Green hydrogen supply potential on the Arabian Peninsula

Francesco Benetti

Delft University of Technology

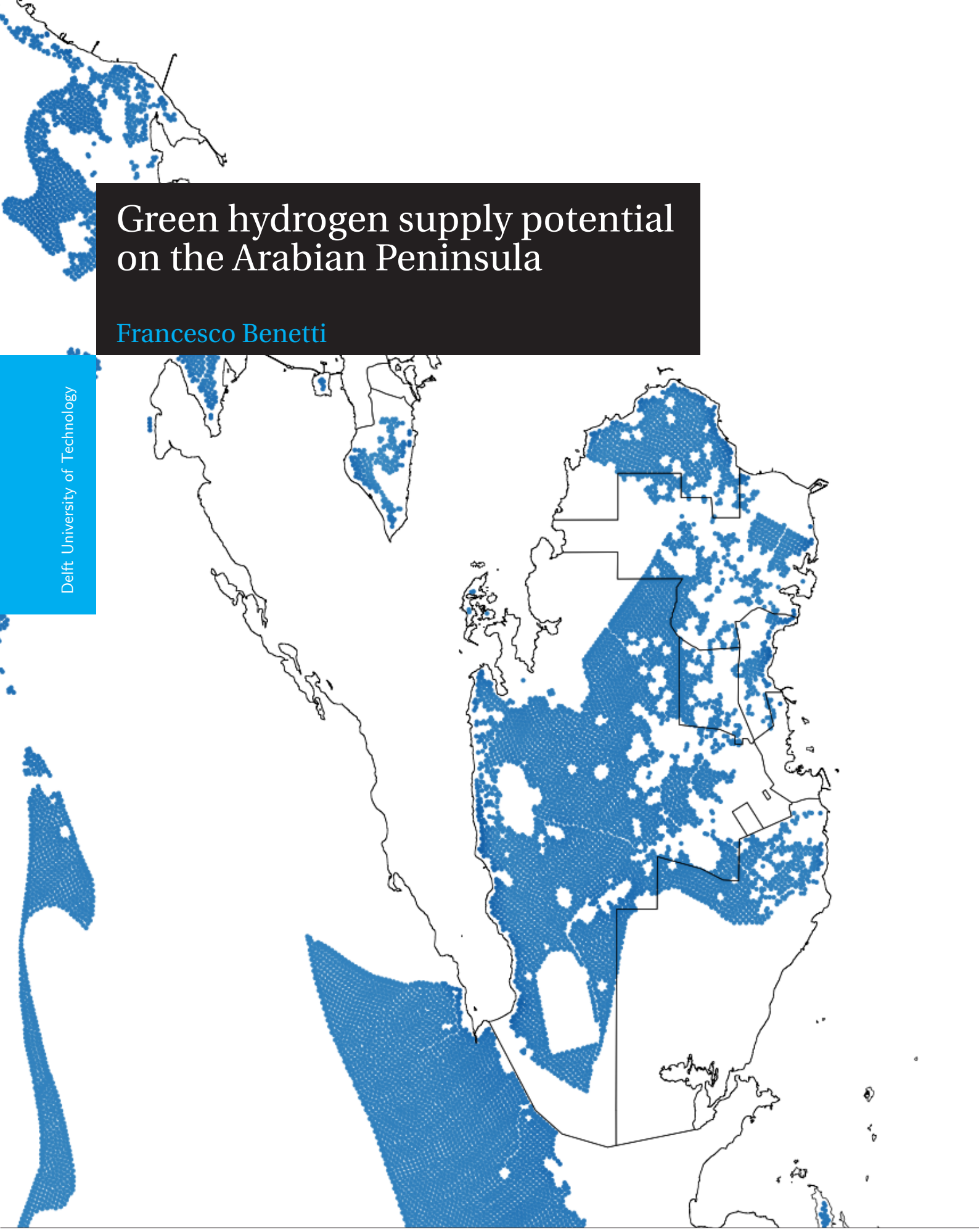

TU Delft Delft University of Technology

JÜLICH Forschungszentrum

Challenge the future

Delft University Of Technology

Master of Science Thesis

Green hydrogen supply potential on the Arabian Peninsula

Author: Francesco Benetti

Supervisors at TU Delft: Prof. A. Smets, Prof. B. Dam

Supervisor at FZJ: Dr. H. Heinrichs

May 11, 2021

Faculty of Electrical Engineering, Mathematics and Computer Science (EEMCS) · Delft University of Technology

TU Delft Delft University of Technology

JÜLICH Forschungszentrum

Contents

List of Figures

List of Tables

Acronyms

BEV	Battery Electric Vehicle
BOF	Basic Oxygen Furnace
BOS	Balance of System
CAPEX	Capital Expenditures
CCI-LC	Climate Change Initiative - Land Cover
CCUS	Carbon Capture Usage and Storage
CF	Capacity Factor
CHI-RSD	Cumulative human impacts: raw stressor data
DHI	Diffuse Horizontal Irradiance
DNI	Direct Normal Irradiance
DRI	Directly Reduced Iron
DSMW	Digital Soil Map of the World
EAF	Electric Arc Furnace
EIA	US Energy Information Administration
ERA5	European Centre for Medium-Range Weather Forecasts Re-Analysis version 5
ESA	European Space Agency
ESM	Energy System Model
EU	European Union
EV	Electric Vehicle
FCEV	Fuel Cell Electric Vehicle
FCHEV	Fuel Cell Hydrid Plug-in Electric Vehicle
FINE	Framework for Integrated Energy System Assessment
FLH	Full Load Hours
GADM	Global Administrative Areas
GCC	Gulf Cooperation Council
GDP	Gross Domestic Product
GEBCO	General Bathymetric Chart of the Oceans
GH2	Gaseous Hydrogen
GHG	Greenhouse Gases
GHI	Global Horizontal Irradiance
GHSL	Global Human Settlements Layer
GIS	Geographic Information System
GLAES	Geospatial Land Availability for Energy Systems
GPCA	Gulf Petrochemicals and Chemicals Association
GSA	Global Solar Atlas
GWA	Global Wind Atlas
H-DR	Hydrogen Direct Reduction
HBI	Hot-Briquetted Iron
HVAC	High Voltage Alternating Current
HVDC	High Voltage Direct Current
IEA	International Energy Agency
IEC	International Electrotechnical Commission
IEI	Intersect of Exclusive Economic Zones and IHO areas
IRENA	International Renewable Energy Agency

LAEA	Lambert Azimuthal Equal Area
LCOCEH	Levelised Cost Of Combined Electricity and Hydrogen
LCOE	levelised cost of electricity
LCOH	levelised cost of hydrogen
LEA	Land Eligibility Analysis
LH2	Liquified Hydrogen
LHV	Lower Heating Value
LNG	Liquified Natural Gas
ME-OGFM	Middle East Oil and Gas Field Map
MENA	Middle East and North Africa
MERRA-2	The Modern-Era Retrospective Analysis for Research and Applications version 2
METN	Middle East North Africa Electricity Transmission Network
NASA	National Aeronautics and Space Administration
NREL	National Renewable Energy Laboratory
OF	OpenFlights
OPEC	Organization of the Petroleum Exporting Countries
OPEX	Operating Expenses
OSM	OpenStreetMap
PBL	Planet Boundary Layer
POA	Plane of Array
PTC	PV USA Test Conditions
PV	photovoltaics
RES	Renewable Energy Sources
RESKIT	Renewable Energy Simulation toolkit for Python
SCM	Submarine Cable Map
SRTM	Shuttle Radar Topography Mission
TAC	Total Annual Costs
TSAM	Time Series Aggregation Module
UAE	United Arab Emirates
UK	United Kingdom
UN	United Nations
UNCLOS	United Nations Convention on the Law of the Sea
US	United States of America
USGS	United States Geological Survey
VRES	Variable Renewable Energy Sources
WDPA	World Database on Protected Areas
WEF	Water-Energy-Food

Symbols

bbl/d	barrel per day
kW_p	kW peak

1 | Introduction

The hydrogen sector is receiving renewed interest from important political and financial institutions across the world. According to the European Commission, the sector is set to play a fundamental role in the energy infrastructure of the future. Among the reasons behind this prediction is the possibility to employ hydrogen as both an energy vector and an energy storage medium. Besides, hydrogen could also be used as feedstock in sectors whose emissions are hard to abate, such as the ammonia and steel production sectors. Green hydrogen, i.e. hydrogen produced using renewable electricity, would therefore be able to contribute significantly to the climate goals of the Paris Agreement. [1]
The considerations just made particularly apply to the countries of the Arabian Peninsula. In fact, high insulation [2] and significant wind speeds [3] can be observed over parts of their territory if compared to many other regions of the world, which results in a high potential for renewable electricity production. Besides, the countries are committed to diversify their economy through investments in the clean energy sector, while they currently rely almost exclusively on fossil fuels [4].

The objective of this thesis is to create and study an optimised fully renewable energy system model for the countries of the Gulf Cooperation Council (GCC)[1] for the year 2050. Green electricity and hydrogen will be used to satisfy the energy and feedstock demand of the power, ammonia, steel and road&rail transport sectors. The export of liquified hydrogen will also be considered. Therefore, the following research goals have to be achieved, each one building on the ones preceding it:

- Determining the portion of land and sea able to host open-field PV panels and wind turbines
- Determining the potential and feed-in timeseries of open-field PV and wind energy
- Determining the electricity generation cost of open-field PV and wind energy
- Deriving the main features regarding the installation and operation of the optimised energy system model under different scenarios
- Calculating the costs of the system. This includes, among others: i) the calculation of the economic benefits of a cooperation scheme based on the exchange of energy commodities among different countries and ii) the economic benefits of sector coupling

In terms of novelty of the present work, even if similar studies have been conducted for other regions of the world such as Europe [5–7], only one other fully renewable energy system model is reported in literature considering the GCC countries [8]. Besides, this source does not offer any information on the decarbonisation of the transport, ammonia and steel sectors, while it also adopts a lower spatial resolution than the one used here.

The report is structured as follows. First, chapter 2 offers an overview of the possibilities and challenges regarding the use of green hydrogen in the selected energy and industrial sectors. Also, geopolitical information is reported laying the foundation for an energy system model of the area under exam. Next, chapter 3 describes the methodology adopted to determine the area where VRES can be installed as well as their potential and electricity-related generation costs. Chapter 4 is also dedicated to methodology, but it is focused entirely on the set-up of the energy system model. The upcoming chapters 5 and 6 thoroughly describe the results obtained by applying the methodology reported in chapter 3 and 4 respectively. After this, results are summarised and discussed in chapter 7, where a comparison with other studies is also conducted. Finally, chapter 8 contains the conclusions of this work together with some recommendations for improving and/or continuing it in the future.

[1] Yemen, the only country of the Arabian Peninsula outside the GCC, is excluded due to the reasons explained is subsection 2.3.4

2 | Background Information

This chapter consists of three parts. To begin with, section 2.1 gives an overview of the importance of green hydrogen in a sustainable energy system and quantifies the CO_2 savings made possible by this technology. Secondly, section 2.2 discusses one of the main challenges related to green hydrogen production, namely the water-energy-food nexus. Lastly, section 2.3 is devoted to the study of the Arabian Peninsula itself, its geopolitical situation and the possibilities of liquid hydrogen shipping based on multiple considerations.

2.1 Potential role of green hydrogen

This section is divided in two. The first subsection explains why green hydrogen can play a crucial role in a future sustainable energy system. The second and last subsection quantifies the CO_2 emissions that could be avoided by implementing green hydrogen in three key sectors: power, raw material feedstock for industrial processes (simply referred to as "feedstock" from now on) and transport.

2.1.1 Need for hydrogen

The shift from the traditional energy mix to a more environmentally sustainable one based on renewable energy sources such as solar and wind naturally leads to an increased need for energy storage technologies [9, 10]. As the weather changes continuously, sun and wind energy potentials fluctuate as well; the result is a variable electricity feed-in associated with solar panels and wind turbines [11]. The energy demand, however, is not always as flexible [12]. Therefore, energy storage is needed as a link between the demand and production side of the energy system.

The variation pattern of the solar and wind electricity feed-in curves can be appreciated on multiple time scales, ranging from the order of seconds to that of months or years [13]. Therefore, the question arises if existing energy storage technologies are well suited to cover these fluctuations, and at which are better for each time-scale.

Two reports published respectively by International Renewable Energy Agency (IRENA) and the World Energy Council in 2019 both show the dominating role of Li-ion batteries in recent world-wide energy storage installations, once pumped hydro is excluded from the analysis [14, 15]. This phenomenon is mainly due to their use in electric vehicles, whose development is being supported in many countries following concerns over the sustainability of the current state of the transport sector [16]. At the same time, Li-ion batteries have also performed well in utility scale projects, such as the Hornsdale Power Reserve in Australia. Therefore, on the short-term time scale this technology seems to be up to the challenges posed by generation intermittency. However, in addition to issues such as safety [17] and sustainability [18], it is well known that Li-ion batteries' efficiency decreases with storage time: they can lose up to 5% of their stored energy for each month of inactivity due to self-discharge reactions [19]. Moreover, capacity and power are not decoupled for this type of technology [20], meaning that if only extra capacity is needed, the designer is forced to oversize the rated power of the system. This means that economy of scale poorly applies here, so that gain margins increase only relatively slowly with growing size of the system.
As a consequence, modern Li-ion batteries are being challenged by other technologies in the mid-term storage applications (3-4 hours and above) and are surely not the optimal solution for long-term storage (days, weeks), as can be observed for example in the techno-economic analysis of Zeng Li et al. [21]: at large scale, technologies such as pumped hydro and compressed air are more cost-effective. Today, these two technologies are associated with the lowest capital costs per unit of energy, as it is also reported in S. Hameer et al. [22], under the condition that the natural resources they depend on are easily available. In fact, the authors also highlight a big disadvantage for these two energy storage solutions: they require special site conditions. Simply put, they cannot be arbitrarily installed anywhere. What is more, pumped hydro and compressed air come with another problem, which is not mentioned in most techno-economic analyses such as those just cited: they allow the storage of energy, but not its transport. In other words, another energy carrier is needed in the absence of power lines in the proximity. In fact, since these installations have be located close to specific cites, they might end up being located very far from energy demand or production centers. Therefore, the nearest possible grid connection point may also be located very far away, meaning that expensive grid infrastructure has be built to allow the correct functioning of these storage plants.

In the light of the information just reported above, it is difficult to state for sure which existing energy storage technology is best suited for long-term or large-scale applications. Hydrogen does solve the problems of site and grid dependency just mentioned, but it is not the only possible way to do so: many other options exist, as best shown in Figure 2.1. Therefore, why has it been hydrogen to gain so much momentum in the last years, even to the point of being defined as a "key priority" by the European Commission [1]? The reason put forward by the Commission is that hydrogen can be used not only as energy storage and carrier but also as feedstock, allowing it to be implemented in sectors of the utmost important for society, such as industry, power, transport and buildings, potentially preventing a significant part of CO_2 emissions. The same point is made by Brandon and Zurban, who call hydrogen "an energy revolution" [23]. The opportunities and implications of a world-scale hydrogen system are such that specialists commonly use the expression "hydrogen economy" to refer to them. Some challenges remain significant, particularly the necessity of massive initial investments to build the necessary infrastructure, but also for this problem promising solutions have been investigated, most notably the conversion of the existing natural gas grid to hydrogen purposes, resulting in a dramatic reduction of overall costs [24].

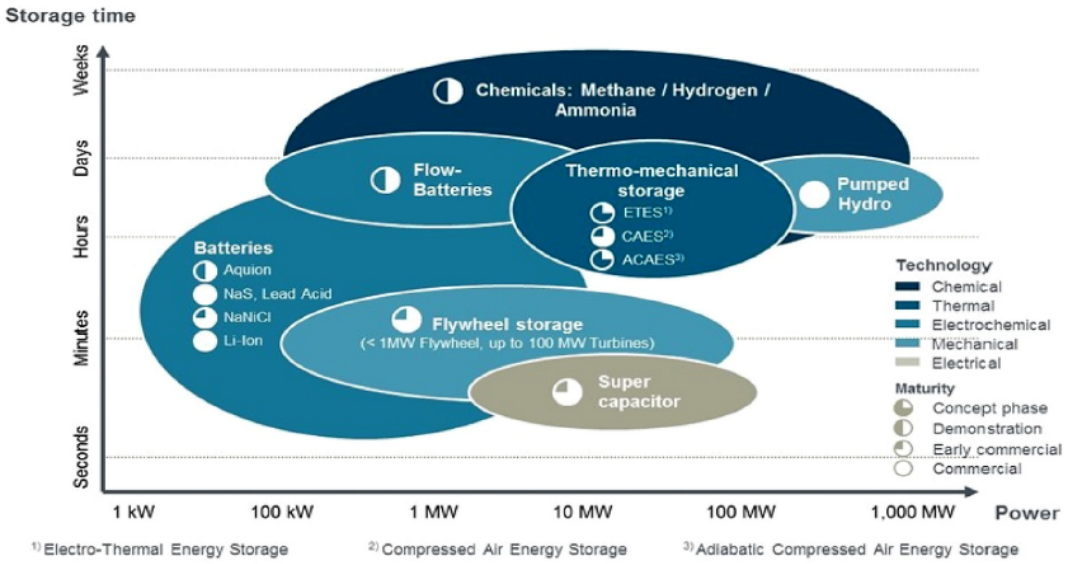

Figure 2.1: Comparison between different storage technologies [25]

If hydrogen can be effectively coupled to existing sectors as they are, it could also continue to be employed as these undergo critical transformation in the future. Actually, hydrogen is needed to facilitate the second big revolution that has to happen in the energy sector in order to meet the 2 °C target set by the UNFCCC Paris Agreement: electrification. In fact, in order to limit the damages of global warming, the electrification rate in final energy demand must increase [26]. Moreover, in the ideal case of a fully renewable system, the absence of electrification and hydrogen integration would inevitably lead to an unsustainable amount of biomass demand [27].

Therefore, the key takeaway in terms of large-scale energy system design and energy policy-making is that the main goal of hydrogen should be to support the creation of a highly-electrified flexible energy system. This does not mean that hydrogen-based heat production will not be necessary in the future: it is reasonable to suppose that thermal sources will still be required to some extent. In any case, the heat sector is outside the scope of the present work.

2.1.2 Sector coupling

In the following subsection a brief overview is given of how sector coupling is technically realised and how significant its CO_2 impact may be for the planet, with special focus on the Arabian Peninsula, which will be thoroughly analysed in the following chapters. The sectors covered here and whose energy demand is later modelled in the study are: power, chemical feedstock for industrial processes (steel and ammonia) and road

and rail transport. As it often happens with definitions, the three categories identified are linked and may partially overlap, which is why further clarifications are included in each sector's description.

Before delving deeper into the three categories identified, it is necessary to mention a few key points, which are often source of confusion or errors when reporting CO_2 emissions. Firstly, global warming is a result of all Greenhouse Gases (GHG) emissions, of which CO_2 is only a part, although a very significant one: 80.5% in 2018, followed by CH_4 with 11.3% [28]. In 2016, about 31% of all methane emissions were fugitive emissions. These are indirect emissions of the oil&gas sector and are therefore difficult to include in calculations about specific emissions of sectors dependent on fossil fuels. For this reason, and also because they represent only a relatively small fraction of total GHG emissions (5.6% in 2016, as shown in Figure 2.2), it is common to refer only to CO_2 emissions coming from fossil fuel burning when discussing the energy sector (Figure 2.3). These should not be mistaken for total emissions expressed in CO_2eq, where potentially all GHG could be included and which would be more comprehensive. [29]
Secondly, emissions can be generally devided between energy and non-energy emissions. Non-energy emissions were approximately 26.8% in 2016 and are mainly due to agriculture (Figure 2.2); as such, they are not accounted for in the calculations that will follow. [29]

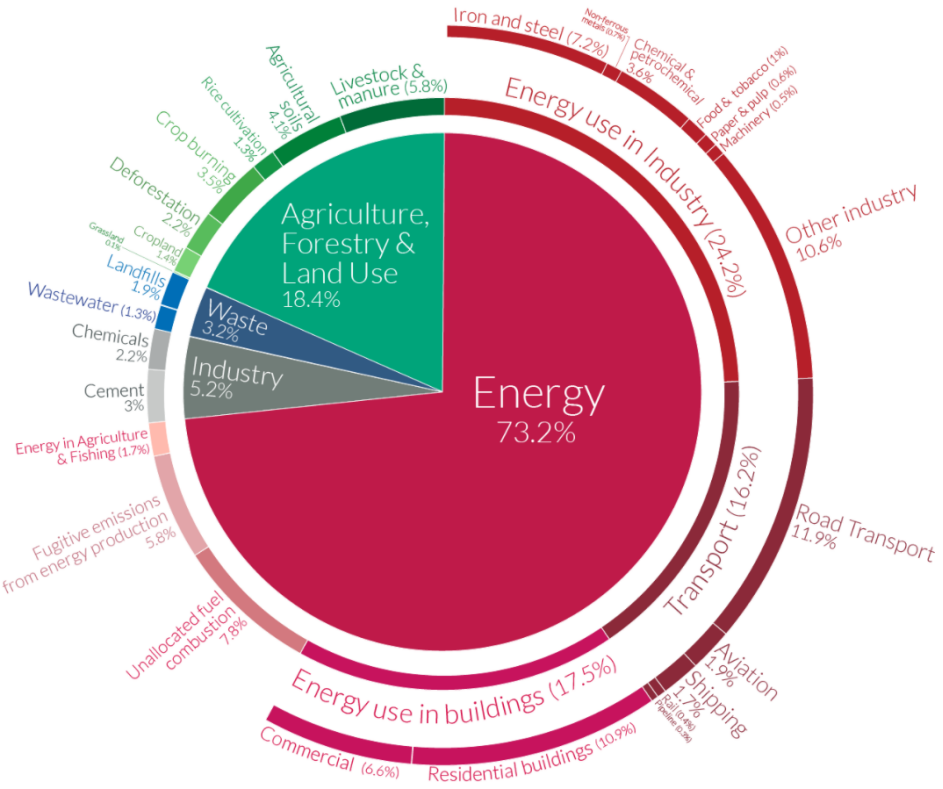

Figure 2.2: Breakdown of global GHG emissions by sector in 2016. Total is 49.4bn tonnes CO_2eq [29]

Power sector

In order to clarify the role of the power sector in carbon emissions, it is useful to provide the breakdown of the CO_2 emissions stemming only from the combustion of fossil fuels (33.5bn tonnes in 2018 [30]), so that the role of the power sector can be bettered measured. This is reported in Figure 2.3. The power sector, represented in light blue, is responsible for 41,7% of these emissions, meaning 14bn tonnes CO_2 [30]. In addition to this, the power sector also produces different GHG gases, namely methane (CH_4) and nitrous oxide (N_2O), although these are considerably less than those related to CO_2 [31]. For example, in Italy, the average amount of non-CO_2 GHG emissions in terms of CO_2eq is around 0.41% of CO_2-type emissions [31]. Given the relatively small relevance of non-CO_2 emissions in the power sector, the ratio for Italy can be applied globally. Now that all GHG emissions stemming from the power sector have been derived, keeping in mind that total GHG emissions were 49.4bn tonnes CO_2eq in 2016 [29], the power sector is then found

responsible for approximately 28.5% of total GHG emissions.

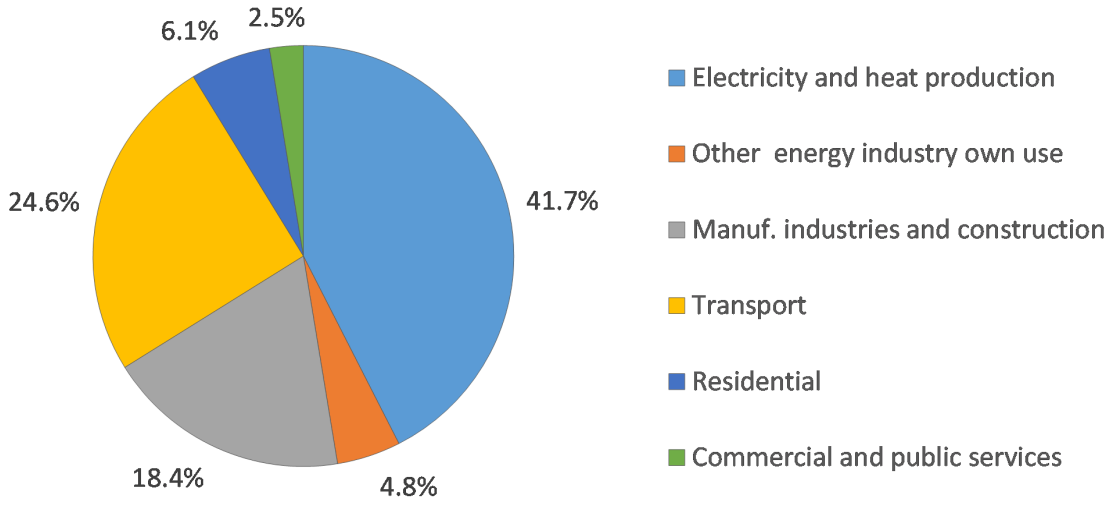

Figure 2.3: Breakdown of global CO_2 emissions from fuel combustion by sector in 2018 [30]

In order to bring GHG emissions associated to the power sector close to zero, hydrogen is not directly the solution, but rather a consequence. In fact, the first necessary condition is that power generation itself becomes carbon-neutral. Multiple ways can be undertaken to obtain this result. In this work, a total shift to renewable energy sources is considered, particularly wind and solar ones. Therefore, decentralisation and discontinuous electricity supply are serious challenges that need an adequate response in terms of (long-term) storage. Hydrogen could give the necessary flexibility needed by the system [1]. This is why hydrogen is a possible indirect solution to the problem of emissions from the power sector, or rather a potential consequence of the direct solution offered by renewables.

The hydrogen-renewables combination plays out in this way: when an excess of electricity is produced, this energy is used to power an electrolyser, which splits water into hydrogen and oxygen. Electrolysers can be placed in multiple locations and in particular close to renewable power plants, effectively adapting to their decentralised installations over the country. In the case of green hydrogen, upscaling its production means upscaling also that of green electricity and ultimately renewables installations. The opposite conversion process from hydrogen to electricity is then possible through the use of fuel cells, with water as the only by-product of this reaction. Fuel cells can be employed either next to the electrolysers or close to physical demand sites: in fact, once hydrogen is produced it can be transported under different forms (compressed gas or liquid, just to mention two of them).

Supposing that hydrogen was indeed sufficient to provide the necessary storage capacity to an electricity sector fully powered by renewable sources, how much GHG emissions could be avoided? It is very difficult to assign two different shares of total power demand (and therefore of GHG emissions) to electricity and heat respectively. However, the International Energy Agency (IEA) estimates that electricity was responsible for as much as 90% of all emissions from the power sector [32]. Keeping in mind the figures for the power sector already mentioned during this discussion, a carbon-free supply of electricity would save around 25.6% of total GHG emissions.

The role of the power sector in terms of CO_2 (and hence GHG) emissions is even greater in the Arabian Peninsula. In fact, the carbon-intensity of electricity produced there is on average higher than many other countries in the world, as it is reported in Figure 2.4 [33].

The reason for this is simple: the almost entire production of electricity in the Arabian countries is based on fossil fuels. Detailed data about this topic is provided by IRENA for the GCC countries, meaning all states of the Peninsula except for Yemen. The graph reported in Figure 2.5 shows that the Gulf States generally rely on natural gas as their main source of electricity, with countries such as Saudi Arabia and Kuwait also exploiting oil and its products for approximately 40% and 60% respectively, which leads to even higher CO_2

intensity values. Important to notice, renewable power is almost absent from the mix. [4]

A final interesting piece of information is that, in the case of all countries of the Arabian Peninsula, a GHG-free electricity supply would directly lead to no emissions in the whole power sector. In fact, given the high temperatures over the entire duration of the year in the region, no heat production is required. [34].

Transport

There is no doubt that an effective energy transition strategy would have to drastically reduce GHG emissions from the transport sector. Figure 2.2 shows that transport was the fourth largest emitting sector in 2016 at 16.2% of global GHG emission. Road transport is the main contributor to this number, registering a 11.9% of all emissions and almost three quarters of those of the entire transport sector. [29]

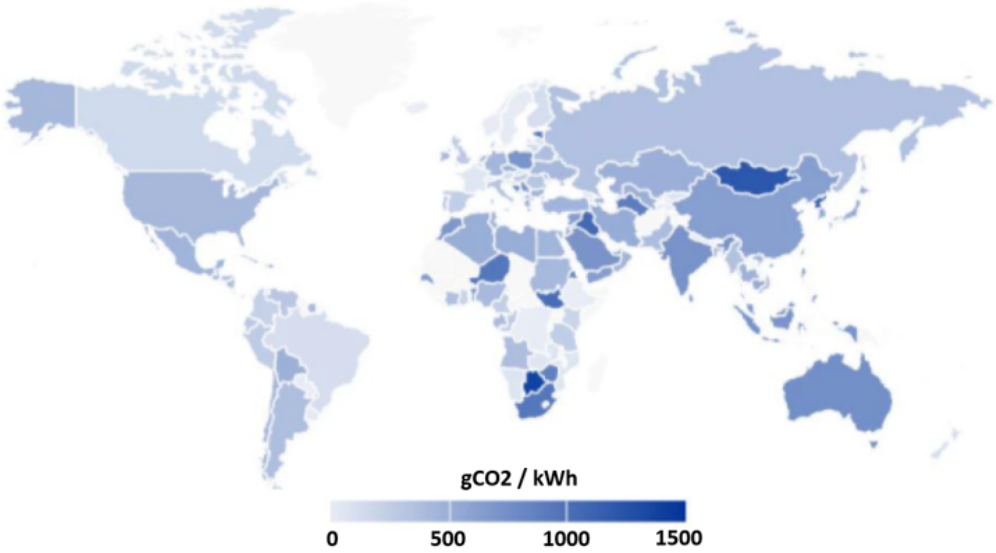

Figure 2.4: Carbon intensity per unit of produced electricity by country [33]

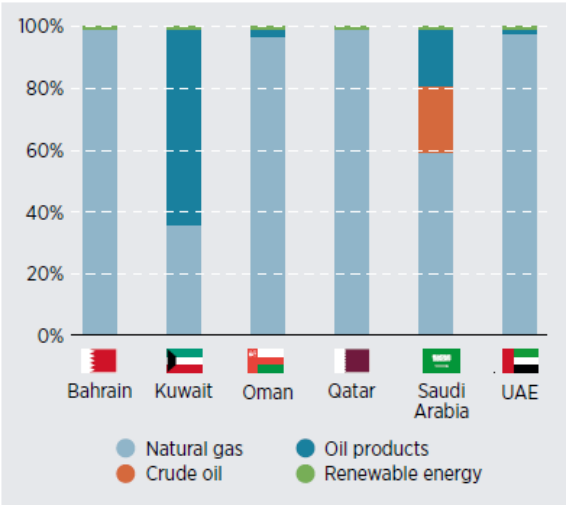

Figure 2.5: Breakdown of electricity generation in the GCC countries by source [4]

In order to effectively achieve sustainability goals, multiple countries around the world are setting goals and plans to foster the penetration of electric vehicles in the transport sector. However, these actions are seldom followed by bans on fossil fuel vehicles or other legislative acts, so that law enforcement remains an issue [35]. In spite of this, Electric Vehicles (EVs) are definitely going to play an important role in the future and

compete with conventional ones [36]. EVs can be grouped in two main categories: Battery Electric Vehicles (BEVs), whose power source is a battery, and Fuel Cell Electric Vehicles (FCEVs), which primarily rely on fuel cells.

In general, the Arabian countries are at a very early stage of this process. What is sure however is that the United Arab Emirates (UAE) are leading the change in the region: the Emirati government has declared their intentions to continue the installation of charging points (200 in 2018) and also stated that they are aiming to get 42,000 EVs running by 2030. Saudi Arabia, currently lagging behind, is also expected to develop a significant EV market in order to achieve its "Saudi Vision 2030", especially after the country signed a Memorandum of Understanding with the United Kingdom in this sense. [37]

The deployment of electric vehicles alone, however, would not be sufficient to transition to a more sustainable scenario. This needs to happen together with a shift of the power sector to emission-free technologies. This is even more true for countries such as those of the Arabian Peninsula, which heavily rely on fossil fuels for electricity. Eventually, the full green electrification of vehicles would require an immense amount of renewable energy, which would in its turn lead to the need for seasonal storage, given the almost constant energy demand of the road transport sector during the year. This topic has already been addressed at the beginning of this section, where we conclude that hydrogen is a good solution in this sense. Therefore, the hydrogen infrastructure could even gain initial momentum from the need for seasonal storage generated by the sales of BEVs, although only when their overall demand rises significantly. It is difficult to say which of these two power train technologies will eventually gain the largest share of the market. In fact, most studies usually conclude that both will probably have a role in the future of road transport, indicating BEVs as the best option for short-distance trips and lightest vehicle, while FCEVs as well-suited for the other cases [38, 39]. G.J. Offer et al. even suggest that the best EV option for the next future would be that of a Fuel Cell Hydrid Plug-in Electric Vehicle (FCHEV), which combines battery grid charging options and hydrogen fuel cells [40].

Unfortunately, heavy-duty commercial vehicles are way harder to be run on electricity [41]. However, a considerable share of road transport emissions (29% of total CO_2 transport emissions in 2018 [42]) would not become GHG-free unless this happens or alternative green fuels are used: in both of these cases, hydrogen can be considered. In fact, hydrogen can either be used to directly produce electricity, or as chemical feedstock to produce hydrogen-based liquid fuels such as ammonia or synthetic liquid hydrocarbons, which are more energy-dense [41]. Since the current study focuses on electricity and hydrogen alone as energy carriers, the choice of fuel cells will be made when modeling hydrogen demand. Fuel cell electric trucks, in fact, have already been proven a possible solution for decarbonisation [43], whereas hybrid or hydrogen trains are starting to or close to being commercialised in different countries, for example Germany and the Netherlands [44].

In the case of a zero-GHG scenario, aviation and shipping, other important emitters in the transport sector, are also expected to rely on hydrogen-based or other liquid fuels due to volume constraints, unless radically new designs are found [41]. In any case, as hydrogen demand stemming from aviation and shipping cannot be directly allocated to individual countries, the scenarios developed in this study will not include these sectors in the analysis, but will only account for road and rail transport.

Feedstock for industry

So far, we only analysed how hydrogen could be used as an energy carrier or energy storage solution. However, another opportunity offered by green hydrogen is to be employed as feedstock in some very important but polluting industries, namely those producing steel and ammonia, allowing them to become almost carbon-neutral. For both, electrolysis-based green hydrogen is offered as an alternative option to technologies based on fossil fuels.

Firstly, we consider the case for ammonia (NH_3). This chemical product is essential to the manufacturing of fertilisers, and it registered a global production 144 million metric tons in 2018 [45]. This is responsible for around 1% of all GHG global emission [46]. Ammonia production is particularly important for the Arabian Peninsula, which hosts three of the 20 largest-producing countries worldwide: Saudi Arabia, Qatar and Oman [45], with overall production in the GCC area adding up to 13 million tonnes in 2018 [47]. The production of this commodity in the region is projected to increase, but should then stabilise in 2030 at around 16 million tonnes [47].

Currently, ammonia production mainly relies on a well-established synthesis process called Haber-Bosch (H.-B.), which takes a mixture of gas as input, the required elements being H_2 and N_2. In its turn, this mixture (a version of syngas where nitrogen is also present) is obtained in a previous step where air, water and a fossil fuel react at high temperature [48]. The reaction for which water and methane combine to give hydrogen is called steam reforming and it is the most common way to produce hydrogen to date. The most efficient and frequently employed fuel for steam reforming is natural gas, but coal and others can also be used, as shown in Figure 2.6. [49]

Therefore, hydrogen and nitrogen can also be produced separately, with nitrogen obtained for example through cryogenic air separation (for large-scale plants) or pressure swing adsorption (PSA, for small-seize plants) and hydrogen obtained through steam reforming. [50]

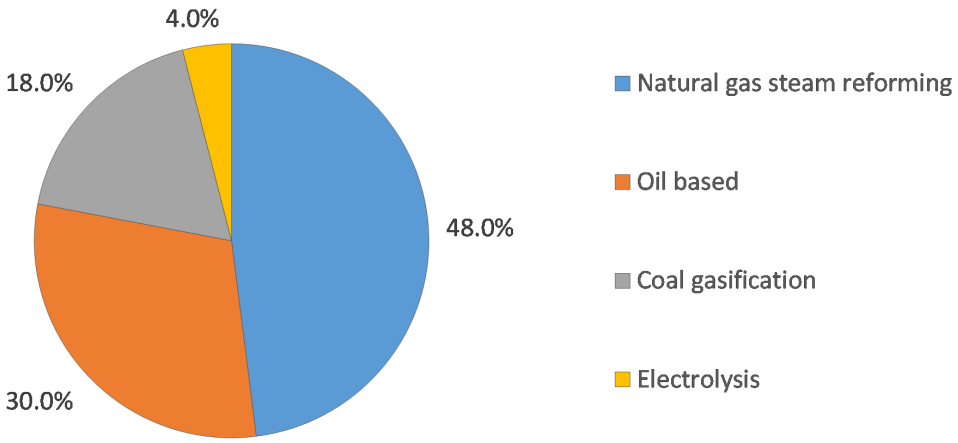

Figure 2.6: Breakdown of global hydrogen supply by production method [49]

A different process is described by Pfromm, which aims at producing hydrogen and nitrogen separately using renewable electricity [48]. On the one side, nitrogen is obtained through the cryogenic air separation process already mentioned above. On the other, hydrogen is obtained through renewable-powered electrolysis. The two are then combined to create ammonia using the Haber-Bosch synthesis. Electrolysis constitutes the near total of the energy demand for the whole process, which is around 10 MWh per tonne of ammonia. [48]

The second sector that could use green hydrogen as feedstock is that of iron and steel. The sector is called as such since steel is iron containing a low amount of carbon (lower than 1%) [51]. The potential reduction in GHG emissions for this sector is even greater, and can be observed in Figure 2.2: approximately 7% of total GHG emissions and an even higher share of energy emissions alone [29]. The largest demand for steel (around 52%) is to be found in the building and infrastructure sector, with mechanical equipment and the automotive industry following at 16% and 12% respectively [52]. In 2019, world crude production was equal to 1,870m tonnes, with China as the top producer by far (as it is also the case for ammonia) at roughly 1,000 million tonnes. The countries of the Arabian Peninsula, on the contrary, are not as relevant for the type of feedstock under study: only Saudi Arabia is a somewhat important producer, making it to the 20th position with a tonnage of 8.2 million [52]. Among the other countries, the Arab Emirates produced 3.3 million tonnes of crude steel in 2019, Qatar 2.6 million and Oman 2.0 million. The steel capacity for Kuwait and Bahrain is reported by the OECD Steel Committee as equal to 1.4 million and 0.2 million tonnes respectively [53]. Therefore, the GCC countries today come to produce 17.7 million tonnes of steel overall. According to the numbers presented above, this would account for almost 1% of the world total production.
Although of a very small size compared to the top steel-producing countries, it can be argued that the steel sector is key to the diversification plan that GCC countries have to pursue to enhance their economic stability, since steel making from hydrocarbons would reduce the dependency on oil&gas exports. This is also an effective strategy to pursue given the availability of such a feedstock at a low price [54]. The same applies to the fertilisers (hence ammonia) sector and in general the manufacturing industry to which steel and ammonia belong [54]. Moreover, increasing the size and competitiveness of the steel and ammonia sectors through a diversification plan would also mean gathering know-how that can later be used to convert the system to run on green hydrogen feedstock, as we consider in this study for the year 2050.

The IEA has recently published an outlook for steel demand and production in 2050, where two different scenarios are considered. In the more ambitious approach in terms of sustainability goals, steel production does not grow globally after the year 2025, reaching 2,000 mln tonnes. In the other scenario based only on existing or announced policies, production reaches instead 2,500 million tonnes in 2050. Here, the Middle-East strongly increases its production thanks to the availability of natural gas at a low price: in the Stated Policies Scenario, this more than doubles reaching almost 4% of the world total. It should be noted however that the Middle East region includes other non-African countries, most notably Iran, which has a steel market size comparable to that of Saudi Arabia. In the case of a green hydrogen economy scenario such as that considered in the present study, the countries of the Arabian Peninsula could still increase their steel output if they maintain a competitive edge over the other countries in terms of levelised cost of electricity and therefore levelised cost of hydrogen and eventually cost of steel produced. [55]

Steelmaking can be either referred to the process itself of iron reduction, or to the full process of transforming iron ore into steel, of which iron reduction is only one step. There are two main ways to obtain steel. The first and conventional process is divided in ironmaking and steelmaking itself. Ironmaking is realized in a blast furnace, to which coke (derived from coal), limestone and iron-ore products are fed; steelmaking follows in a Basic Oxygen Furnace (BOF), where scrap can also be added. The newer technology produces iron in the first process directly from iron under the form of pellets or equivalent alternatives or even raw, without this having to undergo any previous physical or chemical reaction, hence the name Directly Reduced Iron (DRI); then, steel is obtained in the Electric Arc Furnace (EAF), which requires a considerable amount of electricity to work and which can also use scrap. The two different workflows can be observed in the diagram in Figure 2.7. [51]

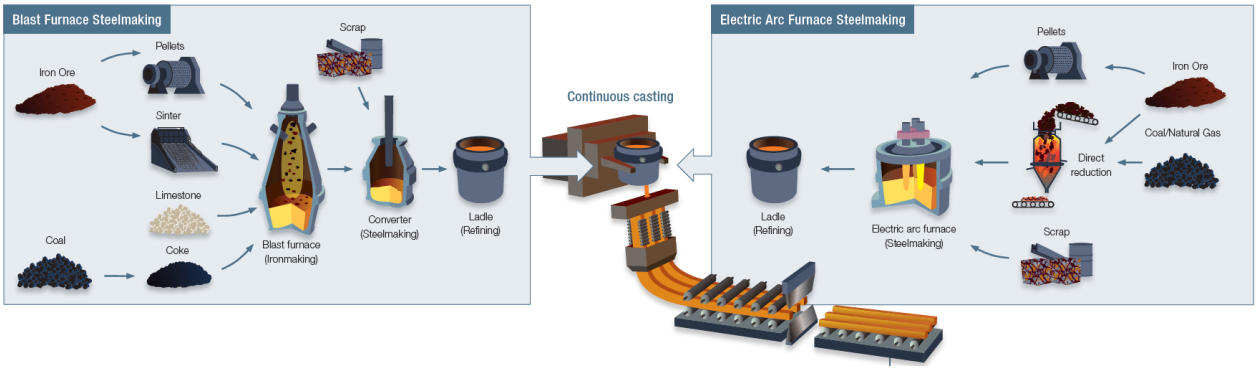

Figure 2.7: Overview of the two main steelmaking technologies [56]

As just mentioned in the previous lines, steel scrap can be used to reduce the necessary amount of raw materials, since steel can be recycled without its properties being negatively affected [57] (attention must be paid however to the presence of impurities [58]). In fact, the IEA indicates that scrap makes up 30% of newly produced steel, with iron ore constituting the remaining 70%. At the same time, 80 to 90% of used steel is recycled. This makes sense not only economically, but also environmentally, as the energy input for scrap in an electric arc furnace is 8 times lower than that of iron ore in a traditional blast furnace [55]. Of the 750 million tonnes of scrap available in 2017, 630 million were effectively used by the iron and steel industry [59]. The Worldsteel Association expects the amount of scrap availability to rise to 1300 million by 2050, meaning a 67% increase in just over 30 years [59]. Considering the use of the EAF technology with iron ore and scrap as feedstock materials, and assuming a feedstock-to-steel conversion efficiency of 89% as indicated in [58] for the EAF, scrap would then cover as much as 58% of the steel demand value of 2000 million tonnes reported in the more sustainable scenario of the IEA [55]. Besides, the ratio of scrap over the total amount of feedstock input in the EAF would also allow for a good dilution of the impurities present in scrap.
Scrap recycling is just an example of a broader strategy that the iron and steel sector is expected to follow in order to reduce its emissions, namely that of energy efficiency. In fact, this is indicated as an effective approach for the sector by the Worldsteel Association [57]. More precisely, the IEA forecasts that an average efficiency improvement of 1.7% will be achieved every year until 2030 [60].

The biggest challenge in reducing carbon emissions from the production processes highlighted above (BOF, DRI) is that fossil fuels are not only used as fuel to provide electricity or heat, but they also provide the

necessary elements for the chemical reactions to take place, just as it happens for ammonia. Typically, CO produced through fossil fuels is the reducing agent for iron; however, also hydrogen can serve this purpose, eliminating the need for polluting materials. The same problem mentioned for ammonia applies here: hydrogen is primarily obtained through the carbon-intensive process of steam reforming. Therefore, the same solution should apply: green hydrogen and electricity. This idea is investigated by Vogl et al. [61], who create a model for a H-DR process such as that already implemented in the HYBRIT project developed by Vattenfall. More precisely, green iron is produced according to the two following chemical reactions in Equation 2.1 and 2.2 [61]. The authors model energy demand as a linear function of scrap, which, albeit a simplification, allows to study the system for any percentage of scrap used as input.

$$Fe_2O_3 + 3H_2 \rightarrow 2Fe + 3H_2O_{(g)} \tag{2.1}$$

$$Fe_2O_3 + H_2 \rightarrow 2FeO + H_2O_{(g)} \tag{2.2}$$

The authors, however, indicate that the overall energy emissions of steel would still be greater than zero, due to the iron ore extraction and generation phases. At the moment, iron ore production is CO_2 intensive: in China its life-cycle GHG impact is equal to 250 kg CO_2eq per tonne of iron ore fed into the blast furnace, with most emissions due to fuel consumption for energy production [62]. These emissions could be avoided, for example, in the case of a fully developed hydrogen economy where these steps are performed by electric machines powered by green hydrogen and/or where Carbon Capture Usage and Storage (CCUS) is a mature technology.

Finally, some emissions would still remain due to the use of materials such as lime and carbon in some specific phases of the process. The latter of the two could be made carbon-neutral if the carbon was derived from biomass or CCUS techniques instead of fossil fuels. In any case, these material-related emissions would account only for around 3% of those associated to the traditional BOF technology. [61]

Now that the key points of green hydrogen production have been described, it is possible to understand the overall H-DR production process of Vogl et al. [61], which is reported in Figure 2.8. The only new feature is the presence of Hot-Briquetted Iron (HBI), which is just a hot and compact form of DRI. The direct reduction process takes place in the shaft to which iron ore pellets and hydrogen are fed. The latter is obtained through hydrogen electrolysis, with the possibility to also rely on hydrogen storage. Finally, steel is created in the electric arc furnace, in which scrap, carbon and lime are used together with DRI.

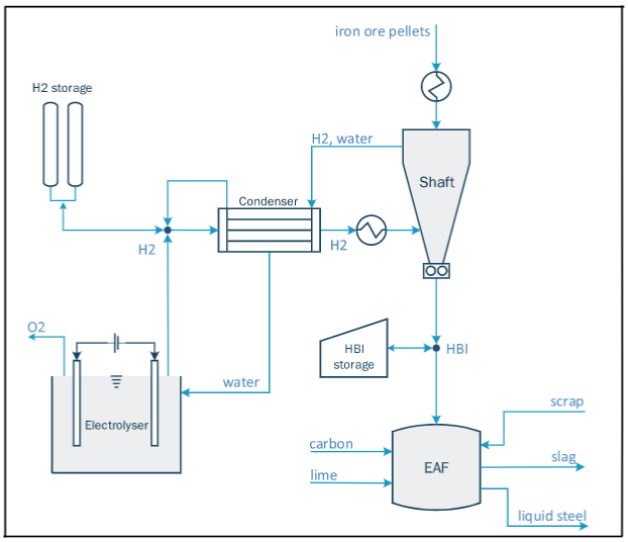

Figure 2.8: H-DR green steel production process through hydrogen proposed by Vogl et al. [61]

2.2 Potential challenges with green hydrogen

This section is devoted to the analysis of some challenges connected with green hydrogen production, namely pure water supply for electrolysis and land competition for the installation of renewable energy technologies.

In the previous chapter, the climate benefits offered by green hydrogen in terms of GHG emissions reduction have been highlighted. Producing hydrogen via electrolysis, however, gives rise to a challenge, namely that of water usage. In fact, traditional electrolysers must be fed with pure water, which is very hard to find in the Arabian Peninsula.

Fresh water supply is actually one of the biggest issues for the people living in the Arabian Peninsula already. In fact, the water resources are not just among the lowest per unit of area, but also per inhabitant [63]. In fact, in addition to the absence of rivers and lakes on the surface and limited rainfalls, groundwater resources are scarce and often face salinity problems. These issues are worsened by many factors including inefficient use and water pollution. Finally, a rapidly rising demand (due to a rapid population increase and fast economic development) further contributes to the water scarcity problem. [64]

The energy sector plays an important role in the issue of water supply. In fact, water and energy are interpendent, meaning that they are both necessary for and dependent on each other. For this reason, the expression "water-energy nexus" has been created to describe this phenomenon. In order to explain the role of the water-energy nexus in the Peninsula, we take the case of Saudi Arabia, the biggest and most populous country of the Peninsula, and also the most water consuming.
Saudi Arabia heavily relies on desalination: 70% of the water used by the nation has to be desalinated, with 18% of total desalinated water output worldwide being registered in this country alone. On top of this, the demand for desalinated water is growing at an impressive rate of 14% a year. As a consequence, it is reported that 10-20% of Saudi Arabia's energy demand and half of the oil domestic use are consumed by this sector.
On the other hand, water is needed by the energy sector. In fact, this type of final use is associated with the second highest water demand after agriculture. Water is needed for refining petroleum, in which case it has to be pure, and in general in all steps of fossil fuels extraction and processing and also for cooling thermal plants. It must be noted, however, that the water use for industrial applications is low compared to agricultural and domestic ones. [65]

Given the critical role of freshwater in the current energy system of the Arabian Peninsula, would the situation worsen once hydrogen is introduced in the system as an energy source partly replacing fossil fuels? In other words, would it take more fresh water to produce the same amount of energy through green hydrogen instead of fossil fuels? The answer is: not significantly. The water required specifically for green hydrogen electrolysis is of 9 liters of pure water per kg of final product [66], as can be also derived from a simple mass balance equation of the electrolysis reaction. On the other hand, the production of green hydrogen would reduce the consumption of fossil fuels, meaning that significant water savings would derive from it as well [67]. Since refining needs around 2.2 liters of fresh water per kg of gasoline output and since the energy density of gasoline is one third of that of hydrogen, the amount of water required per unit of energy would only increase by approximately 36% if the energy system was converted from fossil fuels to green hydrogen [67]. This number could even decrease if one considers that water is also used as coolant in thermal power plants, which would then be replaced by green hydrogen power plants; however, this reduction cannot be always considered in freshwater saving calculations, since industrial cooling systems can also run on salt water [68]. On the energy side, desalination does not have a significant role compared to electrolysis: considering the Lower Heating Value (LHV) of hydrogen (33.3 kWh/kg_H2) and an electrolyser having an efficiency of 70%, 48 kWh/kg_H2 of electricity are needed for electrolysis, whereas 0.2 kWh/kg_H2 are consumed for distribution and desalination using thermal power plants (and even less considering solar and wind power plants). [67].

A workaround for the problem of water scarcity could be the use of direct seawater electrolysis. Research is indeed ongoing on this topic, and it shows that the coasts of very arid regions (such as the Arabian Peninsula) would be the most suitable to host this new technology. This is also true for spatially constrained offshore applications, which is also relevant to the present case: offshore oil&gas platforms reaching end of life could be converted to this purpose, effectively reducing infrastructure costs. Although the prospects of seawater electrolysis look promising, it is still early to say if this technology could be applied on a very large scale level

such as that required for the present study. Furthermore, traditional electrolysers can rely on years of use in the energy industry, which is essential to reduce investment risk. Therefore, direct seawater electrolysis is not included as a hydrogen production option. [69]

Finally, it is worth mentioning another issue connected with competition for resources, namely that of food supply. As already mentioned in the previous paragraph, agriculture is also strongly linked with water. Moreover, once we consider the case of green hydrogen, renewable energy technologies are included in the system, particularly PV panels and thus solar farms. Therefore, while wind farms do not generally interfere with local crops, solar farms increase land competition with agriculture [70]. In the case of the Arabian Peninsula, the "water-energy-food nexus" is particularly critical. In fact, in addition to the reasons given above, the fact that only a very small fraction of all the GCC region is arable should be considered [71]. Therefore, the agricultural areas found in the territory under study will not be considered for the installation of PV panels, meaning that all fertile regions (and not just croplands) will be excluded in the land eligibility analysis.

2.3 Geopolitics

After having analysed the main potential benefits and challenges of green hydrogen in section 2.1 and section 2.2, the focus is narrowed down to description of relevant aspects of the Arabian Peninsula for the research goals of this study. The first two subsections that follow are devoted to the study of the land and of its natural energy resources respectively. Subsection 2.3.3 gives an overview of the different countries in the region and of the political relationships among them, whereas subsection 2.3.4 describes the relationship between them and the other countries in the world. Finally, the last subsection describes the options for Liquified Hydrogen (LH2) exports via ship based on the current oil&gas terminals and maritime choke points. While the first two sections are necessary to create a model of the energy production system, the remaining three sections are needed to understand with whom and how the energy commodities produced on the Peninsula could be exchanged.

2.3.1 Land

Due to various constraints (population settlements, physical obstacles exc.), not all land can be used to install VRES. Hence, it is important to have an overview of the physical characteristics of the Arabian Peninsula. This covers an area of 3,100,000 km^2, which can be observed in Figure 2.9. This is slightly larger than India and approximately one third of the United States. The maximum length of the region is 1,900 km (left-side), while it reaches up to 2,100 km of width (bottom-side). From a political point of view and according to the definition given in most sources, the Arabian Peninsula consists of 7 countries, which can be observed in Figure 2.9a together with their neighbouring states [72]. Ordering them from the largest to the smallest, they are: Saudi Arabia, Yemen, Oman, United Arab Emirates, Kuwait, Qatar and Bahrain [73].

The Peninsula is surrounded by water on three sides: on the West, by the Red Sea, on the East, by the Persian Gulf and the Gulf of Oman and on the South by the Gulf of Aden and the Arabian Sea. From the sides, access to the Arabian Sea is possible on the left through the Bab el-Mandeb Strait and on the right via the Strait of Hormuz. The northern border of the Peninsula with the Syrian Desert is not officially established, but the borders of Saudi Arabia and Kuwait are generally indicated for this purpose. Access to the Mediterranean Sea is allowed only by crossing the neighbouring states to the North-West or via the Suez Canal controlled by Egypt. The three straits just mentioned are therefore strategic elements when considering LH2 exports from the Peninsula to Europe or the United States of America (US), as will be explained in subsection 2.3.5. [74]

The center of the Peninsula is occupied by desert, while parts of the coasts are some of the few areas to offer habitable land with possibilities for settled agriculture [74]. However, a considerable amount of cultivated fields can also be found in central Saudi Arabia, running parallel to the left side of the desert [76]. Mountains rise on the western portion of the Peninsula, slowly decreasing northeastward towards the fertile crescent and southeastward towards the Gulf of Oman, where they rise again to create another mountain range. Water is scarce: no river or lake of significant size can be found over the entire territory [75].

The almost entire region is extremely dry and hot, with infrequent and low precipitation [77]. In fact, no

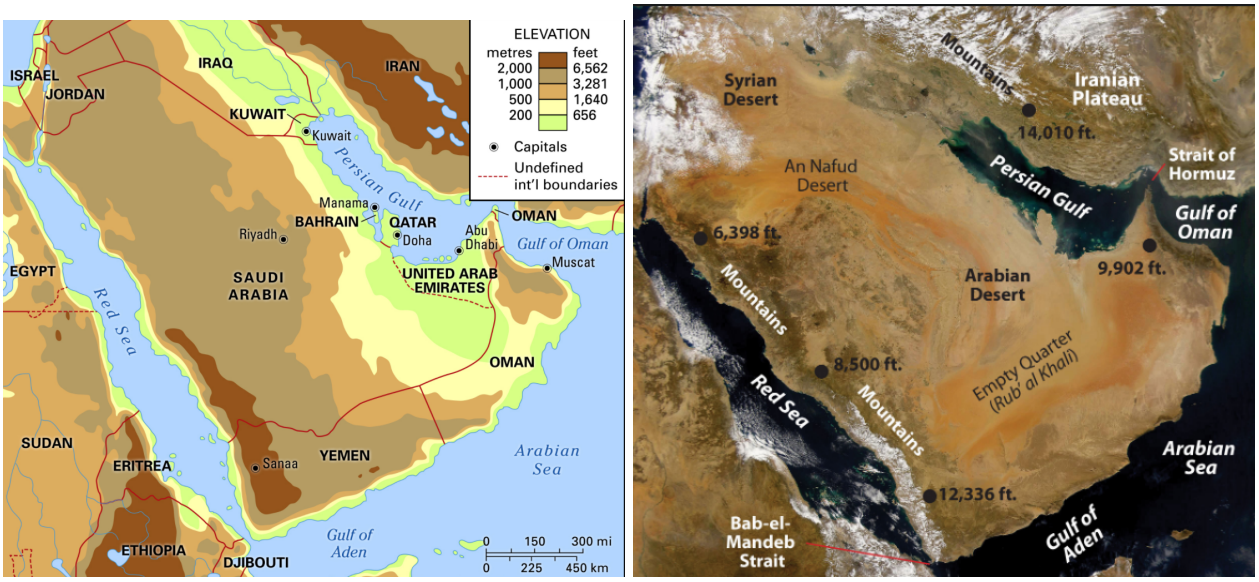

(a) Topographic map [74] **(b)** View from above [75]

Figure 2.9: Different physical maps of the Arabian Peninsula

country registers heat production over the entire year [34]. Only the southwestern part of the region (Yemen) enjoys more abundant precipitations and therefore a mild steppe climate [77]. The average temperatures for the month of January and July can be observed in Figure 2.10.

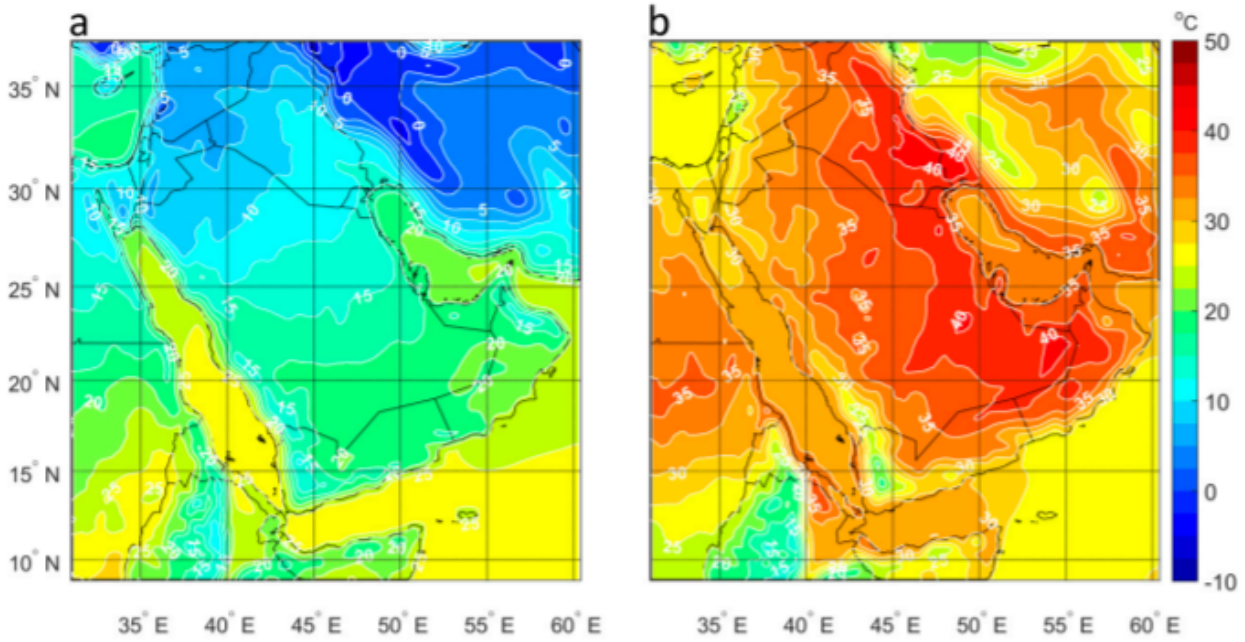

Figure 2.10: Mean temperature distribution at 2 m of height during January (a) and July (b) - average over the years 1986-2015 [77]

2.3.2 Natural energy resources

In order to explain the importance of VRES for the Peninsula in the future, one should start by describing the importance of fossil energy sources for its current economy, even though this may seem counter-intuitive. This region is known for its incredibly large reserves of oil and gas, a fact which applies (although to a lesser

extent) to the entire Middle-East[1]. The discovery of oil in multiple locations of the region was made during the first half of the XX century mainly by the British, but new fields keep being discovered to date [79]. The greatest amount by far of these energy sources is found offshore in the Persian Gulf and onshore in the stretch of land surrounding it [80]. At the end of 2019, the Middle East was found to possess 38% and 48% of the entire world reserves of natural gas and oil respectively [81]. If one considers only the states of the Peninsula excluding Yemen (so the GCC countries), the shares of natural gas and oil reserves become 21% and 29% [4]. It follows that production and exports are also high. Just to give an idea, in 2017 Qatar and Saudi Arabia were among the top 8 gas producers in the world, whereas the same Saudi Arabia together with the UAE and Kuwait were among the top 9 oil producers [4].

The abundance of hydrocarbons in the Arabian Peninsula has led to the modern economy revolving around them, especially when it comes to exports and fiscal revenue. However, the instability of oil prices and geopolitical tensions affecting them have shown the risks of this economic model. Furthermore, in spite of their amount, oil and gas reserves are limited and will eventually expire. Besides, competition from alternative energy sources is increasingly challenging the status quo of the industry where gas had long been the cheapest way to produce electricity. [4]

Therefore, all governments of the GCC have recognized the need for diversification [4]. This means first of all depending less on oil&gas exports (growing the local manufacturing industry for example), but also gradually relying less on oil&gas in general. The main beneficial effect on the local economy would be that of making it more resilient in case of fluctuating oil prices, but there is more to it. In fact, in pursuing diversification policies governments hope to achieve two more goals. Firstly, to create high-value jobs for locals. Secondly, to attract private investors more. In fact, the role of the private sector will probably be the key to expand non-oil activities [82].

For the GCC countries, diversification of the economy means first of all diversification of the energy sector: in other words, increase of the renewables' share in the energy mix. Even when considering electricity generation alone, where penetration of wind and solar is generally easier, almost 0% of the total was coming from these sources in 2016 [4]. However, the case for renewable energy installations in the Peninsula is particularly strong: many regions are underpopulated and not fit for other purposes, while solar potential is very high and that of wind is also considerable. As both land availability and sun and wind energy potential will be thoroughly analysed in the following chapters, we only report here in Figure 2.11 and Figure 2.12 the solar and wind energy distribution maps for world and the Arabian Peninsula to give a qualitative idea of their potential use.

From Figure 2.11, it can be observed that the Arabian Peninsula is characterised by a significant solar potential in terms of Direct Normal Irradiance (DNI), like the entire MENA region, although it does not come close to the average values of the countries such as South Africa or Australia [2]. Besides, wind power is also relatively high if compared with the majority of other regions in the world, with average power being close to that of northern Europe but still inferior, for example, to that of North Africa or the United Kingdom [3].

A closer look at the Peninsula (Figure 2.12) proves that the areas with higher solar potential are those in the North and South West, peaking at around 2775 kWh/(m^2year) [2]. The pattern for wind power is different, with the best areas for energy production found in the central-western, north-eastern and south-eastern part of the Peninsula, where wind speed is generally above 7 m/s [3]. In particular, along the coasts of Oman overlooking the Arabian Sea the record wind speed is set at almost 10 m/s, with very high potential also offshore in that area.

Overall, judging from the distribution of wind and solar energy resources in the region with respect to other countries in the world (Figure 2.11), it is difficult to say whether the Peninsula is better suited for the installation of PV panels rather than wind turbines. In any case, none of the two should be excluded in advance from the research of the optimal energy system. In fact, not only both wind and solar potential are high: these two technologies also have variable power outputs that could often balance each other peaking at different times and points in space. This effect could therefore reduce the costs for energy storage installations.

[1] According to [78], the Middle East includes the states of the Arabian Peninsula (Saudi Arabia, Kuwait, Qatar, Bahrain, United Arab Emirates, Oman, Yemen), some African states (Lybia, Egypt, Sudan), plus the territories of Turkey, Cyprus, Syria, Lebanon, Iraq, Iran, Israel, the West Bank, the Gaza Strip, Jordan, Egypt and Libya. Other states are also considered according to different sources

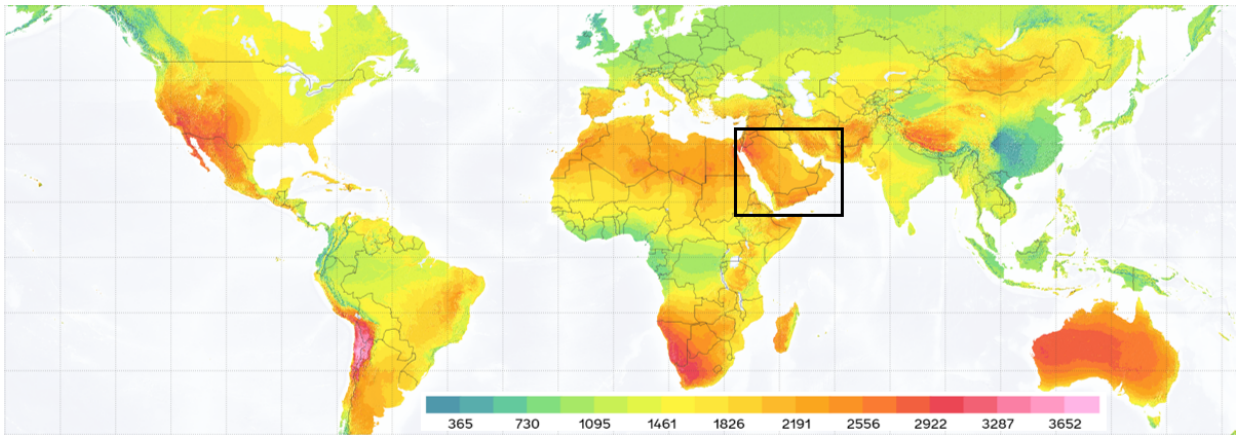

(a) DNI distribution $[kWh/m^2year]$ - average over the years 2007-18

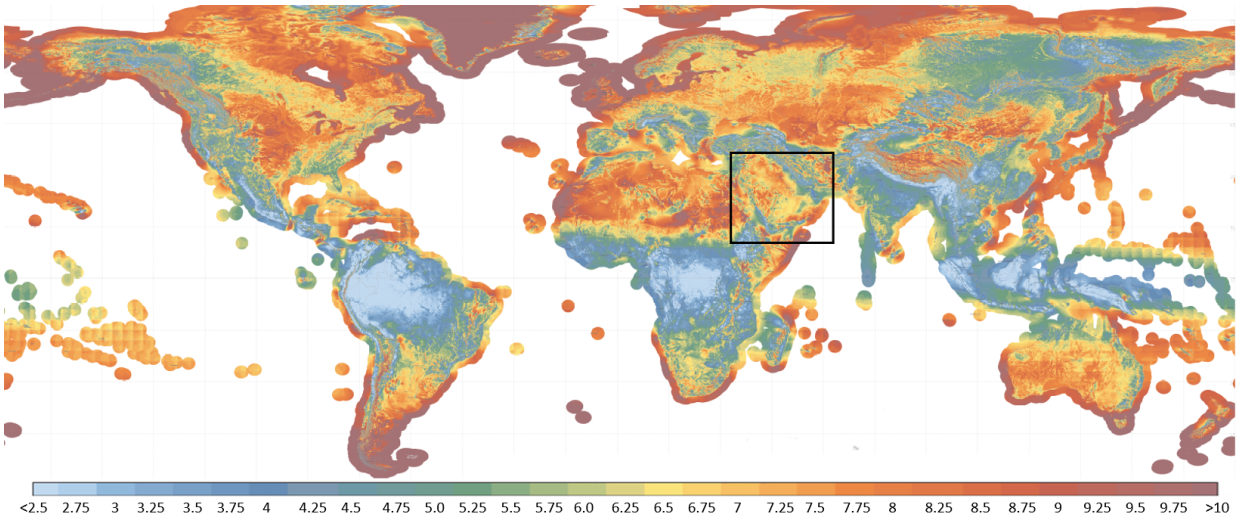

(b) Wind speed distribution at 100m $[m/s]$ - average over the years 1998-2017

Figure 2.11: Solar (a) [2] and wind (b) [3] energy potential distribution worldwide. The Arabian Peninsula is framed in black

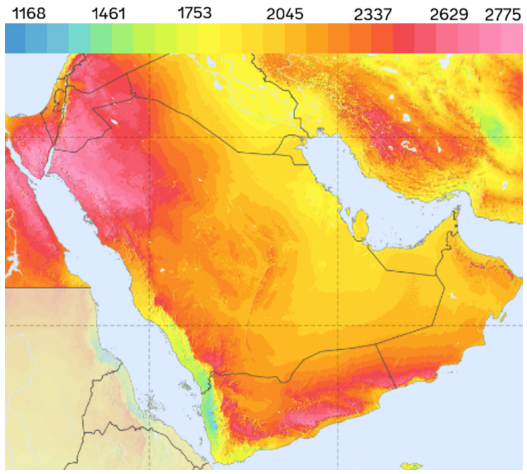

(a) DNI distribution $[kWh/m^2year]$ - average over the years 1999-2018

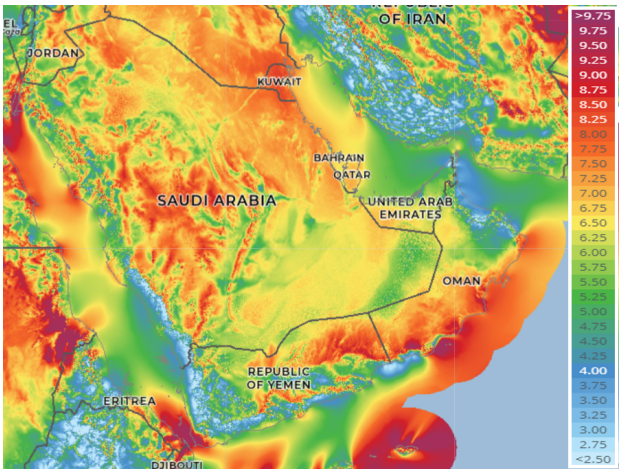

(b) Wind speed distribution at 100m $[m/s]$ - average over the years 1998-2017

Figure 2.12: Solar (a) [2] and wind (b) [3] energy potential distribution over the Arabian Peninsula

2.3.3 Arab states in the Peninsula

Designing an energy system which comprehends different countries implies the knowledge of the conditions at which energy commodities can be traded among them, if they can be traded at all. This, in turns, leads to the need to understand the political relationship between the different countries composing the Peninsula. The political chessboard reported in Figure 2.13 is a result of very recent historical events: borders, governments and alliances are largely a result of the British colonisation of the Persian Gulf in the XIX and XX centuries [83] and of the US's influence over the past sixty years [84]. This is particularly true for the northern region of the Peninsula, where the US led two wars in 1990 and 2003 to avoid any modification to the balance of power in the region, especially in Kuwait.

Figure 2.13: Political map of the Arabian Peninsula [72]

As a consequence of these events, the political arena still sees a lot of action. Although the inhabitants of the region share similar language (Arabic), religion (Islam) and political systems (monarchies or similar, except for the Republic of Yemen), tensions are often high, especially between the closest western allies (Saudi Arabia and the UAE) and the remaining states of the Persian Gulf (Qatar and Bahrain). These conflicts intensified recently after the Arab Spring, which also provoked a civil war in Yemen, which currently hosts what is the largest humanitarian crisis worldwide. [85]

The sheer size of the Arab states might be misleading when trying to judge the political power and influence they exert in the region. First of all, as mentioned in subsection 2.3.2, the oil&gas reserves are almost entirely located in the central-eastern part of the Peninsula and offshore in the Persian Gulf, meaning that the largest share of wealth and power is concentrated in Saudi Arabia's Eastern Province, the UAE, Qatar and Bahrain. Yemen, in the south-western part of the Peninsula, was already producing less oil than the other countries of the region; with the civil war, production fell even further as well as the level of wealth [86, 87]. Oman, situated in the bottom-right corner of the Peninsula, represents a sort of in-between situation, both in terms of oil production and of GDP per capita [86, 87].

There is another important factor to the weight of the Arab states in the political events shaking the Peninsula: population. Figure 2.14 shows that the population is primarily distributed on the coastal areas, with very low population density in the central region, with the exception of Riyadh, the capital of Saudi Arabia [88]. This is a consequence of the distribution of fossil resources in the region (subsection 2.3.2) and of the natural

characteristics of the land (subsection 2.3.1). For these reasons, in spite of a huge difference in size, the population of Yemen is close to that of Saudi Arabia [89]; besides, all states have a comparable number of inhabitants if one only considers the coastal region overlooking the Persian Gulf [88]. Due to the fact that also oil and gas resources are located mainly in this area [78], great competition for leadership arises among the Gulf states, both in political and economic terms [90].

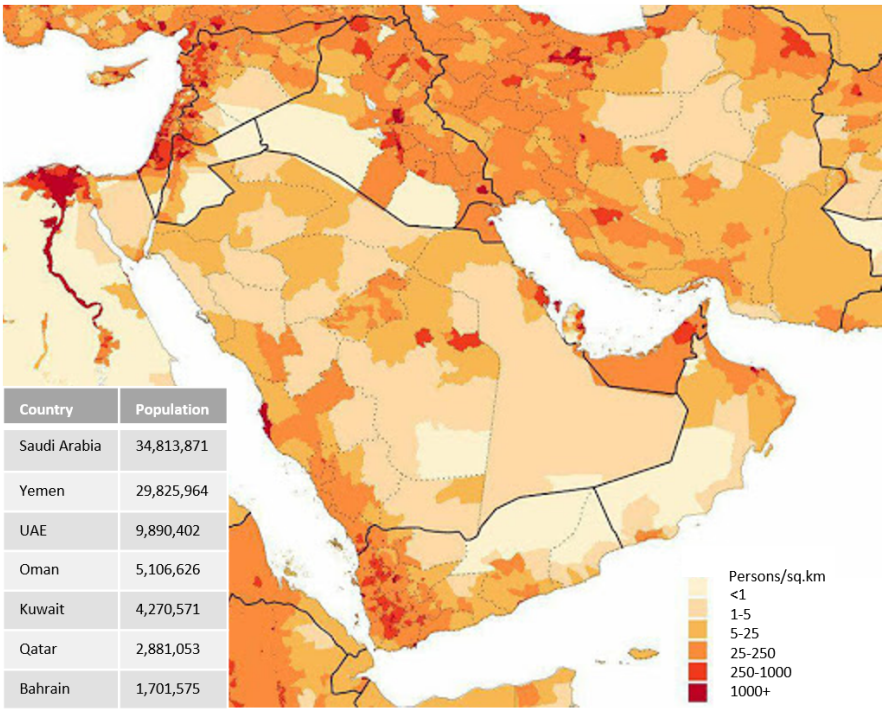

Country	Population
Saudi Arabia	34,813,871
Yemen	29,825,964
UAE	9,890,402
Oman	5,106,626
Kuwait	4,270,571
Qatar	2,881,053
Bahrain	1,701,575

Figure 2.14: Infographics of population in the Arabian Peninsula in 2020 [88, 89]

Although the older British colonies bordering the Persian Gulf are trying to impose themselves as leaders in the region, they are political allies from an official point of view: all of them, in fact, are part of the strategic alliance called GCC (Gulf Cooperation Council). Although reportedly created to foster social and economic development across the countries of the Peninsula, the alliance was formed in 1981 in order to coordinate military defense forces in the region in response to potential external attacks. In fact, two years before the six gulf countries (Kuwait, Bahrain, Qatar, Saudi Arabia, United Arab Emirates, Oman) came together to sign a constitution in Abu Dhabi (1981), the Soviet Union had launched the invasion of Afghanistan (1979), while one year earlier Iraq had started a war with Iran (1980). [91]

With the passing of time, the countries have indeed cooperated not only for defense purposes, but also in economic terms: the internal market is essentially free for people, although some restrictions remain on goods and services, whereas the countries have also been coordinating their oil exports to some extent [91]. In any case, the GCC block has already formally established a customs union and is working to achieve it [92]. However, the member countries have difficulties in coordinating their policies [82].

Probably one of the most important events in terms of cohesion of the group was the joint military support of the GCC states to Bahrain's government during the 2011 protests that invested the country [93]. In spite of an effective response to the Bahrain crisis, political bonds among the group are again at stake. In 2017 Saudi Arabia imposed a blockade on Qatar, the UAE, Bahrain and Egypt, following a purported hack of Qatar's governmental website where comments were made on behalf of Qatar in support of destabilizing political groups active in the region. The countries later asked Qatar to cut its ties with Iran, Turkey and Islamic groups such as the Muslim Brotherhood, but the country refused [94]. The local news agency Al Jazeera, however, hints at a possible reconciliation under the guidelines of the United Nations (UN) [95].

Since it is unlikely that the GCC could break up without major consequences in the Middle East political arena, many countries are in fact interested in keeping peace in the region, most notably the US. Therefore, we can reasonably suppose that a hydrogen system such as that which will be created in this study will

encompass all countries of the GCC, including Qatar, with energy commodities being exchanged freely among them.

The situation is far from close to a resolution in Yemen. Following the Arab Spring of 2011, chaos broke out in the country. Previously, relationship between Yemen and the neighbouring Saudi Arabia had progressed, especially after the unification of Yemen under president Saleh, an ally of Saudi Arabia. However, the country has hosted Marxist ideas and a wide-spread anti-US sentiment which prevented it from joining the GCC over the years leading to the Arab Spring. When this broke out, the Houthi rebellion (dating back to 2004) transformed into a proper civil war between the government and the group. In 2015, Saudi Arabia intervened, leading a military operation in Yemen with the backup, among others, of the United States. [96]

However, the military operation commanded by Saudi Arabia was not decisive: the Houthi rebellion is still ongoing. In 2019, the Houthis claimed the drone and missile attack that hit oil facilities in Saudi Arabia, compromising as much as 50% of their oil production [96]. In 2020, the UN declared that the weapons used in the air-strike were of Iranian origin [97]. Iran is indeed supporting (at least ideologically) the Houthi movement, as these are part of the Shia just like Iran and contrarily to the majority of GCC members, who are Sunnis. In fact, Iran hopes to extend its influence across the Gulf at the expenses of Saudi Arabia, whose intervention in Yemen is seen by Iran as an unlawful attempt to conquer the region [98]. The US will not be able to mediate, as they are also involved in an ongoing economic and military warfare with Iran and allied with Saudi Arabia.

In the light of the situation in Yemen just outlined, any kind of trade relationship between Yemen and the GCC countries seems unlikely in the next future, especially considering the diverging interest of major powers such as the US and Iran in the region. Accession of Yemen to the GCC could happen only many years from now, but that is anyway unsure. Besides, the lack of political and social stability in the long term would probably hinder the development of new green hydrogen infrastructure in the country. In fact, considerable investments are needed and soon if the Arab countries want to achieve a hydrogen economy by 2050, but this will very hardly happen in Yemen, where the risks associated with investments will remain high for an unknown number of years. For all these reasons, the current studies will not include Yemen in the energy system that is designed. This decision is also backed-up by the fact that most available data sources and papers usually adopt a GCC perspective rather than considering the whole Arabian Peninsula.

Following the considerations made for Yemen, another very small region is excluded from the subsequent land eligibility analysis: this is a 120 km^2 portion of the Persian Gulf located close to the south-eastern coasts of Qatar, defined as “contested” among multiple countries [99].

2.3.4 International political relationships

Since the scope of the current study goes beyond energy auto-consumption in the Peninsula to investigate the export of LH2 as well, international political relationships become important too. In fact, these contribute to determine the routes and final destination of energy exports. Given the importance of oil in the modern world, GCC countries are involved in different international organisations and have tightened political bonds, formally or otherwise, with different nations across the world. These ties are however often conflicting, either because strategic allies are competing with each other, or because GCC states do not all take the same side.

First and foremost, Saudi Arabia, the UAE and Kuwait are members of the Organization of the Petroleum Exporting Countries (OPEC). The organization includes some African states, most notably Algeria and Lybia, while also including Iraq and Iran. Given the tensions between certain members of the association, oil production coordination falters repeatedly. Qatar left OPEC in 2019, during the blockade imposed on it primarily by Saudi Arabia. Tensions are often high also with Russia and the United States, by far the two world biggest oil producers together with Saudi Arabia, who consequently positions itself as the ”de facto” leader of the OPEC group [81].

Also important from an economic point of view, but even more from a political perspective, all GCC countries are members of the Arab League. The League was created in 1945 on the wave of growing nationalism in response to continuous colonialism at the hands of European countries [100]. Nowadays, the organization includes all North African countries and all countries of the Arabian Peninsula. The association is also opposed to Israel and in general to the intervention of non-arab major powers in the region, most notably the

US. This formal stance is however in contrast with the close relationship between the US and the biggest GCC countries. In any case, the Arab League is on the path to achieve a free-trade zone among the participating members [101]. Within the League, an important and solid relationship is that between Egypt and the GCC countries of Saudi Arabia, United Arab Emirates and Kuwait [101]. This can also be observed by the fact that the majority of northbound oil&gas flows through the Egyptian Suez canal originate in the GCC area [102], making Egypt and the GCC members economically interdependent. Even during the diplomatic crisis of 2017 that saw Egypt back up the GCC sanctions against Qatar, Qatari ships were still allowed to cross the canal [103], also because the United Nations Convention on the Law of the Sea (UNCLOS) international laws forbid the ban of ships from crossing maritime straits [104]. Therefore, it seems that access of all GCC members to the Mediterranean Sea through the Suez Canal will continue to be possible in the future as well.

The main political rival of the GCC countries in the Middle-East is Iran. As a matter of fact, Iran is in a sort of cold war with Saudi Arabia, the two of them trying to prevail as the major power in the region, while it is in better terms with Qatar and Bahrain. The US and UK have so far sided with Saudi Arabia, giving it the upper hand in the international scene. Saudi Arabia and almost all countries of the Arab League are Sunni majorities, whereas Iran follows the Shia; therefore, the two countries try to leverage on religion to back up their claims and influence. Iran has allies in many regions of the Middle-East, including the Houthi group in Yemen, and its area of influence primarily includes Yemen [97], Iraq, Syria and Lebanon [105]. It can then be concluded that these countries will probably not be engaged in LH2 imports from the GCC union in the future, unless the balance of power in the region changes significantly.

In multiple occasions in this and the previous section, we have highlighted the importance of the role of the US and UK in the region. Apart from the US and the UK, other important commercial partners are the European Union (EU) and many Asian countries (Japan, Korea, China, India) [106]. However, when it comes to energy exports, the Asian market is the main destination, and it is predicted to remain so [106]. As demand from OECD countries reduces due to policies for energy independency and sustainability and due to slow economic growth, oil and gas are needed by developing countries such as China and India. For this reason, in 2013, GCC countries saw less than 20% of their crude oil output being purchased by Europe and North America combined, while 70% ended up in Asia [107]. Therefore, although future trade of energy commodities might change once hydrogen replaces fossil fuels, the Asian market seems to be on the path to remain the main energy importer. The US and the European countries might also have a role as importers depending on how much they manage to achieve their energy independency policies.

Finally, North African countries members of the Arab League are allies and thus potential markets, but they are competitors in terms of energy exports. An interest option for a future export scenario could be to consider South-East Africa, where demand should grow and oil&gas reserves are limited [81]. These countries could also create their own local infrastructure for green hydrogen production, but their economies are very weak [108] and substantial investments such as those needed for building a new hydrogen infrastructure are therefore difficult to achieve.

2.3.5 Ports

As already mentioned in this section, the energy system which will be designed in chapter 4 will account not only for local consumption of hydrogen, but also for LH2 export. Particularly important to this topic is the analysis of oil and gas terminals already existing in the GCC countries. In fact, this type of infrastructure can be adapted to host the new technology, possibly avoiding the cost of creating new ports for this specific reason. This is particularly true for the LNG facilities. It is also important to notice that existing LNG ship carriers would need very little changes in order to switch to liquid hydrogen exports instead of LNG, which would further lower the initial investment costs of the new hydrogen system. [109]

In order to model the system of hydrogen ports according to what has just been explained, the existing oil and gas terminals in the GCC region were derived from the US Energy Information Administration (EIA) [80] (updated to 2007) and then reported in a simpler way in Figure 2.15. It is interesting to notice that while oil terminals are numerous, there are only 4 LNG terminals, none of which located in the territory of Saudi Arabia. In fact, the almost entire gas reserves in the Persian Gulf belong to Qatar (second largest gas exporter after Russia [4]), while very few other deposits are found offshore elsewhere. The oil terminal present in South Oman is only reported by S&P Global Platts, who published a more recent map for Oman in 2020 [110],

although it must said that the EIA already showed all the infrastructure leading to the future terminal as of 2007. In any case, no more recent map can be found for the other countries of the Peninsula which is also public.

In order to answer the question of where the LH2 carriers might be loaded in the most economically efficient way, another topic should be investigated, namely which shipping routes might be followed by the carriers. However, an issue arises when investing energy exports from the GCC countries, namely that of maritime choke points, meaning congested navigable passages that oil carriers have to go through. An overview of maritime routes followed by crude oil carriers worldwide is visible in Figure 2.16, where choke points also appear together with their associated daily transit oil volumes [102].

Figure 2.15: Location of oil (black) and LNG (red) terminals in the GCC countries [78, 80, 110]

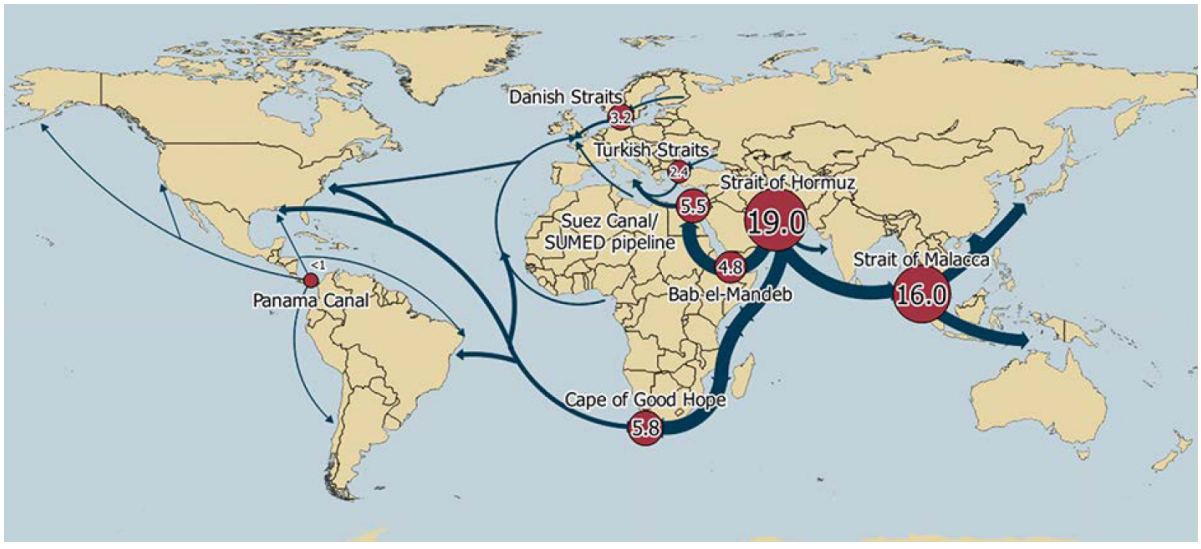

Figure 2.16: Major shipping routes and maritime choke points for oil worldwide. Numbers in million bbl/d [102]

Three of the five world major shipping routes can be found around the Arabian Peninsula, including the very first one, namely the Strait of Hormuz. The others are the Suez Canal & SUMED Pipeline system and the Strait of Bab el-Mandeb. They can be observed in Figure 2.17. For clear geographical reasons, all fossil fuels shipped by any GCC country except for Oman and the United Arab Emirates have to cross one of these points. [102]

The Suez Canal connects almost all continents in the world. Important for the current study is that it is a key export point of LNG for Qatar, but also a fundamental passage for most exports of oil and gas for all the Persian Gulf countries, not only the GCC ones. Almost all northbound flows of oil through the Suez Canal are destined to Europe and North America (78% and 14% respectively in 2016). [102]
A reasonable question would be if new types of carriers such as those transporting LH2 could actually be able to cross the Suez Canal. The answer has already been given above, when saying that these carriers would be very similar to LNG carriers [109]. In fact, some prototypes have already been created following this approach and are documented in literature. In particular, LNG ships with size such as the 160,000 m^3 LH2 ship described in S. Kamiya et Al. [111] normally transit the canal [112], and hydrogen has a lower volumetric density than LNG [109].

Figure 2.17: Major maritime choke points for oil in the Middle East [113]

The Strait of Bab el-Mandeb is also very important: products coming from Asia and the energy exports of the Persian Gulf all have to cross it to reach Europe and North America, since the only alternative would be to circumnavigate South Africa, as shown in Figure 2.16 [102]. Saudi Arabia is an exception, since they can transport oil and gas extracted in the Gulf to the Red Sea using the East-West pipeline that crosses the country horizontally [80]. This strait is often object of piracy and terrorist attacks, and could be considered one of the most dangerous in the world [114]. Its control is also an object of conflict both locally (between the nearby countries in Africa and Arabia) and internationally (notably between the US and China) [114].

Finally, the Strait of Hormuz is the world major choke point for oil and gas. As the largest majority of world reserves is located in the Persian Gulf and the surrounding area, as much as 30% of seaborne-traded oil and other fossil derivatives was crossing the Strait in 2015. The figure for gas is due to the fact that Qatar exported around 30% of all LNG traded worldwide through this choke point. As for crude oil, 80% of the total leaving the strait was destined to Asian markets, notably China, Japan, India and South Korea. [102]

Although the possible shipping routes are now clear, a final issue arises: who can cross the three choke points described? The answer is that it depends. All three straits, given their geopolitically strategic position, have been object of conflicts and wars in recent times after the discovery of oil and gas reserves in the region [115]. If one only considers the political territories in which these territories are located, the Suez Canal belongs to Egypt, the Strait of Hormuz to Iran and Oman while the Bab el-Mandeb Strait to Yemen, Djibouti and to a lesser extent Eritrea [99, 116].
However, sea laws are often contested in the international political scene: the countries just mentioned potentially have the power of closing the straits, although this has dire consequences given the involvement of so many powerful nations in the world, notably the US. In other words, rather than the actual closing of the straits, the countries that control them most often use the closure threat as a political weapon. This is becoming more and more relevant in recent years in the Saudi Arabia vs Iran conflict or the US vs Iran

conflict, which have been described in the previous section. [115]
Therefore, it would be appropriate to mention who controls the straits "in practice", not only which countries own these territories. This is more meaningful but also more subject to errors, since the balance of power is always difficult to define with certainty, especially when so many regions are directly or indirectly involved. As we have explained in the previous subsection, Egypt controls the Suez Canal, but the sphere of influence of other Arab League countries including Saudi Arabia, the United Arab Emirates and Kuwait is also relevant, given their political ties with Egypt [101]. Of the two countries overlooking the Strait of Hormuz, Iran clearly exerts more power thanks to its strongest military [117], but Oman can count on its alliance with the other GCC member states, so that different actors must be considered here as well, namely the GCC block and Iran. Finally, multiple countries have military forces at or close to the Bab-el-Mandeb straits, so that this ends up under the indirect control of some of the most powerful UN nations rather than Yemen or Dijibouti itself [114]. However, piracy attacks in these waters make the area unsafe, as already discussed earlier in this subsection. In any case, it must be reminded that the UNCLOS laws forbid any country to prevent commercial ships from crossing these straits [104], so that a naval block would have dire political consequences. However, this has already happened and could take place again in extreme political situations [115], which must be taken into account when designing a LH2 export system for the Peninsula.

From all the geopolitical considerations made so far, the following conclusions can be drawn. From the point of view of a GCC block of countries led by Saudi Arabia, the best export route for Europe and North America would be the Suez Canal, possibly avoiding the crossing of the Bab el-Mandeb strait using onshore pipelines. It has already been explained, in fact, that the passage of this strait is critical and therefore not a reliable transport route [114]. On the other hand, in order to access the Asian market, carriers should ideally avoid the Strait of Hormuz, as political tensions might result in its closure [115]. This is even more true if all electricity (and hydrogen) in the new energy system is produced onshore and not in the Persian Gulf or close to its shores, as it happens with oil and gas nowadays [80]. This should be the case as onshore open field PV and wind technologies are generally cheaper than offshore [118]. However, this new port set-up would entail the creation of new ports on the coasts of Oman in the south of the Peninsula, where very few terminals are currently present [110]. In any case, due to the fact that political tensions around this gulf are particularly high, the choke point constituted by the Strait of Hormuz is excluded from the land eligibility analysis that follows.

3 | Renewable Potential Assessment Methodology

The following chapter discusses the steps taken in order to assess the potential of Variable Renewable Energy Sources (VRES) in the Gulf Cooperation Council (GCC) area. First of all, a division of the countries under exam into multiple regions is presented in section 3.1. Among other reasons, the regionalisation allows for an effective way to analyze the system and describe results later on. As the adopted workflow consists of two main parts, two sections follow next outlining the method used to quantify the VRES potential in the area. The first step is the identification of eligible land and sea for open-field PV panels and onshore and offshore wind turbines and the subsequent placement of energy farms in those areas, which is described in section 3.2. The second step consists in the implementation of specific design choices for the renewable technologies just mentioned, upon which physical models are applied. In this way, the electricity production potential can be identified together with its costs as described in section 3.3.

3.1 Regionalisation of the territory

Key to the correct quantification of the potential of VRES in the GCC countries is the determination of size and location of geographical areas that can host the installation of these technologies. Therefore, the need arises to find a set of criteria that effectively exclude unfit areas. The whole process just described is referred to as "land eligibility analysis", and the criteria (or constraints) as "land eligibility constraints" [119]. Moreover, two preliminary steps are adopted here, as will be described in this subchapter. The first one is the use of the findings of the Introduction to restrict the area on which the LEA will be run, while the second one is the further division of remaining areas is subregions, hence the name "regionalisation".

First of all, it should be reminded that the considerations of section 2.3 have led to the exclusion of Yemen from the system under exam, leaving the remaining six countries of the Peninsula to be studied: Saudi Arabia, Kuwait, Katar, Bahrain, United Arab Emirates and Oman. Similarly, the Strait of Hormuz and a very small offshore region close to Qatar have also been left out. These exclusion decisions count as sociopolitical exclusion criteria, hence they are included under the "Contested" or "Strategic" category in the list of criteria presented in the following section in Table 3.3. Since it is decided in advance that the above-mentioned areas are being entirely excluded, the effect of these exclusion criteria is immediately applied and these regions are not further investigated, so that the focus of the LEA is entirely concentrated on the land where installations can in theory take place.

After selecting the area where the LEA has to be run, it becomes necessary to divide it into regions. A strong reason for this is to allow the parallelisation of the computational tasks following the LEA and aimed at finding the energy potential of VRES and subsequently their optimal installation layout. In this way, computational time is significantly reduced. The second argument is that different policies and laws typically apply to different regions, even if these belong to the same country. Therefore, it is reasonable to spatially divide VRES installations accordingly.

In the case of onshore land, the georeferenced file with region boundaries offered by the Global Administrative Areas (GADM) database [116] is used: this covers the whole globe and is cited by Caglayan et al. among others [6]. The division of the GADM dataset are based on administrative areas and usually contain multiple possible levels of division, from the individual country itself down to division in small provinces. The first regional level below the country level and called "GID1" is deemed sufficient for the current study. Actually, splitting further the biggest regions of Saudi Arabia could have also been a valid approach, but unfortunately the dataset does not provide any further division beyond the "GID1" level for this particular country.
Overall, 49 regions can be found onshore, for a total of 2.33 million km^2. For each of these, a name and an identifying alphanumeric code at the regional level can be found in the GADM dataset [116]. For each region, the code contains the abbreviated name of the country, the GID level of the region and an ID number to distinguish it from the other regions of the same country. Since the GID level is chosen as 1 everywhere, a simpler alphanumeric code is derived from the GADM definition by removing the GID level number. For example, "ARE.1" stands for Arab Emirates - region 1. The other abbreviations are "SAU' for Saudi Arabia, "KWT" for Kuwait, "BHR" for Bahrain, "QAT" for Qatar and "OMN" for Oman. In order to more clearly present the onshore regions, each of them is also associated with a unique ID integer in the range 1-49, which is the total number of regions found in the GCC area; in doing this, all regions of the same country are

associated with consecutive integers. The result of this process is shown in Figure 3.1, where the ID numbers of onshore regions are reported in black. It is important to notice that some areas are not contiguous but they still belong to the same region (or administrative area). This irregular distribution is the result of physical features of the territory but also of disputes for strategic locations over the past, as already explained in subsection 2.3.3 [90]. For more information on any given region, refer to Table 3.1.

As an equivalent of the GADM for offshore regions could not be found, the exclusive economic zone of each country is adopted according to the Intersect of Exclusive Economic Zones and IHO areas (IEI) dataset [99], which only contains divisions at the country level and is also mentioned by Cagalyan et al. [6]. The only further division at the sub-national level is performed for the territorial waters of Oman, which are divided into those belonging to the Arabian Sea and those belonging to the Gulf of Oman, as this is considered by the author as the only clear example of regional division offshore. This is especially true because the Gulf of Oman is shared with Iran, while Omani territorial waters in the Arabian Sea are not.
As the only divisions in the offshore area are due to national sea borders, apart for the contiguous waters of Oman, no alphanumeric code exists for them at the regional level. A custom one is then created, following the country abbreviations used for onshore regions and adding a letter which describes the sea to which the region belongs: “p” for Persian Gulf, “o” for Gulf of Oman, “a” for Arabian Sea and finally “r” for Red Sea. A unique ID number is assigned also in this case following a clock-wise order starting from the waters of Kuwait: these numbers are reported in white in Figure 3.1. The other information regarding the offshore regions is inserted in Table 3.2.

Finally, in order to allow for a correct implementation of the LEA later on, an appropriate spatial reference system has to be used. In fact, since area calculations are performed on each region individually during this process, two requirements have to be satisfied by the reference system: 1) the area of each region has to be preserved and 2) its overall shape must not be deformed significantly. In particular, not meeting the second condition would create problems when merging the regions together in the following steps. The issue of spatial reference systems is well know in literature, since giving an accurate 2-dimensional representation of some aspects of a 3-dimensional object (Earth) always comes at the cost of reducing the accuracy of other parameters [120–122].
The first condition just mentioned imposes the use of a Lambert Azimuthal Equal Area (LAEA) reference system, whereas the second suggests centering it within the GCC area itself in order to reduce the distortion of shapes [120–122]. Finally, a LAEA is created whose origin is placed in the center of Saudi Arabia. This is thus giving a slight priority to the shape of Saudi regions with respect to the other ones, since here regions are bigger and borders are thus more difficult to merge after splitting. In any case, the respect of original distances is manually checked for all countries revealing no distortion at the km level.

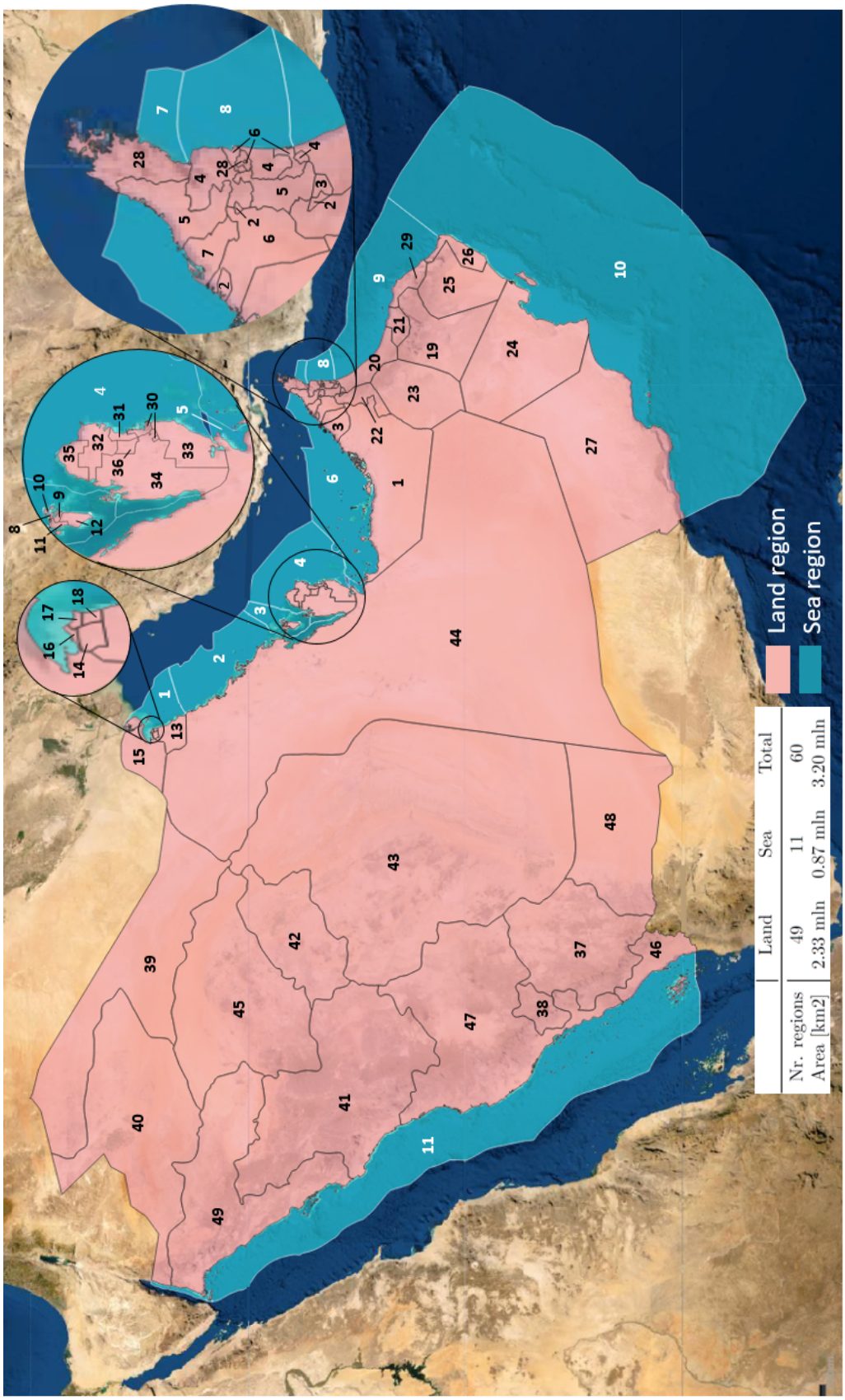

Figure 3.1: Overview of all regions through the regionalisation process. Their corresponding ID is reported in black (land) or white (sea). Non-contiguous areas may belong to the same region following territorial disputes over the past

Table 3.1: List of regions selected through the regionalisation process together with their identification code

ID	Region name	Code	ID	Region name	Code
1	Abu Dhabi	ARE.1	26	Ash Sharqiyah South	OMN.8
2	Ajman	ARE.2	27	Dhofar	OMN.9
3	Dubai	ARE.3	28	Musandam	OMN.10
4	Fujairah	ARE.4	29	Muscat	OMN.11
5	Ras Al-Khaimah	ARE.5	30	Ad Dawhah	QAT.1
6	Sharjah	ARE.6	31	Al Daayen	QAT.2
7	Umm al-Qaywayn	ARE.7	32	Al Khor	QAT.3
8	Capital	BHR.1	33	Al Wakrah	QAT.4
9	Central	BHR.2	34	Ar Rayyan	QAT.5
10	Muharraq	BHR.3	35	Madinat ash Shamal	QAT.6
11	Northern	BHR.4	36	Umm Salal	QAT.7
12	Southern	BHR.5	37	‘Asir	SAU.1
13	Al Ahmadi	KWT.1	38	Al Bahah	SAU.2
14	Al Farwaniyah	KWT.2	39	Al Hudud ash Shamaliyah	SAU.3
15	Al Jahrah	KWT.3	40	Al Jawf	SAU.4
16	Al Kuwayt	KWT.4	41	Al Madinah	SAU.5
17	Hawalli	KWT.5	42	Al Quassim	SAU.6
18	Mubarak Al-Kabeer	KWT.6	43	Ar Riyad	SAU.7
19	Ad Dakhliyah	OMN.1	44	Ash Sharqiyah	SAU.8
20	Al Batinah North	OMN.2	45	Ha’il	SAU.9
21	Al Batinah South	OMN.3	46	Jizan	SAU.10
22	Al Buraymi	OMN.4	47	Makkah	SAU.11
23	Al Dhahira	OMN.5	48	Najran	SAU.12
24	Al Wusta	OMN.6	49	Tabuk	SAU.13
25	Ash Sharqiyah North	OMN.7			

Table 3.2: List of sea regions selected through the regionalisation process together with their identification code

ID	Region name	Code
1	Kuwaiti part of the Persian Gulf	KWT.1p
2	Saudi Arabian part of the Persian Gulf	SAU.1p
3	Bahraini part of the Persian Gulf	BHR.1p
4	Qatari part of the Persian Gulf	QAT.1p
5	Saudi Arabian part of the Persian Gulf	SAU.2p
6	United Arab Emirates part of the Persian Gulf	ARE.1p
7	Omani part of the Gulf of Oman	OMN.1o
8	United Arab Emirates part of the Gulf of Oman	ARE.2o
9	Omani part of the Gulf of Oman	OMN.2o
10	Omani part of the Arabian Sea	OMN.3a
11	Saudi Arabian part of the Red Sea	SAU.3r

3.2 Land eligibility analysis methodology

In the previous section, 60 sociopolitical regions have been identified overall for land and sea in the GCC area. Now, the method will be discussed which was used to assess which portions of these regions are eligible for the installation of one or more technologies among the selection under exam, namely open-field PV panels and onshore and offshore wind turbines. To achieve this goal, land and sea exclusion criteria are identified with the help of existing literature. Following this step, computational tools are used to obtain GIS files containing the placements for VRES parks.
For the sake of brevity, we will often refer to the land and sea eligibility analysis only as LEA, therefore extending the meaning of the word "land" to the entire land and sea area covered by the GCC countries.

3.2.1 Land and sea eligibility constraints

The LEA is a very important step for the analysis of renewable energy systems [70]. However, chapter 1 already mentioned the fact that no study has been published featuring an exhaustive LEA of the whole GCC area. The reason for this should not be searched in the region under exam itself: as illustrated by the authors of the study "Evaluating land eligibility constraints of renewable energy sources in Europe" [70], the definition of LEA constraints in general was not sufficiently explored by previous literature. This means that even though multiple studies contain examples of LEA for VRES, there was no omni-comprehensive framework of land eligibility criteria until the publication of their research [70]. Building on the work of Ryberg et al., Caglayan et al. expanded the list of constraints to account for marine regions as well [6].

As their work comprehends almost all LEA contraints in a very-well organised way for both onshore and offshore regions, the models of Ryberg [70] and Caglayan [6] are chosen as the main source for the methodology adopted in this study. Therefore, some clarifications are immediately required. In fact, the LEA conducted by the authors is applied only to Europe. However, Ryberg has made sure to define its constraints in such a way that their definition remains valid in all other regions of the world. For example, the exclusion of too inclined terrains through the slope angle can be applied to the countries in Europe as well as everywhere else. In the same way, Caglayan used the same approach when creating her offshore LEA framework.

Even though the identified LEA frameworks are found valid irrespective of the geographical location under consideration, a few adjustments are needed when applying them to the Arabian Peninsula. This is true for two main reasons: 1) the lack of some (very few) potential constraints from the chosen frameworks and 2) the need of increasing the land exclusion associated to some constraints due to local macro-environmental factors. In practice, this last point consist in changing the so called "buffer" around the areas excluded. In fact, each exclusion criterion translates not only in an area that is identified as unfit for VRES installation, but also in a buffer around it which is also excluded from the energy potential calculations.

The exact decisions taken to implement and slightly change the eligibility framework of Ryberg and Caglayan will be discussed in this subsection one technology at a time. Before that, the entirety of the constraints considered is presented in Table 3.3. Overall, 41 constraints are used to assess land eligibility in GCC countries. According to the definitions of Ryberg, they are divided in four groups: sociopolitical, physical, conservation and economic. Sociopolitical criteria exclude regions where installation would be physically possible, but impossible in practice due to elements related to human societies and their activities or creations. A similar rule is used for the category "conservation", where installations are forbidden due to environmental constraints, including landscape, flora and fauna conservation. This is radically different from the criteria category "physical", where the very characteristics of the land make installation of VRES impossible. Finally, economic constraints limit the overall potential by excluding regions where VRES are surely economically inefficient. The table also shows the name of the data sources where geographical information was taken from according to each criterion. This can be easily accessed since they are all publicly available.

It should be noted that some differences are visible with respect to the original framework of Ryberg. First of all, two sociopolitical constraints (military areas and borders) are added as suggested by Heuser [123]. These criteria are found particularly suitable for the current case given the political tensions mentioned in section 2.3. Two more sociopolitical constraints are also deemed necessary following the considerations made there regarding contested regions (notably Yemen) and strategic regions (shipping choke points). Since whole regions are identified by these constraints, these are simply excluded *a priori* from the study, meaning that no LEA is conducted on them, as it has been already mentioned in the previous section and in chapter 2. In

fact, this allows to focus on the effect of ineligibility constraints in areas where the actual feasibility of VRES installations is not known in advance. Finally, the criterion "historical sites" is added to the list to better match the keywords of the OpenStreetMap (OSM) database.

Table 3.3: List of all land eligibility criteria applied to the Arabian Peninsula, together with the database on which they are based

Type	Nr.	Exclusion Criterion	Technology			Data source
			Open-field PV	Onshore wind	Offshore wind	
Sociopolitical	1	Urban settlements	x	x		GHSL [124]
	2	Rural settlements	x	x		GHSL [124]
	3	Airports	x	x		OF; OSM [125, 126]
	4	Primary roads	x	x		OSM [126]
	5	Secondary roads	x	x		OSM [126]
	6	Agricultural areas	x	x		CCI-LC [76]
	7	Railways	x	x		OSM [126]
	8	Power lines		x	x	METN; SCM [127, 128]
	9	Historical sites	x	x		OSM [126]
	10	Recreational areas	x	x		OSM [126]
	11	Leisure & Camping	x	x		OSM [126]
	12	Tourism	x	x		OSM [126]
	13	Industrial areas	x	x		OSM [126]
	14	Mining Sites	x	x		OSM [126]
	15	Oil&Gas pipelines		x	x	ME-OGFM [80, 129]
	16	Military areas	x	x		OSM [126]
	17	Borders	x	x	x	GADM, IEI [99, 116]
	18	Marine shipping routes			x	CHI-RSD [130]
	19	*Contested regions*	x	x	x	GADM, IEI [99, 116]
	20	*Strategic regions*			x	GADM, IEI [99, 116]
Physical	19	Slope (general)	x	x		SRTM [131]
	21	Elevation	x	x		SRTM [131]
	22	Lakes	x	x		OSM [126]
	23	Rivers	x	x		OSM [126]
	24	Coast	x	x	x	GADM [116]
	25	Woodlands	x			CCI-LC [76]
	26	Wetlands	x	x		CCI-LC [76]
	27	Salt Flats		x		DSMW [132]
	28	Moving sand / Sand dunes	x	x		DSMW [132]
	29	Water depth			x	GEBCO [133]
Conservation	30	Habitats	x	x	x	WDPA [134]
	32	Biospheres	x	x	x	WDPA [134]
	33	Wildernesses	x	x	x	WDPA [134]
	34	Bird areas		x	x	WDPA [134]
	35	Landscapes	x	x	x	WDPA [134]
	36	Reserves	x	x	x	WDPA [134]
	37	Parks	x	x	x	WDPA [134]
	38	Natural monuments	x	x	x	WDPA [134]
Econ.	39	Slope (northward)	x			SRTM [131]
	40	Global horizontal irradiation	x			GWA [3]
	41	Wind speed at 100m		x		GSA [2]

As for the physical criteria, the original "ground composition" criterion is here translated specifically into "moving sand or sand dunes", since sand areas are not excluded as a whole, and into salt flats. These criteria are then added to the list in place of the original, which only defines unstable ground in general terms. Such clear breakdown of the "ground composition" criterion allows the use of the authoritative Digital Soil Map of the World (DSMW) database to implement it, which will be described later in more detail. Moreover, the northward slope criterion is moved to the economic constraints group as deemed more appropriate. The solar irradiation criterion is kept, even though the Global Solar Atlas (GSA) clearly shows that no area falls below the minimum GHI recommended value of 1070 kWh/(m^2year) [2].
However, the most important difference with respect to the original framework of Ryberg is the absence here of two economic constraints, namely electricity grid connection and road access. The main reason put forward for this choice is that the evolution of the electricity and transport infrastructure from here to 2050 cannot be predicted with certainty, while the use of these constraints strongly impacts the results of the LEA. Therefore, applying these constraints risks to wrongly reduce the potential of VRES in the region by a considerable amount. In fact, it is desirable that the results found in terms of VRES potential are as generally valid as possible, which would not be the case once the current grid and road system are taken into account for the connection and access constraints.

What is more, the choice of a unique constraint in terms of distance of any energy installation to the grid risks to be inaccurate no matter its value. In fact, the economic viability of the connection distance depends on how cheaply electricity can be produced at the site, which cannot be known in advance. Besides, it could be the case that dedicated connection roads or lines are created for VRES installations with particularly low values of LCOE or for other reasons. About the electricity grid in particular, energy-intensive industrial facilities could also be directly constructed close to isolated areas to avoid the need for connection lines.

It is now possible to more thoroughly discuss the exact methodology applied for some of the different eligibility criteria for each technology, starting from open-field PV.

Open-Field PV

For open-field PV, the buffer for each criterion is derived either from Ryberg [119,135] or from Heuser [123]. Besides, Ryberg's [135] coverage factor describing the actual specific peak power of open-field PV is also applied in this case. In fact, the resolution of 100 m chosen for the LEA means that smaller geographical elements may be not be detected and excluded by the analysis, so that Ryberg's conservative value fits the present case as well.

The main modelling decision to be taken in this case is that regarding sand areas. In fact, chapter 2 has already shown that a great portion of the Arabian Peninsula is covered by deserts or areas with a considerable amount of sand. A simple approach could be to exclude all areas where sand is found. However, this would not be correct. In fact, there exist solar farms which are not only located in sandy areas, but also subject to sand storms, for example the Bahdla solar park, which is installed in the Indian region of Rajastan [136]. Consequently, for these areas as well as for the whole territory of the Peninsula, increased operational costs may have to be considered to account for the more frequent need of cleaning services, without which the panels' efficiency could drop by as much as 50% [137]. However, the next section shows that these extra cost do not necessarily occur.
Sand areas, however, are not all eligible for the analysis. In fact, moving sands or sand dunes do not offer a stable enough surface for the installation of solar technologies [138]. Accordingly, this type of ground is identified by the filtering keys of the DSMW database by the Food and Agriculture Organization and then excluded using the same buffer as in Kevin et al. [139], even if this buffer was originally referred to solar thermal installations. In fact, if the buffer is safe for solar thermal installations when it comes to ground instability, it is more so for PV installations, which are lighter since they do not rely on heavy pipes filled with hot fluid (often molten salts).

Salt flats are another constraint. In the case of PV, however, it was not possible to find any source explicitly advising against this type of ground for the installation of the technology. Besides, some parks exist located close to salt flats, such as the Cauchary solar farm in Argentina [140]. Hence, salt flats are not considered in the LEA for open-field PV.

Finally, it is important to notice that the ineligibility attribute is applied not only to already cultivated fields, but to all fertile areas in general, in order to take into account the scarcity of fertile regions in the GCC

area and the consequent land competition issues between VRES installations and agriculture (section 2.2). Besides, the buffer distance for agricultural areas is increased to 1000 m from the original value of 0 m used by Ryberg [135]. This buffer is chosen to be the same as that Ryberg used for rivers, as water is subject to the same scarcity problems just mentioned. The higher buffer allows to compensate for errors that might arise from the land classification of the chosen database, and to include areas around cultivated fields which are not cultivated but necessary for cultivation-related activities (transit zones, small containers, etc.). In fact, it is better to have a positive margin of error here rather than a negative one in order to make sure that the potential land usage of the agricultural sector is not underestimated. This increase in the buffer distance will not be considered for onshore wind installations, as they impact land usage way less than PV. As will be shown in chapter 5, this assumption increases the impact of agricultural land exclusions from 1.4% to 4.7% of the total, with a strong impact particularly in the smallest regions of Kuwait and Bahrain, where agricultural land exclusions rise from from 20% up to 70% of their associated region.

All these considerations lead to the creation of Table 3.4, where the buffer for each exclusion criterion for PV is reported together with the reasoning behind it. Overall, 32 criteria are adopted. In particular, the criterion "contested regions" here only refers to the exclusion of Yemen from the eligible areas. The buffer distance for this criterion is chosen to be the same as the the buffer for national borders of Heuser [141], which means that the buffer areas excluded by these two criteria coincide.

Onshore wind

As already anticipated, in the case of onshore wind it is possible to extract the vast majority of buffer values from Ryberg [119]. Still, some few items have to be derived from Heuser [123] or Caglayan [6], as was already the case for PV.

Although almost all buffers are different, similarities with the methodology used for PV can be found. First, the fact that moving sands and sand dunes are considered as ineligible areas for the installation of wind farms due to land instability reasons. This is even more true in this case, given the higher weight of this technology with respect to PV. The buffer is once again taken from the buffer for solar thermal technologies. In fact, heavy towers can be found both in wind farms and solar thermal plants (heliostats), so that the same buffer should apply to both. Sand areas that do not fall in these categories are classified as eligible as it happened for PV, as the Dhofar wind farm in Oman shows that wind turbines such as those of General Electric can be effectively placed in these regions [142]. Secondly, the fact that agricultural areas are excluded from the analysis, thus adopting a more conservative approach than that of Ryberg, which is necessary also in this case because of the land competition issues already mentioned for PV and better described in section 2.2. Chapter 5 shows that this assumption leads to an overall land exclusion of 1.4% in the GCC area and of maximum 20% in some small regions of Kuwait and Qatar and in one region of Saudi Arabia.

However, some important differences are present for onshore wind with respect to open-field PV, notably the presence of more constraints: oil&gas pipelines, power lines and salt flats, whereas the economic exclusion criterion is wind speed and not northward slope.

As for oil&gas pipelines, up-to-date georeferenced maps showing these elements are not available for free. The best source publicly available in this sense is the ArcGIS website, which reports the same map of the authoritative source already mentioned in subsection 2.3.5 [80] in a suitable georeference system. The map cannot be downloaded, so a screenshot must be taken and then the map must be then again manually georeferenced. This allows for pipelines to be drawn manually with good precision. On the negative side, the map is updated only to 2007.

As for the salt flats additionally included in the list of exclusion criteria, these are found as inappropriate for the construction of heavy systems such as wind turbines. In fact, Kevin [139] indicates this type of ground as ineligible even for solar thermal technologies, also offering an exclusion buffer for salt flats. The same approach is adopted here for wind turbines, as similar weights can be reached by these two technologies, as explained earlier.

To summarise all the points just made, Table 3.5 reports all 35 exclusion criteria adopted for the onshore wind LEA together with their buffer and the reference used. Also in this case, the only contested region is that of Yemen, whose buffer is identical to that of the "Border" criterion also included, as explained earlier for PV.

Table 3.4: List of all exclusion criteria adopted for the open-field PV LEA, together with the corresponding buffer value and the methodology used to determine it

Type	Nr.	Exclusion Criterion	Buffer		Rationale a/o reference for buffer
Sociopolitical	1	Urban settlements	200	m	[135]
	2	Rural settlements	200	m	[135]
	3	Airports	0	m	large airports [135]
	4	Primary roads	300	m	onshore wind equivalent [119]
	5	Secondary roads	200	m	onshore wind equivalent [119]
	6	Agricultural areas	1000	m	rivers [135] due to WEF-nexus
	7	Railways	200	m	onshore wind equivalent [119]
	8	Historical sites	1000	m	tourism [135]
	9	Recreational areas	1000	m	tourism [135]
	10	Leisure & Camping	1000	m	[135]
	11	Tourism	1000	m	[135]
	12	Industrial areas	300	m	onshore wind equivalent [119]
	13	Mining sites	200	m	onshore wind equivalent [119]
	14	Military areas	1000	m	[123]
	15	Borders	500	m	[123]
	16	*Contested regions*	500	m	borders [123]
Physical	17	Slope (general)	>10	°	[135]
	18	Elevation	1750	m	[135]
	19	Lakes	1000	m	[135]
	20	Rivers	1000	m	[135]
	21	Coast	1000	m	[135]
	22	Woodlands	0	m	[135]
	23	Wetlands	1750	m	[135]
	24	Moving sand / Sand dunes	4000	m	solar thermal equivalent [139]
Conservation	25	Habitats	500	m	[135]
	26	Biospheres	500	m	[135]
	27	Wildernesses	500	m	[135]
	28	Landscapes	0	m	[135]
	29	Reserves	500	m	[135]
	30	Parks	0	m	[135]
	31	Natural monuments	1000	m	[135]
Econ.	32	Slope (northward)	>3	°	[135]
	33	GHI	<1070	$\frac{\text{kWh}}{\text{m}^2\text{year}}$	[135]

Table 3.5: List of all exclusion criteria adopted for the onshore wind LEA, together with the corresponding buffer value and the methodology used to determine it

Type	Nr.	Exclusion Criterion	Buffer		Rationale a/o reference for buffer
Sociopolitical	1	Urban settlements	1200	m	[119]
	2	Rural settlements	800	m	[119]
	3	Airports	5000	m	large airports [135]
	4	Primary roads	300	m	[119]
	5	Secondary roads	200	m	[119]
	6	Agricultural areas	0	m	[123] due to WEF-nexus
	7	Railways	200	m	[119]
	8	Power lines	200	m	[119]
	9	Historical sites	1000	m	tourism [135]
	10	Recreational areas	1000	m	tourism [135]
	11	Leisure & Camping	1000	m	[119]
	12	Tourism	1000	m	[119]
	13	Industrial areas	300	m	[119]
	14	Mining sites	200	m	[119]
	15	Oil&Gas pipelines	500	m	offshore wind equivalent [6]
	16	Military areas	1000	m	[123]
	17	Borders	500	m	[123]
	18	*Contested regions*	500	m	borders [123]
Physical	19	Slope (general)	>17	°	[119]
	20	Elevation	2000	m	[119]
	21	Lakes	400	m	[119]
	22	Rivers	200	m	[119]
	23	Coast	1000	m	[119]
	24	Wetlands	0	m	[119]
	25	Salt flats	2000	m	solar thermal equivalent [139]
	26	Moving sand / Sand dunes	4000	m	solar thermal equivalent [139]
Conservation	27	Habitats	200	m	[119]
	28	Biospheres	0	m	[119]
	29	Wildernesses	0	m	[119]
	30	Bird areas	1000	m	[119]
	31	Landscapes	0	m	[119]
	32	Reserves	0	m	[119]
	33	Parks	0	m	[119]
	34	Natural monuments	500	m	[119]
Econ.	35	Wind speed at 100m	<4	m/s	[119]

Offshore wind

The majority of exclusion criteria and buffer values used for this technology are taken from Caglayan [6]. Applying her methodology in this case presents some difficulties. First and foremost, related challenges lie in the lack of a ready-made database not only for the oil&gas pipelines (as is the case of onshore wind), but also for the power lines and the shipping routes in the maritime regions here considered. The procedure already discussed in this section, consisting in georeferencing and then manually drawing all the lines of an existing map has to be repeated in this case, with the additional challenge of many submarine cables being close to each other.

The LEA is made more complete by adding the "Borders" constraint, which is absent in the analysis of Caglayan but reported in Heuser [123] for onshore wind. In fact, borders are strategic geographic areas not only onshore but also offshore. Besides, a sea area reported as object of conflict among three GCC countries is also excluded from the available regions as was done for Yemen. Finally, the Strait of Hormuz, identified as a strategic region in section 2.3, is immediately removed from the eligible areas through the new constraint "Strategic regions".

To summarise, Table 3.6 contains all information on the exclusion criteria used for offshore wind, namely type of criterion, buffer and reference used to derive it. It should be noted that in this case, all conservation constraints except for that of bird areas are summarized in the criterion "Protected areas" , following the example of Caglayan [6]. Effects of LEA constraints in contested and strategic regions will not be studied, as these regions are simply removed from the analysis, as anticipated in section 3.1.

Table 3.6: List of all exclusion criteria adopted for the offshore wind LEA, together with the corresponding buffer value and the methodology used to determine it

Type	Nr.	Exclusion Criterion	Buffer		Rationale a/o reference for buffer
Sociopolitical	1	Power lines	500	m	[6]
	2	Oil&Gas pipelines	500	m	[6]
	3	Marine shipping routes	3000	m	[6]
	4	Borders	500	m	onshore wind equivalent [123]
	5	*Contested regions*	500	m	borders [123]
	6	*Strategic regions*	500	m	borders [123]
Physical	7	Coast	15000	m	[6]
	8	Water depth	<1000	m	[6]
Conservation	9	Protected areas [1]	3000	m	[6]
	10	Bird areas	5000	m	[6]

3.2.2 Modeling and implementation in GLAES

Having identified all exclusion criteria that need to be applied during the LEA and once all the necessary databases are collected, the phase of implementation begins. A fully programmatic approach is adopted by making use of the computational tool called Geospatial Land Availability for Energy Systems (GLAES) developed by Ryberg et al. [70]. The model, written in Python 3 language, is open-source and can be downloaded online [70], while all of its dependencies are also open-source. Besides, GLAES is built on top of two well known tools: GDAL [143] and SciPy [144]. Due to these libraries, GLAES is able to process many types of different geospatial files, which proves particularly helpful in this case.

The starting point of the workflow followed by GLAES consists in the input of the geometry on which exclusions will be run. Shapefiles containing the regions identified in section 3.1 as vectors are loaded in the program one at a time in a loop. As already anticipated when discussing the regionalisation step, the files are loaded from the GADM database [116] using a LAEA reference system having its origin in the center of Saudi Arabia, which allows to study each region individually respecting its geagraphical dimensions and

[1] Includes all exclusion criteria of the conservation group (nr. 25-31) of Table 3.3, excluding bird areas

overall area. The pixel resolution for the geospatial file used is 100m, meaning that each pixel has an area of 1 km^2.

The following step of the workflow consists in the exclusion of the first criterion. A georeferenced data source is input containing the element to be excluded either in the form a vector (typically a .shp fle) or in the form of a raster (typically a .tif file). This is first converted into the reference system of the region under exam, then a boolean matrix is created on top of it, each cell representing a pixel of the region. The matrix is initially filled with "True" values (ones), meaning that the area is all available. Then, if the data source input is a vector file, the user must specify the attributes common to the elements to exclude from the region and present in the file. On the other hand, if the data source comes in the form of a raster image, the user has to specify the scalar values associated to the pixels that have to be removed from the available land. For example, in the case of a topographic map showing ground elevation, the user can remove all pixels/areas above a threshold value of altitude. In addition, an exclusion buffer can be added around the ineligible area elements. Following these specifications, GLAES changes to "False" (zeros) the values of the cells of the boolean matrix associated to the area elements identified as ineligible. This process is well represented in Figure 3.2.

The first exclusion terminates when the whole data source has been analysed and applied to the boolean matrix. Then, the process starts over for the following constraint: a new data source is added, and a new matrix is created. The combined effect of this and the previous matrix can easily be obtained by multiplying the elements of the first and the second matrix element-wise. GLAES thus accounts for multiple ineligibility criteria which can sometimes overlap. For illustrative purposes, the visual representation is offered in Figure 3.3 of the combined effect of the "airports" and "pipelines" exclusions in a portion of region QAT.4 in western Qatar.

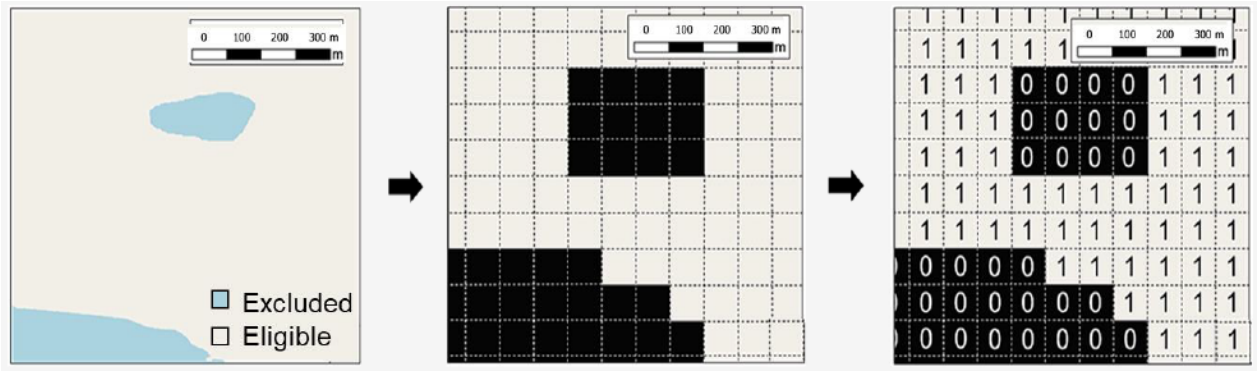

Figure 3.2: Creation process of the exclusion Boolean matrix operated by GLAES [145]

This process is repeated iteratively for any additional constraint until all exclusion criteria have been accounted for. Finally, a raster image is created from the boolean matrix representing the eligible land in the region. As an example, figure Figure 3.4 illustrates the final result of the exclusions operated by GLAES for region QAT.4 in Qatar in the case of onshore wind turbines. The two values coming from the boolean matrix are translated into black ("False": no availabily) and white ("True": available). The two airports shown in Figure 3.3 are displayed also here in brown to allow a comparison with Figure 3.3, but they are not an output of GLAES.

With the creation of the final image representative of the eligible and ineligible land, the LEA can be considered finished. GLAES can also offer the values of eligible and ineligible land, so that valuable information is retrieved at the end for postprocessing purposes. Furthermore, there is another important step that is performed by GLAES: the placement of VRES in the available areas identified. In the case of solar farms, the shape of the farms is typically in between that of a square and circle, so that they can effectively cover all the area available, while the separation distance is calculated considering the center of contiguous parks. This distance is set to around 1 km, so that the typical PV farm is associated with a capacity of 50 MW, according to Ryberg's coverage factor (more details on this factor are given in section subsection 3.3.1) [135]. The value of 50 MW is chosen to be 50% more than the current average size of a solar farm in the Middle East (34 MW in 2015) [146], as it has been shown that larger solar farms are becoming more and more frequent

all over the world [147]. Besides, in this study the PV farms with areas below 0.10 km^2 (i.e. approximately 5 MW) are discarded. Few solar farms today are in fact below 0.05 km^2 [148], and again the tendency to build larger farms should be considered [147].
The placement of wind farms is less straightforward. In fact, following the approach of Jäger [149], Ryberg [135] suggests considering a higher distance between turbines in the main wind speed direction for the area of the placement, whereas a lower buffer is used in the perpendicular direction to the one just described . Therefore, for onshore wind farms a value of 8 times the rotor diameter is used in the main wind speed direction, while the perpendicular distance is only 4 times the rotor diameter. For offshore wind farms, the two buffers considered are 10 and 4 times the rotor diameter respectively, as in the model of Caglayan [6].

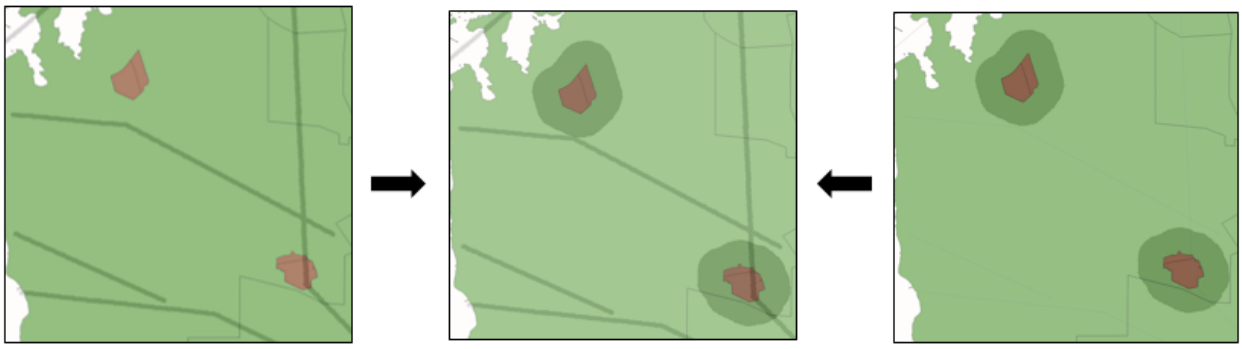

Figure 3.3: Combination process of the effects of two different exclusions criteria (airports, pipelines) on a portion of QAT.4 operated by GLAES

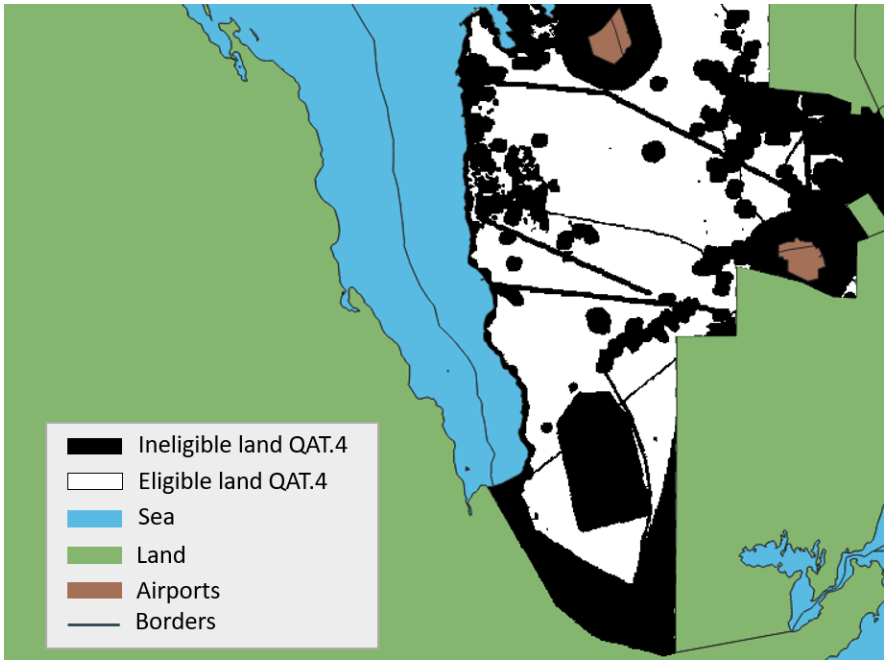

Figure 3.4: Image created by GLAES as a final result of the onshore wind LEA conducted on QAT.4. Airports and surrounding regions are reported as well for geographical reference

To complete the overview of the workflow of GLAES, Figure 3.5 shows the placements of solar farms and onshore wind farms in the form of vector geometries for the region of Qatar already used in Figure 3.4 and 3.3. Once again, the two airports in the region are also represented to offer the reader a geographical reference.

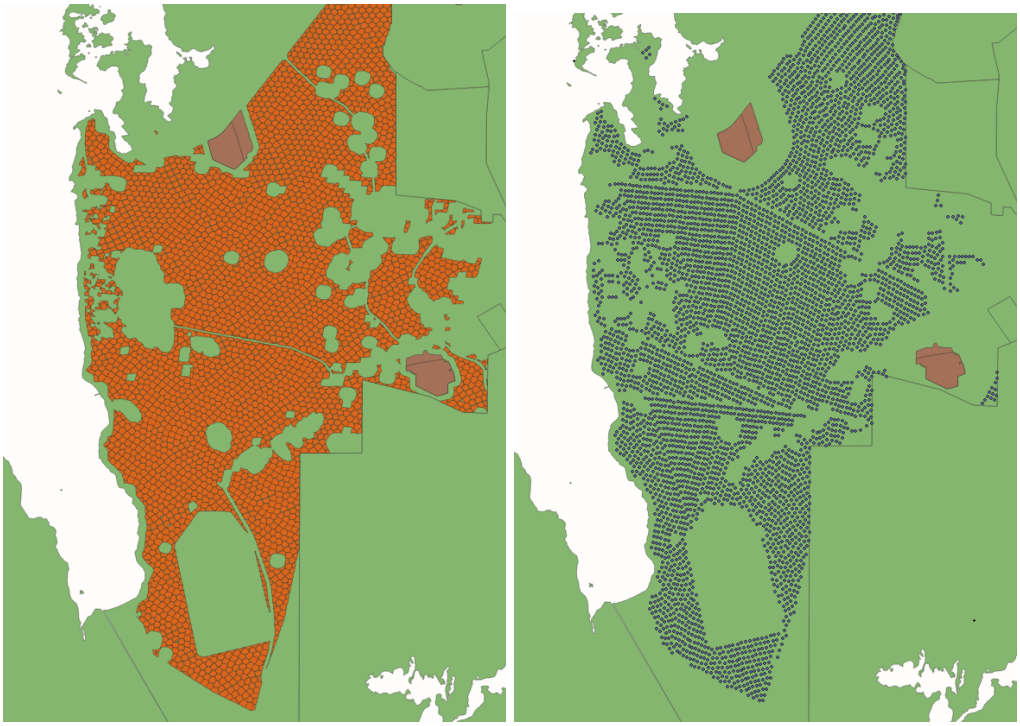

(a) Solar farms **(b)** Wind farms

Figure 3.5: Placement of VRES technologies in QAT.4 operated by GLAES after the LEA. Airports and surrounding regions are reported as well for geographical reference

3.3 VRES analysis methodology

In order to assess the potential for VRES in the GCC countries, two main steps are needed. First of all, the choice of appropriate solar and wind technologies to be installed in the eligible locations, which is described in subsection 3.3.1. Secondly, the implementation of physical models that can combine the techno-economic parameters previously defined with weather data to derive the energy potential for each installation. These models are described in subsection 3.3.2. In each subsection, the same order will be followed which was used earlier in this chapter to present the methodology for the LEA; this means that open-field PV will appear first, followed by onshore wind and finally offshore wind.

3.3.1 VRES technologies

The current subsection is aimed at explaining the choice of VRES technologies, whose most relevant techno-economic parameters will also be presented. The process always consists in deriving a baseline reference technology from available literature or datasheets and then projecting it to 2050 in the ways that will be described.

Open-field PV

In order to identify a suitable future open-field PV technology for European countries, Ryberg [135] starts by performing a simulation with a very large selection of current PV modules over multiple locations scattered across the continent, using the workflow that will be described in the following subsection. One module outperforms the others in all locations: the WSx-240P6 by Winaico [150]. As this holds true also for the hot and dry parts of Europe, the WSx-240P6 is considered for the GCC area as well. However, more considerations are necessary before concluding that this module is indeed a good choice for the Arabian Peninsula and before describing how its techno-economic parameters are projected to the year 2050.

To begin with, the WSx-240P6 uses polycrystalline sylicon. In general, this should indeed be preferred over monocrystalline sylicon in the case the system is not size-constrained, due to its lower costs per kW_p [151]. In the specific case of the Peninsula, though, two more elements should be accounted for when choosing the PV technology. One is the large presence of sand, and thus of dust, whereas the second is the high average temperature registered over the year. These characteristics have already been described in subsection 2.3.1. While polycristalline silicon is subject to lower efficiency losses at higher temperatures than multicrystalline one [152], it suffers less from efficiency losses in dusty environments [153]. Since transmittance losses due to soiling can exceed 50% in only 4 months of dust exposure without cleaning [154], priority is given here to dust-related concerns. This decision, together with the lower cost of polycrystalline cells, confirms the choice of the WSx-240P6 module.

Once the reference module is identified, some of its parameters must be projected to the year 2050 examined in this study. This is done following the projections of Fraunhofer ISE [155]. This source is very authoritative and offers different scenarios to choose from. In particular their so called "conservative" scenario is adopted here as done by Ryberg to make sure not to overestimate open-field PV potential. In this way, the values for Capital Expenditures (CAPEX), Operating Expenses (OPEX) and efficiency under PV USA Test Conditions (PTC) reported in Table 3.7 are obtained. Accordingly, the theoretical ground coverage factor would be of 4.17 m^2/kW_p. However, this value must then be corrected due to the fact the modules are distanced to reduce self-shading and allow maintenance, but also that auxiliary elements are required for the installation of a PV farm (access roads etc.). Besides, an additional increment of the coverage is needed to account for the exclusion of some features (smaller roads, individual buildings etc.) from the LEA which were too small compared to the resolution value of 100 m used. As indicated by Ryberg [135], the final coverage becomes 20 m^2/kW_p. All other technical parameters, such as temperature-related coefficients, are directly taken from the specifications reported by Winaico and so they are not reported here [150].

Table 3.7: Main techno-economic parameters of the open-field PV systems used for the VRES simulations

Parameter	**Value**
Module	Winaico WSx-240P6 [135, 150]
Technology	Polycrystalline [135, 150]
Efficiency (PTC)	24 [135, 155] %
Coverage (actual)	20 m^2/kW_p [135, 155]
CAPEX	500 €/kW_p [135, 155]
OPEX	1.7 %/a CAPEX [135, 155]
Economic lifetime	25 years [135]
Interest rate	8% [135]
Tilt angle	as from Equation 3.1 [135]
Azimuth angle	Due-south [135]

Moreover, some additional considerations should be made regarding the phenomenon of soling in relation to the value of OPEX. On the one hand, it is true that soiling increases the necessity of cleaning, which would imply an increase in maintenance costs [156]. On the other hand, the cost of labor in these countries is very low, which leads to reductions in the operational costs [157]. As these two phenomena impact CAPEX in opposite ways, its value is reasonably left unchanged.

Finally, system (or installation) design characteristics are also important for open-field PV simulations. Ryberg's analysis shows that for Europe, a fixed-tilt system is always more cost-efficient than a single- or dual-axis tracking system [135]. Following the same considerations made for the choice of the PV module, a fixed-tilt system is adopted here as well. In order to determine the optimal tilt of the PV modules, latitude of each PV farm is used following a simplified version of the model of Ryberg [135] according to Equation 3.1. As for the azimuth[2], this is not optimised but the south-oriented direction is used, as this is shown to be best option across a broad range of locations [158].

$$\text{tilt}\,[^\circ] = 42.3277 * \arctan(1.5 * |\,\text{latitude}\,[rad]\,|\,) \tag{3.1}$$

[2]Angular displacement between the north and the horizontal projection of the vector normal to the module

Onshore wind

In order to determine which turbine should be placed in each location, a future reference wind turbine is first defined in accordance to Ryberg [135], and then scaled depending on the local wind speed. For the type of wind turbine, an upwind three-bladed turbine is chosen, having horizontal axis and pitch control. The turbine taken as baseline (i.e. as "most common type") is the Vestas V136 [159]. This is a relatively new turbine but, as reported by Ryberg [135], its specifications should already fall within the ranges of common wind turbines by 2030.

The assumption that the V136 will actually be the baseline turbine by 2050 implies by itself that technological improvements are achieved without having to model them directly, which is a big advantage. In fact, the V136 would then replace the standard models of the present, which necessarily have poorer performance. Therefore, only cost improvements need to be modelled. In practice, the assumption on the future baseline turbine is implemented in the simulations by ensuring that a turbine with the exact specifications of the V136 is installed in all sites having the same wind speed registered at today's wind farms on average. Using a broad selection of wind farm installation sites, Ryberg finds this value equal to 6.7 m/s. [135]

The same selection of wind sites is used to correlate specific capacity and hub height of wind turbines installed there with the average wind speed registered at the site at 100 m of height, which is extracted from the Global Wind Atlas (GWA). The two fitting functions resulting from this process then allow to scale the hub height and capacity of the wind turbine depending on the site's wind speed, under the condition that the rotor diameter remains constant at the value of the baseline wind turbine (136 m). Ryberg [135] further modifies these functions to make sure that the values of the baseline V136 are returned if the wind speed value of 6.7 m/s is input in the equations. Besides, in order to keep the ground-to-blade-tip distance above 20 m, a lower constraint of 88 m is imposed on the hub height. The two design formulas are reported below in Equation 3.2 and 3.3.

$$\text{hub height}\,[m] = 1.240910 * exp(\,-0.849766 * ln(\text{wind speed}\,[m/s]\,) + 6.187994\,) \tag{3.2}$$

$$\text{specific capacity}\,[kW_p/m^2] = 0.900260 * exp(\,0.537690 * ln(\text{wind speed}\,[m/s]\,) + 4.749177\,) \tag{3.3}$$

In order to determine the cost of the onshore wind turbines used in this study, Ryberg [135] considers various sources and derives the final value of 1100 €/kW$_p$ for the CAPEX of the baseline turbine in 2050. To scale the CAPEX for different wind turbines, the National Renewable Energy Laboratory (NREL) models are used [160, 161]. The value of OPEX used by Ryberg is used here as well assuming that the cost of extra maintenance due to sand infiltration balances out the lower cost of labor. In the end, the techno-economic parameters of the baseline V136 turbine in 2050 and of the scaled onshore wind turbines are reported in Table 3.8. The actual values of the scaled design specifications will be presented later in the results of chapter 5.

Table 3.8: Main techno-economic parameters of the onshore wind turbines used for the VRES simulations

Parameter	Value - V136 projected to 2050	Value - scaled onshore turbine
Diameter	136 m [135, 159]	136 m [135, 159]
Hub height	120 m [135, 159]	as from Equation 3.2 [135]
Capacity	4.2 MW [135, 159]	as from Equation 3.3 [135]
CAPEX	1100 €/kWp [135, 159]	as from NREL models [135, 160, 161]
OPEX	2 %/a CAPEX [135]	2 %/a CAPEX [135]
Economic lifetime	20 years [135]	20 years [135]
Interest rate	8% [135]	8% [135]

Offshore wind

Similarly to the approach adopted by Ryberg [135], Caglayan [6] sets up a procedure to optimise the design of future offshore wind turbine based on defining a wind turbine for the year 2050 and scaling it according to local weather and physical parameters. Unfortunately, her model has not already been implemented in

the tool used for the simulations, so that it could not be used for the current study. Implementing it should be considered for future work on the topic, especially because it could also be used for different regions of the world. Here, the choice was made to install the baseline turbine identified by Caglayan [6] and reported in WindEurope [162] in all offshore locations, without optimising its design, since this option is not yet implemented in the existing tools.
However, the foundation type of the turbines is allowed to change according to water depth: monopiles and semi-submersible foundations are used if water depth is below or above 100 m respectively. In fact, these types of foundations are almost always shown to be cheaper than their respective alternatives: jacket and floating spars [6].

In order to make sure that the turbines employed in the model reflect future cost reductions, Caglayan [6] first finds the current costs of the turbines using the NREL [160, 161] cost models already mentioned for onshore wind with the addition of a more recent NREL offshore model [163] specifically for the Balance of System (BOS). In this case, water depth and distance from coast are the important cost variables, as they affect the cost of the BOS (which includes the foundation). Then, the costs are scaled to the CAPEX value of 2300 €/kW$_p$ of the chosen baseline offshore wind turbine [162], which is derived from literature studies projecting offshore wind turbine costs to the year 2050 [6], as considered here.

Table 3.9: Main techno-economic parameters of the offshore wind turbines used for the VRES simulations

Parameter	Value - WindEurope projected to 2050	Value - scaled offshore turbine
Diameter	212 m [6, 162]	212 m [6, 162]
Hub height	128 m [6, 162]	128 m [6, 162]
Capacity	13 MW [6, 162]	13 MW [6, 162]
Foundation	monopile [6, 162]	monopile or semisubmersible [6]
CAPEX	2300 €/kWp [6, 162]	as from NREL models [6, 160, 161, 163]
OPEX	2 %/a CAPEX [6]	2 %/a CAPEX [6]
Econ. lifetime	25 years [6]	25 years [6]
Interest rate	8% [6]	8% [6]

In this case, OPEX could indeed be reduced in order to account for lower labor cost. On the other hand, the use of a non-optimised wind turbine will already increase the average LCOE of the offshore installations and thus the OPEX value of 2% of CAPEX is left unchanged to counter-balance this effect.

3.3.2 Modeling and implementation in RESKIT

Now that a suitable selection of VRES technologies for the system under consideration has been identified together with their design specifications, it is essential to describe which physical models are used and how these are implemented in practice, which is the scope of this subsection. The modelling steps will be described separately for each technology, in the same order adopted for the previous subsection. For the computational simulations, the RESKIT is used [164]. Similarly to the tool employed for the LEA (GLAES), RESKIT is developed in Python 3 and publicly available. Apart from significant computational power required to handle weather data, VRES simulations necessarily rely on multiple lists of arrays of significant size. Besides, the temporal dimension must also be considered in addition to the spatial one. For these reasons, in addition to GDAL [143], the packages xarray [165] and netCDF4 [166] are also used by RESKIT. These and all other dependencies of the tool are publicly available.

When it comes to the actual workflows used for the both PV farms and wind turbines simulations, these consist of two high-level blocks, which are run in sequential order. First, the weather parameters are arranged in a way that effectively allows them to be used for the simulation of each VRES placement. In the second block, the adjusted weather data is input to the physical models. Without post-processing, the direct output of the simulations would be multidimensional netCDF files, one for each VRES placement. Each file would contain the geographical location of the placement, its design specifications and an hourly time series of the capacity factor for that specific turbine or PV farm (thus 8760 values overall). To derive the electricity feed-in time series for each placement, the capacity factors should simply be multiplied by its capacity. The workflows are valid for a single wind turbine or PV farm, but they can be applied to multiple technologies in parallel depending on the available computational power.

However, post-processing is required for multiple reasons. First and foremost, because the tool used to optimise the energy system later on does not accept netCDF files directly as input. Secondly, because assigning a degree of freedom to each individual wind turbine and PV farm would dramatically increase the computational time of the optimisation process. Therefore, placements must be somehow clustered, each cluster having a degree of freedom. In practice, this means that multiple turbines or PV farms will be modelled as a single "bigger" representative turbine or PV farm. The capacity of this representative technology is given by the sum of the capacity of all placements composing the group.
As with all simplifications, some information is inevitably lost in this process. However, this loss can be limited by employing an appropriate method for grouping. Here, two criteria are used. The first one is that grouping is based on the geographical proximity of elements. In other words, a maximum distance of 450 km is allowed between two placements within the same group. This ensures that the weather conditions discrepancies are reduced among the same group, which in turns implies similar design characteristics, as these depend only on the weather conditions at each location. In a second step, each spatial group is further divided according to the LCOE, with up to 11 potential clusters defined overall for each spatial group. In fact, under relatively similar weather conditions and design characteristics ensured by the same spatial group, placements showing similar LCOE are necessarily associated with similar capacity factors. This is because once the design has been assigned using weather sources, LCOE only depends on the capacity factor. In the way just described, VRES placements end up in the same cluster only if they show very similar design and time-series, which eventually reduces the impact of averaging.

As for the weather data sources employed, use is made mainly of the European Centre for Medium-Range Weather Forecasts Re-Analysis version 5 (ERA5) [167] dataset. The data provided by ERA5 is the output of a climate model, and not of direct measurements. Although this might imply a lower accuracy of the datasets, the advantages are the availability of a higher number of different weather variables and the possibility to adopt the same source at any latitude and longitude; besides, the need of pre-processing the weather data is also avoided, reducing computational time [135]. The ERA5 has a spatial resolution of 30 km and a time resolution of one hour over the years 1980 to the present, with a new release including the years 1950-1970 expected soon. In order to reduce computational time, data from the year 2015 was used for the simulations of this study. It should also be noted that since a different data source was used here with respect to that used by the creators of the original VRES models, the workflow had to be adjusted accordingly.
Moreover, two additional weather sources are used to a lower extent for onshore VRES simulations, namely the GWA and the GSA [2, 3]. For the purpose of these simulations, these offer long-run average values with a higher spatial resolution for the values of wind speed, DNI and Global Horizontal Irradiance (GHI). In particular, the GWA average covers the years 1998-2017 with a resolution of 270 m, whereas the GSA average was performed over the years 2007-2018 with a resolution of 1000 m.

It is now possible to delve deeper into the actual models used for the simulations. These have been already extensively described by Ryberg [135] (onshore VRES) and Caglayan [6] (offshore wind). Therefore, only the main steps are here explained.

Open-field PV

The simulation procedure adopted for open-field PV contains numerous steps, as shown in Figure 3.6 [135]. As with all VRES simulations in this work, two main sequential set of procedures are followed, namely the processing of weather data and the actual simulation of the technology [135]. The directions of the workflow in the case of the absence of DNI from the datasets or in the case of time-dependent tilt and azimuth are not discussed here, since for the current case DNI is available from ERA5 [167] and a fixed tilt is chosen.

For open-field PV simulations, the following parameters are read from the data source: northerly surface[3] wind speed, easterly surface wind speed, surface pressure, surface temperature, GHI and DNI. In addition to weather data, the location of the PV farm under exam should be input, together with the techno-economic parameters of the modules and of the system (the latter being tracking system, tilt and azimuth). [135]

The first operation run on the weather data is to process location, pressure and temperature to obtain zenith

[3] At 2 m of height

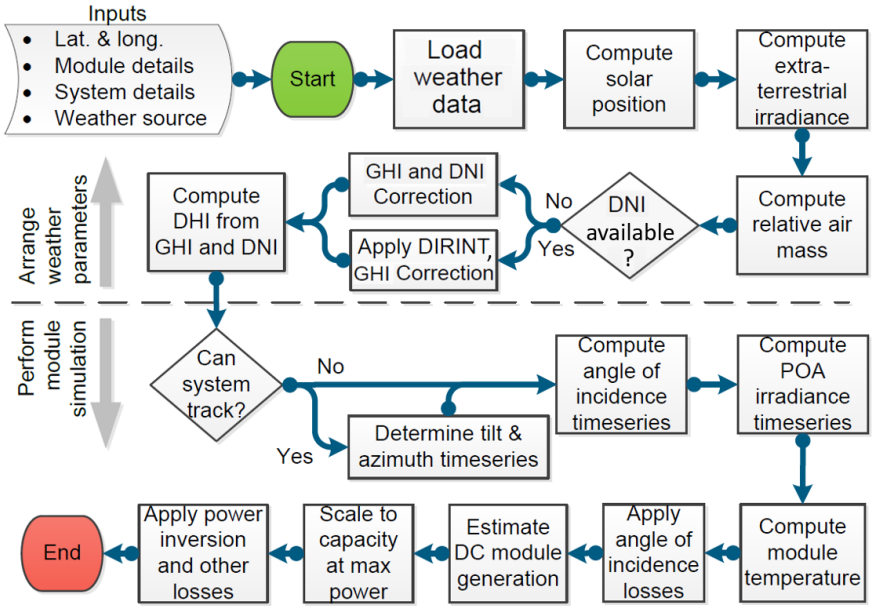

Figure 3.6: Workflow implemented for the simulation of each open-field PV in RESKIT. Adapted from Ryberg [135]

angle[4], solar altitude[5] and solar azimuth angle [6], which together determine the solar position, meaning the direction of the vector which connects the center of the Earth to the sun [135]. Here, terrain elevation is also required, so that the path to the EU-DEM elevation dataset is specified as well [168]. Then extra-terrestrial irradiance is computed using the solar constant (1367 W/m^2) and the hour of the year, while air mass is obtained in function of the zenith angle [135].

The next step is intended at adjusting the values of GHI and DNI to the GSA, which is characterised by a significantly higher spatial resolution. Therefore, the ERA5 irradiation time series are each multiplied with a factor which forces their yearly average value to be the same as the GSA long-run yearly average value. The corrected GHI and DNI are then combined with the zenith to return the Diffuse Horizontal Irradiance (DHI) values over the year. [135]

In order to compute the Plane of Array (POA) irradiance[7] it is first necessary to determine the time series of the angle of incidence of the direct sun beams on the modules of the PV farm. In the case of fixed-tilt, the time-series always contains the same value, which is the angle between the solar position and the vector normal to the module. Once this information is know, the three components of the POA can be determined. The direct POA component is found through zenith, incidence angle and DNI; the ground-reflected one through GHI, tilt angle and albedo (supposed constant at 0.2); finally, the sky-reflected component uses DHI, DNI, air mass, extra-terrestrial irradiance, zenith, angle of incidence and tilt angle. [135]

Before summing up the POA components, each is multiplied by a coefficient that accounts for transmittance losses, which ultimately depends on the angle of incidence, the angle of refraction (and so the refraction coefficients of air and glass through Fresnel's law) and the module coating's extinction coefficient and thickness (here assumed 4 m^{-1} and 2 mm respectively). The coefficients for the reflected components of POA, however, are estimated through the module's tilt with a simplified set of equations, as the use of the angle of incidence would require the integration over the whole sky or ground for each hour of the year, resulting in difficult and computationally demanding calculations, while not being the focus of this thesis. [135]

The final value of POA is then used in the following step, which is in its turn composed of two parts. First, the cell temperature is computed through air temperature, surface wind speed and POA. The POA and the

[4]Angular displacement between solar position vector and its vertical projection
[5]Angular displacement between horizon and sun. Complement of zenith angle
[6]Angular displacement between the north and the horizontal projection of the solar position vector
[7]Total irradiance hitting the surface of the PV module (plane of array). Since the PV modules are tilted, POA is different from GHI, which refers to the total irradiance hitting an horizontal surface (tilt = 0°)

value of cell temperature just found are then combined with the module's technical parameters to obtain the theoretical power production of the module in watts [135]. This is done according to the Single Diode physical model of De Toto [169], which has also been employed for some of the previous steps. The remaining part of this process simply consists in dividing the power just obtained by the rated power of the module, which returns the capacity factor [135].

At the end of the workflow, a loss correction factor of 18% is applied to the capacity factor which accounts for electrical and soiling losses. This value was obtained by Ryberg from literature for Europe, but it is also accepted here even if the environment is subject to a considerable amount of sand. In fact, it is supposed that the lower cost of labor allows for a more frequent cleaning, so that the same soiling losses are generated under the same OPEX costs, as explained in the previous subsection when describing the choice of the PV modules. [135]

In order to derive the electricity feed-in time series, the capacity factor of the PV farm should then be multiplied by the capacity of the PV farm. In turn, this can simply be obtained by the product of the PV farm's area and the coverage factor of 20 m^2/kW_p already discussed in the previous subsection as well. [135]

Onshore wind

In the case of onshore wind, the workflow is shorter, as reported in Figure 3.7 [135]. Besides, the design specifications input at the beginning of the workflow strictly depend on the individual technology (wind turbine), and not also on system (or installation) characteristics, as in the case of PV (tilt, azimuth and tracking strategy). In fact, the control mechanism is always the same (pitch-control) as well as the general set-up (three blades, upwind, horizontal axis) [135].

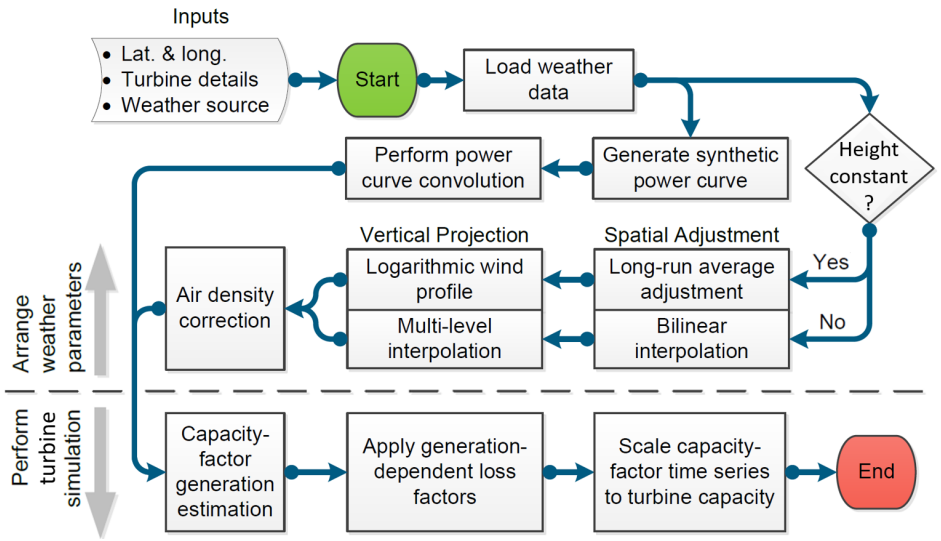

Figure 3.7: Workflow implemented for the simulation of each onshore wind turbine in RESKIT. Adapted from Ryberg [135]

Initially, the location of the turbine under examination is input together with its design characteristics, namely hub height, capacity and specific capacity, which is derived from the constant rotor diameter and capacity. At the same time, the relevant weather variables are loaded from ERA5. These are: northerly wind speed at 100 m, easterly wind speed at 100 m, Planet Boundary Layer (PBL) height, surface pressure and surface temperature. [135]

Two parallel steps follow next. The first one is aimed at adjusting the values of wind speed. If these are available always for the same height in the data source (as in the present case), then these are scaled with a constant factor ("long-run average adjustment") [135], so that their overall yearly average is the same as the long-run yearly average offered by the GWA, whose spatial resolution is higher [3]. Then, the wind speed is fitted to the hub height of the turbine through a logarithmic profile [135], using the roughness length

corresponding to the terrain type specified by the European Space Agency (ESA) [76]. The logarithmic law is however applied only until the PBL height should the hub height of the turbine exceed this value [135]. Finally, air density is corrected first by interpolating bilinearly with the neighbouring cells and then by taking into account the values of hub height, pressure and temperature, while ensuring the conservation of kinetic energy [135].

The second step happening parallel to wind speed adjustment is that of the creation of a power curve for the turbine specified. To be precise, this step is a sort of bridge between the arrangement of weather data and the simulations of the turbine, although it is reported in the first category since it is does not relate the technology with the weather data time series yet. First a so called "synthetic power curve" is generated depending on the specific capacity of the turbine. This is created based on the fitting curves applied to a large number of existing turbines and describing the relation between specific capacity, wind speed and capacity factor. According to Ryberg [135], new turbines being developed, such as the one used as baseline in his work and in the current one tend to have a lower specific capacity and hence higher full load hours. After this step, a Gaussian curve is convoluted around the synthetic power curve to account for the uncertainty of wind-related physical phenomena. In simpler words, as the actual power produced by a wind turbine fluctuates around the theoretical value of the synthetic power curve within a range of uncertainty (or error), an appropriate "smoothing" must be applied to the synthetic power curve to obtain results closer to the actual production of the turbine. The parameters of the Gaussian function are in turn found by comparing the actual and theoretical production of different wind farms. [135]

Once the weather parameters have been arranged and used to derive necessary information in the way just described, the corrected power curve and corrected wind speeds are combined to obtain the capacity factor (one for each hour of the year), which is found using the fitting curves already mentioned for the creation of the synthetic power curve: for each combination of specific power and wind speed, only one capacity factor exists. An additional correction must be implemented this time directly on the capacity factor, to account once more for power losses (turbulence and wake effects, turbine misalignment, power conversion and transport and others); this is done comparing real production data from different wind farms as already described. The last step is simply to multiply the corrected capacity factor time-series by the wind turbine capacity, so that the electricity feed-in time series is obtained. [135]

Offshore wind

The workflow adopted for offshore wind and developed by Caglayan [6] is a slight simplification of the onshore equivalent shown in Figure 3.7 [135]. Consequently, three main differences can be found. The first one is that, independent of the datasets available, bilinear interpolation is chosen to correct wind speed instead of the long-run average adjustment. This is because the GWA does not always contain values for some offshore locations, although this could be solved in future releases [3]. Secondly, the air density correction is not implemented, as Ryberg shows that it does not affect results significantly [135]. It should also be reminded that since no terrain type variations are registered offshore the same roughness length is used everywhere and equal to 0.0002 m [6].

4 | Energy System Model

This chapter presents the methodology adopted to design the Energy System Model (ESM) of the GCC countries for the year 2050, on which most of the research goals of this study depend. In order to study the system, a set of different scenarios have been created: these are first described in section 4.1. Then, section 4.2 describes how the different components of the system are modeled. It should be noted that deriving the generation potential and costs of fixed-tilt PV panels and wind turbines requires a considerable effort, which is why the previous chapter 3 is entirely dedicated to this purpose. Following the description of the system components, section 4.3 concludes this chapter by explaining the main characteristics of the optimisation process implemented in this work.

4.1 Scenarios design

This section describes the different scenarios designed to set up the ESM. In order to answer the research question regarding the behaviour of the ESM, three scenarios are deemed as essential, as they envisage three very different but relevant set of conditions for the operation of the ESM. Therefore, these scenarios, hereon called "main" scenarios, are analysed in depth in each of their system components. Furthermore, an additional category of scenarios is also created; differently from what has just been described, only a selection of their results is sufficient to answer the different research goals presented in chapter 1. The scenarios belonging to this second category are referred to as "functional" scenarios from here onward.

Of the three main scenarios, the cooperation scenario is the one that could be considered as the reference one, since it features the maximum flexibility that the system can rely on. In fact, cross-country exchange of energy commodities is allowed, while hydrogen demand is distributed over the territory and required in the gaseous form. In this as in all other scenarios, the amount of electricity demand is derived from the projections of the power sector for the year 2050 [170], while that of hydrogen from the projections of the transport [170–176], ammonia [45, 47, 48, 173, 177] and steel [52, 55, 61] sectors. The methodology adopted to obtain demand from various sources has already been described in subsection 4.2.5.

The other two main scenarios are built by varying some important aspects of the cooperation scenario. In particular, the isolation scenario sees the removal of powerlines and pipelines connecting different countries. This feature allows to observe the different layout of the system when flexibility is reduced by forbidding cross-country exchange; besides, the increase in costs due to the lack of international cooperation is also obtained.

Instead, the export scenario is the same as the cooperation scenario, but without the presence of local hydrogen demand. Instead, it envisions the concentration, liquefaction and export of hydrogen at three ports, which are supposed to be located in the regions of SAU.5, OMN.9 and ARE.1. The choice of the location of at least one port on both the Eastern and Western coasts of the Peninsula allows for shipping to Asia and Europe (or North-America) respectively avoiding to cross the dangerous Bab-el Mandeb strait. Similarly, the presence of two ports for Asian exports located in the Arab Emirates and Oman respectively allows the ships of the GCC to avoid the Persian Gulf should political tensions arise with Iran, who could threaten a block of the Strait of Hormuz. Given the potential costs reduction offered by converting existing oil&gas infrastructure to hydrogen purposes [109], the port of the Arab Emirates would be more economycally advantageous [80], but it would also force ships to cross the Strait of Hormuz. On the contrary, OMN.9 does not present this problem, although oil&gas infrastructure is not as developed as in the Gulf regions [80]. The geopolitical considerations influencing the decision of the location of the ports can be read in more detail in section 2.3. The region of SAU.5 is chosen over other regions neighbouring the Red Sea as it contains the majority oil&gas terminals present on the coast [80].
As for the technical characteristics of the system in this scenario, the amount of overall hydrogen demand is considered to be the same as the national hydrogen demand in order to allow for a more meaningful comparison with the cooperation scenario. In fact, considering both local and export demand would lead to a way higher amount of hydrogen demand than in the cooperation scenario. Besides, in this way it is possible to observe the effects on the system of concentrating high amounts of hydrogen demand in few selected locations. Using the projections regarding the destination markets of the oil&gas exports of the Peninsula [102], hydrogen exports are accordingly split as 20% to Western countries and 80% to Asia, which

is further evenly split in the two ports in ARE.1 and OMN.9. Contrarily to the method adopted by Heuser et al. [141], liquid hydrogen storage at the port is not considered due to safety considerations [178]. Instead, constant liquefaction is implemented together with gaseous storage. This last assumption further increases safety, since not all hydrogen necessarily needs to be concentrated in a single location.

In order to facilitate the understanding of the scenarios described so far and of those that will follow suit, Table 4.1 reports the main features defining each of the scenarios designed in this study. These are divided in the two macro-categories used to described them, namely the "main" and the "functional" group. The group of functional scenarios is typically built around one or two of the three main scenarios just described. For example, the electricity-demand and hydrogen-demand scenarios are the same as the export scenario in which hydrogen demand and electricity demand of the power sector respectively have been excluded from the system. Comparing their results with the export scenario, these two scenarios allow to observe the cost benefits of sector coupling. The export scenario is preferred over the cooperation scenario since a higher energy demand is needed because of the additional electricity demand due to liquefaction, which might lead to more benefits from sector coupling.

Table 4.1: Main features of the scenarios designed in this study

Type	Name of scenario	Electricity demand	GH2 demand	LH2 demand	Cross-country exchange	CAPEX variation
Main	Cooperation	x	x		x	
	Isolation	x	x			
	Export	x		x	x	
Functional	Electricity-demand	x			x	
	Hydrogen-demand			x	x	
	Isolation-electricity-demand	x				
	Isolation-hydrogen-demand			x		
	CAPEX PV -30%	x	x		x	x
	CAPEX PV -10%	x	x		x	x
	CAPEX PV +10%	x	x		x	x
	CAPEX PV +30%	x	x		x	x
	Only-wind	x	x		x	x
	CAPEX ON -30%	x	x		x	x
	CAPEX ON -10%	x	x		x	x
	CAPEX ON +10%	x	x		x	x
	CAPEX ON +30%	x	x		x	x
	Only-PV	x	x		x	x

Similarly to what has just been explained, the isolation-electricity-demand and isolation-hydrogen-demand scenarios are the same as the two functional scenarios described above, with the additional feature typical of the isolation scenario, namely the fact that cross-country exchange is forbidden. This allows to derive the LCOE and levelised cost of hydrogen (LCOH) at a country level, which is particularly useful to compare results with other sources from literature, in particular Aghahosseini et al. [8] for the LCOE and Heuser et al. [123] for the LCOH. In the case of the isolation-hydrogen-demand, only the country of Oman and Saudi Arabia are considered, since results are available from Heuser et al. [123] only for these countries. The export demand is considered to be the same as the national hydrogen demand, which again is not included in the system, while each nation relies on the port present in its territory according to the export scenario.

Finally, ten additional scenarios are designed by varying the investment costs of either PV or onshore wind technologies in the cooperation scenario, as these make up the majority of the total annual costs observed at the end of optimisation. The name of these ten scenarios specifies the entity of the variation of investment costs and the technology affected by it. For example, "CAPEX PV +10%" indicates that the capital costs

of PV panels are multiplied with 1.1 before running optimisation. However, two out of the ten functional scenarios just introduced are named without following this rule: these are the "only-wind" and "only-PV" scenarios. The name is useful to understand that only one technology is being used by the system, although this is obtained following the same methodology as for the other scenarios. In fact, the only-wind and only-PV scenarios are obtained by increasing the costs of PV panels and wind turbines respectively by several orders of magnitude. Among the different goals of the last ten functional scenarios here considered is to check that all results are consistent with the ones obtained in the other scenarios. Also, it is interesting to observe how sensitive the system costs are to these CAPEX variations.

4.2 System components model

This section describes the methodology used to design the ESM, also reporting the techno-economic parameters used for each technology present in the system. Each macro-component of the system is described in a separate subsection, according to the following order: sources, transmission, conversion, storage and demand. The energy commodities considered in this study are hydrogen and electricity. Since hydrogen can only be obtained from other sources, the sources component only includes electricity generation technologies, whereas hydrogen is produced through conversion technologies.

4.2.1 Electricity sources

The only electricity sources considered in this study are wind turbines and open-field fixed-tilt PV panels. Their potential is obtained following the methodology described in chapter 3 and it has already been reported in chapter 5. This subsection discusses instead the key postprocessing steps applied to the time series obtained with the VRES simulations, so that these can be input in the ESM. Furthermore, the absence of electricity sources in the model other than those already mentioned is discussed. Both these two topics have already been partly addressed in section 2.3 and section 3.3, but repeating some of the main concepts here helps to better understand the ESM.

The best natural sources of renewable electricity in the Arabian Peninsula are wind and solar energy [4]. The exclusion of tracking technologies for PV has already been motivated by citing the work of both Ryberg [135] and Caglayan et al. [173], who compared the economics of fixed-tilt PV and tracking PV in multiple locations in Europe for the year 2050, coming to the conclusion that fixed-tilt PV is more economically efficient. Since this was proven also in locations where DNI is the same as most regions of the Arabia Peninsula [2], the technology was excluded from this study as well. It should be said, however, that other sources report a share of single-axis tracking PV in the optimal energy system of both Europe [5] and the MENA region [8]. In the end, in order to limit the complexity of the system, single-axis tracking PV is not included in the model according to the results of Ryberg [135] and Cagalyan et al. [173] just mentioned. On the contrary, concentrated solar power could very well be a good solution for the system, since its efficiency rises with increasing temperature, contrarily to PV technologies [179]. However, this technology is not yet available in RESKIT [164], meaning that it cannot be included in the model.

Hydropower is by far the most exploited Renewable Energy Sources (RES) in the word [81]. The Arabian Peninsula, however, is one of the most arid regions in the world, featuring no important water body [75]. Therefore, this source cannot be considered in the energy mix. Something similar could be said regarding biomass crops, since food scarcity is already an issue due to the absence of water just mentioned [71]. This means that only urban waste could be used for this purpose. Indeed, as reported by IRENA [15], biomass and also geothermal energy could in theory offer interesting opportunities for energy production, but their potential remains currently unexplored. Consequently, these two sources are also excluded from the model, leaving only wind turbines and fixed-tilt PV as the two sources available to the system to produce electricity.

In theory, it would be possible to input each single wind turbine and solar farm in the optimisation tool, but this would make the model too complex. Therefore, multiple VRES installations are clustered and modeled as a single one. The capacity of this "clustered" technology is obtained with summation of the individual placements' capacity, whereas its feed-in time series with averaging. The clusters are identified based on similarity of LCOE or location, which results in grouping of technologies which feature similar design and feed-in time series. This has already been thoroughly described in subsection 3.3.2.

Finally, an additional modeling decision is taken in order to include offshore regions in the ESM. The problem is that by connecting offshore regions to multiple onshore regions, as suggested by the fact that they extend over larger portions of the coast, offshore regions could act as a bridge between onshore regions, something which does not happen in reality. This problem is further enhanced by the fact that transmission lines have to be modeled without any transmission costs and hence be more cost-efficient than onshore ones. This is because transmission costs for offshore wind turbines have already been included in their techno-economic parameters and hence in the LCOE associated to them. Therefore, due to the set-up of the model, each offshore region can only be connected with one onshore region. This is chosen as the region with the longest part of coast extending approximately over the center of the offshore region. For the very big SAU.3r and OMN.3a offshore regions, however, SAU.5 and OMN.9 are chosen, since the best wind potential is found to be located off their coasts and it is not evenly spread over the whole offshore territory near the coast. Keeping in mind that transmission costs have already been accounted for in the case of offshore regions, their potential can therefore be modeled as part of the potential of the onshore region each of them is connected to. The advantage is that the number of regions effectively present in the model decreases from 60 to 49, hence reducing optimisation time.

4.2.2 Transmission

This subsection describes the methodology that was adopted in order to model the transmission system of electricity and hydrogen. This includes determining the layout of the powerlines and hydrogen pipelines, as well as the techno-economic parameters which are necessary to describe them. The electricity grid is discussed first, followed by the hydrogen network.

Currently, all GCC states are connected through an electricity network system, the so called GCC electricity grid [180]. This project was designed in the 1990s with the original idea of creating a 5-GW High Voltage Alternating Current (HVAC) line [180] to connect these countries. However, only 2.4 GW of capacity are reported by IRENA [181], who also point out that the grid is used exclusively as an emergency system. In fact, its capacity is also lower than the individual current peak demand estimated by Toktarova et al. [170] for any other GCC state by at least 50%. Besides, the capacity of the line connecting Saudi Arabia and the Arab Emirates is 20 times lower than the latter's current peak demand.

Almost all different regions of Saudi Arabia are connected with at least another one among them [182]. In fact, although the national electricity system consisted of four isolated grids up to 2009, important connections have been realised with long High Voltage Direct Current (HVDC) lines, especially to connect the eastern and the western part of the country [183], which are also those with the highest population [184]. In spite of the relatively high capacity of Saudi Arabia's grid with respect to the other Arab countries, experts point out that its transmission system could only withstand 14 GW of renewable electricity. This is as low as one fourth of its current peak demand. [182]

The information just given shows that in a system powered only by VRES and which connects all GCC states, grid expansion should grow by several times. This is even more true once we consider the additional energy demand of hydrogen due to sector coupling and the fact that demand has been shown to increase significantly over the period 2020-2050, as explained in subsection 4.2.5. Moreover, it is not possible to know in advance which part of Saudi's current grid are adequate to withstand high VRES penetration, while the design of the GCC interconnection grid dates back to more than 20 years ago [180]. Therefore, a new grid is modeled for the year 2050. However, it is reasonable to suppose that the new lines will gradually replace the old ones, so that the same layout of the current grid is kept. The main transmission powerlines are made available by the World Bank Group [127]. The database can also be used to determine the location of the energy demand of a given region, which is chosen as the location of its main grid connection. In order to reduce the complexity of the system, in fact, the entire energy demand of a region is supposed to be concentrated in a single point, referred to as the energy demand center. Furthermore, to ensure demand is met also in the case of a sustained shortage, the few regions [1] which are currently isolated are connected to the nearest region, while their demand center is located at the center of their territory. These regions are typically located in areas with low population and in the outermost part of the system, with the exception of KWT.2. More grid connections could be added to the system to increase safety, but this would also add fixed costs to the system, so that the proposed methodology constitutes a reasonable compromise between costs and safety.

[1] These regions are: SAU.3, SAU.4, SAU.12, OMN.9, OMN.6, OMN. 10, QAT.6, QAT.7, KWT.2

Keeping in mind all these considerations, Figure 4.1 is created showing the regional energy demand centers and the transmission lines connecting them.

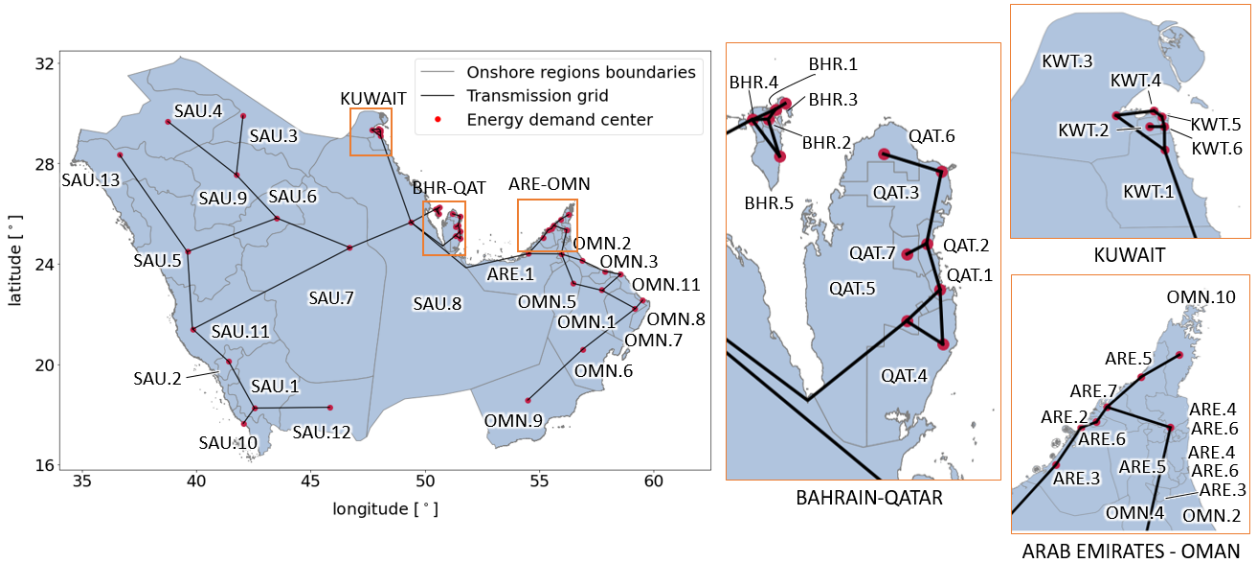

Figure 4.1: Modeled transmission grid for both electricity and hydrogen for the year 2050

As discussed so far, both HVAC and HVAC lines are present in the GCC area. It is difficult to state in which share they will make up the future capacity of the electricity transmission system, as both present advantages and disadvantages. Since the accurate modeling of a grid is out of the scope of this thesis, HVAC lines are supposed to be installed everywhere. Losses have to be modeled linearly due to the linearity of the optimisation tool [185]. A value for this parameter is offered by the IEA [186], who also reports current prices for HVAC grids. Future cost reductions are instead based on the projections of the reference scenario of the European Commission [187]. All parameters mentioned so far are reported in subsection 4.2.2. The length of transmission lines is obtained calculating the eucleadian distance between regional demand centers and multiplying it by 1.3. In fact, similar correction factors have already been used in literature [188].

Table 4.2: Techno-economic parameters of transmission technologies

	Economic lifetime [a]	**Investment costs [€/MWkm]**	**Fixed OPEX [%/a CAPEX]**	**Variable OPEX [%/a CAPEX]**	**Energy losses [%/1000km]**
Powerlines [186, 187]	60	800	1.5	2	7
H2 pipelines [173]	40	185	0.5	0	0

Looking at existing oil&gas pipelines installations over the Peninsula, it is observed that these often run parallel or close to powerlines. Therefore, for the purpose of this work it is reasonable to suppose that the future hydrogen network will have the same layout as the electricity grid. In reality, the existing pipelines are more developed than the electricity grid in the East due to the presence of oil&gas reservoirs, while the opposite happens in the West. These differences are not implemented in the model since the future hydrogen network will be less influenced by the extraction of hydrocarbons. Besides, even if the existing pipes could be initially converted to host hydrogen in order to save costs [109], this study assumes completely new hydrogen pipelines. This is because installations are supposed to happen in 2050, i.e. 30 years from now, which is more or less the economic lifetime of natural gas pipelines [189].

The techno-economic parameters used to model hydrogen pipelines are taken from Caglayan et al. [173], who modeled an energy system to satisfy electricity and hydrogen demand in Europe in the same year considered in this study. In particular, the authors ignore hydrogen transport losses. This seems reasonable also looking at current transport losses in the methane long-distance distribution sector, which are reported around 0.6

% for Russia, a leading country in this business [190]. The chosen techno-economic parameters are reported in Table 4.2, together with those adopted for powerlines, as mentioned earlier in this subsection. The table allows to show that even though powerlines have a longer economic lifetime, they are significantly more expensive than hydrogen pipelines when considering the same amount of energy transported per unit and length. In particular, the effect on costs of the variable OPEX associated to powerlines is comparable to that of CAPEX, as revealed by the optimisation results of chapter 6.

4.2.3 Conversion

This subsection reports the criteria used to model the conversion components of the ESM. The main conversion steps taken into account in this work are those considering the passage from electricity to hydrogen and viceversa. These are modeled according to the work of Caglayan et al. [173], since these authors have created a system including the technologies modeled here and keeping the same time horizon for cost projections, even if Europe is the geographical area they are considering. Only one technology is implemented for electrolysis, but multiple are available for reconversion. In this way, different combination of costs and efficiency are possible depending on the scarcity or abundance of VRES and the high or low need of reconversion processes. Flexibility in this sense could be further increased by considering multiple electrolysers having different efficiencies and costs, but the forecast of additional future techno-economic parameters for other technologies is complex and out of the scope of this thesis. It should also be pointed out that hydrogen compression after electrolysis is neglected here as well. In fact, Heuser et al. [123] show that the costs of compressors contribute to less than 1% of total annual costs, whereas the related energy losses do not surpass 1% of total generation.

Due to the existence of scenarios featuring hydrogen exports, a hydrogen liquefaction technology is also necessary. The liquefier model is taken from Heuser et al. [191], since their work is the only one available in literature offering results for individual countries of the GCC and will therefore be used for comparing the LCOH in subsection 7.2.3.

Finally, all techno-economic parameters used for the conversion technologies are reported in Table 4.3. The efficiency of the electrolyser, as well as that of the liquefier, is referred to the amount of electrical energy lost in input for the production of one unit of hydrogen energy in output. Conversely, the efficiency of the reconversion technologies considers the losses of hydrogen energy per unit of electrical energy produced. The energy associated to hydrogen is based on its LHV of 33.3 kWh/kg [173].

Table 4.3: Techno-economic parameters of conversion technologies

	Economic lifetime [a]	**Investment costs** [€/kW]	**Fixed OPEX** [€/kWa]	**Variable OPEX** [€/MWh]	**Energy efficiency** [%]
PEMEL [173]	10	500	15	0	70
PEMFC [173]	10	923	0	7.5	51
SOFC [173]	10	1500	2	0	70
H2 Gas Engine [173]	20	715	4	7	48.5
H2 OCGT [173]	25	504	5	7.5	40
H2 CCGT [173]	25	760	11	2.4	60
H2 liquefier [191]	20	182	8	0	82

4.2.4 Storage

In line with the methodology followed for conversion technologies, the storage tehnologies are modeled according to the work of Caglayan et al. [173], as reported in Table 4.4. However, the current work excludes the use of pumped-storage hydroelectricity due to the scarcity of water resources in the region [75], as already explained in subsection 4.2.1. Besides, salt caverns also have to be excluded, although this is due to the lack of sufficient data publicly available. In fact, even if maps can be retrieved showing the approximate location of salt caverns over the Peninsula [192], a very extensive and detailed amount of data is necessary

to estimate the potential of these caverns for hydrogen storage [173]. Finally, liquid hydrogen storage at ports is also excluded from the scenarios where it would be relevant, namely those where hydrogen is shipped abroad. This is because gaseous storage is safer than liquid hydrogen storage [178], while concentrating the entire hydrogen storage capacity at ports alone could further increase safety risks. Besides, storing hydrogen as liquid would limit the flexiblity of the system significantly, since this cannot be transported back to the regions unless re-gasification is used. Other forms of hydrogen storage, such as organic carriers, are excluded as well due to time-constraints.

Table 4.4: Techno-economic parameters of storage technologies [173]

	Economic lifetime [a]	**Investment costs [€/kWh]**	**OPEX [%/a CAPEX]**	**Self discharge [%/month]**	**Charge/Discharge losses [%]**
Li-ion battery	22	151	1	3	5
GH2 vessel	20	7.5	2	0	0.5

4.2.5 Electricity and hydrogen demand

This subsection explains the methodology chosen to model the electricity and hydrogen demand of each region in the energy system for the year 2050. The sectors considered for this purpose are those extensively described in subsection 2.1.2, namely power, road&rail transport and finally feedstock for industry, which includes ammonia and steel. For each sector, energy demand is estimated at the country level using different sources. Then, this is assigned to the different regions based on the ratio "region inhabitants / country inhabitants", which is computed from the WorldPop database [184]. The regional demand is finally assigned to a regional demand center, whose location is defined as the most important connection of that region to the transmission grid. The role of demand centers and their location have already been reported subsection 4.2.2.

Electricity demand - power sector

The first part of this subsection explains how electricity demand for the year 2050 is modeled. This is derived by the electricity demand estimates of the power sector for the chosen year. This value could be higher due to the additional electricity input required for the ammonia and steel sectors. However, the next subsection shows that this increase would be lower than 3%. Therefore, it is supposed that future electricity demand for ammonia and steel is already included in the estimates of the power sector. Finally, an additional electricity input is needed in case hydrogen liquefaction is considered. However, this is entirely dependent on the hydrogen demand and the efficiency of the liquefier reported in subsection 4.2.3, which is why it will not be mentioned further.

Only one source could be found in literature offering electricity demand projections for the year 2050 for GCC countries specifically [193]. However, Almulla [193] only disposes of estimates from authoritative sources up to the year 2020, after which he arbitrarily assumes a growth rate decline factor of 30% every ten years. Therefore, his model is not adopted here. Trying to retrieve different forecast models for each different country also poses challenges due to the lack of information in literature. Therefore, the predictions of Toktarova et al. [170] are chosen in this work, which offer a value of electricity demand for each country in the world until 2100. These are based on the hypothesis that parity of Gross Domestic Product (GDP) per capita will be achieved in 2100 according to the UN Resolution. The predictions of Toktarova et al. were also able to better predict the actual electricity demand of Saudi Arabia in 2019 as reported by Statista [194] with respect to Almulla [193]. A direct comparison between recent data and short-term predictions is however not able to define the quality of the forecast models in the long term, since the oil price crisis of 2014 significantly impacted short-term economic growth of oil exporting countries [195]. Finally, the use of a single authoritative source such as Toktarova et al. [170] to derive future electricity demand allows for greater consistency in forecasts when considering multiple countries. Besides, the authors also create load time series for each country based on the interpolation and average of different real load curves, which can therefore be directly adopted here.

An overview of total electricity demand in 2050 for all GCC members is offered in Table 4.5. As would be

expected, Saudi Arabia and the Arab Emirates, the most populated countries and with the highest GDP, make up a large portion of total demand at 615 TWh (56%) and 208 TWh (19%) respectively. Bahrain is the country with the least electricity consumption at 28 TWh. Overall, the GCC countries are forecast to require 1098 TWh of electricity.

Table 4.5: National electricity demand projections [TWh] modeled by Toktarova et al. [170] for the years 2020 and 2050

	Arab Emirates		**Bahrain**		**Kuwait**		**Oman**		**Qatar**		**Saudi Arabia**		**GCC**	
Year	2018	2050	2018	2050	2018	2050	2018	2050	2018	2050	2018	2050	2018	2050
Demand	118.0	208.3	24.6	28.2	65.7	98.4	33.4	89.1	41.5	58.4	341.3	615.3	624.5	1097.7

In order to model the system more accurately and according to the regions defined in section 3.1, national electricity demand is distributed at the regional level by using the WorldPop database [184]. More specifically, the amount of population living in each region with respect to the country total is computed from the database and multiplied with the national demand, thus returning a regional demand value. The result is reported in Figure 4.2. It is useful to remind that some regions include territories which are not contiguous, so that their regional code is repeated in the picture. This shows that size is not a good indicator of energy demand. In fact, regions with the same area show great differences. Besides, all countries except Saudi Arabia present small regions with high demand with respect to the country total, for example: ARE.3, QAT.1, BHR.3 and KWT.2.

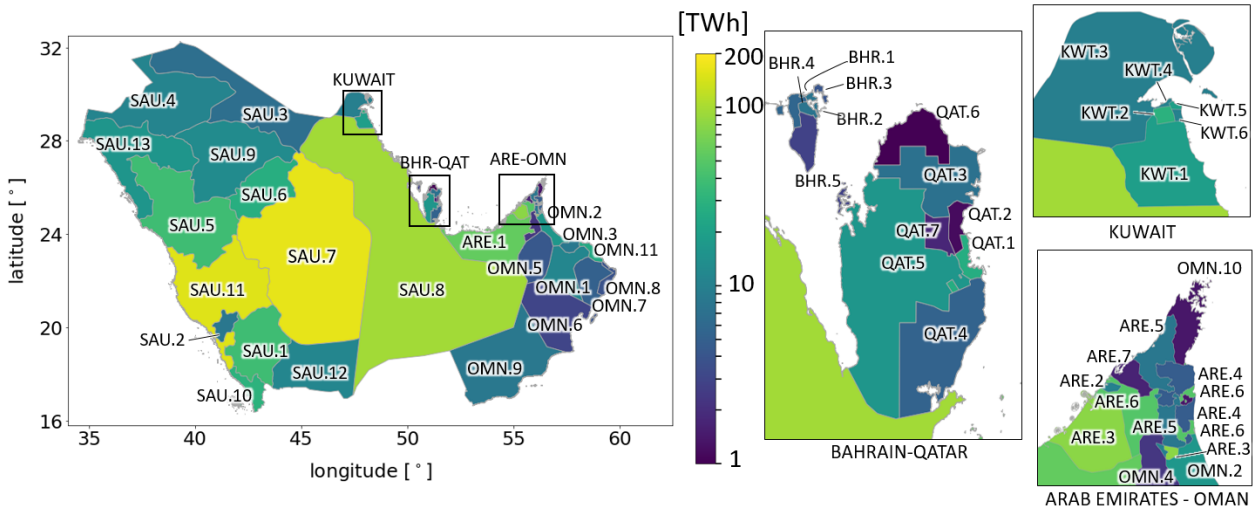

Figure 4.2: Regional electricity demand modeled for the year 2050

Hydrogen demand - transport, ammonia, steel sectors

The last part of this subsection explains how future hydrogen demand is derived for each of the three remaining sectors that are coupled to the system: road&rail transport, ammonia and steel. This is done separately for each of them, as the methods used necessarily have to adapt to the nature of the information available in literature, most of which has already been introduced in subsection 2.1.2. As it will be shown in this subsection, coupling these three sectors leads to an additional electricity demand of less than 3% with respect to the power sector described earlier. Therefore, this is supposed to be already included in the power sector demand.

In the context of this study, a fully developed hydrogen economy is supposed to be achieved. Therefore, the assumption is made that a hydrogen storage infrastructure already exists acting as a buffer at the distribution level. Consequently, the hydrogen demand of each of the sectors coupled to the system is modeled as constant

throughout the year. This is also a conservative approach, as a constant profile does not match well the feed-in time series of solar energy on a daily basis nor that of wind energy on a yearly basis.

The energy required by the whole **transport** sector for the year 2018 at a country level is reported by the IEA [171]. For a reference, the energy currently used by this sector in the whole region is of 73 Mtoe/year, or 849 TWh/year. The energy demand for each country is first of all corrected with the ratio between the efficiency of modern highly-efficient internal combustion engines (36% [172]) and of fuel cells in 2050 (51% [173]) in order to account for the fact that fuel cells will replace combustion engines in transport vehicles. Considering plug-in hybrid vehicles could be an option, but they are not considered here following a conservative approach. In fact, assuming that part of the transport energy demand has to be covered with electricity instead of hydrogen would reduce the required primary energy consumption, since the operation of the electrolysers would be avoided.
The share of road&rail transport to the total transport demand varies considerably depending on the country. Even if this value for the GCC countries could not be retrieved by the author, a pattern is found for other states in the world which shows that the ratio is equal to 70-80% for bigger countries and to 60-65% for smaller ones. Therefore, the median value of 75% is chosen for Saudi Arabia, and 62% for the other GCC members. [174]
Although sources exist in literature forecasting the long-term future energy demand of the transport sector, none could be found specifically for the GCC region. Therefore, the relative increase in time at the country-level is chosen to be the same as that of the electricity sector described in the previous subsection and suggested by Toktarova et al. [170]. In fact, the energy demand of the transport sector for the GCC countries is found to grow at the same speed as GDP [175], while the relationship between GDP and electricity demand obtained by Toktarova et al. [170] is almost linear in the current and estimated future values of GDP of the GCC countries [176]. At the end of the process just described, the future hydrogen demand of the road&rail transport for the region is found equal to 752 TWh.

Current production of **ammonia** for the three largest producing countries in the region (Saudi Arabia, Qatar and Oman) can be retrieved from the United States Geological Survey (USGS) [45]: these combined account for 8.8 Mton_NH3/year. The remaining amount of the total 13 Mton_NH3/year produced in the GCC area is then assumed to be evenly distributed among the other three countries of the Gulf [47]. Following the stoichiometric coefficients of the chemical formula describing ammonia production through nitrogen and hydrogen as indicated in Rivarolo et al. [177], tonnage of ammonia can be converted to kilograms of hydrogen using the value of 177 kg_H2/ton_NH3 for each individual country. In this way, the overall current demand of the GCC region is found equal to 2.3 Mton_H2.
To the best of the author's knowledge, no public source exists estimating the growth of this sector for the area under consideration until 2050. However, the forecasts of the Gulf Petrochemicals and Chemicals Association (GPCA) [47] show that production of ammonia in the GCC countries will grow until 16 Mton_NH3 in 2030, but will then remain stable until 2035, which is the time horizon used for their study. Following the expected trend of the period 2030-2035, the same constant pattern is supposed also for the period 2035-2050. Moreover, the growth rate of the GCC area indicated for the period 2018-2030 and equal to 23% is applied to all countries. Finally, hydrogen demand is converted to energy demand using the LHV of hydrogen and equal to 33.3 kWh/kg_H2 [173]. The assumptions made so far lead to an overall hydrogen demand of 94 TWh for the GCC area in 2050.
In order to produce ammonia, nitrogen is also required in the proportion of 823 kg_N2/ton_NH3 [177]. As shown by Pfromm [48], only 243 kWh/ton_N2 are needed to perform criogenic air separation. Accordingly, 3 TWh of electricity would be directly used in the region by the ammonia sector in 2050. This value does not get close to even 1% of the electricity demand of the power sector, and is therefore neglected.

Finally, the **steel** sector is considered. Current production of each country in the GCC region is obtained from the World Steel Association [52]: 17.7 Mton_steel are produced overall. In order to convert steel demand into hydrogen demand, the model of Vogl et al. [61] and based on the DRI steelmaking process is chosen, as anticipated in subsection 2.1.2. This requires the knowledge of the amount of scrap used as feedstock, which is set at 58% following the world projections of scrap and steel production for 2050, as also thoroughly discussed in subsection 2.1.2. Following this assumption, the value of 21 kg_H2/ton_steel can be obtained from Vogl et al. [61]. In this way, current hydrogen demand is calculated for each country, with an overall value of approximately 0.4 Mton_H2 observed for the GCC area, approximately 6 times lower than that of the ammonia sector.

Again, it was not possible to find sources projecting the growth of the steel sector until 2050 for the specific countries considered here. However, the IEA [55] published projections for the Middle East as a whole and considering the same time horizon: these are used here. Two scenarios are made available by the IEA, under the respective conditions of "business-as-usual" or "sustainable" development, which have been also discussed in subsection 2.1.2. The sustainable development scenario is chosen by the author since one of goals of the energy system modeled in this study is to reduce GHG emisssions as much as possible. Accordingly, an overall growth of 66% for the period 2019-2050 is adopted for all countries. This leads to an overall future hydrogen demand of 21 TWh for the ammonia sector in the GCC region.
Calculating the electricity directly required by the DRI process is straightforward: using the value of 900 kWh/ton_steel indicated by Vogl et al. [61], the steel sector modeled here is found to require approximately 26 TWh of electricity in 2050. Although this value is way higher than that of the ammonia sector, it only represents 2% of the future energy demand of the power sector and is therefore neglected also in this case.

Table 4.6 reports the hydrogen demand for the year 2050 modeled in the way just described for each country and sector considered in this study. Road&rail transport accounts for almost 87% of the overall hydrogen demand, which is found to be 867 TWh at the GCC level. This is lower than the demand estimated for electricity, but corresponds to a higher theoretical primary energy input due to the necessary conversion steps needed to produce hydrogen from electricity. Contribution of ammonia is also significative at around 11% TWh, with only 2% of the remaining demand due to steelmaking. As observed for the power sector, Saudi Arabia and the United Arab Emirates are associated with the highest hydrogen demand at 540 TWh and 129 TWh respectively. Due to the methodology just explained, the values registered by Saudi Arabia, Qatar and Oman are found to be no more than 20% lower than those of the power sector, whereas the energy demand of the other countries shows a greater difference: between 35% and 50% less.

Table 4.6: Current[2]and future national hydrogen demand [TWh] modeled in this study

Country		**Arab Emirates**		**Bahrain**		**Kuwait**	
Year		2018-19	2050	2018-19	2050	2018-19	2050
Demand	Road&Rail [170–176]	65.0	114.6	6.6	7.6	27.2	40.7
	Ammonia [45, 47, 48, 173, 177]	8.3	10.2	8.3	10.2	8.3	10.2
	Steel [52, 55, 61]	2.3	3.8	0.1	0.2	1.0	1.6
	Total_H2	77.0	128.6	15.1	18.0	36.4	52.5
Country		**Oman**		**Qatar**		**Saudi Arabia**	
Year		2018-19	2050	2018-19	2050	2018-19	2050
Demand	Road&Rail	21.1	56.2	19.8	27.9	279.9	504.5
	Ammonia	10.0	12.3	18.3	22.5	23.6	29.0
	Steel	1.4	2.3	1.8	3.0	5.7	9.6
	Total_H2	32.5	70.9	39.9	53.4	309.2	543.1
Countries		**GCC**					
Year		2018-19	2050				
Demand	Road&Rail	419.5	751.6				
	Ammonia	76.6	94.3				
	Steel	12.4	20.6				
	Total_H2	508.5	866.6				

Finally, the national hydrogen demand is distributed at the regional level based on the number of inhabitants

[2]Current hydrogen demand of both the road&rail [171] and the ammonia sector [45, 47] refers to the year 2018, whereas current demand of the steel sector [52] to the year 2019

of each region with respect to the corresponding country total, as already explained earlier. Since the same method was adopted for this purpose, the resulting colormap reported in Figure 4.3 is very similar to that of electricity. This is also due to the fact the contribution of Saudi Arabia to the total GCC demand is significantly higher than that of other countries for both the power and the transport sector, while the overall value of demand is similar for both hydrogen and electricity. However, the zooms offered on the right side of Figure 4.3 allow to see a strong difference for the Arab Emirates and Kuwait, which is especially visible in regions: kWT.1, KWT.2, ARE.6, ARE.3 and ARE.1 (the latter being instead reported in picture on the left side). Their colors are darker in this case, since the national hydrogen demand for these two countries is almost half as the electricity demand reported earlier.

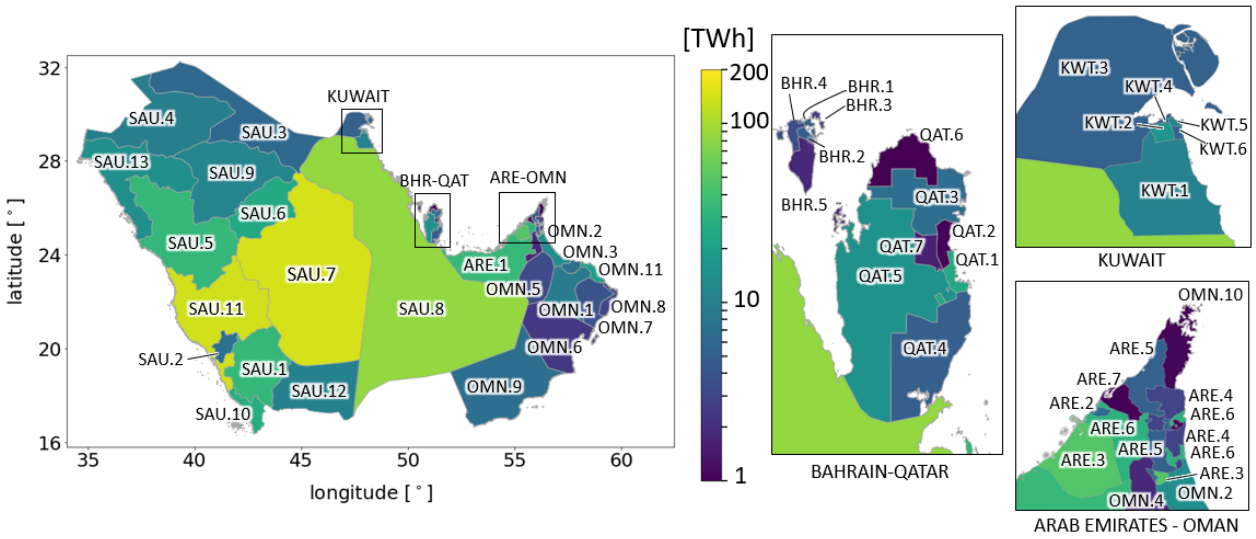

Figure 4.3: Regional hydrogen demand modeled for the year 2050

To finish this subsection, the temporal profile of electricity and hydrogen demand is reported in Figure 4.4. As already mentioned, hydrogen demand remains is modeled as constant, whereas electricity demand varies significantly over the year, with peak values approximately twice as high in the summer than in winter due to cooling applications. Differences can also be appreciated on a daily level between the different periods of the year. In particular, a more constant and regular profile of electricity demand is observed in summer than in winter.

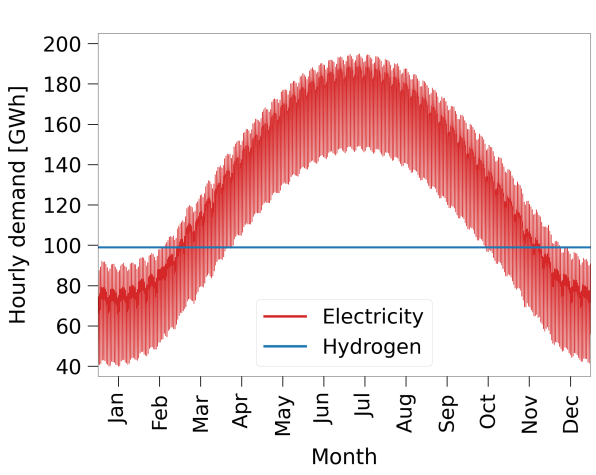

(a) Yearly demand time series

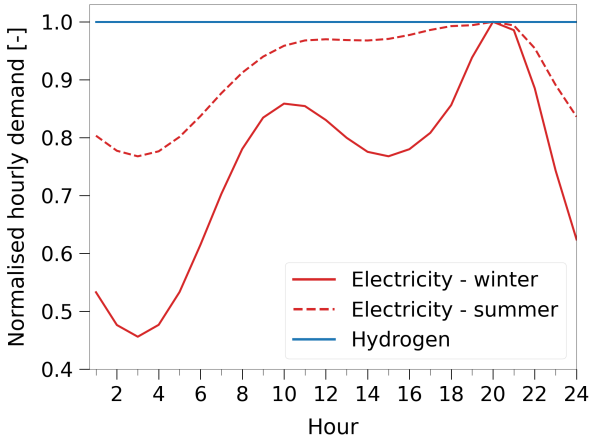

(b) Daily demand time series. Values are normalised with respect to the daily maximum of each curve

Figure 4.4: Temporal profile of overall electricity [170] and hydrogen demand in the GCC area

4.3 System optimisation in FINE

This section will report some important information related to software used to obtain the optimal operation of the system. Some elements regarding this topic have already been introduced in other parts of this work, but repeating them here briefly helps to understand the new items which will also be discussed.

The software, called Framework for Integrated Energy System Assessment (FINE), is an open-source tool based on a linear optimisation algorithm which is aimed at optimising the economic costs of the system. Therefore, the minimum of the objective function describing Total Annual Costs (TAC) is achieved by FINE [185]. The cost models used for the different system components have already been presented in the previous section 4.2. The need to use linear cost models should be regarded as a modeling simplification, since this is typically not the case. In particular, it does not account for economy of scale effects, in particular the existence of fixed costs which do not scale with capacity.

Apart from the goal of optimisation and the algorithm it relies on, the spatial and temporal resolution of the energy system are two very important parameters. As for the spatial resolution of the system, the territory is modeled as a set of nodes where different forms of energy can be generated, absorbed, converted or stored. These nodes can be interconnected and therefore exchange energy. The GCC countries are modeled as a system of 49 nodes determined by the location of the regional energy demand centers, which have already been introduced in subsection 4.2.2. Each offshore region is incorporated in one onshore region according to the method indicated in subsection 4.2.2. While all VRES are modeled as if they were producing electricity in their respective regional node, more than one representative PV farm and wind turbine is typically present in each region, since VRES are clustered taking into account a maximum distance of 450 km and their LCOE, as reported in detail in subsection 3.3.2.

More complicated is the discussion of the temporal resolution characterising the system. The feed-in time series of electricity generation input in the system are provided with an hourly-resolution, which is also the chosen duration of a time-step describing the operation of the system. However, in order to reduce computational time, the generation and load data given in input is preprocessed. From the 365 different daily profiles specified for each generation cluster and demand center, a reduced set of typical days is obtained through hierarchical time series aggregation [196]. To perform this step, FINE uses an open-source package called Time Series Aggregation Module (TSAM) [197]. One the best features of the time series aggregation algorithm used by FINE is that it allows the system to size the storage components based not only on intra-period needs, but also on inter-period needs. In simple words, long-term storage is considered by optimisation, something where many other energy system models fall short [196]. For this work, 30 typical days are chosen following the sensitivity analysis performed by Caglayan et al. [173]. In particular, their optimisation results perfectly converge at 30 typical days, while their system is more complex than the current one both in terms of number of technologies considered and total amount of nodes. What is more, a deviation of TAC of only 4% is already achieved by her system at 15 typical days, suggesting that the value of 30 typical days should be particularly reliable.

5 | Renewable Potential Assessment Results

In the previous chapter 3 and 4 we have offered a thorough description of the methodology used to achieve the research goals described in the Introduction. In particular, chapter 3 has outlined the approach adopted to determine the eligible land for the installation of Variable Renewable Energy Sources (VRES) and their associated potential. Therefore, it is now possible to show the results of this analysis, which is carried out in the following way. First, section 5.1 is dedicated to the outcome of the Land Eligibility Analysis (LEA). Then, the technical potential of VRES in the countries under exam is reported in section 5.2. In both of these sections, each technology will be treated separately, although comparisons among them are offered in several passages of this chapter.
The same region and country name abbreviations presented in section 3.1 are used in this chapter as well, so that it is always possible to find there the information for each of the territories referred to in the following graphs.

5.1 Eligible Land Results

In this subchapter, the results of the LEA are presented for each technology in the following order: open-field PV, onshore wind and offshore wind. There are multiple elements of interest that can be treated when assessing the outcome of the LEA. In fact, apart from the values of available land worked out for each country, it is also interesting to see which exclusion criteria are most influential and in which regions. Therefore, multiple charts are created from the results of each technology, so that these can be studied from different perspectives. An important aspect to stress here is that the areas excluded by different criteria may overlap on the map especially because of the use of buffer zones, so that sum of exclusions reported on a given region may exceed 100%, as it is often the case with smaller regions. However, the software used is able to recognise these cases and count these overlapping exclusions only once. Finally, it should be reminded that the regions labelled as "strategic" or "contested" have been removed during the regionalisation process, so that these exclusion criteria do not appear here.

Open-field PV

As a start, an overview of the areas excluded by GLAES as ineligible is offered in Figure 5.1, where these are represented in black. What stands out immediately is the almost entire exclusion of the southern part of Saudi Arabia. The main factor contributing to this effect are the dunes of Rub'al Khali, extending in the center-right side of southern Saudi Arabia, but a large portion of terrain is also covered by the Al-'Uruq al-Mu'taridah natural reserve at the southern border with Oman, whereas the western side, bordering with the Red Sea, is also largely excluded due to the Asir mountains. The north-western side also features a significant reduction of available land for similar reasons, with the continuation of the mountain escarpment to the left, the presence of another desert, the Al-Nafūd, and a series of major natural reserves in the north. The stripe of ineligible land stretching between north and south is the third biggest desert in the region, namely the Al-Dahnā. These types of constrains are also resulting in significant exclusions in the east, especially in the eastern region of Oman overlooking the Gulf of Oman and in the United Arab Emirates. In general, the eastern stripe of land of the Peninsula, hosting the majority of the population and industrial activities related to oil& gas extraction, sees numerous exclusions due to either settlements or coastline constraints. Finally, agricultural areas and agricultural settlement exclusions result in what appear as black dots to the left of the Al-Dahnā desert. In fact, satellite images show cultivated fields of circular form which are typical of these desert regions. These dots should not be confused with the others scattered around the mountainous regions, which are due to slope or elevation constraints, since the transition from flat to elevated and inclined terrain is not sharp.
Following these exclusions, at the end of the LEA only around 15% of the Arab Emirates and Bahrain are eligible for VRES installations, as is reported in the table of Figure 5.1. Other coastal states such as Kuwait and Qatar also see relatively high exclusions at 40% and 62% respectively. Oman is the state with the lowest relative exclusion at 26% and the second largest area available in absolute terms among the GCC states (0.23 million km^2). Finally, the LEA halves the available area of Saudi Arabia; in spite of this, the state has four times more eligible land than all the other countries combined at almost 1 million km^2. Overall, 1.22 million km^2 can be used for VRES installations.

A more detailed breakdown of the effects of the LEA on each single region of the GCC countries is given in Figure 5.2. Thanks to these graphs and keeping as a reference for the regional codes the abbreviations presented in section 3.1, the exclusions described above can be further explored. In particular, numerical comparisons can be made between the country level and the regional one. For example, looking at the first chart reported (Arab Emirates), one can see that the first region, ARE.1, constitutes the almost entire area of the country and features an exclusion slightly above 80%, which is in fact very close to the exclusion value of 85% obtained at the country level.
Another interesting observation is that the smallest regions of each country typically see the highest exclusion. This trend can be explained with the fact that regions tend to reflect the distribution of the population, so that a small region typically implies a high concentration of human settlements, which are then classified as ineligible land. Saudi Arabia, however, shows a different pattern, with a very high exclusion in its biggest region (SAU.8), due to the presence of the Rub'al Khali desert. For this extremely large country, in fact, the highest exclusions are not due to the concentration of people but to the location of mountains, sand dunes or reserves.

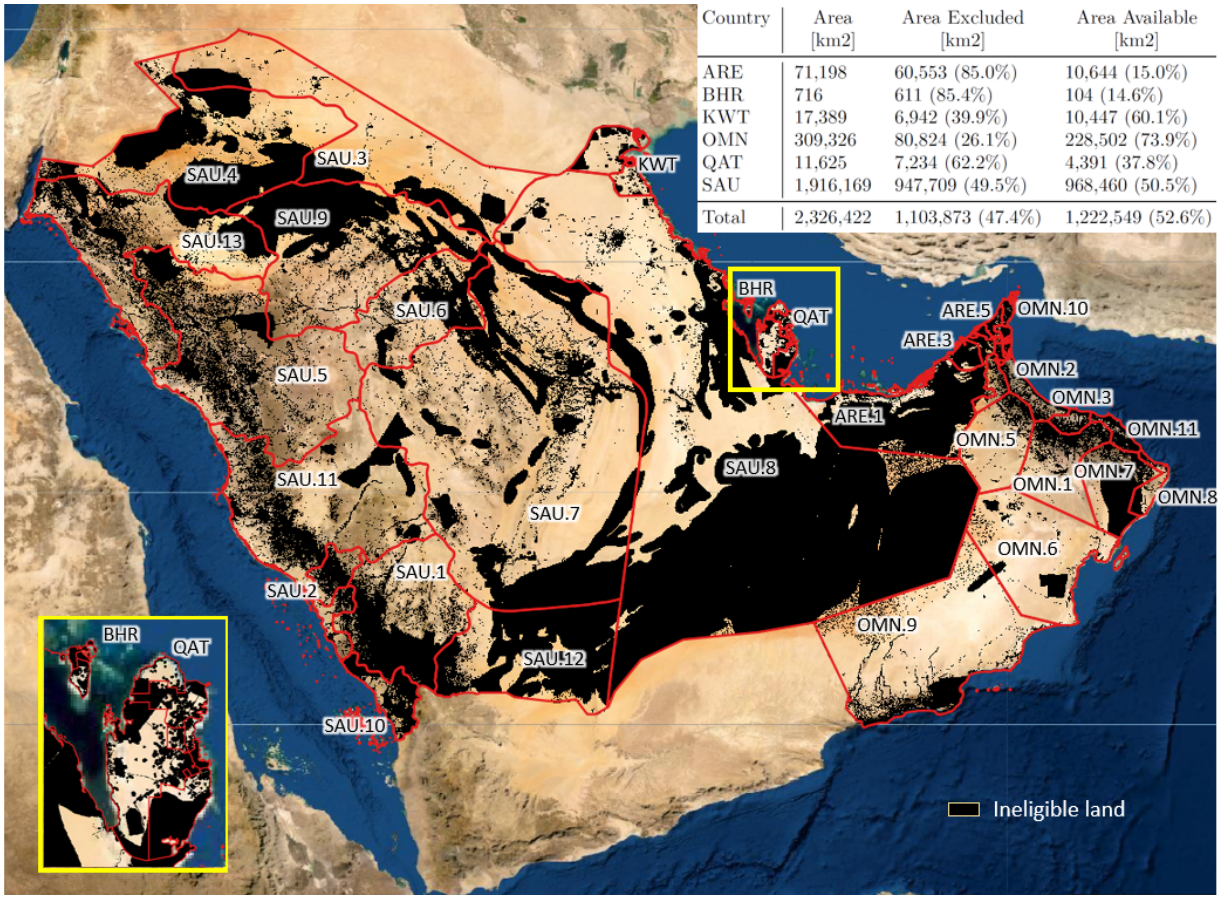

Figure 5.1: Map of land areas excluded by the open-field PV LEA and overall country-wise exclusion results

In order to better measure the effect of the constraints on an individual region, the chart of Figure 5.3 was created. This is in line with the analysis carried out so far. For example, the third row shows that agricultural areas lead to considerable exclusions not only in smaller countries but also in some regions in Saudi Arabia, registering a value of 40% in SAU.10, following the pattern of circular cultivated fields mentioned earlier. Urban settlements lead to total exclusions in some coastal regions on the East, as also mentioned before. Moreover, the criteria of sand dunes, slope and reserves highly affect the availability of land in many large regions, as can be observed in some columns associated to Saudi Arabia. Colours associated with high exclusions can also be found in some of the top-left squares of the figure. However, as these are usually affecting tiny regions, their overall effect should not be overestimated.
Interestingly enough, the values of slope (general and northward) found in the matrix show that this is the

main exclusion associated to mountains, and not elevation, as best exemplified in the columns representative of Oman. The slope criterion, however, should be treated with great care since it can also be triggered by the slope of sand dunes.

Now that the system has been considered in all its parts, it proves beneficial to wrap up the analysis by looking at the overall effect of land exclusion criteria on the GCC area as a whole. To do so, the double pie chart of Figure 5.4 is created. Not surprisingly, sand dunes score first at almost 25%. What is remarkable, though, is the value itself of this constraint, corresponding to more than 0.5 million km^2, especially considering the fact that sand areas were not entirely excluded (only sand dunes and moving sands were). The second place is taken by reserves, with a 8.7% of the overall territory. Following close, northward slope registers 7.3%. Therefore, the greatest three exclusions on the GCC area belong to three different macro-categories of criteria, namely physical, conservation and economic going from the highest to the lowest value of the top-three. In spite of the presence of mountains in vast areas of Oman and Saudi Arabia, the elevation constraint is seldom activated, leading to an overall exclusion as low as 1.2%. Of the 32 exclusion criteria used, the bottom half combined account for less than 2.5% of land excluded. Another meaningful take-away is that rural settlements result in higher exclusion than urban ones, as well as secondary roads lead to more areas excluded than primary ones. This is because although urban centers and primary roads are bigger and are associated with higher individual buffer values, they are less frequent, so that the effect of buffers becomes more evident for rural settlements and secondary roads.

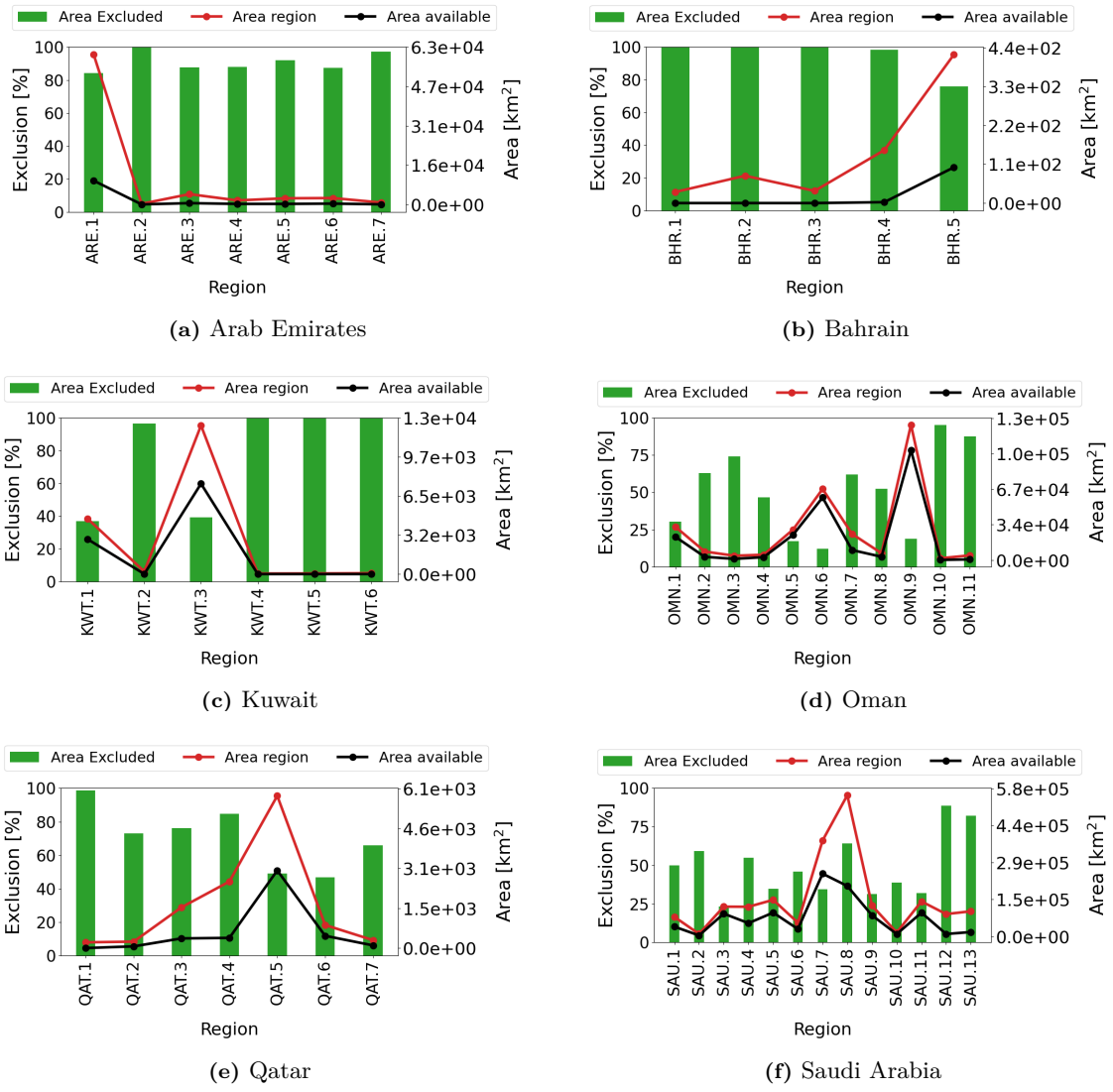

(a) Arab Emirates **(b)** Bahrain

(c) Kuwait **(d)** Oman

(e) Qatar **(f)** Saudi Arabia

Figure 5.2: Representation of the results of the open-field PV LEA on each region

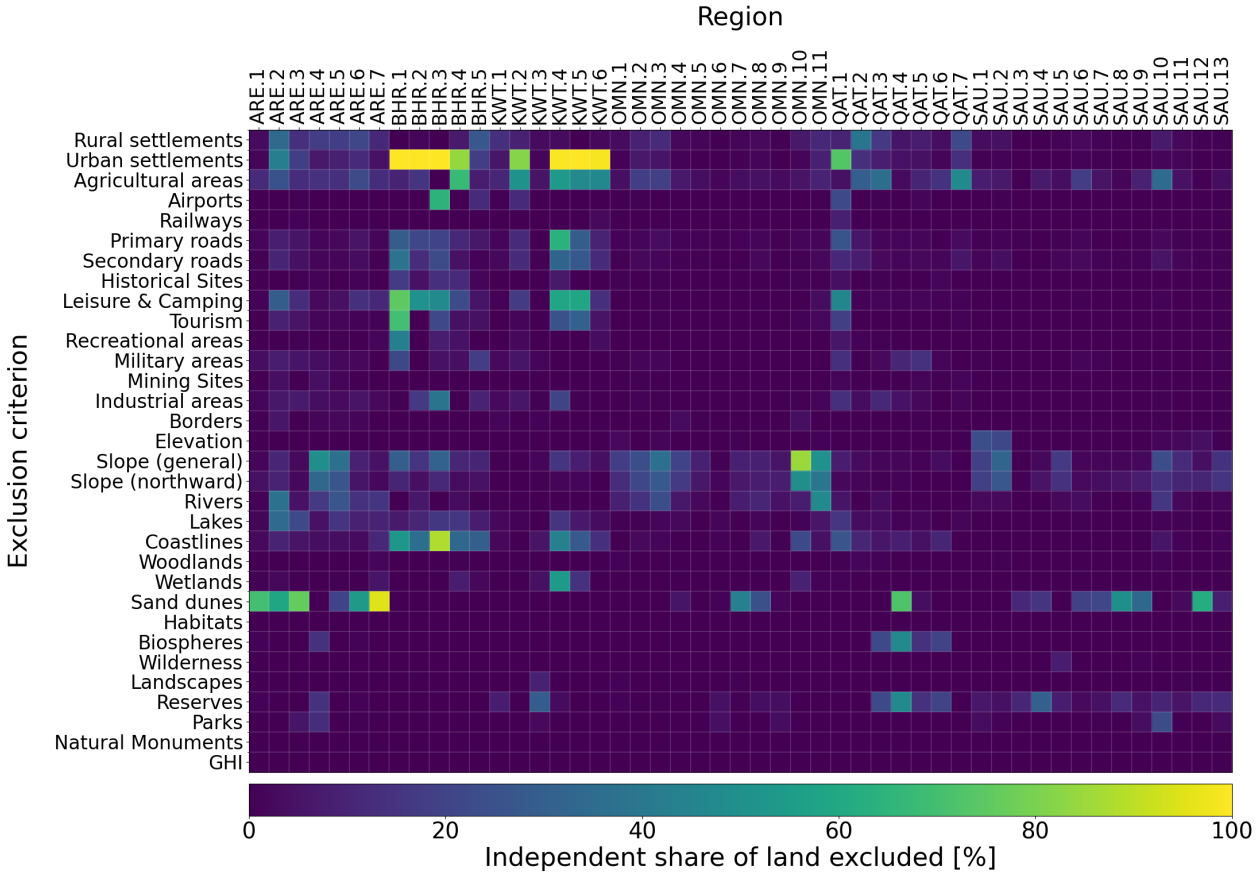

Figure 5.3: Matrix plot of individual land exclusion operated by each eligibility criterion on each region - open-field PV

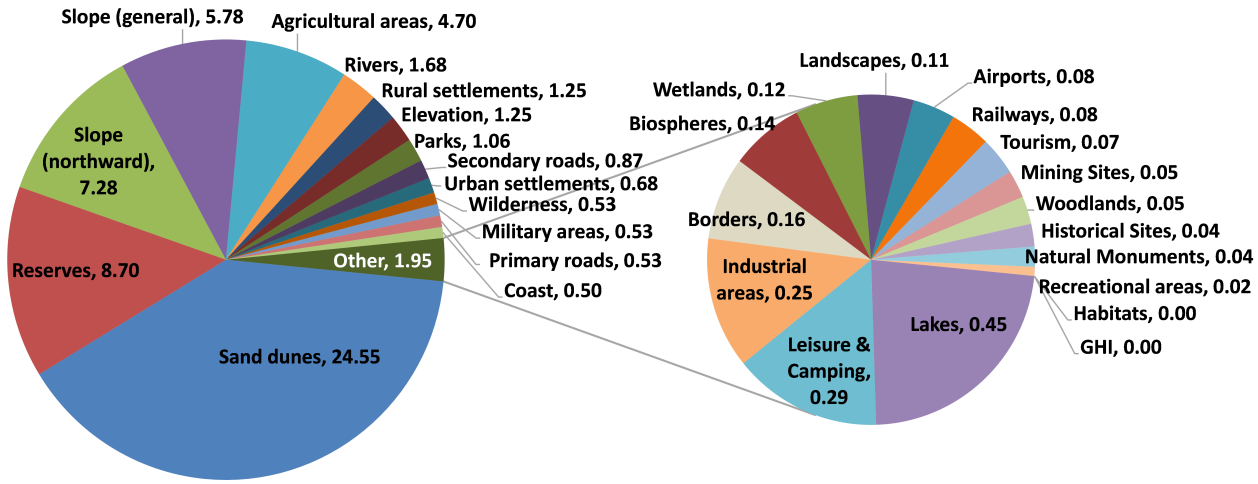

Figure 5.4: Share of total individual land exclusion operated by each eligibility criterion on the entire GCC area - open-field PV

Onshore wind

Once the outcome of the LEA for open-field PV is clear, many similarities can be found with the results of the LEA for onshore wind, as the eligible land identified by this analysis does not differ significantly from what described so far. As a matter of fact, the map of eligible land for onshore wind turbines reported in Figure 5.5 may look the same as that of Figure 5.1 at a first glance. However, a more careful comparison reveals some differences, which need to be investigated in this phase. The most evident one is the reduced area of land excluded in mountainous regions, which stems from the relaxation of the general slope criterion from 10° to 17° and from the absence of the northward slope economic constraint from the onshore wind analysis. Therefore, even if more exclusion criteria are used in this case, the LEA ends up identifying more portions of terrain as available. More precisely, the total amount of land available for onshore wind installations in the GCC regions increases to 58.3% compared to 52.6% in the case of open-field PV.
The other features showing different results between the exclusion map of onshore wind and open-field PV are more subtle and difficult to identify here. However, some are actually visible already. For example, the more stringent buffer values used for rural and urban settlements lead to larger black dots along the main road running parallel to the north-eastern border of Saudi Arabia, while the relaxed constraint of agriculture leaves more space for wind turbines among the fields cultivated close the eastern part the road. This stretches from Bahrain to Jordan in the north-west and can actually be visualised by following the dots just mentioned. Moreover, the effect of the new exclusion criteria for oil&gas pipelines and power lines can be observed in this step. In fact, since the buffer for both primary and secondary roads has been left unchanged, the new thin black lines appearing in the map are necessarily caused by the presence of either the oil&gas or the electricity grid.

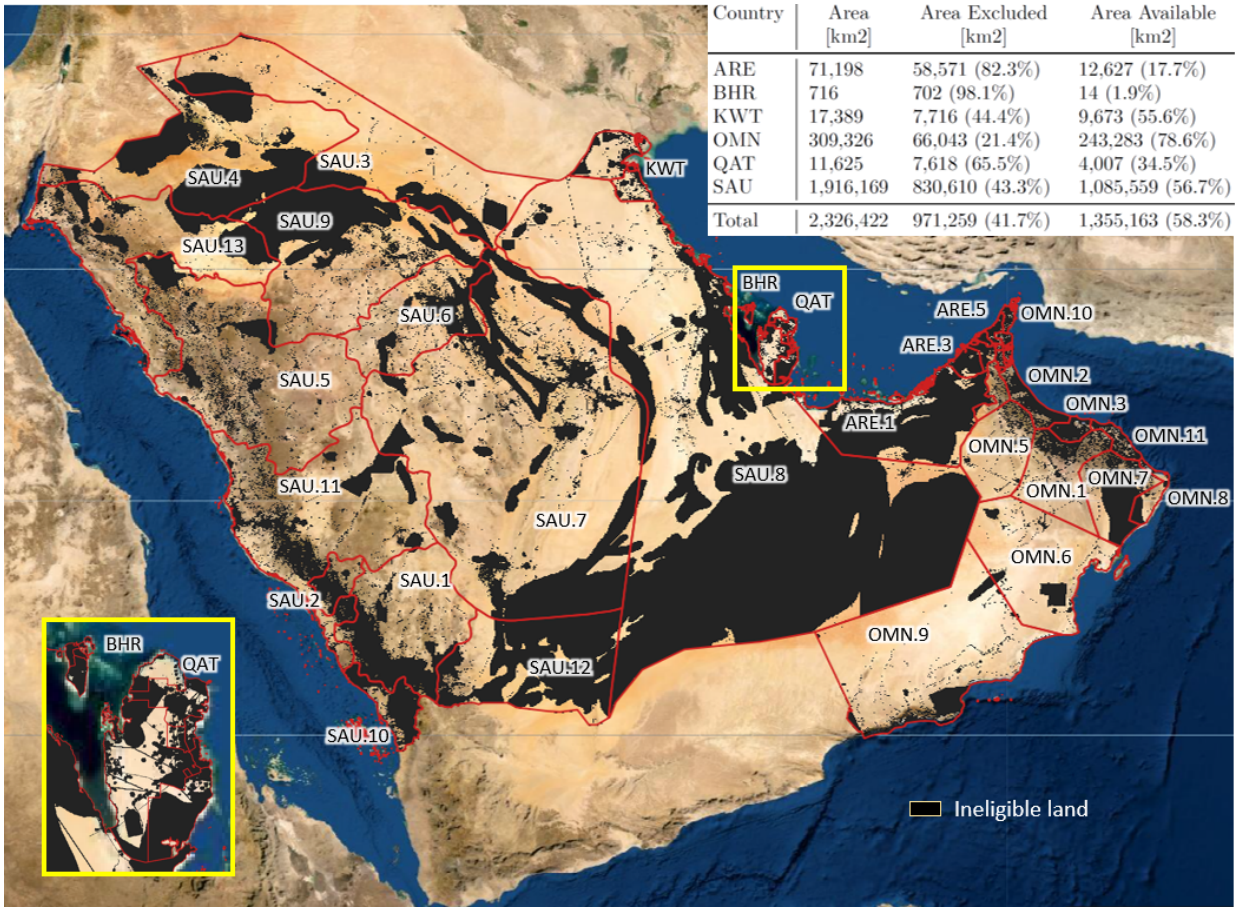

Figure 5.5: Map of land areas excluded by the onshore wind turbines LEA and overall country-wise exclusion results

On a country level, it is easier to refer to the graphs of Figure 5.6 and 5.7 in order to spot the differences, comparing them with Figure 5.2 and 5.3. First of all, the bar charts show that regions ARE.4 and ARE.5 see their share of excluded land decrease by 5-10%. A comparison between the two exclusion matrices reveals

that this is due not only to the reduced effect of slope but also to that of rivers and lakes, whose exclusion buffer distance is lowered in the case of onshore wind. On the contrary, BHR.5 is now entirely excluded as a consequence of the more stringent buffers for urban and rural settlements, but also for airports, whose new elevated buffer (5000 m) becomes extremely influential on such a small region. Since the other regions of Bahrain are once more identified as unavailable, installations of onshore wind turbines is basically impossible on the whole country. As for Kuwait, the only remarkable difference can be observed in KWT.1, its second largest region. Although the reduced buffer for agricultural areas implies a lesser effect of its associated criterion, oil&gas pipes and most importantly the increased buffer for rural settlements lead to 15% more of its territories being excluded from the available land. Similarly, the interplay between an increased exclusion buffer for settlements and a reduced exclusion buffer for agricultural areas leads to the differences in terms of available land also in QAT.2, Qat.3, QAT.5 and QAT.6. As for Oman and Saudi Arabia, multiple regions present differences. Although in the smaller regions this result is also caused by the effects of settlements, agricultural areas and water bodies, slope is usually the main factor to the discrepancies in the final outcome of the LEA between the open-field PV case and the onshore wind one.

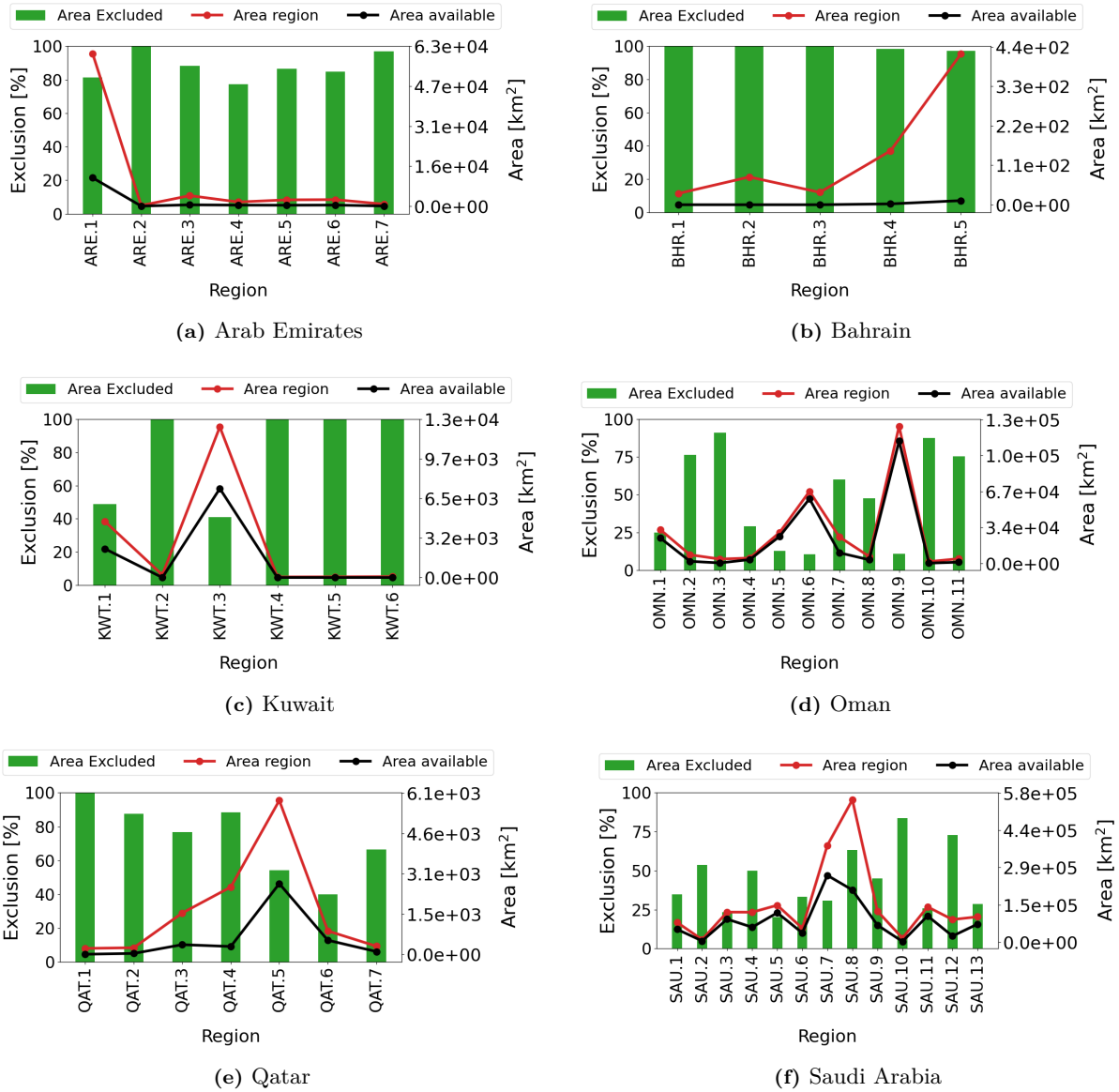

(a) Arab Emirates

(b) Bahrain

(c) Kuwait

(d) Oman

(e) Qatar

(f) Saudi Arabia

Figure 5.6: Representation of the results of the onshore wind turbines LEA on each region

Finally, following the same order used to describe the results of open-field PV, the analysis is concluded by introducing a double pie chart indicating the independent exclusion of each land eligibility criterion on the overall GCC area (Figure 5.8). The greater exclusion is achieved by sand dunes, with the exact same values of 24.55% obtained for open-field PV. The second place is also taken by the same constraint as PV, namely reserves, although here only a slightly different value is found, in spite of the exclusion buffer having decreased significantly. This result can be explained by the fact that natural reserves are few and large portions of land, meaning that their own area determines the result way more than the buffer associated to it. The first and probably greatest difference between the LEA for open-field PV and onshore wind is registered at the third place in order of overall exclusion. In the absence of northward slope and with the constraints for general slope, agricultural areas and rivers all relaxed, the criterion of rural settlements rises to the third spot with 2.8%, more than twice as much as it registered for open-field PV. General slope remains an important constraint at 2.5%, while the exclusion due to low wind speed (economic constraint) ranks fifth at 2%. All other exclusion criteria each score less than 1.5% of exclusion on the whole territory.

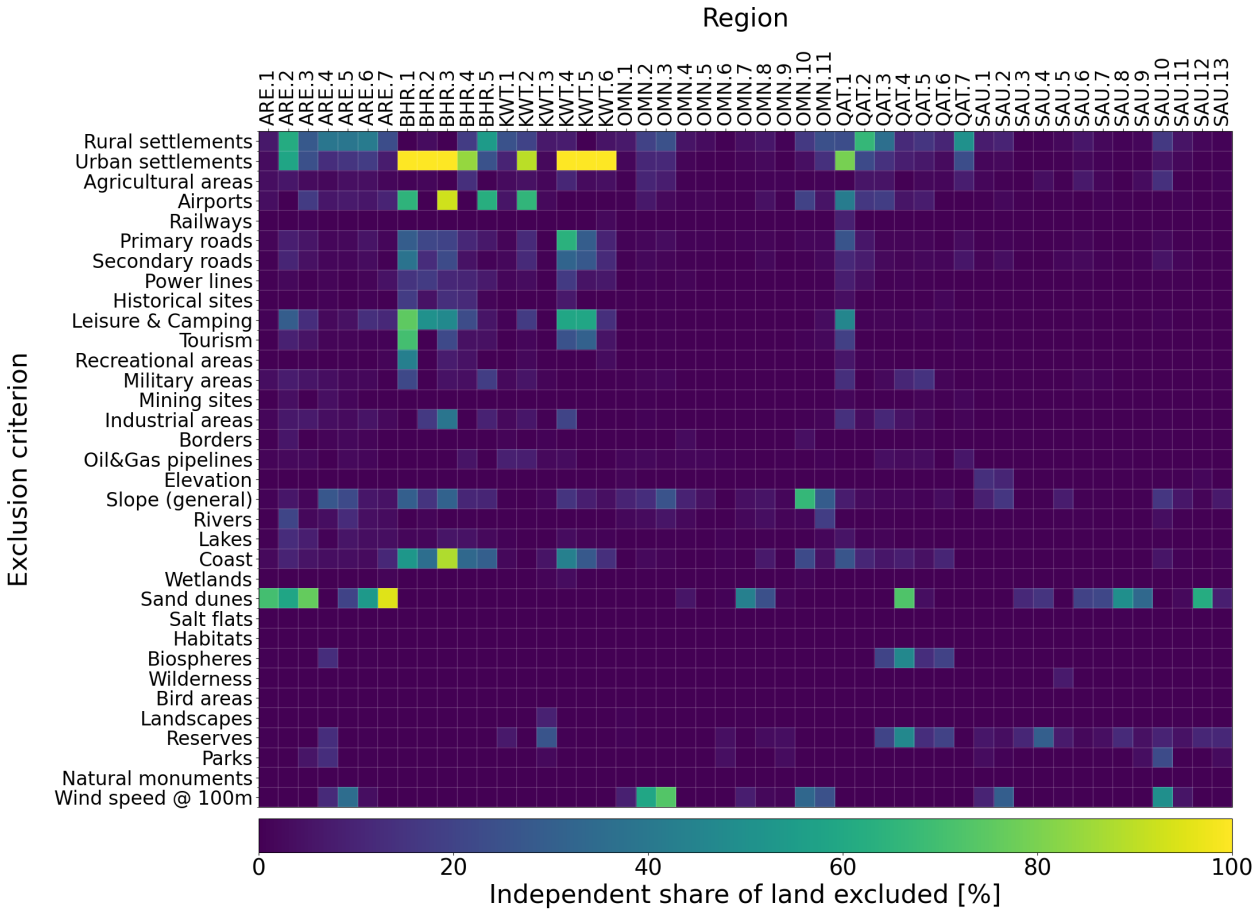

Figure 5.7: Matrix plot of individual land exclusion operated by each eligibility criterion on each region - onshore wind turbines

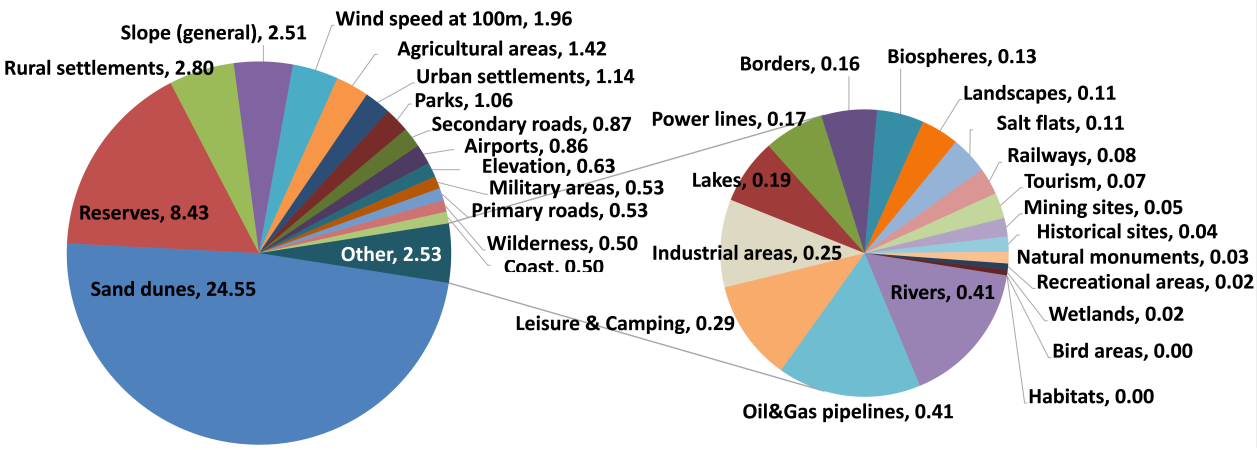

Figure 5.8: LEA Share of total individual land exclusion operated by each eligibility criterion on the entire GCC area - onshore wind turbines

Offshore wind

Lastly, the results of the offshore LEA will be now discussed. To begin with, the country associated with the vastest maritime area before the application of the exclusion criteria is Oman now, whose waters span 0.55 million km^2, whereas Saudi Arabia ranks only second at 0.22 million km^2, despite being the only country present in both the Persian Gulf and the Red Sea. The other GCC countries considerably lag behind in terms of territorial possessions offshore. After the LEA, however, the situation changes dramatically, as best shown in Figure 5.9. A quick look is sufficient to understand that offshore wind is not a viable option for the almost entirety of Oman waters. This strongly limits the offshore wind potential for the entire Peninsula, as those waters had been shown to possess the highest amount by far of wind resources in subsection 2.3.2. Only a tiny portion of the Arabian Sea is eligible, which is shown to be around 90% in Figure 5.10. The reason is immediately offered in Figure 5.11, which indicates water depth as the main cause of the exclusion at approximately the same value of 90%.
Since the reduction of the eligible sea of Saudi Arabia is way lower than that of Oman, the country comes to rank first again also in the case of sea eligibility for offshore wind, and by a considerable margin: 103,000 km^2 against only 37,000 km^2 for Oman. The vast majority of this area is located in the Red Sea, but around 60% of Saudi territorial waters in the Persian Gulf are also eligible (Figure 5.10). In the west, the exclusion is relatively high due to combined effect of shipping routes, coastlines, submarine cables and water depth, as indicated by Figure 5.11, even if the available sea found there is still higher than Saudi possessions in the Persian Gulf. Protected areas also influence the result, but these are typically located around the islands, so that they are usually already covered by the coast criterion already.
After Saudi Arabia and Oman, Qatar and the Arab Emirates follow at around 23,000 km^2 of available sea each, with overall exclusions of 26% and 54% respectively. For them, as well as for Kuwait and Bahrain, the exclusion is mainly due to large buffer associated with coasts.

In general, the map of Figure 5.9 shows the presence of multiple straight lines crossing the seas. Keeping in mind the buffers used for offshore wind (subsection 3.2.1), one can conclude that the larger black stripes find their origin in shipping lanes, whereas the narrower lines could either be power lines of oil&gas pipes. However, the Red Sea does not feature any oil&gas extraction activity, meaning that the narrow lines can only be representative of power lines. In fact, Figure 5.11 shows the value for this constraint as zero in that region. The matrix shows that this is true in almost all cases, as the cells of submarine cables are often higher than zero also in other maritime areas, whereas those of oil&gas score zero in many instances, and do not surpass 10% anywhere.
However, trying to read exact values from the matrix is not simple for such a low and narrow range of exclusion values such as those accomplished by power lines and oil&gas pipes. Therefore, the influence of these criteria can be better understood from the last graph presented in this region, which is reported in Figure 5.12. This clearly shows that pipelines only account for the exclusion of 0.3% of the whole offshore area, whereas power lines score a relatively high value of 4.2%. Shipping routes, although less frequent, have a way larger buffer, which is why they rank higher than power lines at 5%. Coasts can be found at the second

place at around 17% of sea excluded, whereas water depth is the main exclusion criterion at 59%. Borders have not been mentioned so far, in fact they score only slightly above 1%. In the end, the overall exclusion is found at 77.6% (Figure 5.9), so that the eligible sea falls just short of 0.2 million km^2.

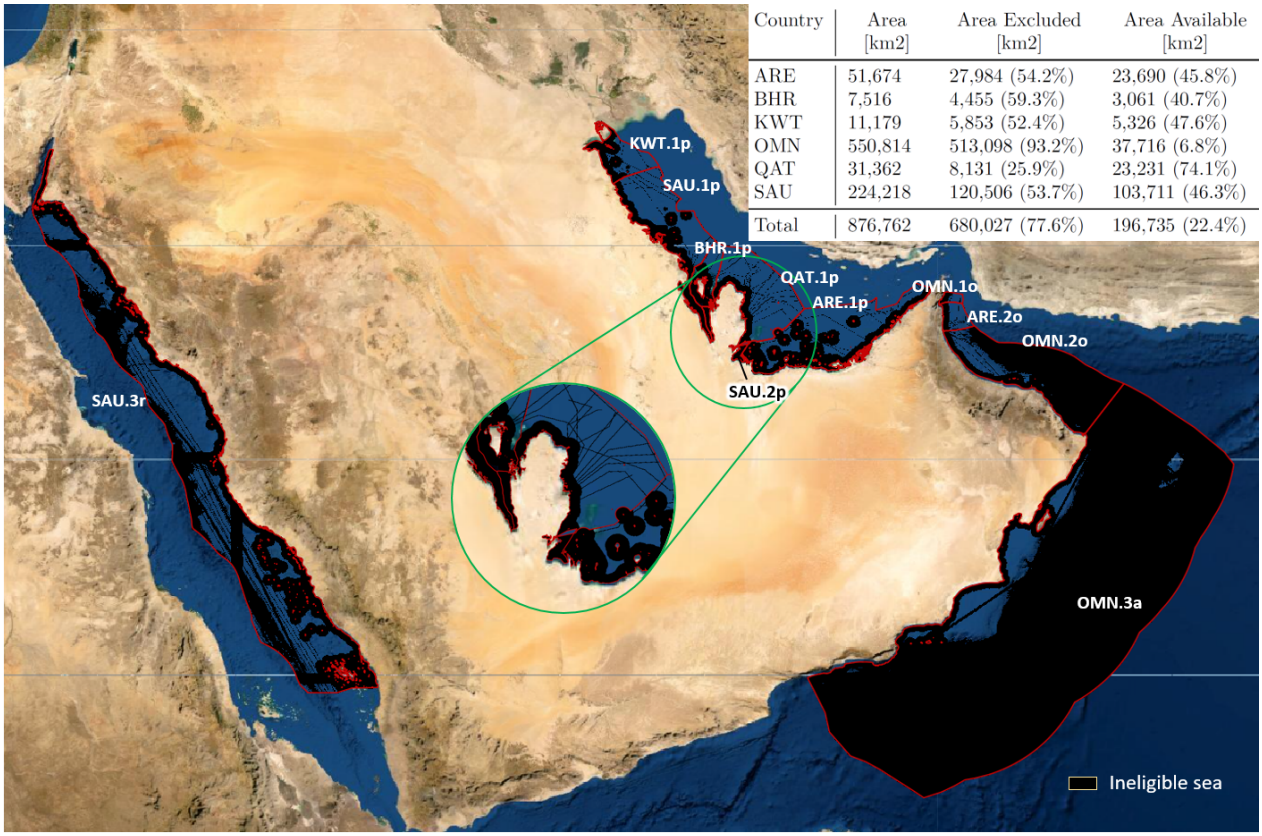

Country	Area [km2]	Area Excluded [km2]	Area Available [km2]
ARE	51,674	27,984 (54.2%)	23,690 (45.8%)
BHR	7,516	4,455 (59.3%)	3,061 (40.7%)
KWT	11,179	5,853 (52.4%)	5,326 (47.6%)
OMN	550,814	513,098 (93.2%)	37,716 (6.8%)
QAT	31,362	8,131 (25.9%)	23,231 (74.1%)
SAU	224,218	120,506 (53.7%)	103,711 (46.3%)
Total	876,762	680,027 (77.6%)	196,735 (22.4%)

Figure 5.9: Map of sea areas excluded by the offshore wind turbines LEA and overall country-wise exclusion results. The zoom helps to notice the presence of pipelines and submarine powerlines close to Qatar's coasts

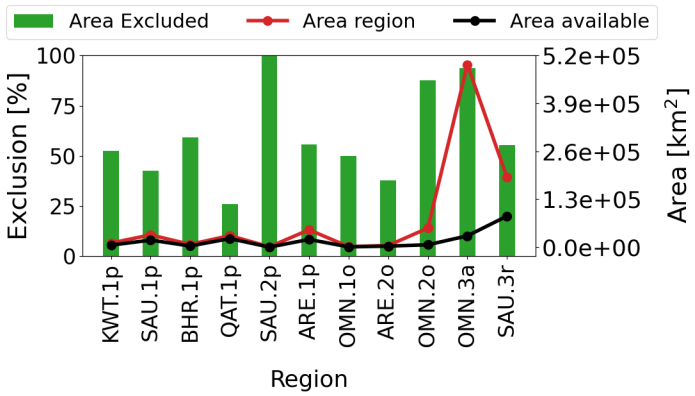

Figure 5.10: Representation of the results of the offshore wind turbines LEA on each region

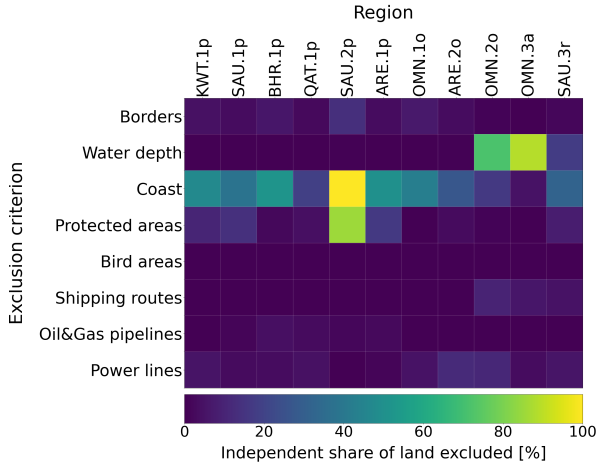

Figure 5.11: Matrix plot of individual land exclusion operated by each eligibility criterion on each region - offshore wind turbines

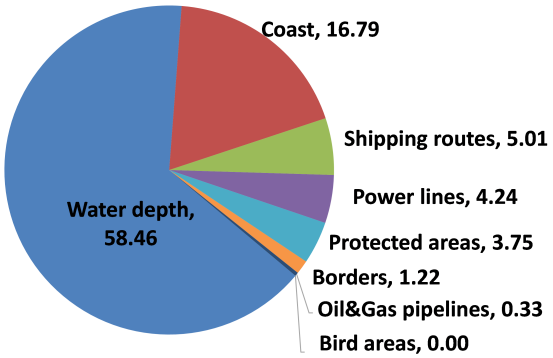

Figure 5.12: LEA Share of total individual land exclusion operated by each eligibility criterion on the entire GCC area - offshore wind turbines

5.2 VRES potential results

The current subchapter is devoted to the analysis of the potential of VRES in the GCC area. This is directly impacted by the outcome of the LEA described in the previous section, which should be kept in mind when approaching this section. The results for each renewable technology will be described following a "bottom-up approach". This means that first the main characteristics of the individual VRES placements are shown; then, the focus is shifted to the regional level, and finally to the national and supra-national level (GCC area). For the regional analysis of onshore technologies, however, relatively small states (Kuwait, Qatar, Bahrain) are still presented at the country level for a better comparison. Besides, their significantly modest size implies that very little solar or wind potential variations are registered among their different regions, meaning that almost the same LCOE is calculated everywhere, which reduces the interest of looking at them at the regional level. The VRES potential of the United Arab Emirates is also studied in the same way as that of the smaller states just mentioned, since the almost entire territory of this country is composed just by one of its seven regions, and since these overall have a size inferior to the average Saudi region.
Each of the steps described above has a different purpose. The goal of checking individual VRES placements is to make sure that they have been designed according to the method described in chapter 3 and therefore in a sensible way. In order to do this, use is made of the main statistical properties of the distribution function describing the techno-economic parameters of all placements. On a regional level and above, the focus is narrowed down only to the cost, efficiency and potential of VRES. As for LCOE, here the average value is presented weighted with the generation potential of the placements. The average FLH, synonym of the efficiency of the technologies potentially installed in the region, are derived by dividing total generation and total capacity, so that they can be directly compared with other sources in literature which use the same approach.

Open-field PV

As mentioned in the introduction of this subchapter, the results obtained with RESKIT are first presented for the individual VRES placements. Table 5.1 reports the outcome of the statistical analysis conducted on all PV farms at the end of the simulation. First and foremost, tilt angles are designed between 17° and 30°, with half of the panels placed between 21.6° to 25.8°. The range of tilt angles therefore is only slightly inferior to that of the latitude coordinates of the Arabian Peninsula, something which is also observed in literature [198]. In particular, Jafarkazemi et al. [198] report an optimal tilt angle of 22° for Abu Dhabi, whereas the model used here finds an average value of 23.5° for the region ARE.1, where Abu Dhabi is located. Moreover, as anticipated in subsection 3.2.2, the parameters set in the tools correctly lead to a mean rated power of the PV farms close to 50 MW and to a minimum value slightly above 5 MW, with the maximum at 8 0MW. The variation is due to the fact that the placing algorithm of GLAES has to adapt to irregular shapes of eligible

areas (especially near region borders), and that each location contains a different share of net available area. Capacity Factors (CFs) are relatively concentrated around the average of 21.8 %, as the standard deviation is registered at only 1.4%. This is in accordance with the values reported for LCOE, whose ratio "standard deviation / mean value" is very close to that of the CFs. Besides, the ratio max / min for these two parameters is almost identical. These trends should indeed be observed, as the cost of electricity differs among PV farms only due to their capacity factor, since the CAPEX per capacity is fixed to a constant value (same design).

Table 5.1: Statistical analysis of the results output by RESKIT across all PV farms

Paramet.	**Tilt** [°]	**Capacity** [MW]	**CAPEX** [€mln]	**Generation** [GWh]	**Avg. CF** [1] [%]	**LCOE** [c€/kWh]	**FLH** [h]
mean	23.6	45.3	22.7	86.4	21.8	2.91	1909
std. dev. [2]	2.8	10.4	5.2	20.3	1.4	0.18	126
min	17.0	5.5	2.7	9.0	18.2	2.22	1592
25%	21.6	45.5	22.7	84.5	20.9	2.84	1828
50%	23.5	49.0	24.5	91.8	21.5	2.94	1881
75%	25.8	51.0	25.5	97.4	22.2	3.03	1947
max	29.7	80.0	40.0	161.7	28.4	3.48	2491

The variation of LCOE in space is probably the most important result of the simulations in RESKIT. In fact, this is among the main drivers of the optimisation of the energy system. For this reason, the value of LCOE of each placement is reported through a scatter plot based on its latitude and longitude. The resulting colormap is shown in Figure 5.13.
Good match can be observed between this colourmap and the DNI map already reported in Figure 2.12a, which indicates that the workflow adopted for the simulations works as expected. In particular, the locations which can produce electricity at the lowest price are located in north-western Saudi Arabia at close to 2.2 €c/kWh. At the other end of the price spectrum, the highest values for LCOE are registered at some of the outermost regions both to the East (Pesian Gulf) and the West, with vast territories at 3.2 €c/kWh or above. The maximum value is actually 3.5 c€/kWh, as can be read in Table 5.1.

The description just made helps to explain the results of Figure 5.14. SAU.10, looking over the Red Sea and bordering Yemen, registers the highest average LCOE at 3.25 €c/kWh. Following next in descending order are the states of Kuwait, Qatar and the Arab Emirates, all of which are in fact sited on the coasts of the Persian Gulf, which is less promising in terms of solar potential, as mentioned earlier. This is not ideal in terms of energy system design, as the eastern and western coasts are also characterised by the highest concentration of population and therefore energy demand, as mentioned in subsection 2.3.3. The figure also shows that the majority of territories feature an average value of LCOE above 3.0 €c/kWh. This particularly holds true for Oman's regions, even though OMN.9, its potentially largest elecricity-producing region and neighbouring Yemen, is below this threshold.
Not surprisingly, SAU.7 and SAU.8, by far the largest regions in the GCC area, show the highest energy potential at 23,000 and 18,000 TWh respectively. SAU.8, the vast Saudi region neighbouring all other coastal states, is larger than SAU.7, where the capital is located. However, given the land eligibility exclusion of the Rub'al Khali desert and the different solar distribution potential suggested by the different average LCOE prices, SAU7 overtakes SAU8 in the ranking of the energy potential. In general, there is a huge discrepancy in energy production between the smallest countries (Kuwait, Qatar, Bahrain) and individual regions of the bigger ones (Oman and Saudi Arabia), but differences of up to two orders of magnitude are also visible among different regions of the same country when it comes to Oman and Saudi Arabia.

[1] Average capacity factor
[2] Standard deviation

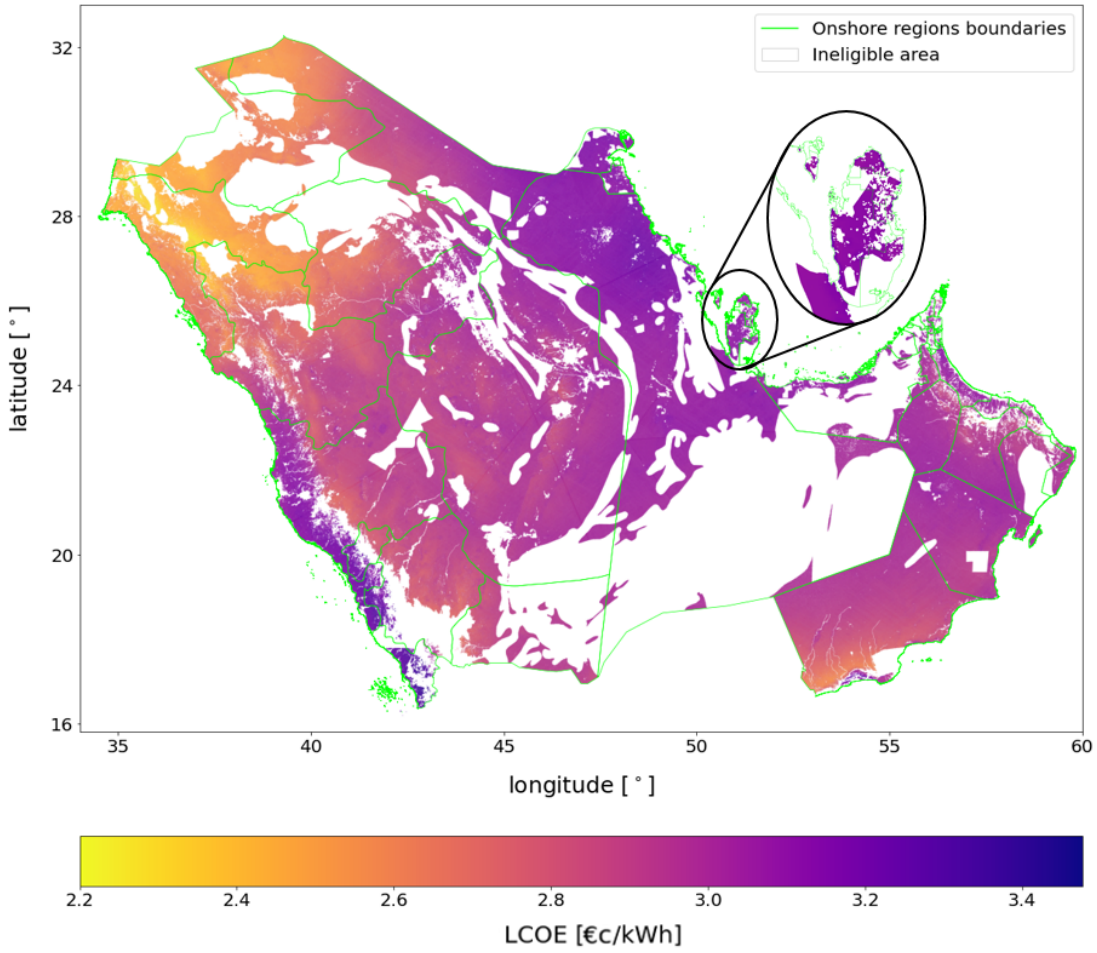

Figure 5.13: Distribution of LCOE of PV farms over the GCC area

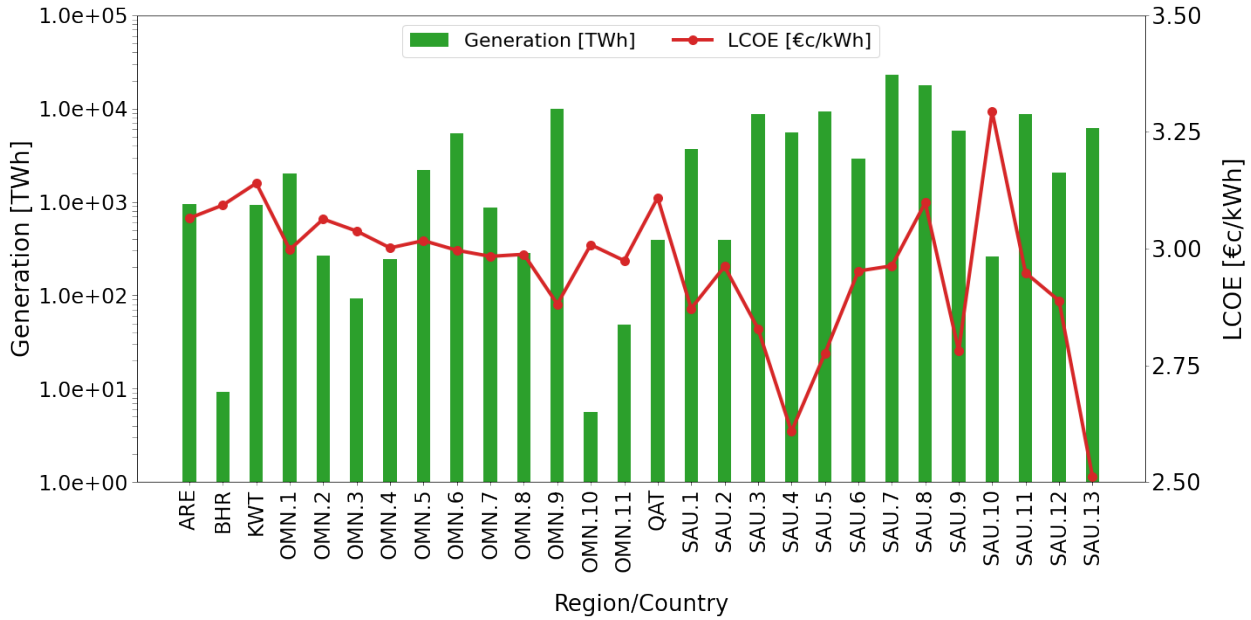

Figure 5.14: Energy potential and LCOE of open-field PV in the GCC area - bigger countries (Saudi Arabia, Oman) are represented at the regional level, the others (Arab Emirates, Bahrain, Qatar, Kuwait) at the national level

A comparison exclusively at the national level is realised in Figure 5.15, which shows the cumulative capacity of PV farms installed in each GCC country as a function of LCOE. Apart from total capacity, the graph is able to show two more important parameters. First, the absolute minimum and maximum LCOE of each state, which is determined by the extremes identified by each curve on the x-axis. Secondly, the maximum value of LCOE at which the vast majority of PV farms are installed, which is defined by the portion of the curve preceding its flat final section. There, the expansion rate of VRES in accordance with eligible land reaches close to its maximum. In fact, the subsequent trait of the curve showing a derivative only slightly above zero is associated with relatively small amounts of VRES installations.
What immediately catches the attention is the substantial difference in terms of capacity among different countries, which naturally results from the size of total (and eligible) land composing each state. Saudi Arabia and Oman both feature more than 10,000 GW of capacity each, whereas Kuwait and the United Arab Emirates register the same installations at around 500 GW. This last result is due to the fact that even though Kuwait has a far smaller territory than Kuwait, the land eligibility excluded more than 80% of the Arab Emirates. Qatar is associated with more than 100 GW of PV farms, whereas Bahrain falls well short 10 GW.
Due to their far greater extension over the Peninsula and consequently their exposure to different solar radiation intensity, installations in Saudi Arabia and Oman exhibit a larger range of LCOE. This results in their associated curves appearing as less steep in the graph. In particular, the LCOE range for the overall installations in the GCC area shown in Table 5.1 is found to coincide with that of Saudi Arabia. For Oman, the installation of more than 98% of PV capacity stops at around 3.05 €c/kWh, whereas the same share is reached by Saudi Arabia at 3.2 €c/kWh. As already mentioned, this point is not the end value of the curve, but the point at which its derivative becomes zero.

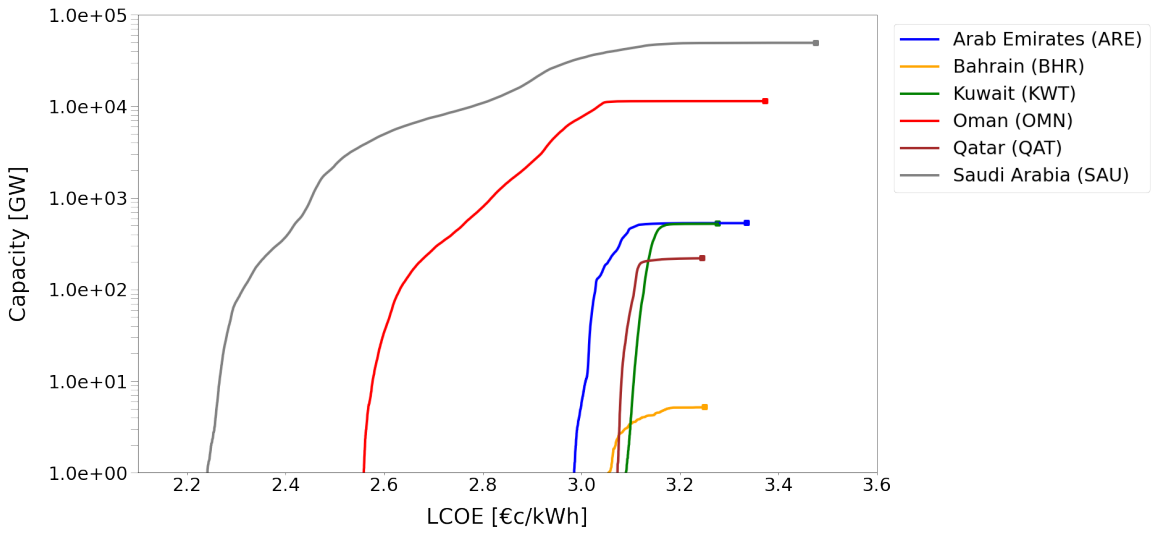

Figure 5.15: Cumulative capacity of PV farms in function of LCOE in the GCC area at the country level

Finally, the summary of the potential of open-field PV in the GCC area is reported in Table 5.2. This shows that the cost of electricity generated through solar power is almost the same in any state if one considers the average LCOE weighted with total generation, with the overall value found at 2.9 €c/kWh, which is exactly the same as that of both Oman and Saudi Arabia. These states are also characterised by the highest average FLH, meaning that the solar potential per unit of eligible area is higher on average over their territory. This is in line with the observations made for Figure 5.13, indicating a higher LCOE in the north-eastern part of the Peninsula. Open-field PV potential in terms of capacity and generation over the entire GCC area is registered at 62,107 GW and 118,349 TWh respectively, most of which comes from Saudi Arabia (49,418 GW and 94,631 TWh).

Table 5.2: Potential of open-field PV in the GCC area at the national and supra-national level

Country	Capacity [GW]	Generation [TWh]	Avg. LCOE [€c/kWh]	Avg. FLH [h]
ARE	531	958	3.1	1805
BHR	5	9	3.1	1789
KWT	522	920	3.1	1762
OMN	11411	21440	2.9	1879
QAT	219	391	3.1	1780
SAU	49418	94631	2.9	1915
GCC	62107	118349	2.9	1906

Onshore wind

The type of analysis just proposed for open-field PV is now repeated for onshore wind. Therefore, the properties of wind turbines output by RESKIT are reported in Table 5.3. In this case, it is particularly interesting to compare the baseline turbine with those installed here. The mean value of capacity of the placements coincides with that of the baseline turbine, and the mean hub height is also very close to the reference (121.5 m and 120 m respectively). Considering the fact that the baseline turbine is set at the reference wind speed of 6.7 m/s, whereas the average wind speed in the GCC area is 6.6 m/s [3], this is an expected result. The entire range of allowed values of hub height is effectively applied, as there are considerable differences of wind speed over the territory under consideration.
Here, the ratio "standard deviation / mean value" for the average capacity factor is significantly different. In fact, if in the case of PV the capacity was only influenced by the share of eligible area of a solar farm, here the design of the individual technology is also an important variable. Another information that can be obtained from the table is that LCOE, as well as FLH and so average CF, show huge variations over the GCC area, which is due to very different wind speeds over the territory, as observed in Figure 2.12b. In particular, LCOE reaches over 30 €c/kWh, so more than 6 times the mean. However, a side check was conducted showing that 14% of wind turbines exhibit a cost above 10 €c/kWh and 8% above 20 €c/kWh.

Table 5.3: Statistical analysis of the results output by RESKIT across all onshore wind turbines

Paramet.	Hub height [m]	Capacity [MW]	CAPEX [€mln]	Generation [GWh]	Avg. CF [%]	LCOE [€c/kWh]	FLH [h]
mean	121.5	4.2	4.2	10.6	28.4	5.38	2489
std. dev.	14.8	0.3	0.4	2.7	5.4	2.50	472
min	88.0	3.2	4.0	2.4	8.0	2.02	702
25%	111.8	4.0	4.0	8.8	24.9	3.94	2185
50%	118.8	4.2	4.1	10.6	28.6	4.70	2502
75%	128.0	4.4	4.2	12.4	32.2	5.86	2824
max	186.0	6.5	7.0	34.5	61.1	32.3	5356

In order to effectively understand the distribution of LCOE over the territory being investigated, Figure 5.16 is created. The aspect of the colourmap is very close to the wind speed map of Figure 2.12b, as expected. Particularly sudden variation of LCOE can be observed in correspondence of two geographical features: mountains and deserts. The first are found along the coasts close the the dark purple areas, whereas the latters are primarily located close to the white areas in the central regions, which are in fact excluded by the LEA. It is therefore not rare to register values at the extreme opposites of the LCOE spectrum in the span of few hundreds meters.

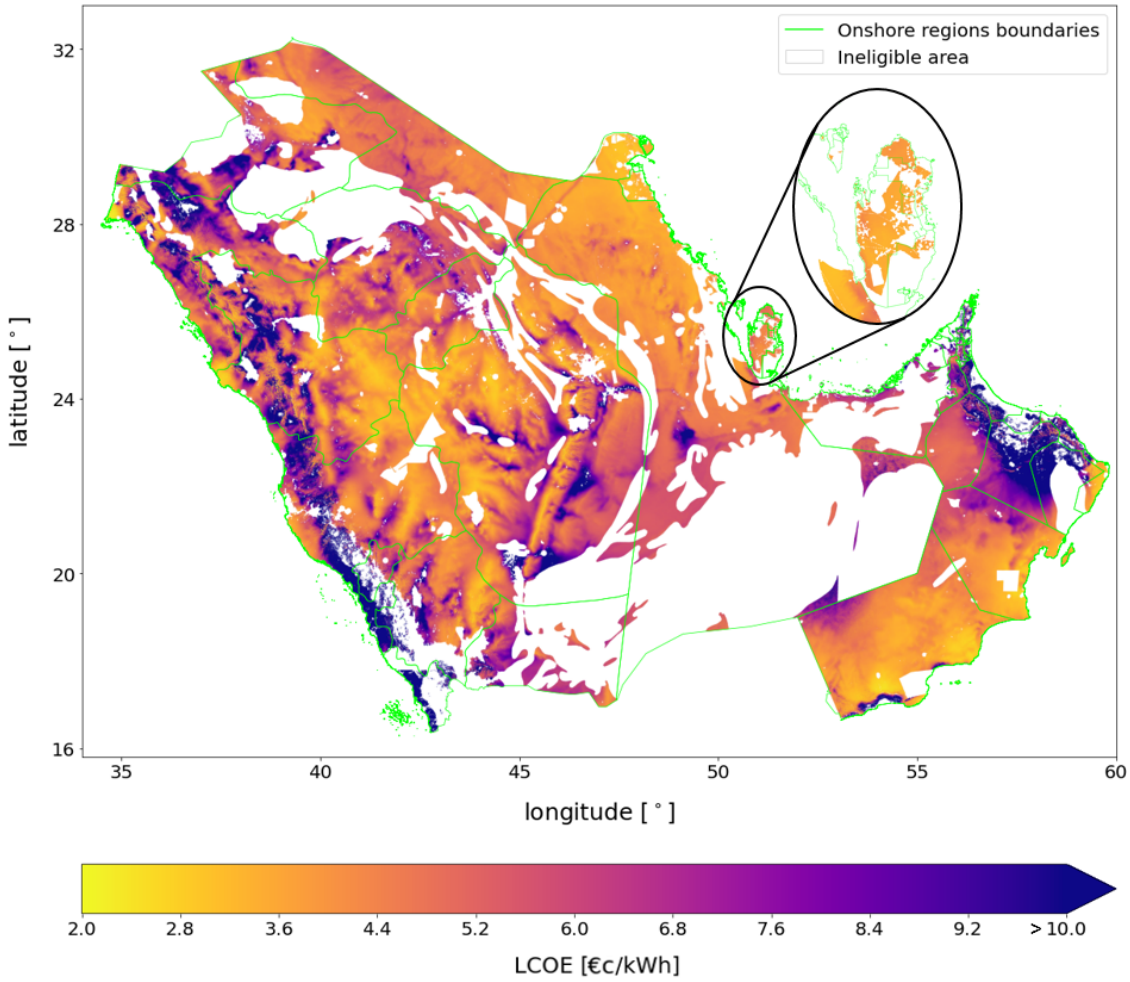

Figure 5.16: Distribution of LCOE of onshore wind turbines over the GCC area

The extreme differences just mentioned are confirmed by Figure 5.17, which reports the average of LCOE at the region or country level depending on the size of the state, together with the associated generation potential. While most regions feature LCOE of around 5.0 €c/kWh and thus close to the mean value reported by Table 5.3, 6 regions exceed 8.0 €c/kWh. These are located mostly in Oman, particularly to the East, and are characterised by a small territory mainly occupied by the Al Hajar mountains. However, the highest average value is registered in SAU.10 at 16 €c/kWh. Once again, due to their considerable area, SAU.7 and SAU.8 score best in terms of energy potential, but this time they do not go beyond 5,000 TWh. The third place is also occupied by the same region as in the case of PV, namely OMN.9. The difference is that OMN.9 also enjoys the third lowest LCOE at 4.0 €c/kWh. As for the remaining 4 coastal states, similar potentials are found again in the range of 80-280 MWh, with the exception of Bahrain: in this case, production falls short of 1 TWh and is therefore negligible if compared to the other states. This is almost exclusively due to the LEA, as a far higher potential would otherwise be registered since the average wind speed is above 6.5 m/s in more than half of the country [3]. Contrarily to what observed for PV, Qatar and Kuwait register among the lowest average LCOE. In particular, Kuwait scores the absolute best just above 3.0 €c/kWh, exactly the same price found for PV.

A comparison at a country level among all GCC members is offered in Figure 5.18. The x-axis is cut at 8.0 €c/kWh to better compare the different countries and because after this value no curve shows a significant increase as installations become very rare. Onshore wind turbine placements in Qatar range between 4.0 and 6.0 €c/kWh, whereas those of Kuwait, between 3.0 and 6.0 €c/kWh. However, the majority of turbine installations for Kuwait happens below 3.3 €c/kWh, whereas that of Qatar below 4.0 €c/kWh. Saudi Arabia and Oman show a far greater extent of LCOE, but more than 80% of their installations is concentrated in

the first 15% of the price range, which was calculated in a side-check. Such considerable cost difference were not observed for PV farms. Finally, Bahrain's capacity is extremely low (0.1 GW) and concentrated around the same price of 4.5 €c/kWh already reported in Figure 5.17.

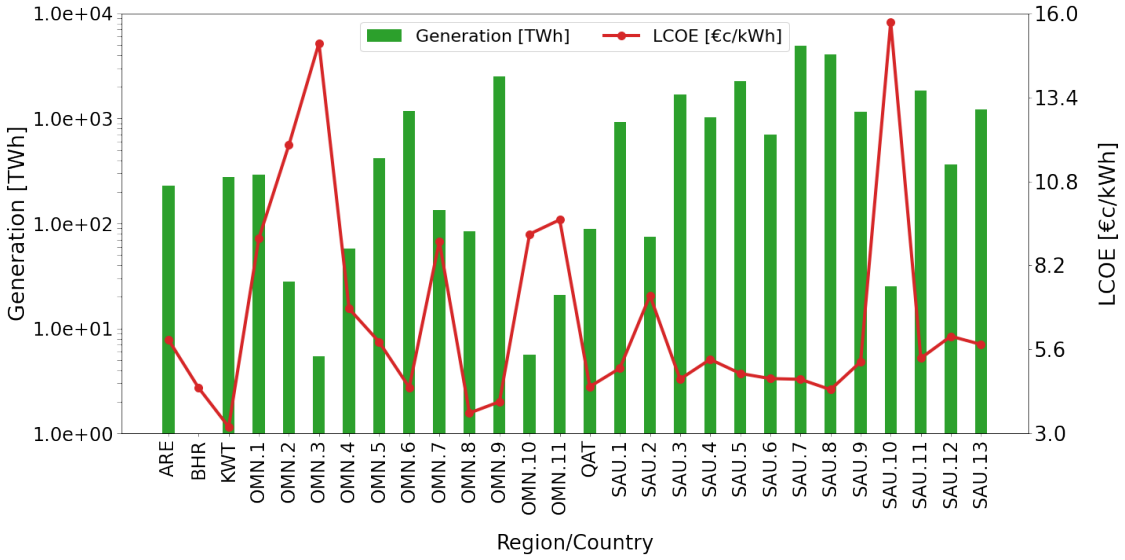

Figure 5.17: Technical potential and LCOE of onshore wind turbines in the GCC area - bigger countries (Saudi Arabia, Oman) are represented at the regional level, the others (Arab Emirates, Bahrain, Qatar, Kuwait) at the national level

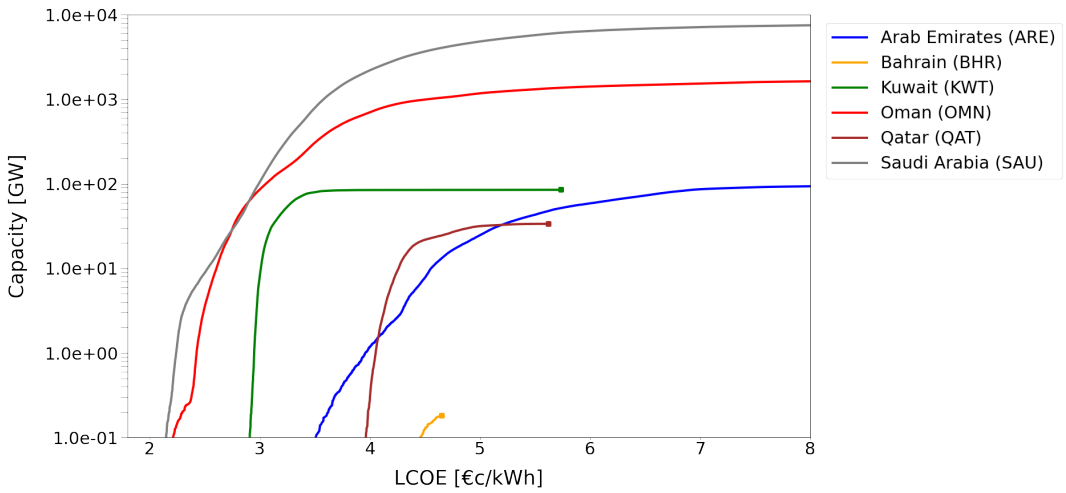

Figure 5.18: Cumulative capacity of onshore wind turbines in function of LCOE in the GCC area at the country level. The x-axis is cut at 8.0 €c/kWh

Table 5.4 offers the summary of the results in terms of potential for the GCC countries and area as a whole. The total capacity for the region is found at 10,155 GW, whereas the generation is 25,613 TWh. Saudi Arabia is responsible for around 80% of it and Oman for the vast majority of the remaining 20%. The FLH associated to these values span the range of ∼2300-3300 h/a. This is considerably higher than the FLH observed for PV; however, average LCOE values are also higher due to the higher investment costs. The Arab Emirates are overall the regions with the highest cost of electricity at 5.9 €c/kWh, whereas Kuwait holds the lowest price also at a state level with 3.2 €c/kWh. On a supra-national level, the GCC area features an average cost of 4.9 €c/kWh, which again is dictated by the price of Oman and Saudi Arabia, whose LCOE are almost the same. This similarity among the two countries could not be predicted just by looking at the

LCOE colormap of Figure 5.16 as in the case of PV, given the irregular distribution of wind energy resources over the Peninsula.

Table 5.4: Potential of onshore wind in the GCC area at the national and supra-national level

Country	Capacity [GW]	Generation [TWh]	Avg. LCOE [€c/kWh]	Avg. FLH [h]
ARE	101	230	5.9	2270
BHR	0.2	0.5	4.4	2702
KWT	85	278	3.2	3271
OMN	1833	4729	4.8	2580
QAT	34	88	4.4	2628
SAU	8102	20287	4.9	2504
GCC	10155	25613	4.9	2522

Offshore wind

Offshore wind is the last technology analysed in this section. First, the statistical analysis conducted on the individual placements is reported in Table 5.5. Even if capacity was chosen to be the same for all offshore turbines, water depth and shore distance vary and therefore impact the cost significantly. The table shows that turbines are potentially placed in waters up to approximately 1550 m deep and also as far as 243 km from the coast. Due to huge variations of these parameters as well as wind speed, LCOE also shows an extremely wide spectrum, from around 5.0 €c/kWh to almost 100 €c/kWh. In spite of this, the ratio "standard deviation / mean" for LCOE is only 30% higher than that of onshore wind turbines, meaning that extreme values are relatively rare as observed for onshore wind. FLH are distributed over the range ∼2900-4800 h/a, which is narrower than that of onshore wind, which could be due to the fixed design. In any case, as all turbines are identical, this value is influenced solely by the wind speed.

Table 5.5: Statistical analysis of the results output by RESKIT across all offshore wind turbines

Param.	Water depth [m]	Shore distance [km]	Capacity [MW]	CAPEX [€mln]	Generation [GWh]	Avg. CF [%]	LCOE [€c/kWh]	FLH [h]
mean	-312	61.0	9.4	23.7	27.1	32.9	11.60	2884
std.dev.	337	34.8	0.0	4.1	8.3	10.1	6.85	885
min	-1557	15.0	9.4	16.4	2.7	3.3	4.97	288
25%	-623	34.3	9.4	20.7	21.3	25.9	7.91	2266
50%	-93	54.1	9.4	23.7	29.1	35.3	9.48	3092
75%	-30	81.6	9.4	26.2	32.4	39.3	13.17	3444
max	-1	243.6	9.4	43.2	45.0	54.7	97.17	4792

The colourmap of Figure 5.19 helps to identify the areas with the highest potential. This is also similar to the wind speed map of Figure 2.12b, meaning that the influence of distance from shore impacts LCOE less than wind speed. In any case, the areas where installation is more convenient are necessarily located close to some portions of the coasts, since almost all locations farther away offshore have been made ineligible by the water depth constraint, as explained in section 5.1. In some points, the LCOE of offshore wind even becomes as low as that of onshore wind, coming close to 5.0 €c/kWh. The best location seems to be that of the southern coasts of Oman, which is in line with the wind speed map of the GWA Figure 2.12b. However, The eastern-most part of the Arabian Sea also features the group of wind turbines farthest away from coast at around 240 km from shore. Their cost is consequently very high, but they are not responsible for the highest LCOE encountered in the GCC area. In fact, after changing the range of the color bar a closer look reveals that while these turbines feature indeed an LCOE above 75 €c/kWh in spite of the high wind speed, the most expensive electricity is produced in the uppermost area of the Gulf of Oman.

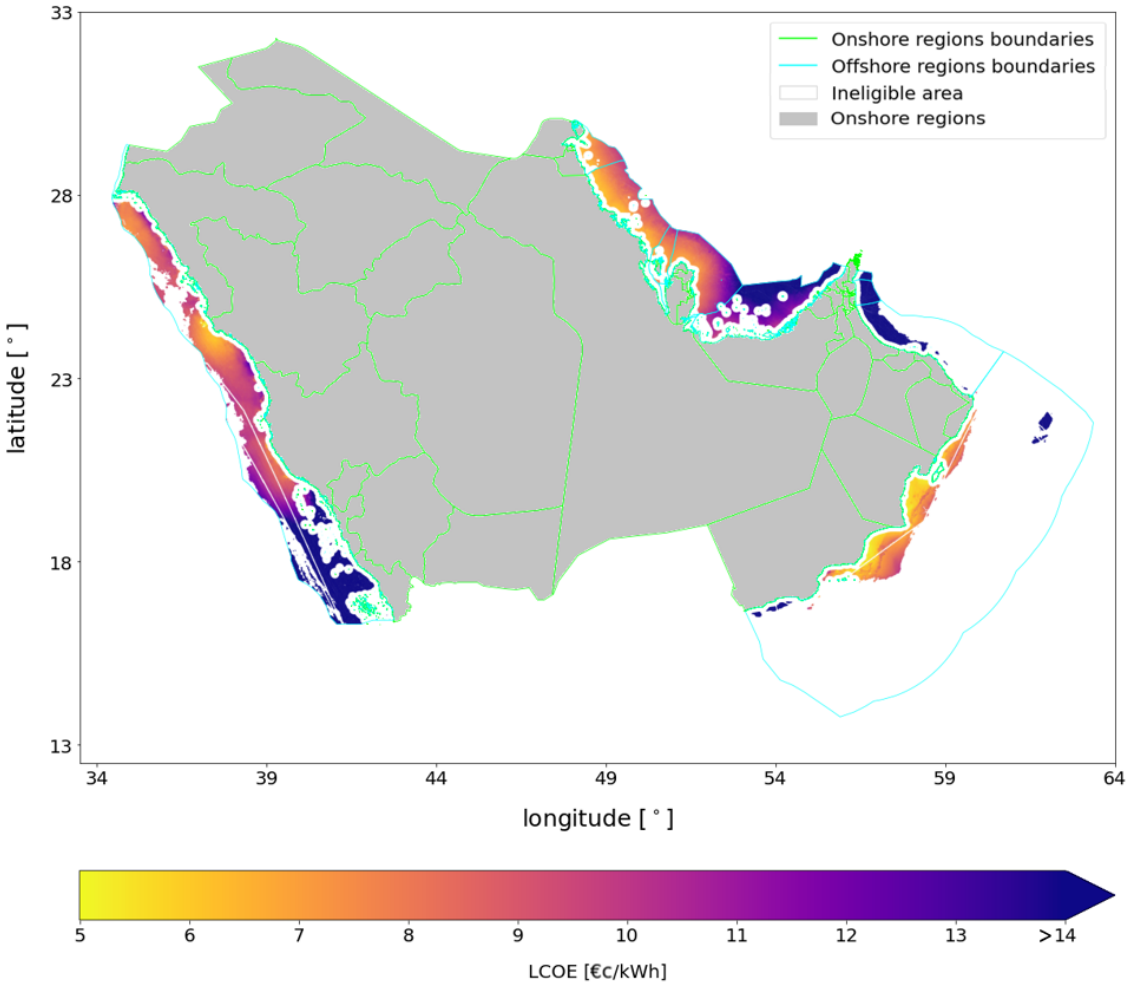

Figure 5.19: Distribution of LCOE of offshore wind turbines over the GCC area

Even when shifting the focus to the regional level and reporting only the average LCOE, differences in cost remain huge. These discrepancies are typically found between the offshore regions of the Gulf of Oman, namely ARE.2o, OMN.1o and OMN.2o, and all the other ones. The most prominent example of expensive energy production is that of 61 €c/kWh reported for OMN.1o, as this is a tiny stripe of water located exactly were the wind speed drops the most. The other regions in the Gulf of Oman also show high values at close to 30 €c/kWh. Due to the low wind speeds as well as their small extension in space, production in these regions is negligible never reaching 40 TWh. In the other seas, better results are found: LCOE remains typically close to 8.0 €c/kWh, with energy production almost always within the range ∼60-600 TWh. The only exception consists in SAU.3r, which corresponds to Saudi waters in the Red Sea: due to its larger extent, production reaches approximately 1500 TWh, with the average cost still relatively low around 10 €c/kWh. In accordance with the colourmap of Figure 5.19, OMN.3a registers the lowest LCOE nearing 7.0 €c/kWh. Therefore, Oman registers both the most and least expensive average cost for offshore wind turbines at the regional level.

Moving up one level and thus adopting a country-wise perspective, Figure 5.21 shows how the cumulative capacity of offshore wind turbines compare to LCOE. What is most interesting to notice is that, differently to what observed for onshore technologies, the capacity of Bahrain surges way closer to that of Kuwait, while Qatar reaches the Arab Emirates. These, in turn, posses almost the same capacity as Oman, which is the biggest difference with respect to the previous cases. In fact, Oman has the vastest territorial waters, but the majority of it is ineligible, while those lying in the Gulf of Oman are characterised by very low wind potential. The graph also shows that placements of most turbines are possible over a wide range of LCOE values, as all curves keep increasing relatively slowly.

In the case of Oman, two sections showing a rapid increase in capacity are visible in the figure: the first one going between the values of 5 €c/kWh and 9 €c/kWh, while the second between 27 €c/kWh and 35 €c/kWh. The latter is more difficult to notice, but of comparable size to the first range, given the logarithmic scale adopted for the plot. More specifically, 70% of onshore capacity is associated with the first price range, and 20% with the second. In other words, turbines are mainly installed in two separate ranges of LCOE, which can indeed be compared to the average cost values of the Arabian Sea and the of Gulf of Oman of 7 €c/kWh and 30 €c/kWh respectively, as shown in Figure 5.20. Two "knees" can also be observed in the curve of Saudi Arabia, with up to 60% of capacity located between 7 €c/kWh and 10 €c/kWh. The second significant LCOE range is instead between 13 €c/kWh and 17 €c/kWh. The pattern just described justifies the average LCOE of 8 and 10 €c/kWh reported for Saudi Arabia's offshore regions SAU.1p and SAU.3r presented in Figure 5.20. However, the curve of cumulative capacity reported for this country in Figure 5.21 extends until 27 €c/kWh. In fact, Saudi Arabia includes areas with very low potential as well, which can be observed in the southern portion of the Red Sea in Figure 5.19.

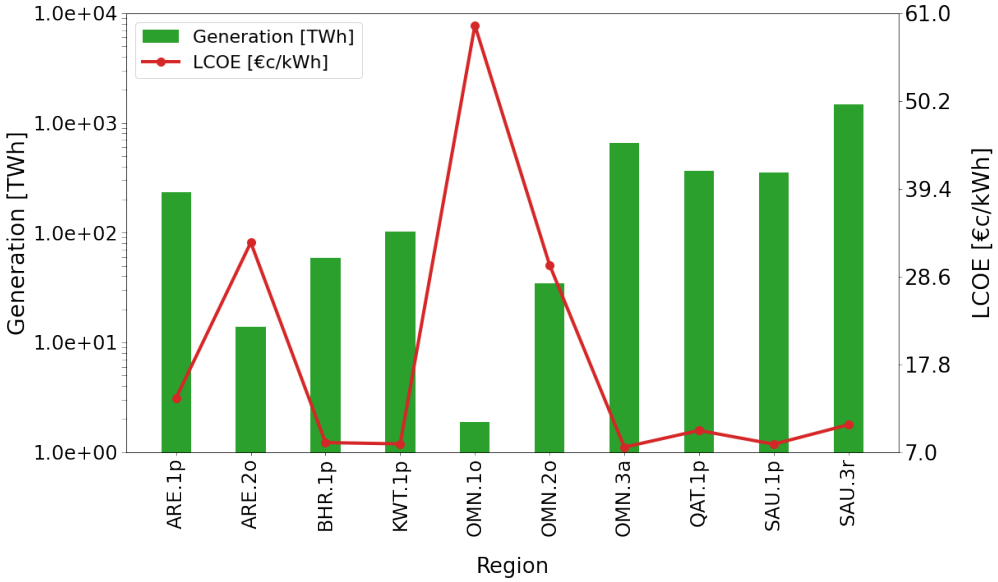

Figure 5.20: Technical potential and LCOE of offshore wind turbines in the GCC area. No data is reported for SAU.2p, as this region is completely excluded by the LEA

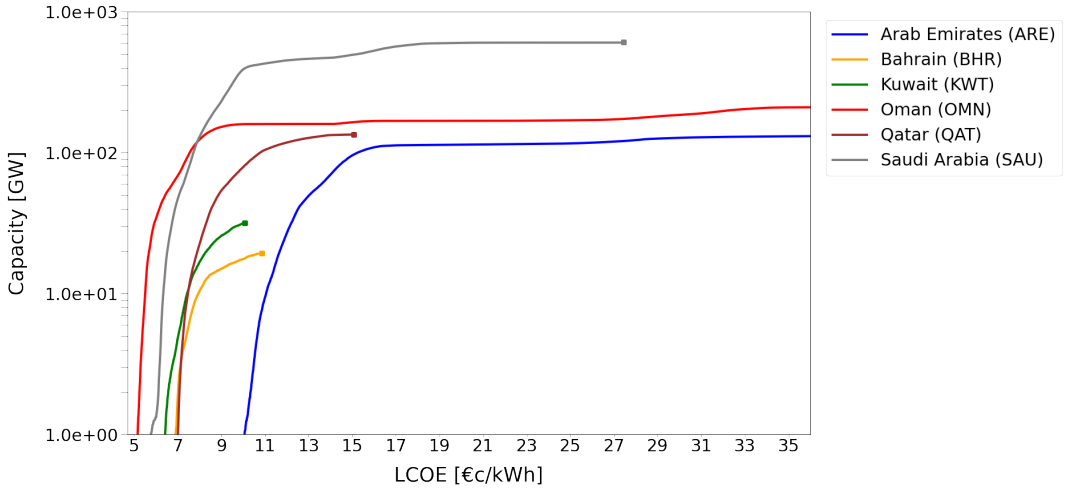

Figure 5.21: Cumulative capacity of offshore wind turbines in function of LCOE in the GCC area at the country level. The x-axis is cut at 18 €c/kWh

Lastly, the potential for the GCC area by country and as a whole is reported in Table 5.6. The results match what has been described so far, as they indicate that the Arab Emirates have on average very low FLH. On the contrary, this variable is high on average for Oman since most of its turbines are located in the Arabian Sea where wind speeds are high. Also in accordance to what has been shown until now, the lowest LCOE is registered again by Kuwait at 8.0 €c/kWh. The region then ends up offering the cheapest installation of wind turbines at both the regional and national level, both onshore and offshore. Production there, however, is low also offshore (102 TWh). The waters of Oman seems to be the second most promising, with 688 TWh at 8.9 €c/kWh on average. On a GCC level, the LCOE is exactly twice as much as that of onshore wind (9.9 €c/kWh and 4.9 €c/kWh respectively), with the maximum electricity producible over the sea at around 3300 TWh, only 13% of the onshore wind case. Although the lack of an optimised design certainly plays a role [6], offshore resources are found to be relatively scarce when compared to onshore ones.

Table 5.6: Potential of offshore wind in the GCC area at the national and supra-national level

Country	**Capacity [GW]**	**Generation [TWh]**	**Avg. LCOE [€c/MWh]**	**Avg. FLH [h]**
ARE	137	248	14.7	1813
BHR	19	59	8.2	3045
KWT	32	102	8.0	3230
OMN	216	688	8.9	3190
QAT	134	368	9.7	2739
SAU	604	1827	9.9	3026
GCC	1141	3292	9.9	2884

6 | Energy System Results

This section presents the results obtained from the optimisation of the energy system following the methodology detailed in chapter 4. In particular, the three scenarios defined as "main scenarios" are discussed in section 6.1. These scenarios are meaningful by themselves, hence the optimised set-up of each of their system components is analysed in depth, always making comparisons across all three scenarios. In the second and last part of the chapter, section 6.2 deals with twelve additional scenarios. These are called "functional", since they are run to obtain specific information regarding the behaviour or the costs of the system. Consequently, only the most important results of the functional scenarios with respect to the research goals of this study are reported.

6.1 Main scenarios results

This section discusses the results of the three main scenarios, namely: the cooperation scenario, the isolation scenario and the export scenario, as described in section 4.1. For this purpose, each component of the system is discussed separately considering all three scenarios, rather than discussing each scenario individually. The system components discussed in subsection 6.1.1 to 6.1.4 are, in order of appearance and reflecting the process chain of green hydrogen supply: generation, transmission, conversion and storage. Lastly, subsection 6.1.5 discusses the three main scenarios from a cost perspective, allowing to confirm and expand some considerations of the previous part of the chapter.

6.1.1 Electricity generation

The most interesting results of optimisation regarding electricity generation lie in the differences and similarities encountered among the three main scenarios relatively to some very specific features of the system. For this subsection, the main focus is on the optimal generation mix of VRES and the location of optimal layout of VRES installations over the Peninsula. Besides, some statements can only be made if all these scenarios are taken into account. Since it is often necessary to mention multiple scenarios when discussing these aspects, each topic is dealt with by mentioning all scenarios which are relevant to it, rather than analysing each scenario separately.

First and foremost, a sanity check has to be performed to make sure that generation is greater than consumption. This consists in comparing the overall electricity generation computed at the end of optimisation with respect to the total equivalent primary electricity demand assigned to the system. This is also necessary in order to fully understand the meaning of the Levelised Cost Of Combined Electricity and Hydrogen (LCOCEH) parameter which will be mentioned in subsection 6.1.5. As explained in subsection 4.2.5, 1098 TWh of electricity and 867 TWh of gaseous hydrogen are required by the system in both the cooperation and the isolation scenario. Considering the efficiency of the electrolyser of 70% assumed for the modeling, the overall theoretical primary electricity demand would amount to 2337 TWh. As reported in Table 6.1, the actual production from VRES comes very close to this number at 2402 TWh and 2422 TWh for the cooperation and the isolation scenario. This means that, excluding the losses occurring during electrolysis, the system efficiency is very high at around 97% in both cases. This is line with the high efficiencies assumed for the transmission and storage technologies, also suggesting that the less efficient re-conversion technologies are not widely used, as subsection 6.1.3 will prove more in detail. Once liquid hydrogen export is considered and hydrogen liquefiers are consequently installed, an additional input of around 8.5% of electricity is needed bringing total generation at 2607 TWh. Considering the hydrogen losses of 2% on the liquefier and the 6.8 kWh of electricity needed to liquefy one kilogram of hydrogen as reported in Table 4.3, the theoretical primary electricity demand would rise at least to 2540 TWh. Ignoring again losses on the electrolyser and the liquefier as well, the same system efficiency of 97.3% is found for the export scenario as for the cooperation scenario.
Following these considerations, the significant losses the system faces considering the sheer sum of hydrogen and electricity demand with respect to electricity generation must be almost entirely linked to the hydrogen production chain. In particular, comparing final energy demand with primary electricity generation, the losses of the system as a whole are equal to 18% and 25% in the case of gaseous and liquid hydrogen demand respectively.

Table 6.1: Optimal installations and electricity generation of VRES at the national and supra-national level across the three main scenarios

Parameter	Scenario	ARE	BHR	KWT	OMN	QAT	SAU	GCC
Open-field PV capacity [GW]	Cooperation	113	5	43	112	35	210	520
	Isolation	245	5	115	74	94	262	794
	Export	164	5	45	164	33	193	605
Open-field PV generation [TWh]	Cooperation	172	9	58	176	57	362	833
	Isolation	369	9	182	123	140	418	1240
	Export	266	9	65	256	53	309	958
Open-field PV FLH [h]	Cooperation	1522	1683	1349	1561	1629	1724	1602
	Isolation	1506	1740	1583	1662	1589	1595	1561
	Export	1622	1715	1444	1561	1606	1601	1583
Onshore wind capacity [GW]	Cooperation	23	0	63	124	0	381	591
	Isolation	29	0	8	27	0	403	467
	Export	23	0	65	146	0	367	602
Onshore wind generation [TWh]	Cooperation	42	0	165	384	0	978	1569
	Isolation	52	0	21	72	0	980	1127
	Export	47	0	172	470	0	960	1649
Onshore wind FLH [h]	Cooperation	1826	-	2619	3097	-	2567	2654
	Isolation	1793	-	2625	2667	-	2432	2413
	Export	2043	-	2646	3219	-	2615	2739
Offshore wind capacity [GW]	Cooperation	0	0	0	0	0	0	0
	Isolation	0	18	0	0	0	1.3	19
	Export	0	0	0	0	0	0	0
Offshore wind generation [TWh]	Cooperation	0	0	0	0	0	0	0
	Isolation	0	52	0	0	0	2.6	55
	Export	0	0	0	0	0	0	0
Offshore wind FLH [h]	Cooperation	-	-	-	-	-	-	-
	Isolation	-	2889	-	-	-	2005	2895
	Export	-	-	-	-	-	-	-

After having conducted this brief sanity check, the generation mix can be studied. After observing the LCOE results reported in the previous section 5.2, open-field PV might be expected to be by far the main energy source chosen by the optimisation tool. However, the actual outcome of optimisation is radically different: the share of PV with respect to the total energy generation mix ranges between 35% and 51% according to the different scenarios, whereas onshore wind accounts for between 47% and 65% of the energy produced. This deviation from the expected results can be explained by taking into account the different synergies that can be found between the feed-in time series of either solar or wind energy and that of the modeled energy demand, both on a yearly or daily scale, in order to minimise storage and curtailment. This point will be dealt with in length in section 7.2. As for the important variation in the optimal share of the VRES technologies across the scenarios, this largely depends on the strong reliance of the system on cross-country exchange especially for hydrogen production, as will be explained more in detail in subsection 6.1.2.
Besides, Table 6.1 shows that the case where the system relies more on PV is the isolation scenario, when less flexibility is possible. There, an increase of production from PV is registered across all countries apart from Oman, whereas the opposite trend is observed for onshore wind in Kuwait and Oman, with a relatively slight increase in Saudi Arabia and the Arab Emirates. No wind penetration is observed in Bahrain due to the almost entire exclusion of eligible locations by the LEA, while Qatar also relies exclusively on PV. This last result, however, is entirely due to optimisation reasons and not to the previous LEA, since wind potential in this country is comparable with its total energy demand.

Apart from Bahrain and Qatar, where almost no electricity originates from wind turbines, PV dominates the

generation mix of very few regions. This is shown to be the case in all scenarios where the GCC countries are connected, as can be observed in Figure 6.1 to 6.3. This is also the case for the isolation scenario, although a remarkable difference is shown in Kuwait, where PV achieves a way higher penetration than wind turbines. This is the first hint regarding the particular and sometimes unpredictable synergies that the tool can establish among different VRES depending on the flexibility of the system in order to reduce overall costs.

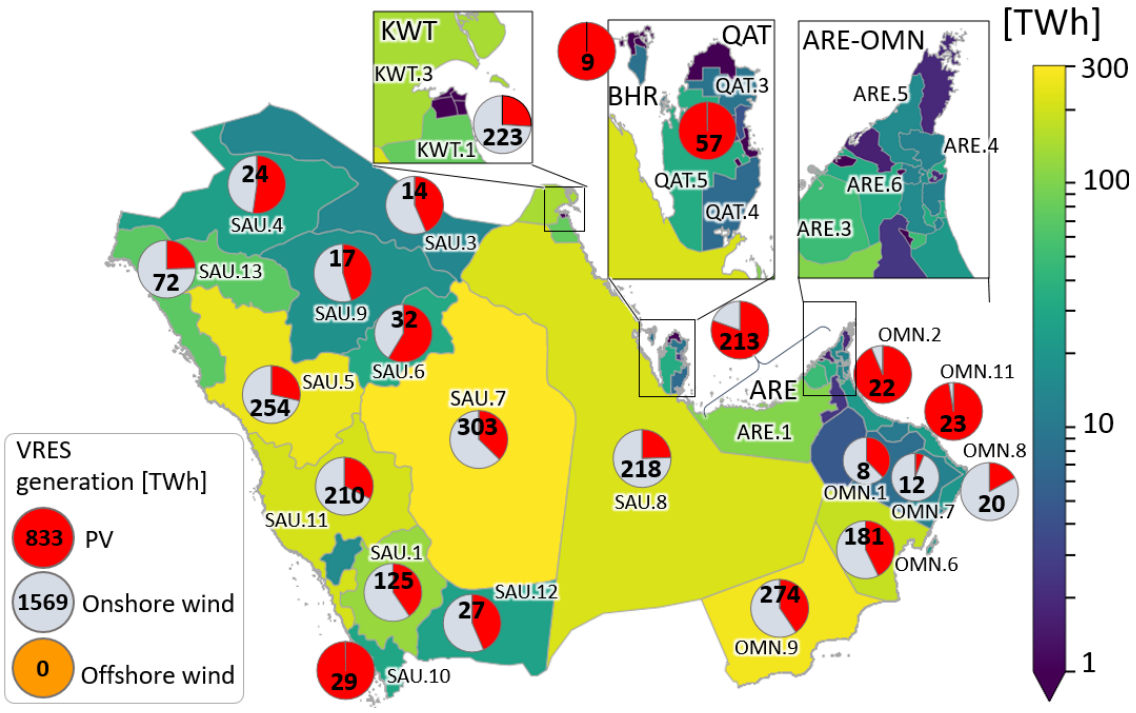

Figure 6.1: VRES electricity generation mix in the cooperation scenario

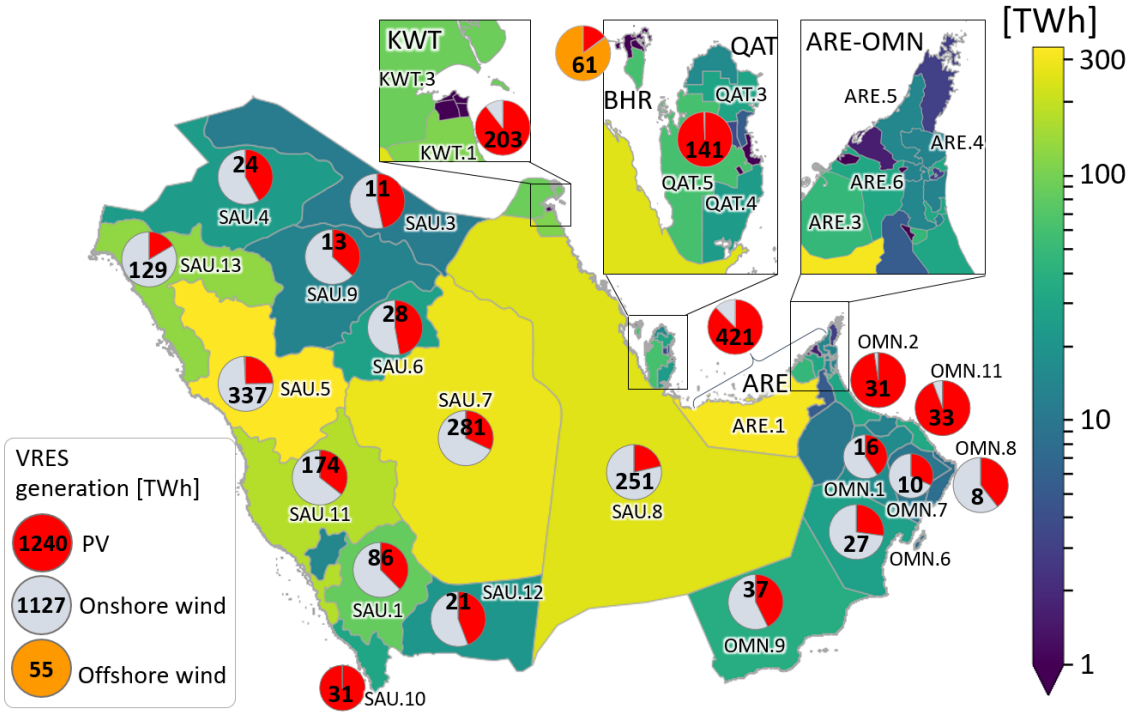

Figure 6.2: VRES electricity generation mix in the isolation scenario

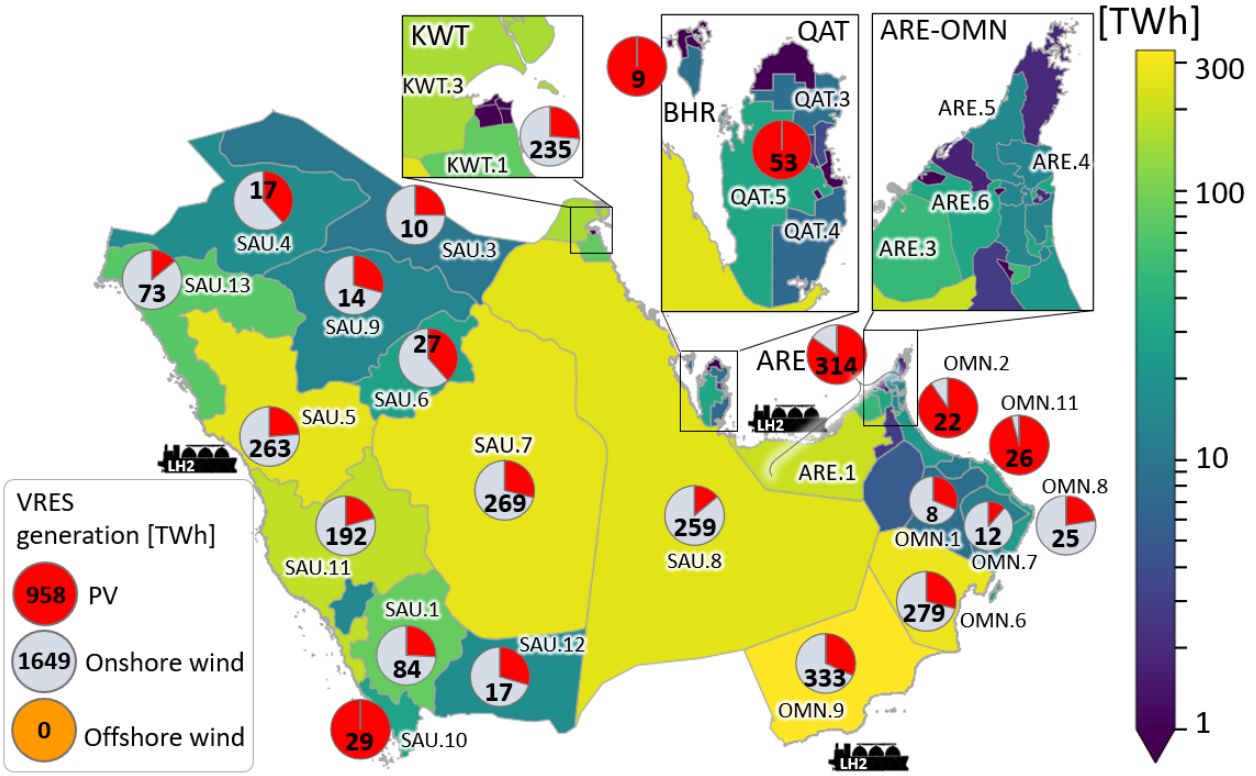

Figure 6.3: VRES electricity generation mix in the export scenario

Among the other regions were PV produces more electricity than onshore wind are a few very small coastal regions of Oman and one in Saudi Arabia, where onshore wind cost is on average high and the overall energy produced low. Together with Qatar, the Arab Emirates are the only area of the system where significant production is registered and where PV stands as the main energy source at the same time in all scenarios. This might also look like an unexpected result, if one considers the fact that the LCOE of PV is on average at its highest in these regions and that of wind is instead relatively low with respect to its cost range in the GCC region. The fact that onshore wind remains on average 30% more expensive than PV in Qatar and even more in the Arab Emirates only partly explain the results, since this situation is observed in many other regions of the Peninsula. Therefore, the next paragraph will now explain the reason for this outcome.
The supposed inconsistency of the results is mainly due to the fact that looking at average costs is misleading. In fact, even small areas with very low LCOE for wind turbines are associated with a high potential if compared to the total demand of the system, meaning that a region with a high LCOE on average might still provide a lot of wind energy for a cheap price in some specific areas and hence be selected by the tool, hence leading to significant wind production in a region with a high average LCOE of wind turbines. For example, the share of onshore wind is low in the case of Qatar, where a low LCOE on average is registered but no wind turbine is found below 4 €c/kWh. On the contrary, the highest-producing regions of Saudi Arabia show similar average costs for wind turbines to that of Qatar, but there some wind turbines can also be found at an LCOE as low as 2 €c/kWh. This information, combined with the fact that the temporal profile of wind production might better fit the electricity and hydrogen demand time series can well explain the energy mix obtained with the simulations. A more detailed discussion on time series is reported in the discussion chapter in section 7.2.

The fact that LCOE is indeed a driver of optimisation as it should be the case is also seen thanks to the absence of offshore wind installations in the cooperation and export scenarios. Only when the countries are forced to rely on their own energy potential, offshore wind is utilised. Apart from a negligible value of 3 TWh registered in the waters of the Red Sea (0.1% of total generation), this resource is used only by Qatar, where the LEA allows for only 9 TWh of PV installations onshore, so that the remaining 52 TWh necessarily have to come from offshore, accounting for 2.2% of total generation in the GCC. Interestingly enough, Bahrain consequently comes close to consuming 90% of its VRES resources, the only state risking to fall short of

renewable energy sources. The Arab Emirates come second in this sense relying on 30% of their VRES, with the other two small states of Qatar and Kuwait following next each at 16% due to the higher availability of eligible land compared to national energy demand.

Although the LCOE of generation technologies is found to affect optimisation, the main factor impacting results remains the balance of production and demand, from which storage costs directly depend. In fact, the analysis of the results shows that wind turbines are used up to the cost of 5.5 €c/kWh against the maximum of 3.4 €c/kWh of PV, as will also be addressed in subsection 6.1.5. It should be said, however, that those exceeding 4.0 €c/kWh are installed to a way lower extent (<10% of the total). The necessity of matching generation and demand in the most cost-efficient way is also the reason why the actual FLH of PV farms are significantly lower than the mean values obtained in section 5.2. Furthermore, the cost-optimal curtailment of PV generation also contributes to explain the large installations of wind turbines in the cost-optimal system set-up. In fact, comparing the theoretical FLH of the PV and wind technologies located in the LCOE range of 0.2-0.4 (where almost all installations come from) with the actual FLH reported in Table 6.1, the curtailment of solar energy is of at least 20%, whereas that of wind turbines is of at least 10%. Moreover, the effects of curtailment should also be kept in mind when looking at the capacity of VRES installed by the tool as reported in Table 6.1, which by themselves could be misleading. For example, in the cooperation scenario the same overall capacity of wind and PV farms is installed, but the FLH of wind turbines and hence their total generation is twice as high as that of PV panels. This is partly due to the fact that wind turbines are already characterised by higher FLH than wind turbines, but this difference is even increased due to curtailment of PV generation.

Apart from the generation mix composition, the influence of demand on the installation of VRES can be noticed when considering the distribution of energy production over the different regions of the Peninsula, as shown in Figure 6.1 to Figure 6.3. However, the behaviour of the system is not so easily explained. In fact, VRES production is high in those regions where a higher electricity demand must be satisfied, but not only there. Considering the cooperation scenario, SAU.5 and even more OMN.9 and OMN.6 are eminent examples of places were demand is relatively low but production is close to the maximum values registered for the Peninsula. Probably, the reason lies in the fact that the regions just mentioned can offer a high amount of wind energy at prices below 4 €c/kWh. Therefore, it can be stated that the system follows two main directives for VRES installations: first, producing electricity and/or hydrogen close to demand, which reduces power transport losses; secondly, producing energy exploiting cheap wind resources. In fact, this source is preferred due to the better match with both the power and hydrogen demand, which is discussed in section 7.2. The next subsection will prove that the location of electricity demand is more influential than that of hydrogen for VRES installations, whereas subsection 6.1.3 proves that wind is particularly favourable for constant hydrogen production.

The considerations just made specifically for SAU.5 and OMN.9 do not apply in the same way to the export scenario. Here the intense production registered by these two regions also stems from the presence of one of the three hydrogen export harbours in the region. The fact that the spatial distribution of VRES depends not only on electricity but also on hydrogen demand is finally proven by the increase of total generation in the Arab Emirates by 50% once the hydrogen harbour is installed in the region in the export scenario. However, this is also due to the extra electricity demand required for liquefaction. Finally, the decrease of total production in Oman in the isolation scenario suggests that most of its energy is being exported abroad, which is indeed proven in the next subsection.

6.1.2 Transmission

Differently to the previous subsection, each scenario is presented independently. This is because the behaviour of the transmission components is in itself longer to describe, so that mentioning all scenarios at the same time might be confusing. Firstly, the cooperation scenario is presented; then, the remaining two scenarios are considered once at a time, making some relevant comparisons between them and the cooperation scenario. For each scenario, two charts are created showing the net flow of either electricity or hydrogen, together with the capacity of powerlines or hydrogen pipelines respectively. In fact, only the combination of net energy flows and transmission capacity allows to have a deep understanding of the mechanisms governing the system behaviour. These maps can be observed in Figure 6.4 to 6.9. Zooms are also necessary to evaluate the role of some very small but key regions in the system.

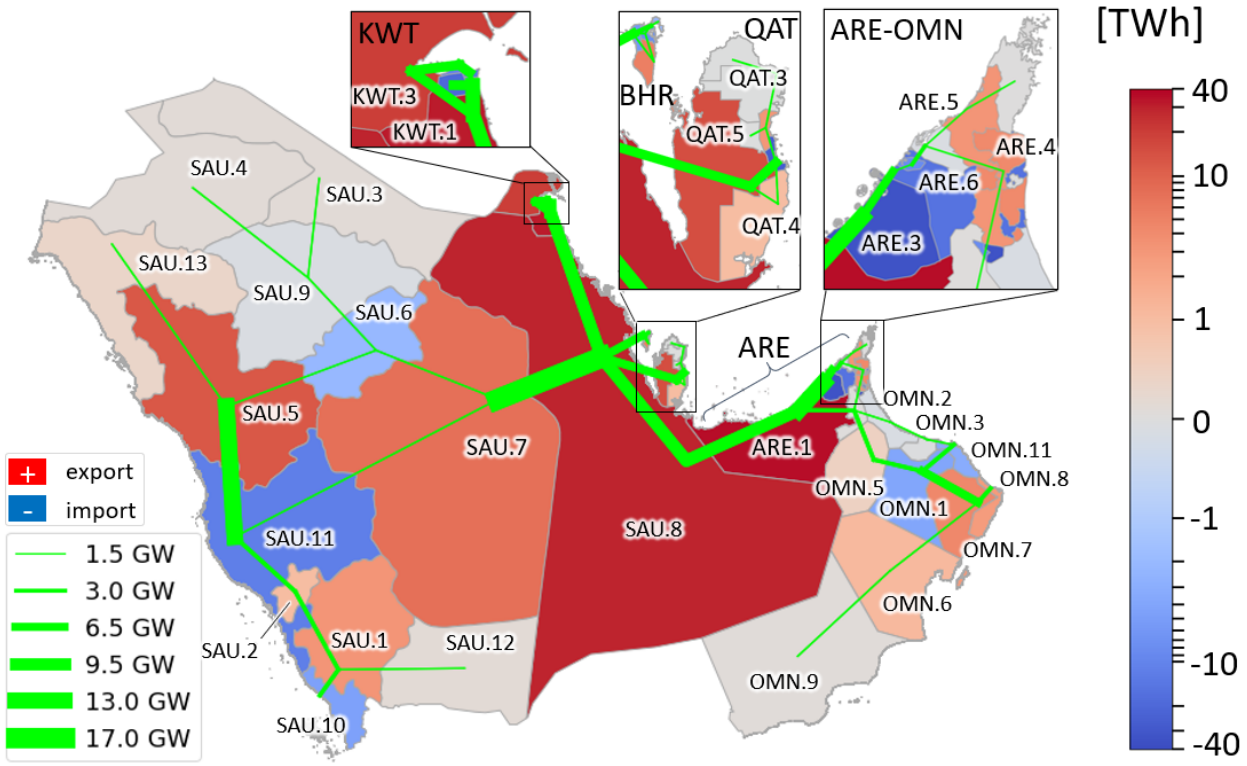

Figure 6.4: Net regional electricity export and powerlines installations in the cooperation scenario

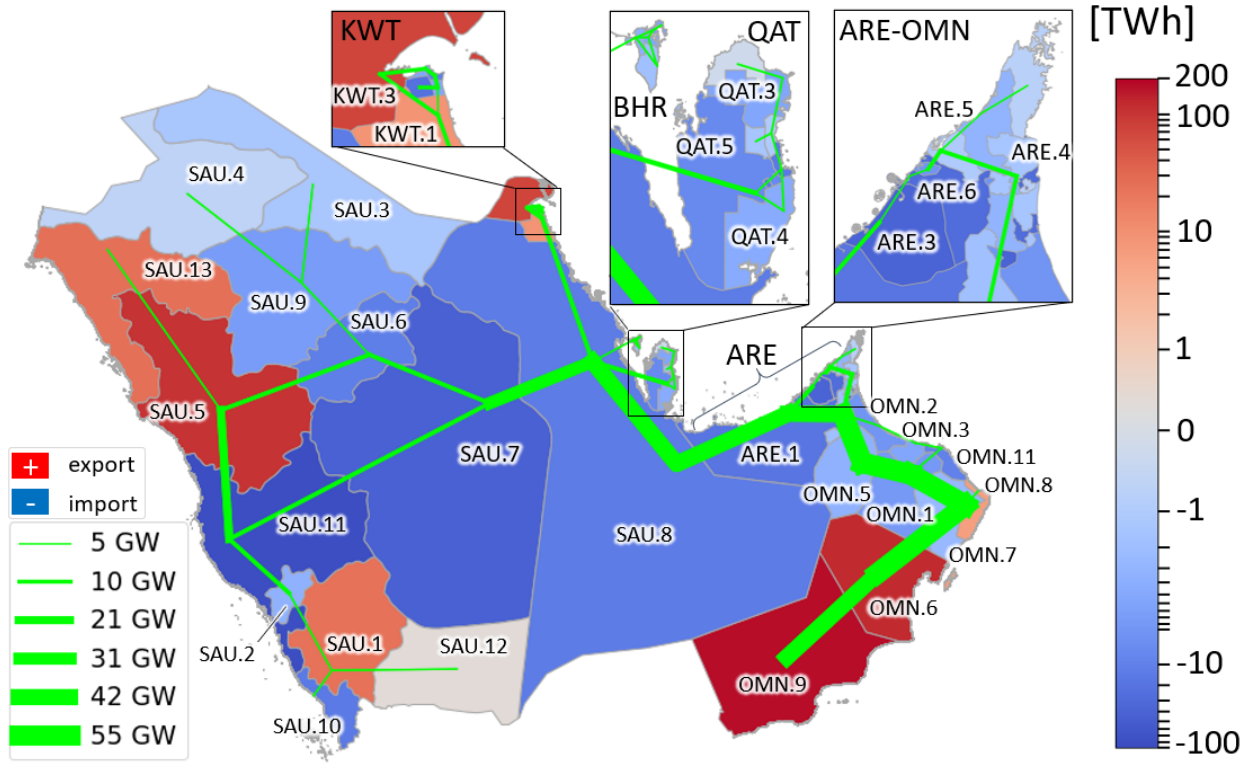

Figure 6.5: Net regional hydrogen export and pipelines installations in the cooperation scenario

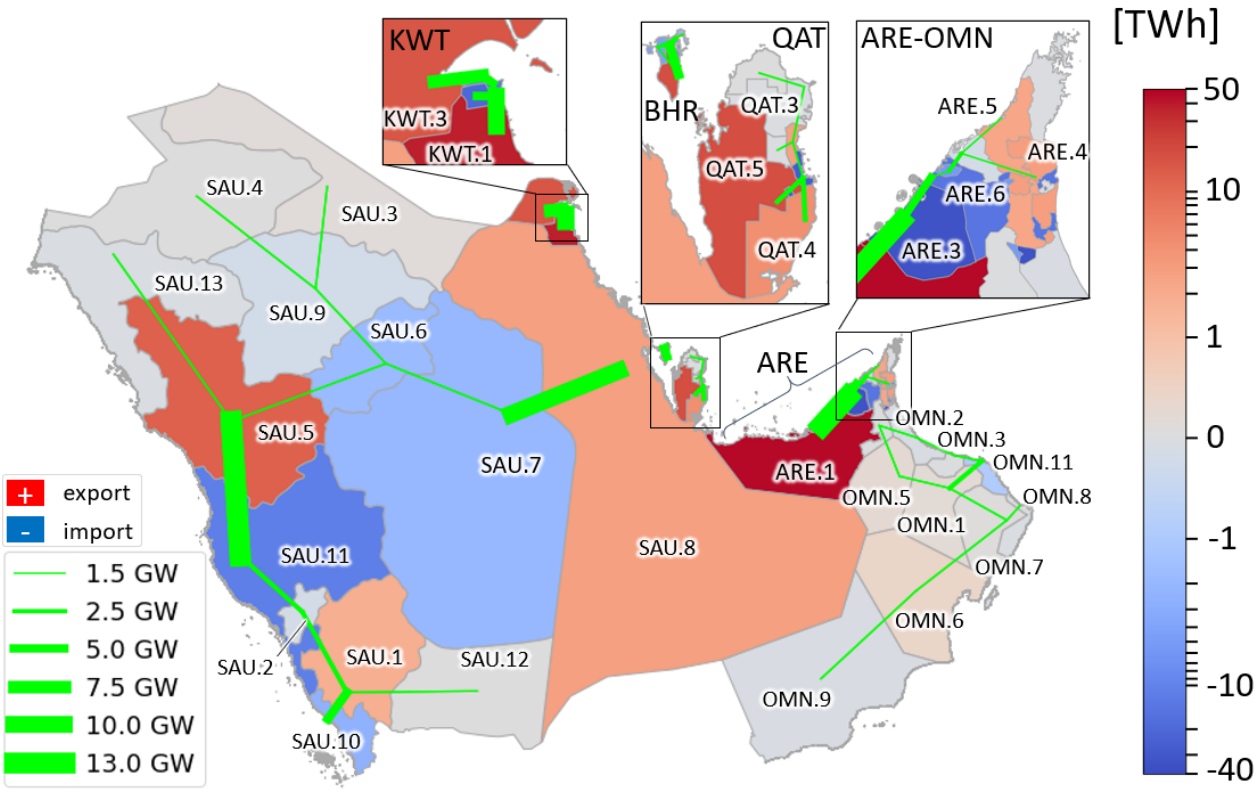

Figure 6.6: Net regional electricity export and powerlines installations in the isolation scenario

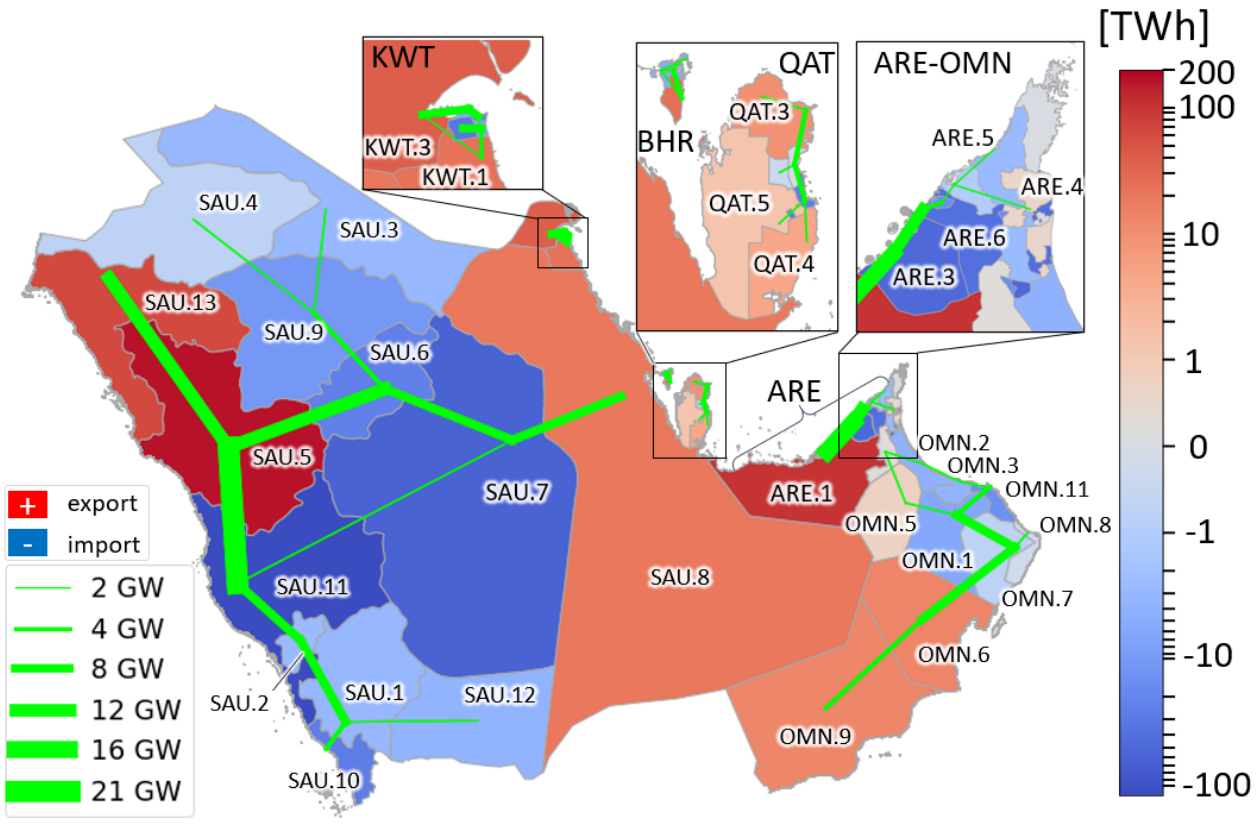

Figure 6.7: Net regional hydrogen export and pipelines installations in the isolation scenario

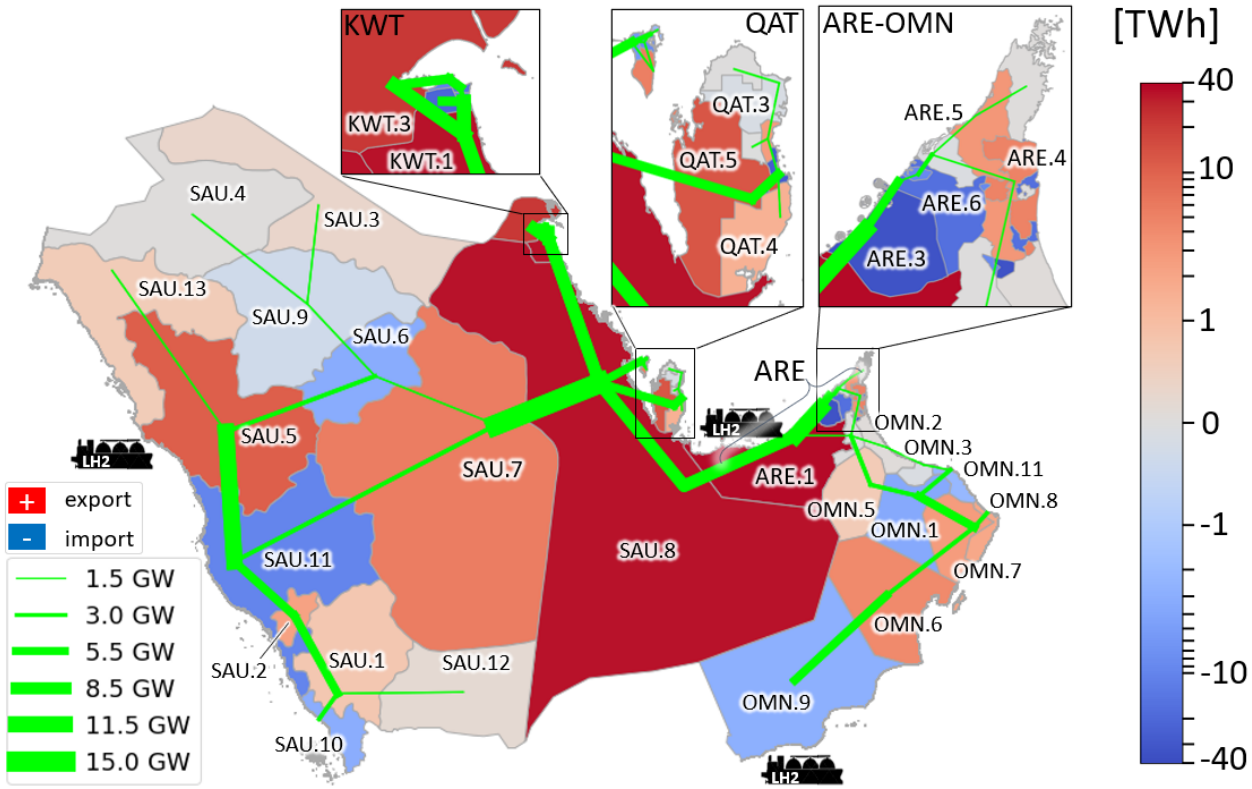

Figure 6.8: Net regional electricity export and powerlines installations in the export scenario

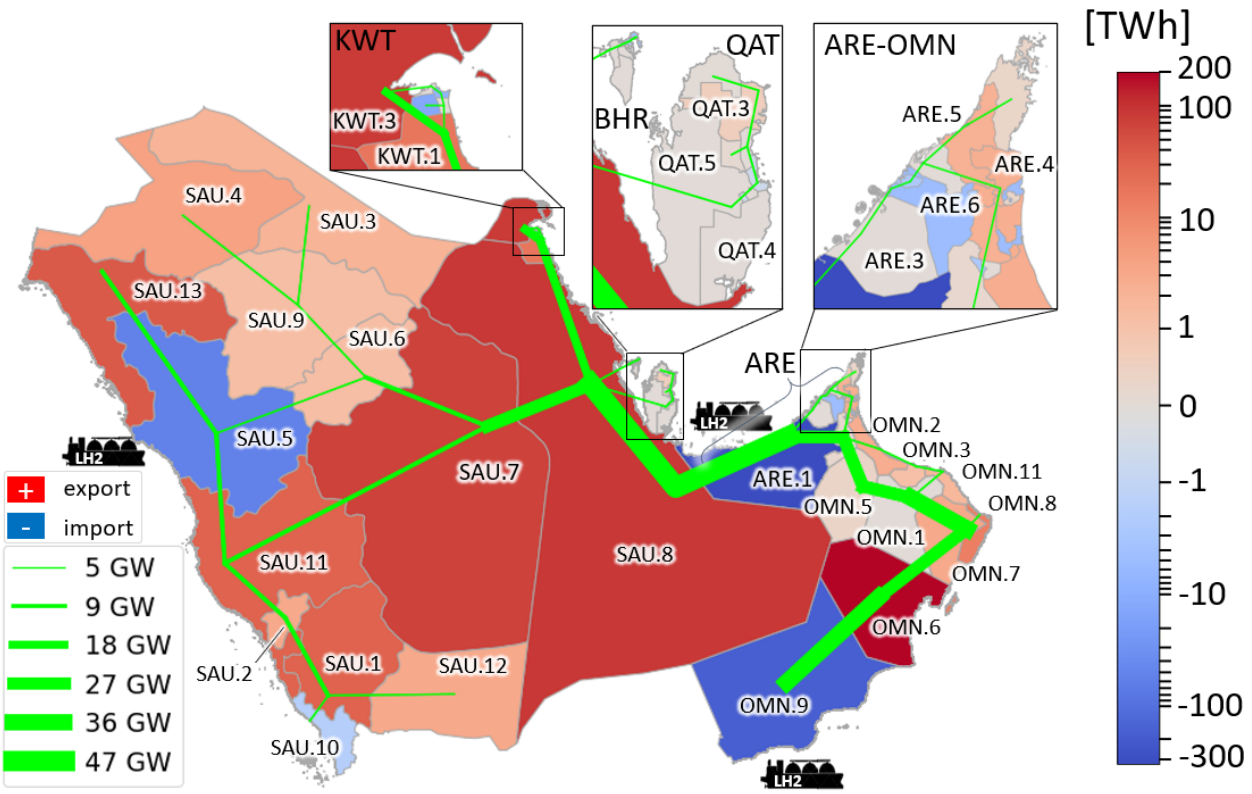

Figure 6.9: Net regional hydrogen export and pipelines installations in the export scenario

The cooperation scenario is the first one to be discussed. Figure 6.4 shows the net exports or imports of electricity registered by each region over the year. Regions associated with a red color produce more power than they consume, whereas those represented in blue take in more power than they generate. The size of each green line composing the electricity grid is representative of the capacity installed in that connection. In this case, the maximum capacity of the powerlines is registered at 17 GW in the connection between SAU.7 and SAU.8. Overall, the electricity grid can count on a capacity of 148 GW, most of which is concentrated in the modeled powerlines connecting the GCC countries. In particular, this portion of the grid runs vertically from Kuwait until the Arab Emirates, with connections featuring between 7 and 10 GW, whereas horizontally it connects Qatar and Bahrain with the easternmost region of Saudi Arabia, namely SAU.8. All GCC states are connected with this region, which explains why the connection with the highest capacity is that linking SAU.8 with SAU.7 and indirectly with the many other regions in Saudi Arabia.

The majority of regions where the GCC connections are present appear as strong energy exporters. This is due to the fact that in these regions most people live and hence more energy demand is also located. In fact, the zooms reported in Figure 6.4 show tiny blue regions acting as strong energy importers, with net import values reaching up to 40 TWh which are provided by the nearby regions. These, in fact, show similar values but in the export range. The proximity between importing and exporting regions can also be observed in other areas of the map, most notably in southeastern Oman and in central and western Saudi Arabia. In particular, SAU.11 seems to be absorbing electricity from all its nearby regions, but mainly from SAU.5, as suggested by its intense red color and the significant capacity of 13 GW connecting it to SAU.11. However, SAU.11 is also one of the highest electricity- and hydrogen-producing regions of the GCC area, as shown in the previous subsection. This leads to an important consideration, namely that intense production is not a synonym of energy excess and consequent export to nearby regions. Viceversa, low-producing regions are often but not always net importers, as exemplified by OMN.8.

The lack of a direct correlation between the amount of electricity/hydrogen produced or the size of a region and its import or export role is even clearer after considering the net hydrogen flows. Those established in the cooperation scenario can be observed in Figure 6.5. Four main hydrogen export regions are found approximately at the four corners of the system, although that of SAU.1 is relatively less significantly. However, the western and eastern side of the Peninsula are relatively poorly interconnected, as suggested by the lower capacity of the pipelines running between them. This implies that the main importing regions in the West ultimately rely on SAU.5, while coastal regions on the East take most energy from Oman and on a lower scale from Kuwait, who satisfies its own local hydrogen demand. SAU.7, the big region located at the center of the system, acts as strong hydrogen importer, as opposed to its role of exporter in the case of electricity. What is most remarkable is the fact that the three major hydrogen export regions mentioned above are all located where the lowest prices of wind energy are registered. Indeed, wind is by far the main component of the generation mix in these areas, as explained in the previous subsection. Therefore, the results seem to show that the electricity required for electrolysis is preferably obtained from wind energy. This point will be finally proven in subsection 6.1.3. Other regions of Saudi Arabia also provide wind energy at the same price, such as SAU.7 and SAU.8, but they feature in the map of Figure 6.5 as hydrogen importers. These regions, in fact, also have to satisfy a high value of hydrogen demand locally, which explains why they appear as net importers.
In the light of what has just been explained, the role of net hydrogen importers of Bahrain, the Arab Emirates and Qatar can be explained. In fact, wind energy here never falls below the threshold of 4 c€/kWh, while wind energy seems to be the favourite technology for the production of hydrogen, as just mentioned in the previous paragraph. In its turn, this in line with the eminent role of wind in the energy mix, particularly in the cooperation and the export scenarios, which was discussed in the previous subsection. The role of wind energy as favourite energy source for the production of hydrogen will be finally confirmed in the next section, which shows that the installation of electrolysers is higher in those regions which can provide the cheapest wind energy.

However, the impact of the techno-economic parameters used to model the system should also be acknowledged with respect to the optimal layout of VRES and transmission installations. In fact, the behaviour of the system is partly due to the fact that no transmission losses are considered for pipelines according to Caglayan et al. [173], which allows the system to transport hydrogen over very long distance in a relatively efficient way, something which is not possible for powerlines, where local production could be preferred in order to avoid power losses. This piece of information, together with the lower cost of hydrogen pipelines and

vessels with respect to powerlines and Li-ion batteries (considering the same amount of energy transported in the two different forms), explains why the total capacity of the hydrogen grid is overall 3.3 times higher than that of the electricity grid, namely 497 GW against 147 GW. The maximum capacity for a single pipeline connection is instead registered at 55 GW, which is also 3.3 times higher than the maximum value of 17 GW of the electricity lines. These results cannot be associated with the difference between electricity and hydrogen demand values, since hydrogen demand is even 22% lower than electricity demand.

The layout of the optimal system configuration for the isolation scenario is radically different. This is necessarily the case given the strong interdependence among the different GCC countries observed in the cooperation scenario, where these are shown to rely on an important transmission system on the eastern side of the Peninsula. Starting from the net electricity flows represented in Figure 6.6, the main difference lies in the stark decrease of electricity export from region SAU.8, which no longer acts as connection point for all other eastern countries. Consequently, the exporting regions of Kuwait, Qatar, Bahrain and the Arab Emirates all see their net outbound flow towards the other regions of the same country increase in order to satisfy national demand, with some of them exporting 50 TWh instead of 40 TWh as observed in the cooperation scenario. This behaviour can be related to the increase of electricity and hydrogen production in these regions once they are disconnected from the common GCC grid. On the contrary, the importing regions continue to absorb similar amounts of electricity overall, with the exception of SAU.7 in central Saudi Arabia, whose electricity balance turns negative only in this scenario. Besides, the minor connection between this region and SAU.11 is here definitely dropped, probably because SAU.7 is no longer able to provide additional energy to SAU.11. The strong powerline connecting SAU.11 and SAU.5 maintains its 13 GW of capacity, just like that between ARE.1 and ARE.3. However, no line is anymore found above this value, with the overall capacity of the grid amounting to 93 GW, 50% less than in the cooperation scenario. Finally, it should be noted that regions in Oman no longer feature significant exports, hinting at the fact that most of its exports are destined to other countries in the cooperation scenario, in particular the neighbouring state of the Arab Emirates.

The differences between the cooperation and the isolation scenario are even stronger once the focus is moved to net hydrogen flows, as suggested by Figure 6.7. Clearly, the three states of Qatar, Bahrain and the Arab Emirates are now forced to produce hydrogen locally, with some of their regions being then converted to hydrogen exporters instead of importers. As regions where demand is concentrated are often small, hydrogen production and export moves to those with a larger amount of eligible locations for VRES. The eastern region of SAU.8 is also converted to a net producer of hydrogen, while it was receiving this commodity from Kuwait and indirectly from Oman in the cooperation scenario. Another interesting difference is found in the higher net imports registered by SAU.11 in this scenario: since demand is the same in both cases, it means that the optimisation process has decreased the amount of hydrogen produced in this region. This must be due to the new exchanges that have to be established between the different regions of Saudi Arabia when this is isolated. Similarly to what happens with the electricity grid, the maximum capacity of hydrogen pipelines is significantly reduced, with the overall capacity dropping to 154 GW, 3 times less than in the cooperation scenario. However, the connections in western Saudi Arabia do not show a decrease in capacity, once more suggesting that the eastern and western side of the Peninsula are strongly independent. The connection between ARE.1 and ARE.3 is even increased from 7 to 14 GW, although this is the only case where such a trend is observed. This increase is due to the fact that no more imports can arrive from Kuwait, forcing ARE.3 to import more hydrogen from its neighbouring regions in the Arab Emirates, most notably ARE.1.

Finally, the export scenario is analysed (Figure 6.8). Even though the entire hydrogen demand is concentrated in the three ports in SAU.5, ARE.1 and OMN.9 since local hydrogen demand is absent, the net electricity flows and powerlines installations seem to be little affected by the new requirements of the system. However, some minor differences can be pointed out. The most significant one is the fact that OMN.9, hosting one of the ports, becomes a net electricity importer, even though only for an overall value of 3 TWh, which is provided by the neighbouring region OMN.6, whose net export increases of a similar amount. Besides, the capacity of connections linking OMN.9, OMN.6 and OMN.7 is increased by two to three times. These changes are most certainly connected with the additional need of electricity required to run liquefaction in OMN.9. An increase of capacity is also found in the southwestern portion of the grid in Saudi Arabia, which is connected with the fact that SAU.2 takes the role of main exporter in the area and has to provide more energy to SAU.11 and indirectly to SAU.10 through SAU.1. However, slightly weaker powerlines are

established among the GCC countries in the East, so that overall almost the exact same capacity of the electricity grid is registered here as in the cooperation scenario, namely 149 GW.

More evident are the differences between the export scenario and the cooperation one when it comes to net hydrogen flows (Figure 6.9). If in the cooperation scenario OMN.9 appears as the first hydrogen exporter in the whole GCC area, in the export scenario it imports 174 TWh of hydrogen, namely half of the hydrogen demand concentrated in its port. Interestingly enough, the other half of this demand, which is necessarily produced locally, is almost the same value of hydrogen that the region was exporting in the cooperation scenario. Furthermore, the region of ARE.1 increases its net imports by ten times, meaning that less than 5% of the demand of its port is produced locally. As PV is the main energy source for this region, the fact the PV is rarely chosen to produce hydrogen is once again confirmed. In fact, significant exports towards this region come from Kuwait, SAU.8 and OMN.6, where wind turbines dominate the generation mix. Another difference can be observed in the nothern regions of Saudi Arabia, all of which still register low net flows of hydrogen, but in the outbound direction, as opposed to the cooperation scenario. Maybe more striking is the role reversal of SAU.5 and SAU.11 in western Saudi Arabia, with the net flow of hydrogen running from south to north in this case. However, this can be easily explained with the fact that hydrogen demand is only found in SAU.5 in the export scenario, while the cooperation scenario is modeled with SAU.11 requiring twice as much hydrogen as SAU.5.
As for the hydrogen transport infrastructure in the export scenario, the maximum capacity of the installed pipelines is equal to 47 GW, less than the value of 55 GW registered in the cooperation scenario. This can be explained with the fact that flows of hydrogen are ultimately directed towards only three regions, so that the system does not have to account for the demand that has to be exported to other regions of the Peninsula in case local demand is present. This phenomenon outweighs the changes in capacity due to the necessity of the regions hosting an harbour to import more hydrogen. Hydrogen connections remain significant among the GCC states and in the traits connecting Oman to the Arab Emirates, although these show a relatively lower capacity than in the cooperation scenario, since less energy is being exported from Oman, which needs to provide hydrogen to its own port. Even though a port is located in SAU.5 in the West, the capacity of its connection with SAU.11 is halved. In fact, also the net import or export of SAU.5 and SAU.11 is also reduced by a similar amount. Overall, the capacity of hydrogen pipelines amounts to 339 GW, that is two thirds of the installations of the cooperation scenario.
Finally, the net import of hydrogen shown by regions where no port and consequently hydrogen demand is located might seem unjustified if no further clarifications are given, even though this amount is never surpassing 13 TWh. The reason for this behaviour of the system should be searched in the conversion components of the system, which are the object of the next subsection. In fact, these show that reconversion of hydrogen to electricity is taking place in those regions which are all net electricity importers too according to Figure 6.8.

6.1.3 Conversion

Among the benefits of a hydrogen economy highlighted in section 2.1 is the supply of long-term storage capacity for energy systems highly dependent on VRES, such as the one modeled in this study. For this reason, the conversion technologies made available to the system allow not only the production of green hydrogen, but also its reconversion to electricity, as already described in subsection 4.2.3. Although up to 5 different reconversion technologies could be theoretically used by the system during the optimisation process, none of the three main scenarios shows that this is a cost-efficient option. To be more precise, the amount of electricity obtained through reconversion ranges only between 21 and 31 TWh, namely 2% and 3% of the overall demand of the power sector. This should mainly be the outcome of the abundant and cheap potential of both wind and solar energy. In fact, curtailment seems to be an economically more viable option than hydrogen storage and reconversion. Besides, synergies can also be established between wind and solar feed-in curves, which also contributes to this effect.
In order to verify to which extent the previous statement is observed for the Peninsula, use can be made of the results of the two only-wind and only-PV scenarios, where the system can exploit only one VRES technology between either onshore wind or PV respectively, while all other conditions are the same as in the cooperation scenario. These two scenarios will be discussed more in detail in subsection 6.2.2. Interestingly enough, reconversion is indeed higher in these case studies, but not significantly: only the only-wind scenario transforms hydrogen back into electricity in a relatively considerable amount, equal to 88 TWh of final electricity demand satisfied in this way, against the 40 TWh of the only-PV scenario, which ranks second for

reconversion. Compared to the 1098 TWh of total electricity demand, however, these numbers are still very low, confirming the fact that hydrogen reconversion is often economically unfavourable. This, however, is not only due to the investment costs of reconversion technologies. In fact, the low utilisation of reconversion technologies is related to the intrinsic inefficiency of the process including both electrolysis and reconversion, which implies an electricity loss of least 50% according to the technologies used in this study. The optimisation process therefore prefers a combination of batteries and curtailment to hydrogen storage and reconversion to electricity. Curtailment has already been discussed in subsection 6.1.1, while electricity and hydrogen storage is the topic of the next subsection.

Even though reconversion technologies are installed in negligible amounts, some considerations can still be made. In both the cooperation and the export scenario, hydrogen gas turbines are the only technologies put in place by the optimisation process. Both the open-cycle and the closed-cycle turbines are present. A reason can be offered to explain why the system might opt for one or the other type of turbine, and that is the required average operation rate of the plant. In fact, in both scenarios just mentioned the average capacity factor of all closed-cycle turbines is above 30%, while that of open-cycle turbines never surpasses 27% and is often around 10%. This is line with the techno-economic parameters of Table 4.3 which assign a higher variable OPEX to open-cycle turbines than to closed-cycle ones.
The considerations just made hold true also for the isolation scenario, although with some differences. Firstly, the average capacity of both types of hydrogen gas turbines is increased in all states except for Bahrain. Here, the system is forced to activate solid-oxide fuel cells, which are the most efficient but also the most expensive reconversion technology among those modeled in this study. This is done in order to waste as little energy as possible during the reconversion process, given the limited amount of VRES available to the country under consideration. When this is done, the capacity factor of the closed-cycle turbines installed in the region drops tremendously to around 4% on average. In spite of the low operation rate, these are here still preferred to open-cycle turbines, most likely because of their higher efficiency, which is essential in the case of Bahrain, as already explained.

As for the location of reconversion technologies, Saudi Arabia only shows the presence of open-cycle turbines, which are installed in the southwestern regions of SAU.10 and SAU.12, with 0.4 GW and 1.6 GW in the export and the isolation scenario respectively. The second largest country of the GCC, Oman, never registers the presence of any reconversion technology. The same happens to Qatar. The case of Bahrain has already partly been discussed, with 3.2 GW of solid-oxide fuel cells and 0.5 GW of closed-cycle turbines in the isolation scenario and around 1 GW of closed-cycle turbines in the other two. These are never placed in BHR.5, the region able to produce most electricity in this country. Kuwait always shows a relatively high capacity of reconversion technologies compared with the other countries, with around 3 GW of hydrogen gas turbines in each of the three scenarios, mostly of the open-cycle type, which are never placed in its biggest regions KWT.1 and KWT.3. Finally, the Arab Emirates host around 1.5 GW of closed-cycle turbines in the cooperation and the export scenario, with the addition of 0.6 GW of open-cycle turbines in the isolation scenario. These are never located in ARE.1. Together with subsection 6.1.2, the information just presented allows for one last consideration regarding reconversion technologies: they are used in relatively small regions and typically in net energy importing regions, or at least never in strong exporting regions. In particular, the regions always showing a capacity greater than zero across all three scenarios are: KWT.2, KWT.5, ARE.2, BHR.1 and BHR.3, while SAU.10 and ARE.6 feature installations across two scenarios. Besides, these regions are usually located far from the center of the Peninsula.

Finally, it is important to discuss the installations of electrolysers across the Peninsula in the three main scenarios, which are reported in Figure 6.10. The three major hydrogen export regions identified in subsection 6.1.2 for the cooperation scenario, namely SAU.5, Kuwait and southwestern Oman score first for electrolyser installations in the two scenarios where the GCC countries can exchange hydrogen among them. Also in accordance with the considerations made in the previous subsection, the production of hydrogen in Oman drops dramatically in the isolation scenario, when no more hydrogen is exported northward towards the other states. Moreover, electrolysers are put in place in the Persian Gulf regions only in this scenario, where Bahrain, Qatar and the Arab Emirates are forced to provide their own hydrogen demand. Kuwait is an exception, as it shows around 25 GW of electrolysers in each scenario. In this case the country produces an amount of hydrogen equal to 78 TWh, which is 75% and 80% lower than the cooperation and export scenario respectively, but still way higher than its hydrogen demand. In fact, 25 TWh of hydrogen are used for reconversion through closed-cycle hydrogen gas turbine, producing around 15 TWh of electricity, which

is 15% of the national electricity demand. Probably the most important difference between the cooperation and the isolation scenario, however, is the installations of 25% more electrolysers when the countries cannot exchange energy among them. As overall hydrogen demand is the same, this means that the average capacity factor of the electrolysers is lower in the isolation scenario, which implies a less cost-optimal utilisation of this technology. In simpler words, more costs are necessary to produce the same amount of hydrogen. In fact, no significant difference in hydrogen production is registered due to reconversion technologies, since their operation is always very low across all three main scenarios with respect to total electricity or hydrogen demand, with electricity obtained through reconversion ranging between 21 TWh and 31 TWh depending on the scenario.

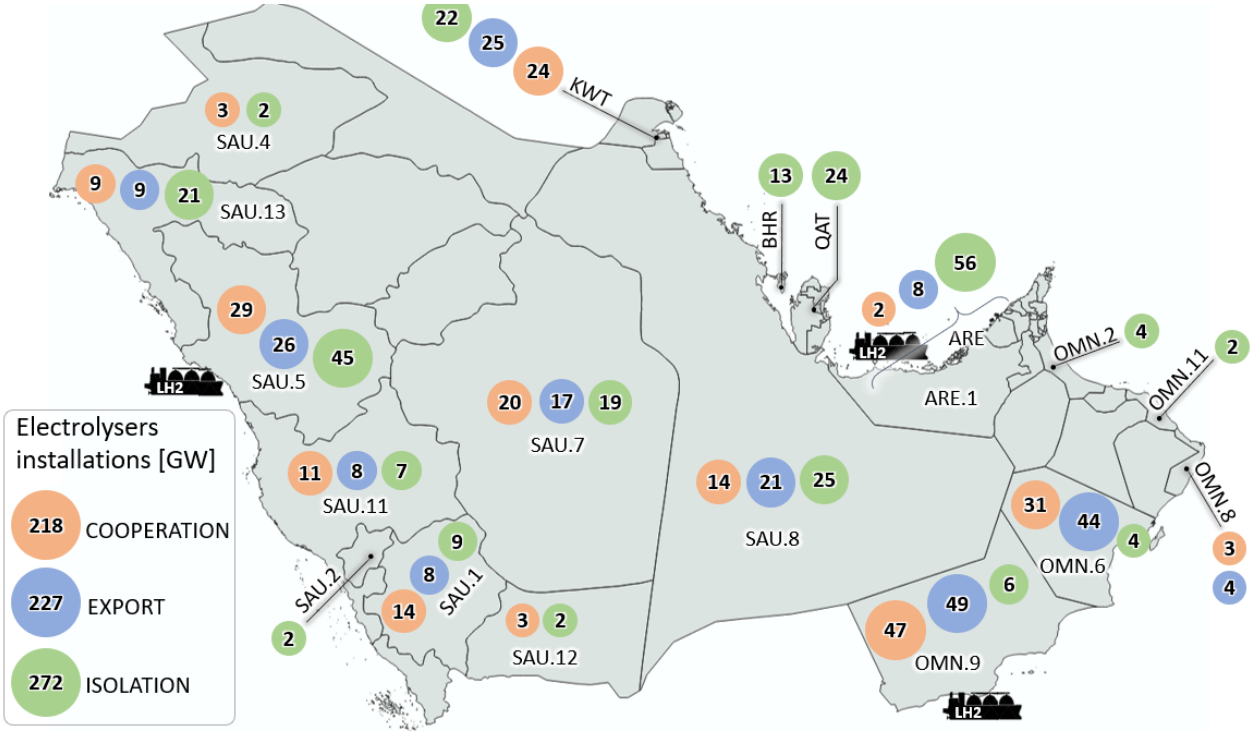

Figure 6.10: Installations of electrolysers across the three main scenarios. Values below 2 GW are not reported

The concentration of all hydrogen demand in only three regions in the export scenario leads to an increase of hydrogen installations in OMN.6, the Arab Emirates and SAU.8 with respect to the cooperation scenario. In fact, these regions host a hydrogen port or are close to one. Surprisingly, installations in SAU.5 and SAU.11 slightly decrease, even though the former hosts one hydrogen port and the latter is located next to it. This suggests that energy is being imported from other regions of the Peninsula and not exported towards them as in the cooperation scenario, as confirmed by comparing the net hydrogen exports of eastern regions in Saudi Arabia in Figure 6.5 and Figure 6.9. Focusing on the three regions where most electrolysers are installed and which do not contain a port, namely KWT.3, SAU.8 and OMN.6, it is possible to observe from Figure 6.9 that these are also the highest hydrogen exporting regions, making up for around 60% of overall hydrogen exports and 42% of total hydrogen demand, equal to 364 TWh. Comparing the amount of hydrogen exported with the energy these three regions generate from VRES in Figure 6.3, it is found that solar energy could not provide more than 30% of the total hydrogen in any of these regions. Moreover, the other two biggest producers of hydrogen are SAU.5 and OMN.9, which together make up 303 TWh, i.e. 35% of overall hydrogen demand, and here PV could potentially cover only 40% of the hydrogen produced. As a similar trend is also verified in other regions, hydrogen generation is found to originate primarily from onshore wind. Using the same method, it can be verified that wind is also the main electricity source to run electrolysers in the export scenario, whereas for the isolation scenario this remains uncertain.

6.1.4 Storage

After having described the three other components of the system in the previous subsections of this chapter, storage technologies are now considered. The three main scenarios will be presented considering one technology at a time, making comparisons between lithium-ion batteries and hydrogen vessels when relevant. Besides, the discussion conducted in the previous subsections of this chapter also proves useful to understand the result of optimisation for storage technologies.

Firstly, the case of batteries is considered. As revealed by Figure 6.11, these are mostly placed along the eastern cost of the Peninsula. While it is true that energy demand is mostly concentrated around this area, this alone does not really explain the exact layout observed at the end of optimisation. In particular, it is striking that Qatar and in particular the Arab Emirates feature several times more battery capacity than some regions of Saudi Arabia, where energy demand is only two or three times lower, both in terms of electricity and hydrogen, as can be observed in subsection 4.2.5. The higher installations in the East could maybe be explained in terms of demand alone only in the isolation scenario, but not in the other two. The reason can neither be found in the net flows of electricity, since very high values of battery capacity are registered in ARE.1 and ARE.3, which are a strong exporter and importer respectively across all scenarios as discussed in subsection 6.1.2. Furthermore, the answer should also not be searched in the total VRES production, since countries producing similar amount of electricity do not show similar values of battery capacity.

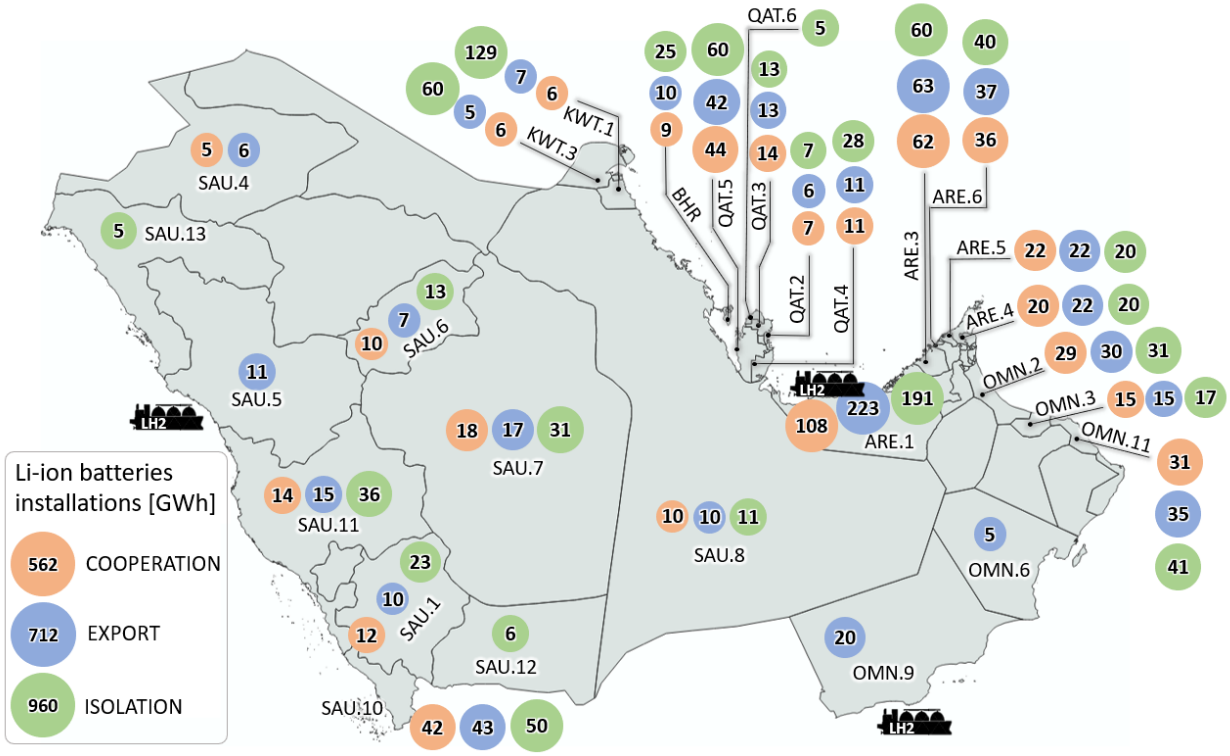

Figure 6.11: Installations of Li-ion batteries across the three main scenarios. Values below 5 GWh are not reported

It is another aspect of the analysis of subsection 6.1.1 to offer the only possible explanation for this aspect of the results: the share of PV sources in the generation energy mix. This is proven by the fact that in both the cooperation and the export scenario all regions registering the highest installations of batteries also produce more than 50% of their electricity through solar energy. Particularly interesting is the fact that the main driver for battery installations is not overall PV production, but rather its share in the mix. This is best exemplified by SAU.10 and the eastern regions of Oman, where demand and production are relatively low but PV is almost the only component of the electricity mix. Once again, the two functional scenarios relying on one single VRES can be used to support the argument proposed. These confirm exactly what just stated. In fact, the battery capacity for the GCC area is of 260 GWh in the only-wind scenario, while it rises to 2400

GWh in the only-PV scenario, as compared to the 560 GWh and 710 GWh of the cooperation and export scenario respectively. This aspect is also analysed in subsection 6.2.2.

Still observing the map of Figure 6.11, it is interesting to note that changing the location of hydrogen demand in the export scenario influences the installations of lithium-ion batteries both in terms of location and size. In fact, while most regions see the capacity of batteries almost unchanged between the cooperation and the export scenario, additional capacity is installed in all regions where a port can be found. In particular, SAU.5 and OMN.9 see the placement of 11 GWh and 20 GWh of batteries once hydrogen demand is concentrated there, while ARE.1 doubles its capacity between the cooperation and the export scenario. Most likely, it is the additional electricity input required for liquefaction by these regions to lead to these results. Keeping in mind the influence of PV share on battery installations, the greater capacity addition of ARE.1 with respect to OMN.9 and SAU.5 is also explained. According to the total operation of batteries, the amount of final electricity demand satisfied by them is found to rise between the cooperation and the export scenario from 18% to 23%, with nominal cycles equal on average to 350 and 360 in the two cases respectively. This suggests that batteries are typically used on a daily basis, although nominal cycles deviate from this average considerably depending on the region, ranging between 250 and 400.
As expected, the isolation scenario leads to the installation of an even greater amount of batteries, meaning 70% more than the cooperation scenario. As noted when discussing the operation of electrolysers in the previous section, using more capacity to satisfy the same energy demand implies a less cost-effective use of a technology. In fact, batteries here run for only 310 nominal cycles on average, with values particularly low in the Arab Emirates and Bahrain. With the new capacity additions of the isolation scenario, 30% of overall electricity demand is satisfied with lithium-ion batteries by the system.

The distribution of hydrogen storage technologies is significantly different from that of batteries just described. Focusing on the cooperation scenario, where hydrogen demand is more evenly distributed over the territory and the system is more flexible, Figure 6.12 shows that the bulk of installations is found in central and western Saudi Arabia and in Kuwait. This deviates significantly from the observations made for batteries, which are mostly found on the eastern and southeastern regions on the Peninsula.

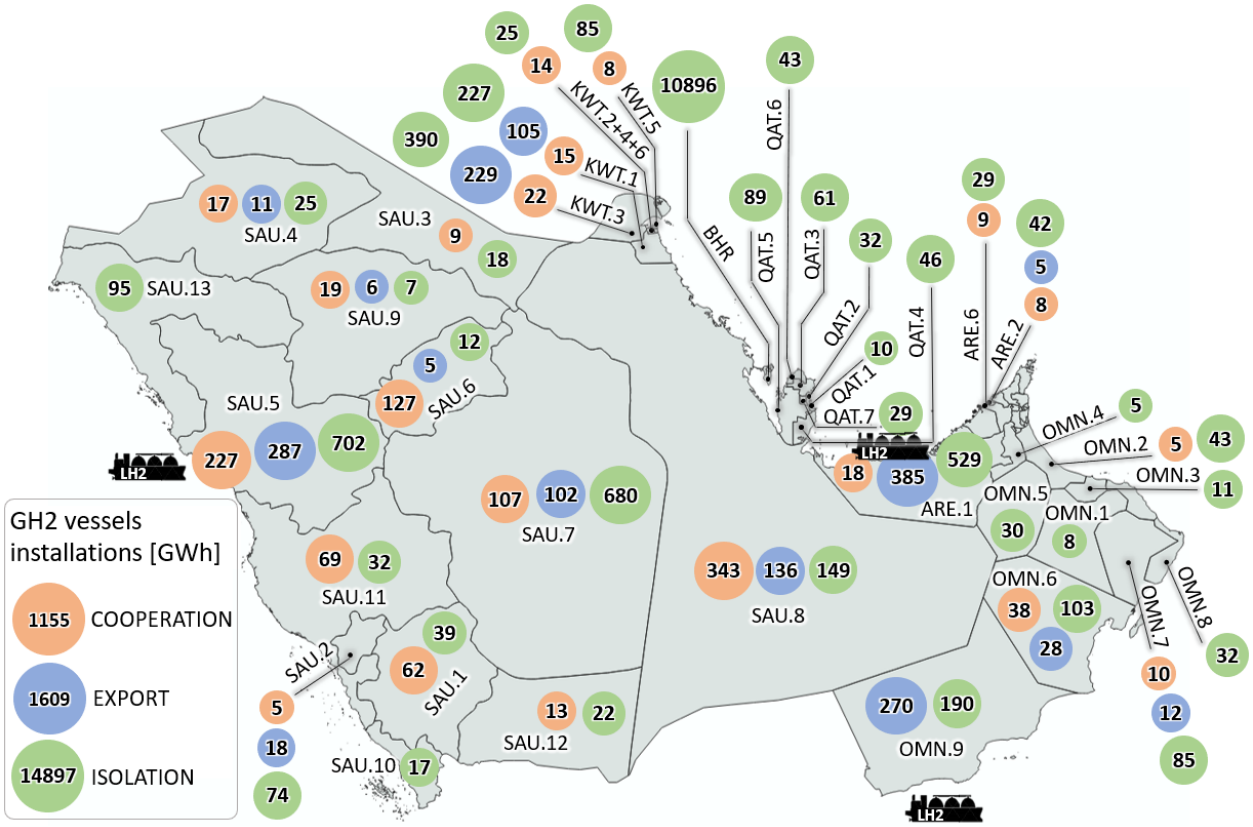

Figure 6.12: Installations of hydrogen vessels across the three main scenarios. Values below 5 GWh are not reported

Finding an explanation for the exact layout of vessels chosen by the optimisation process is not simple, but some points can be made for sure. First and foremost, great capacities are located where high combined electricity and hydrogen demand and production are located, for example in Kuwait, SAU.5, SAU.11, SAU.7 and SAU.8. However, another condition must be verified for this to occur: wind energy share in the energy mix has to be high, approximately above 60%. The two statements are then also able to explain why the Arab Emirates and Qatar, possessing high energy demand and VRES installations, only show little hydrogen vessel installations. A sort of parallel can therefore be established with batteries, which are instead located where PV share is greater. The two criteria offered here to account for vessels installations also explain why OMN.9 produces a lot of electricity through wind, but hosts no vessel. However, there are two exceptions to what discussed so far. The first is constituted by SAU.6 in the cooperation scenario, which has low demand and low production, mostly from PV, but high vessel installations. This region is however a key passage of hydrogen between SAU.7 and SAU.5, which together make up half of the total hydrogen demand of the GCC. Therefore, it is reasonable that hydrogen is stored between these two nodes of the system. The second exception is OMN.6: this region produces a lot of electricity through wind, but has close to no hydrogen demand, so that its 38 GW of vessels would not be expected according to what stated earlier. Probably, the system here has to somehow compensate the extremely high production of hydrogen in OMN.6 and OMN.9 neighbouring it with the extremely low local demand, avoiding the installations of additional pipelines capacity for hydrogen export, which are already extremely high, as described in subsection 6.1.2.

The concentration of all hydrogen demand in the three ports as modeled in the export scenario radically changes the distribution of vessels installations, something which is not observed for batteries. As could be expected, significant installations are created at the three ports, particularly in ARE.1, which hosts almost 40% of all vessels, against approximately 17% for both SAU.5 and OMN.9. Less easy to predict is the dramatic increase of installations in Kuwait, which overall come close to that of ARE.1. Most likely, the country cannot rely anymore on its local hydrogen demand to balance production, so that it is forced to store hydrogen. The lack of local hydrogen demand in SAU.8 has the opposite effect, as vessels in the region are halved in the export scenario with respect to the cooperation one, while total production even increases. This different outcome is arguably due to the fact that the region can now rely on an incredible sink constituted by the neighbouring port of ARE.1, where storage installations are at their record value. In other words, the storage capacity made necessary by the hydrogen production in SAU.8 seems to be simply shifted to ARE.1, so that its own vessels capacity is reduced.

As was the case for batteries, the isolation scenario forces the system to increase its overall capacity of vessels. Supposing not to consider the huge capacity registered in Bahrain, the amount of vessels would still quadruple between the cooperation and the isolation scenario, while that of battery only doubles. This has a very important implication, namely that system flexibility is more important for the hydrogen side of the system than the electric one. As mentioned in subsection 6.1.2, this mainly stems from the costs assumed for the transmission and storage technologies. As for the location of installations, SAU.5 and SAU.7 each hold approximately 40% of the total 1900 GWh installed in the country, most likely as a consequence of their high demand and production of both electricity and hydrogen. The same can be said for SAU.8, although on a lower scale. More importantly, SAU.8 reduces the amount of vessels installed in its territory, highlighting once again the fact that the existence of connections (or lack thereof) between the different GCC countries impact this strategic region significantly, as it hosts the node where the grid of of the different countries converge.
As already mentioned, the capacity of vessels in Bahrain shows a value greater than any other region by at least two order of magnitudes, namely 11 TWh. Besides, it is found that the discharge operation of these technologies offers almost as much energy as the entire hydrogen demand of the country, namely around 18 TWh. This high dependence on hydrogen storage can be explained with the fact that Bahrain cannot rely on an abundant VRES potential; on the contrary, it is forced to use 90% of the total energy available, including very expensive offshore turbines. Besides, this is also due to a more intense use of hydrogen reconversion, most notably through solid-oxyde fuel cells. In particular, reconversion provides over 6 TWh of electricity to the country, thus consuming 9 TWh of hydrogen and leaving only the remaining 9 TWh to satisfy hydrogen demand, so 50% of the total hydrogen produced.
As a side note, while Bahrain could potentially be self-sufficient from an energy point of view according to the results of the optimisation, it is unlikely that the necessary amount of hydrogen vessels can indeed be installed as required. This is because all land made eligible for VRES is occupied almost exclusively by PV panels, while other territories have been mainly excluded due to urban settlements, as reported in

section 5.1. Therefore, no space could be found in reality for such a great capacity of vessels, unless by reducing PV installations to a too great extent. In particular, 41 km^2 of free area would be required at low compression factors, and that is considering only the hydrogen volume of the storage system [199] [1]. This is 36% of the eligible land for PV panels and equal to 104 km^2. Compressing the hydrogen at very high pressure could be considered as an option to save space: this is not an efficient solution, but it would be the only possible one if Bahrain was really to create a completely self-sufficient energy system based on VRES. Underground storage could also achieve this result, although additional work and therefore money has to be considered, unless an efficient reconversion of existing facilities for oil&gas is implemented.

Finally, some interesting figures are discussed regarding the use of hydrogen vessels in the GCC area as a whole. The nominal cycles of vessels are always lower than those of batteries. In the cooperation scenario, 110 nominal cycles are run on average on vessels, three times less than batteries. In this way, they satisfy 12% of overall hydrogen demand, while batteries registered 18% of the final power demand. In the export scenario, overall capacity of hydrogen storage increases from 1155 GWh to 1610 GWh, but the cycles are lower on average, namely 89. Consequently, a less optimal sizing of the hydrogen storage system is registered when hydrogen demand is concentrated at the three ports. In spite of this, the vessels still absorb and provide more energy than in the cooperation scenario, that is 15% of the final demand, against the 23% scored by batteries with respect to electricity demand. As expected, due to the lower flexibility of the system in the isolation scenario, vessels are even more oversized, running only 65 nominal cycles on average to satisfy as much as 31% of final hydrogen demand, even more than the 30% ratio obtained for batteries in the same scenario.

6.1.5 Costs

As explained in section 4.3, the optimisation algorithm of FINE is based on the minimisation of the total annual costs (TAC) of the energy system, which are calculated by the tool based on the techno-economic parameters specified for all the components of the system and reported in chapter 3 and 4. An analysis of the system costs obtained for the three main scenarios is presented in this subsection, concluding the study of the system behaviour in these study cases. The following analysis is able to directly answer two of the research goals of this study. First, to quantify the economic benefits of creating a common energy system based on renewable electricity and green hydrogen for the GCC countries, with respect to the situation in which each country acts independently. This is done by comparing the cooperation and the isolation scenario. Secondly, to calculate how much more or less expensive would the system be when the hydrogen needed to satisfy local hydrogen demand is not consumed locally but instead transported and liquefied at strategic ports in order to be shipped. This is achieved by comparing the cooperation and the export scenario.

The total cost value in billion euros directly retrieved by the objective function can be used to compare results to some extent, but its meaning is limited in a way. Typically, costs are reported in terms of LCOE [€c/kWh] when final energy demand is electricity, or in terms of LCOH [€/kg] when final energy demand is hydrogen. Since in this case final energy demand is composed of both electricity and hydrogen, it is not possible to present the results of the main scenarios in terms of LCOE or LCOH. Therefore, a new cost parameter is created which allows to sum hydrogen demand and electricity demand in a reasonable way, thus allowing to refer costs to energy units. In fact, the chosen parameter normalises costs with respect to the theoretical equivalent electricity demand required by the combined electricity and hydrogen demand modeled for each scenario. In practice, this is obtained by summing the final electricity demand with the theoretical electricity required to run electrolysis and, if relevant, liquefaction to obtain the final hydrogen demand. This parameter is hereon called Levelised Cost of Combined Electricity and Hydrogen (LCOCEH).
The advantage of normalising costs with theoretical electricity demand instead of total primary electricity generated is that, given the same proportion of electricity and hydrogen in final demand, the LCOCEH decreases together with system efficiency, just as LCOE and LCOH do, offering a way to measure the efficiency of the system. Besides, if final demand is exclusively electricity, LCOCEH and LCOE are exactly the same. Similarly, if final demand is only composed by hydrogen, the LCOCEH can be directly converted to LCOH by using the techno-parameters of the electrolyser and the liquefier of Table 4.3. Due to its definition, the relation between TAC and LCOCEH is not the same across all scenarios, since this depends on the type

[1] At ambient temperature and a pressure of 10 bar, hydrogen density is 0.8 kg/m^3 [199]. Using the LHV of hydrogen of 33.3 kWh/kg [173], 409 Mm^3 are required to install 10896 GWh of stored hydrogen. Using a height of 10 m for vessels, 41 km^2 are eventually obtained

of final demand, for example if the hydrogen is required in the gaseous or liquid form. This should be kept in mind when looking at the bar charts reported here and in the following sections, which show TAC in absolute terms and also in terms of LCOCEH. As already mentioned, the LCOCEH can be used to directly compare the variation of system efficiency only if two scenarios feature exactly the same demand. However, comparisons can be made also in other cases, although with some clarifications depending on each single case. The physical meaning of LCOCEH is more difficult to grab than that of the LCOE and LCOH, but this is necessarily the case given the mix of hydrogen and electricity in final demand. Indeed, the LCOCEH represents a sort of compromise between these two commonly used parameters.

The breakdown of costs for all three main scenarios is reported in Figure 6.13. In case the countries formed a single energy system, the TAC would be around 130 €bln/year, which in LCOCEH is approximately 5.6 €/kWh; viceversa, if they decided to act independently, the overall costs would increase by almost 21%. Comparing the isolation scenario with the cooperation one, all components of the system register an increase in costs, except for the transmission ones, highlighting the reduced flexibility of the energy system.

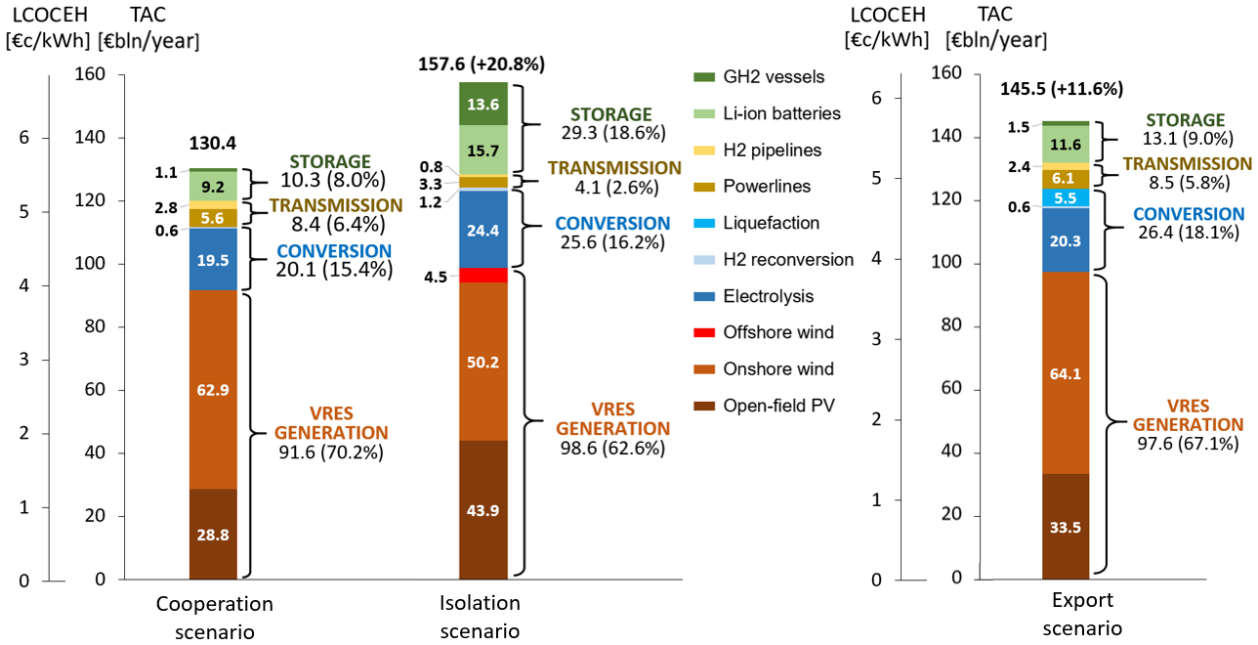

Figure 6.13: Breakdown of total annual costs (TAC) across the three main scenarios. The labels of the cost bars are referred to the TAC axis

Most significant is the increase in storage, in particular hydrogen vessels, which imply a cost of 13.6 €bln/year with respect to 1.1 €bln/year in the cooperation scenario. With regard to this specific result, the eminent role of Bahrain should be acknowledged as explained in subsection 6.1.4: 73% of installations are due to this country. These account for 10 €bln/year in the isolation scenario. However, this country is not responsible for additional costs related to batteries, which are only 0.4 €bln/year in the case of Bahrain when isolated. The cost of VRES generation is also higher, namely 7%. Once again, Bahrain is responsible for a high percentage of this number. However, considering the average LCOE of its wind turbines of 8.2 €c/kWh against the typical cost of electricity generated for the system in the cooperation scenario of 3.8 €c/kWh, the overall generation costs of the GCC would still increase by around 5% even if Bahrain was not considered. Looking at other VRES sources, the share of total costs radically changes for open-field PV and onshore wind turbines. Under a cooperation scheme, wind installations would amount for 2.2 times more costs than PV in total, while the absolute cost of onshore turbines is only 10% higher in the isolation scenario. This is in line with the total energy offered by these sources in the two scenarios as shown in subsection 6.1.1, although some additional considerations will be done with regard to this later on.
Finally, important additional expenses when the countries are isolated stem from conversion technologies, almost entirely from the extra installations of electrolysers. In fact, as already mentioned in subsection 6.1.3, these have to be oversized with respect to the cooperation scenario, running at a lower average capacity

factor.

From what has just been explained, it is clear that Bahrain would tremendously benefit from the cooperation scheme. In fact, the previous considerations allow to state that up to half of the 21% increase of costs of the isolation scenario can be related to this country alone. However, a 10% cost increase is still achieved even not considering Bahrain. In order to verify to which extent each country individually benefits (or otherwise) from a common electricity and hydrogen system, Figure 6.14 is created, where the overall benefit can be evaluated referring to the LCOCEH. In fact, the overall demand is the same in both scenarios, which allows to use this parameter directly, as mentioned earlier.
With respect to the LCOCEH value of 5.6 €c/kWh, all states are found to benefit from cooperation except for Saudi Arabia, which however registers an almost identical LCOCEH when isolated (+2%). Among the other countries, Oman sees its LCOCEH reduce by 4%, while the Arab Emirates, Qatar and Kuwait all enjoy a system 20% to 32% cheaper. As expected, the decrease in costs for Bahrain is by far the highest at 80%. These figures prove that connecting different countries particularly favours those which are characterised by lower VRES potential with respect to their energy demand. In fact, the system is indeed more flexible from their point of view as well as from the general one. On the contrary, costs of bigger countries are not necessarily decreased, as shown by the case of Saudi Arabia, since its system is already highly flexible and is made more inefficient by adding significant values of localised demand to it.

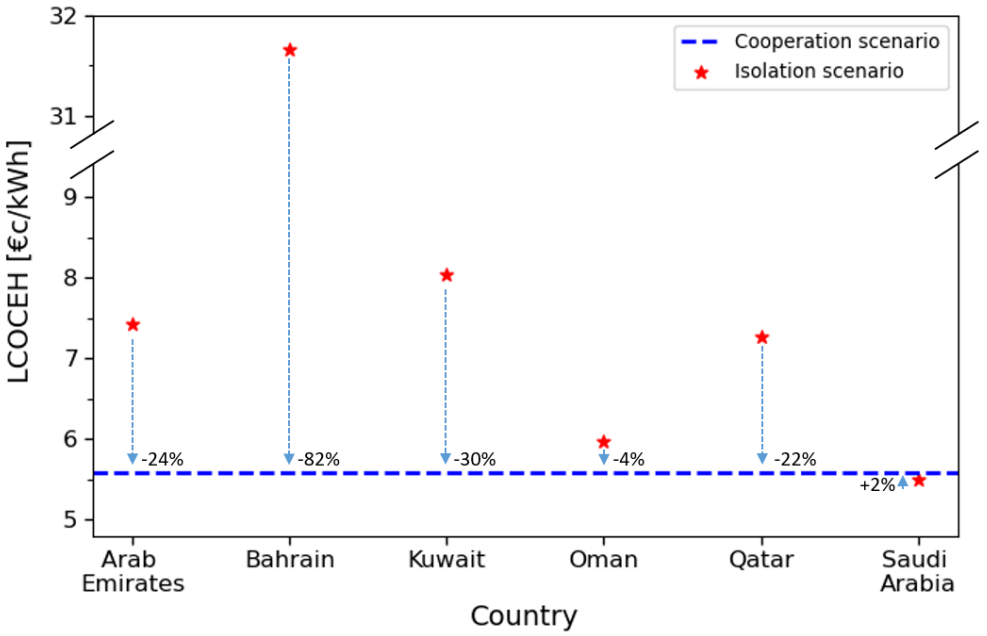

Figure 6.14: Individual LCOCEH of each GCC country in the isolation scenario and LCOCEH of the interconnected GCC system in the cooperation scenario

As anticipated, the costs of VRES with respect to the electricity they produce should also be discussed more in depth. In fact, subsection 6.1.1 has already mentioned the fact that the role of wind energy in the generation mix is unexpectedly high, at least judging from the LCOE values obtained and reported in chapter 5. Particularly interesting is the fact that some wind turbines are chosen to be installed by the tool even if their theoretical price (when no curtailment is considered) is higher than 5 €c/kWh also in the cooperation scenario, when the flexibility is greater. What is also remarkable is that even if the overall costs of PV parks increase together with their installations when the countries are isolated, their actual LCOE is almost unchanged at 3.5 €c/kWh across the cooperation and the isolation scenario, while that of onshore wind turbines increases from 4.0 €c/kWh to 4.5 €c/kWh, which is also due to curtailment. This could be because wind production is connected with hydrogen demand more than PV, while the hydrogen transmission system is cheaper and therefore more intensely exploited than the electric one. Consequently, isolating the countries would mainly impact optimal hydrogen production and consequently onshore wind generation, whose performance drops. This idea is backed up by the results of subsection 6.1.4, where it has

been shown that hydrogen vessels installations (excluding Bahrain) quadruple from the cooperation to the isolation scenario, whereas batteries only double, confirming the higher impact on isolation on the hydrogen components of the system. Another way of explaining the increase in onshore wind costs is to note that these show very different time series among different regions, which allows to create synergies among them in order to reduce curtailment. This phenomenon is limited if countries cannot exchange energy among them. In fact, it is important to point out once again that the higher costs of VRES with respect to the lower values reported in chapter 5 is due to curtailment, which is performed by the optimisation tool to reduce storage installations.

The comparison between the cooperation scenario and the export scenario of Figure 6.13 reveals that liquefying hydrogen increases the overall costs of the system by 11.6%. The additional step of liquefaction does not impact the share of LCOCEH due to electricity generation„ which stays equal to 3.9 €c/kWh. This indicates that the extra 6 €bln/year due to VRES generation are only related to the additional amount of energy required for liquefaction, and not to a higher specific cost of electricity. Even though the relative addition of hydrogen vessels is rather high at 50%, this only slightly impacts the TAC (+0.4 €bln/year), which are instead more affected by the higher amount of batteries (+2,4 €bln/year). The only other difference is due to electrolysers (+0.8 €bln/year), which have to produce 2% more hydrogen due to losses on the liquefiers further down the line and which also show a 2% lower operation rate. Finally, transmission costs are unchanged between the cooperation and the export scenario.
The considerations just made allow to state that the extra costs of the export scenario are almost entirely linked to the additional electricity required by the system, but not to the concentration and relocation of hydrogen demand. In fact, ignoring the cost of the liquefiers themselves, the almost entirety of additional expenses are due to two main factors. First, VRES installations, which however feature the same LCOCEH of the cooperation scenario. Secondly, batteries, which have been shown to be more closely related to electricity demand than hydrogen demand over the previous subsections. This last and very important point will be finally proven in subsection 6.2.1. Clearly, the relatively low costs used to model both hydrogen vessels and hydrogen pipelines influence these considerations, as mentioned already in multiple occasions.

6.2 Functional scenarios results

The study of the main scenarios conducted in the previous section has highlighted interesting aspects of the system behaviour. Therefore, a series of additional scenarios called “functional” has been designed in order to study some of these particular features. In particular, subsection 6.2.1 focuses on the relationship between the generation mix of VRES and the type of energy demand, either in the form of electricity or hydrogen. The discussion also allows to quantify the economic benefits of coupling the electricity and hydrogen demand in a single energy system. Next, subsection 6.2.2 conducts a sensitivity analysis of TAC by varying the CAPEX of either wind or PV technologies. The analysis also allows to delve deeper into the relationship between the type of VRES and storage installations.

6.2.1 Sector coupling for the export scenario

This subsection is intended to better understand the importance of the role of wind energy in the system and to gain further insights into its relationship with the type of final energy demand. Moreover, it allows to quantify the economic benefits of coupling the liquefied hydrogen production chain with the power sector building on the export scenario already presented.

According to the discussion conducted in section 6.1, a particular pattern in the optimisation process was observed which seems to privilege wind farms over PV farms when they show the same theoretical LCOE. In particular, this seems to be the case especially when wind energy has to match constant hydrogen demand. Clearly, electricity is always the same irrelevant of its production method or final use. Therefore, the two following reasons have been pointed out so far to explain this phenomenon. First, the better match between wind turbines’ feed-in time series and the constant hydrogen demand profile assumed here, particularly the hydrogen one. Secondly the possibility to transport hydrogen in a cheaper way than electricity. The second condition, in fact, allows the system to rely on VRES sources located far from energy demand location, including those regions which feature the cheapest wind turbine.

To finally prove the dependency between wind turbines’ feed-in time series and hydrogen demand, the export

scenario is analysed under the condition where the demand of only the power sector or the hydrogen sector has to be satisfied. These functional scenarios are respectively called "electricity-demand" and "hydrogen-demand". The choice of applying variations to the export scenario instead of the cooperation scenario is due to the fact that the primary energy demand required by the latter is higher and therefore a higher benefit should be measured by sector coupling. In the electricity-demand scenario, 1098 TWh have to provided, whereas in the hydrogen-demand scenario, 867 TWh of liquid hydrogen are required, for whose liquefaction 181 TWh of electricity are needed. Consequently, the hydrogen-demand scenario is characterised by a way higher hydrogen demand than electricity demand, where no hydrogen demand is present at all. Conversely, in all main scenarios analysed in the previous section electricity demand is greater than the hydrogen one.

The results turn out exactly as expected. In fact, the hydrogen-demand scenario features a penetration of wind turbines of 57% in terms of installed capacity, while the export scenario is characterised by a perfect balance of PV and wind turbines installations. Conversely, the electricity-demand scenario has less wind turbines installations, although not significantly: 49% against the 50% of the export scenario. In this case, the ratio of the electricity produced by wind turbines with respect to the total generation mix is also decreased by the same small proportion and equal to around 63%. This last result is connected with a new finding, namely that wind energy is the best source not only for hydrogen, but also for electricity production, although to a lesser extent. In other words, the benefits of the wind feed-in time series are observed also with respect to an irregular profile such as that of the power sector, and not only with respect to a constant demand profile such as that modeled here for hydrogen.

The electricity-demand and hydrogen-demand scenario, together with the export scenario of the previous section, allow to measure the cost savings of combining the production of green electricity and liquefied hydrogen with respect to having two separate systems. The result can be immediately obtained by comparing Figure 6.15 with Figure 6.13. The sheer sum of the costs registered by the electricity-demand and hydrogen-demand scenario would amount to 157.2 €bln/year, while the export scenario registers 145.5 €bln/year. This implies a 7.5% cost reduction by coupling the two systems. This improvement is driven by the reduction of storage costs by 15% and that of VRES costs by 8%, while the expenses due to transmission and conversion remain unchanged. Also interesting is the fact that batteries are almost not used in the hydrogen-demand scenario, since hydrogen storage in vessels is more economically convenient in this case. Conversely, in the electricity-demand scenario only batteries are used. Besides, the capacity of hydrogen reconversion technologies is increased from 7 GW to 10 GW, although this remains a negligible number if compared to the overall installed capacity of VRES equal to 669 GW.

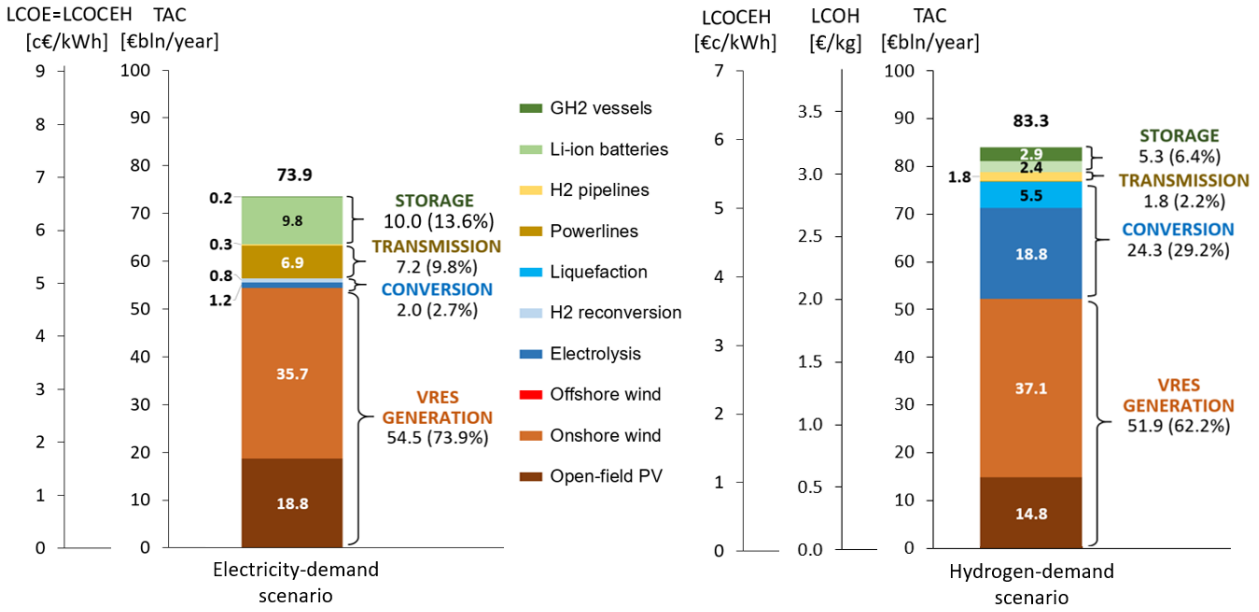

Figure 6.15: Breakdown of total annual costs (TAC) across the electricity-demand and hydrogen-demand scenarios. The labels of the cost bars are referred to the TAC axis

It should be noted that the LCOCEH of the hydrogen-demand scenario is lower than that of the electricity-demand scenario, but not because the overall system efficiency of the hydrogen-demand scenario is higher. In fact, the LCOCEH parameter is able to offer a comparison in this sense only when the penetration of hydrogen in total final demand is the same. This is because the demand value of hydrogen first has to be translated into theoretical electricity using the conversion efficiency of the electrolyser and the liquefier, whereas the demand value of electricity is simply considered as such. In this case, the difference in LCOCEH is due to the fact that the cost of batteries and powerlines in the electricity-demand scenario outweigh that of electrolysers and liquefiers in the hydrogen-demand scenario with respect to the theoretical electricity demand required in the two cases. The LCOCEH of the export scenario is anyway lower than that of each of the two functional scenarios now discussed, which indeed shows an increase in efficiency. Averaging the LCOCEH of the hydrogen-demand scenario and of the electricity-demand scenario and comparing it with the LCOCEH of the export scenario, the same decrease of 7% is found as discussed when comparing TAC, which also proves the reliability of the LCOCEH parameter.

6.2.2 Sensitivity analysis

Subsection 6.1.1 has indicated that wind energy is responsible for around two thirds of the total electricity produced in the cooperation scenario, even though installations in terms of capacity are rather balanced, namely 47% and 53% for PV and wind farms respectively. As already explained, this is due to higher FLH of wind turbines, an effect which is even amplified by the curtailment of PV generation by the optimisation tool. Given the eminent role of wind in the generation mix, it should be expected that varying the cost of wind influences TAC more. In order to verify and quantify this point, ten scenarios are run varying the CAPEX of either wind or PV technologies by different amounts, as reported in Figure 6.16. Among these scenarios, two of them feature the installation of either only PV panels or wind turbines, which is the equivalent of increasing the CAPEX of either wind or PV technologies technologies respectively by several orders of magnitudes.

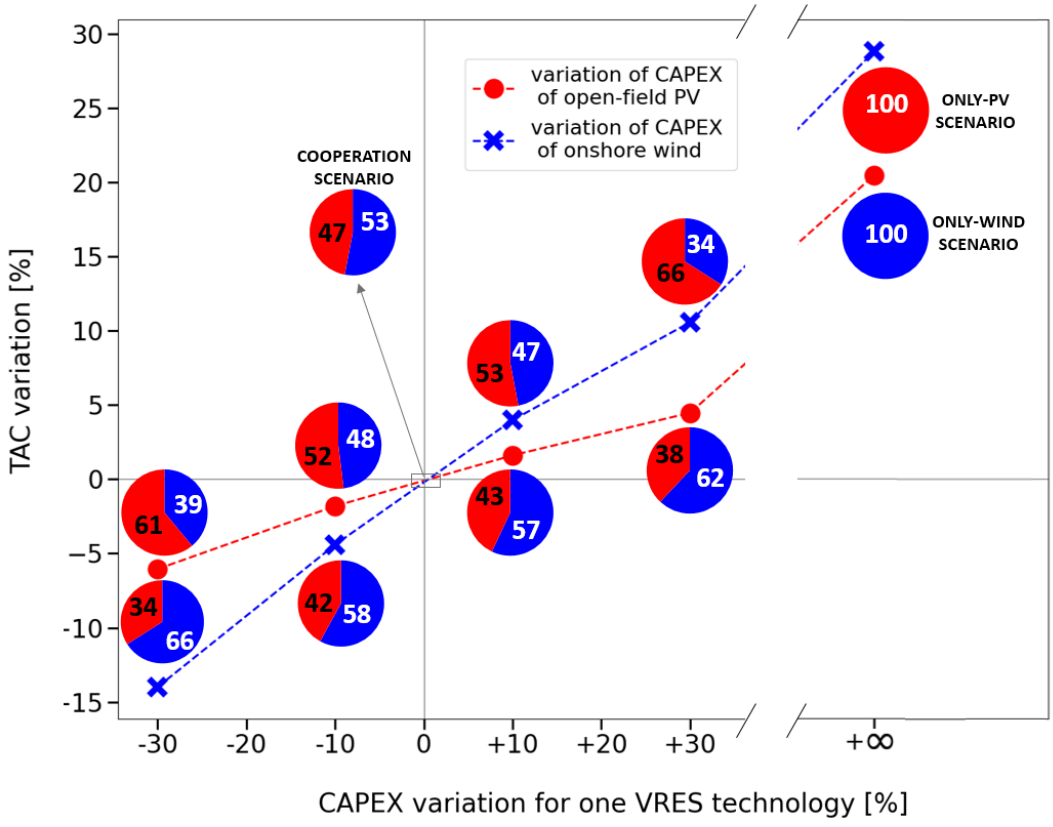

Figure 6.16: Variation of total annual costs (TAC) in function of CAPEX of VRES technologies. The pie charts represent the capacity [%] of open-field PV (red) and onshore wind (blue) with respect to total VRES installations for each different scenario

The sensitivity analysis confirms the higher influence of varying the cost of wind turbines with respect to that of PV panels. In particular, the relative variation of TAC is always around twice as high for the same relative variation in CAPEX of wind turbines than in CAPEX of PV panels in the examined range of -30% to +30% of CAPEX. This almost constant ratio is particularly interesting if one considers the fact that the share of total installed capacity changes considerably across the functional scenarios considered here, adapting to the different cost assumptions of VRES technologies. It could be the case that this phenomenon is due to the fact that the same relative increase in CAPEX for wind and PV leads to absolute variations approximately in the ratio 2:1, since the CAPEX of wind turbines is around twice as high as that of PV considering the same installed capacity. Also interesting is the fact that the rate of decrease of TAC for a decreasing CAPEX is faster than the rate of growth for an increasing CAPEX, a pattern which is registered for both wind and solar technologies. This is because the total costs of the system would be at least 41% lower than in the cooperation scenario if the CAPEX of one technology dropped to zero, while the costs in Figure 6.16 rise only by a maximum of 28% in the scenarios with one technology. The value of 41% just mentioned is found excluding the costs of PV from those of the only-PV scenario, which would then be equal to zero for a -100% CAPEX variation, while the minimum costs decrease would be even greater based on the only-wind scenario. Looking specifically at the curve describing the variation of TAC as a function of the CAPEX of wind turbines, these are found to make up for two thirds and one third of overall installations in the most favourable and unfavourable cost conditions, producing three quarters and half of total electricity respectively. When wind turbines are finally removed from the system and only PV panels are left, TAC increase by almost 30%.
As for the variation of the CAPEX of PV panels, the share of PV capacity with respect to the total ranges from 61% to 38% for a negative and positive variation of CAPEX of 30% respectively. The associated energy produced is half and slightly less than one third respectively. The fact should be stressed that PV production is never able to surpass wind production by more than 1% in none of the ten functional scenarios of Figure 6.16 where both technologies are used. This is true even when PV capacity is found to be two times higher than that of wind farms. When PV panels are removed, the system based only on wind turbines is 20% more expensive than that of the cooperation scenario. Therefore, the increase of TAC due to a generation mix entirely based on wind turbines is significantly cheaper than that of a fully-solar mix, which has been reported at +30%. This is line with the choice of the optimisation tool to produce two times more energy with wind turbines rather than PV panels in the cooperation scenario. The reason for the outcome of optimisation regarding the VRES mix has been already suggested in different occasions by saying that the feed-in time series of wind turbines are found as a better match for the adopted electricity and hydrogen demand time series, allowing to minimise the related storage and curtailment costs. However, as shown by the higher TAC of the only-wind scenario with respect to the cooperation scenario, a combination of wind and solar farms is the best solution for a fully renewable system.

Another trend already highlighted in the previous section is that the installation of batteries is higher in regions featuring a higher penetration of PV in the generation mix, while hydrogen vessels are typically located where a high penetration of wind is found together with a high energy demand. In order to prove these parallel trends between VRES and storage technologies with a higher degree of certainty, a more analytical method is however necessary.
The method used here to gain a clear insight into the relationship of different subcomponents of the system such as PV panels and batteries is to relate the capacity of each subcomponent to the total capacity of the macro-component to which it belongs for different scenarios. Therefore, installations of PV panels are divided by the total capacity of VRES technologies in the system. Similarly, batteries are normalised with the total capacity of storage technologies. The same approach is finally adopted for transmission technologies, since an interesting pattern could be observed for them as well.
Applying the method just explained to all ten scenarios discussed earlier and to the cooperation scenario as well, Figure 6.17 is created. This reports the normalised capacity of batteries, PV parks and powerlines at the end of each optimisation. The relationship that is observed between the system components is highlighted by the dashed red and blue lines, which represents the linear fit of the different scenarios over a certain range of PV share. What is most striking is that the dependency between the normalised share of PV and that of batteries can be fit linearly rather accurately over the whole possible values of PV share in the generation system. Moreover, it can be observed that normalised powerline installations linearly decrease with the share of PV installations up to the value of 70% of total capacity. Looking at the results of optimisation obtained for the case where only wind turbines are present, it is observed that the entire storage system is made up almost exclusively by hydrogen vessels. Instead, the share of batteries increases to 54% of total installations

when only PV panels are used.

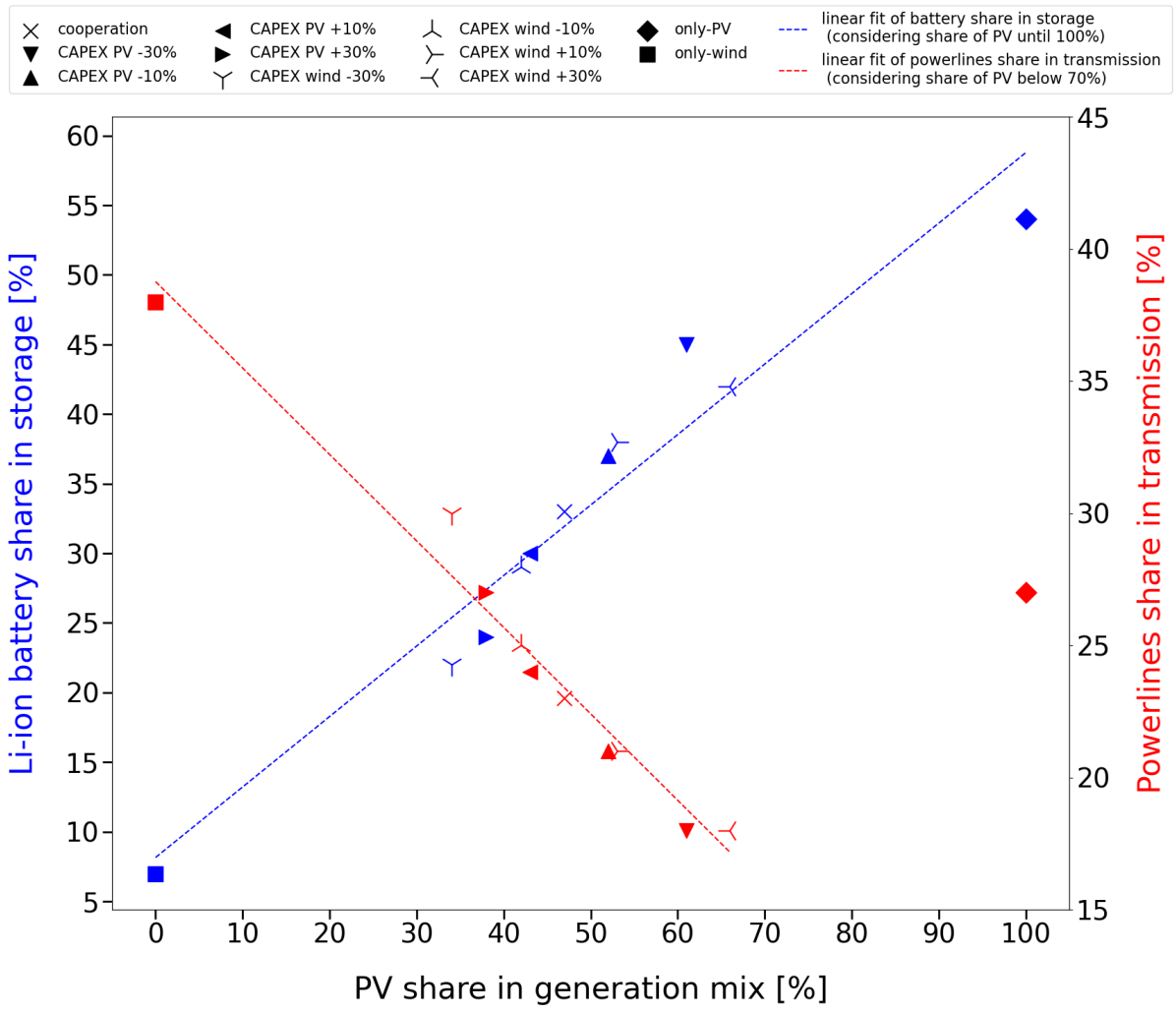

Figure 6.17: Graphical representation of the relation between i) open-field PV installations with respect to total VRES installations, ii) Li-ion batteries installations with respect to total capacity of storage installations and iii) powerlines installations with respect to total capacity of transmission installations. Symbols of the same type but of different colors are the result of different system components of the same scenario

The observations just made confirm once and for all the fact that a higher PV production is associated with a higher amount of batteries. Conversely, hydrogen is by far the preferred way to store energy when wind penetration is increased. This confirms the observations made in this sense in subsection 6.1.4.

7 | Discussion

This chapter discusses the results obtained in this work. Accordingly, it is divided in two parts: section 7.1 revolves around VRES potential and costs, whereas section 7.2 focuses on the different aspects of the ESM. Each section first collects the main findings of the obtained results, critically reflecting on them while accounting for the research goals outlined in chapter 1. Following this step, a selection of the results of this work is compared with other studies. The choice is based on relevance but also on availability of other sources in literature, since not all results can be compared.

7.1 VRES potential discussion

This section is devoted to the discussion of the potential of VRES technologies in the year 2050. Since a thorough analysis of the results has already been offered in chapter 5, only an overview of the main results is now reported in subsection 7.1.1 in a succinct way, which simplifies the task of discussing them in this chapter. Besides, the potential of VRES is related to the future energy demand modeled in chapter 4, while some comparisons with literature are also offered for LCOE prices.
In order to prove the reliability of the models used and presented in chapter 3, a direct comparison of the VRES potential of this and other studies would not be meaningful, as it would not allow to understand where the differences between the results stem from. Rather, these mainly originate from the outcome of the LEA and from that of the VRES simulations. Therefore, an independent comparison of their assumptions and associated results with existing literature is conducted in subsection 7.1.2 and subsection 7.1.3 respectively.
In line with the previous parts of this report, each subsection will deal with one VRES technology at a time, using the following order: open-field PV, onshore wind and finally offshore wind. As always, meaningful comparisons among these three items are also offered when necessary.

7.1.1 Overview of the VRES potential and costs

Based on the LEA and the subsequent VRES simulations, whose methodology and results have been reported in chapter 3 and 5 respectively, the potential of open-field PV, onshore wind and offshore wind in the GCC countries has been obtained. To summarise this result, Figure 7.1 shows the energy potential and the LCOE of the studied technologies for the whole area considered in this study. These can be compared with the energy demand modeled for the system, which is shown in Table 7.1 together with the VRES potential at a country level. In order to have a reference for the numbers that will be presented, it is useful to keep in mind that the most competitive LCOE registered by fossil fuels today is of 5 €c/kWh [200]. Also important to note, the lowest LCOE values found by this work for onshore wind and open-field PV are respectively 50% and 60% cheaper than those observed today for these technologies in the entire MENA region [201].

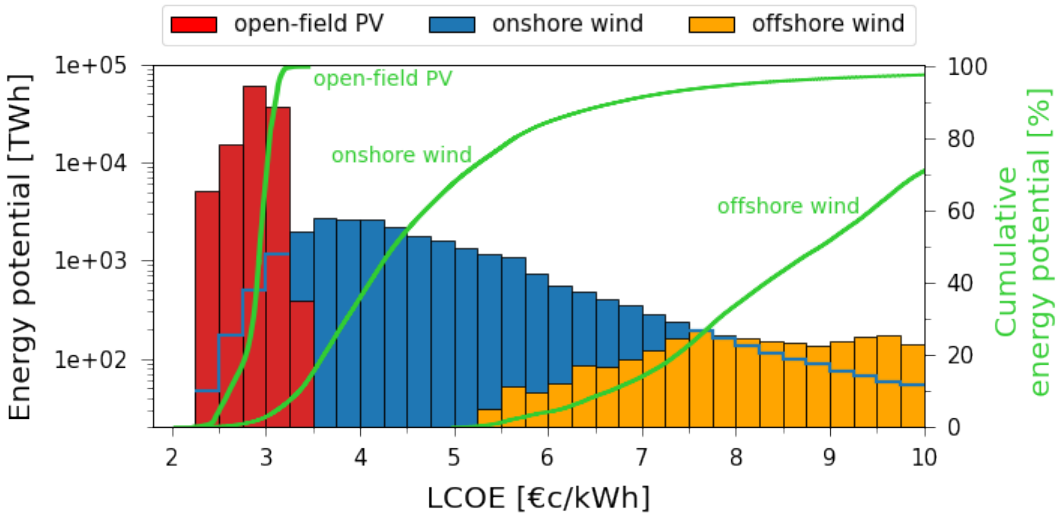

Figure 7.1: Distribution of the overall VRES potential in the GCC area in 2050 over the price range 2-10 €c/kWh. The blue line crossing the bars is related to onshore wind potential where other VRES are also available

Table 7.1: Comparison of VRES potential and energy demand in the GCC area in 2050

Country	Open-field PV potential [TWh]	Onshore wind potential [TWh]	Offshore wind potential [TWh]	Total VRES potential [TWh]	Electricity demand [TWh]	Hydrogen demand [TWh]
ARE	958	230	248	1436	208	129
BHR	9	0.5	59	69	28	18
KWT	920	278	102	1300	98	53
OMN	21440	4729	688	26857	89	71
QAT	391	88	368	847	58	53
SAU	94631	20287	1827	116745	615	543
GCC	118349	25613	3292	147254	1098	867

Unfortunately, to date no scientific study offers an equally detailed breakdown of both VRES potential and LCOE for the Arabian Peninsula. In fact, most studies find the potential of renewable technologies also for the area investigated here, but do not report costs [202–206]. Besides, other studies report future LCOE prices for the countries under exam, but only as average values [8, 205]. Finally, some authors studied the LCOE distribution for the considered countries, but not for future scenarios [207]. Only one study is more complete in this sense, namely that of Fasihi and Breyer [208]. This is able to offer an overview of future LCOE prices for both onshore wind and PV technologies in each area of the globe, but only offers colourmaps and no analytical data on single countries or regions, meaning that only rather coarse estimations can be performed based on that. Therefore, the comparison of LCOE with other studies cannot offer a very effective way to assess the quality of the results obtained for VRES, especially in the case of offshore wind technologies. However, some analogies will still be offered in this subsection using the most meaningful data available in literature for the present case. In order to assess the plausibility of the cost results obtained, the discussion on FLH in subsection 7.1.3 will prove more beneficial. In fact, apart from technology-specific costs, which have been here assumed based on Ryberg [135] and Caglayan [6], FLH are the main driver of the LCOE.

Solar energy is found to be the cheapest and most abundant resource in the Peninsula, with a potential of almost 120,000 TWh distributed between 2.2 €c/kWh and 3.5 €c/kWh. It is meaningful to compare the lower boundary of this price range with the equivalent calculated for southern Spain by Fraunhofer ISE [155] because of two reasons: first, relatively similar values of maximum DNI [2], with Spain registering a 20% lower value than the Arabian Peninsula, secondly, same investment costs used for PV in this study and in Fraunhofer ISE [155]. Even if maximum DNI in Spain is lower, the same lowest LCOE is obtained here for the Peninsula and by Fraunhofer ISE [155] for southern Spain. This can explained with the fact that Fraunhofer ISE [155] supposes a value of 5% for the interest rate, whereas Ryberg [135] and this study use 8%. This difference can lead to a price increase of 20%, as reported by Fraunhofer ISE [155] itself. By using a CAPEX of 390 €/kWh for their 2030 energy system, i.e. 110 €/kWh less than this study, Aghahosseini et al. [8] come to an average LCOE for fixed-tilt PV in GCC countries of 2.8-2.9 €c/kWh. This is only slightly cheaper than this study, since higher OPEX and lower FLH were considered in their study hence counterbalancing the effect of lower CAPEX. Since they start from the same average FLH as this study but half the investment costs (276 €/kW$_p$), Fasihi and Breyer [208] report a significantly lower range of LCOE in 2050 over the Peninsula, namely 1.3-2.0 €c/kWh. Instead, Pietzcker et al. [205] calculate an average value of 3.9 €c/kWh for 2050 referring to the entire MENA region, which can be compared to the GCC area since the average FLH they report are almost the same. The deviation with respect to the results of this study is due to the higher investment costs supposed by the author, approximately twice as much as those adopted here.

Although the majority of the potential of open-field PV is concentrated around a value of 3 €c/kWh in this study, the entire energy demand of the Peninsula could be theoretically satisfied with installations below 2.5 €c/kWh. The electricity generated with solar energy is also sufficient to cover the demand of each country also at a country level, except for Bahrain, which is mainly due to the high fraction of land excluded by the LEA there. For the biggest GCC countries, the potential is approximately two orders of magnitude higher than the national energy demand.

With 25600 TWh, onshore wind is the second largest renewable energy source on the Peninsula. As can be observed in Figure 7.1, onshore wind potential shows a way larger variation of LCOE with respect to open-field PV, which naturally follows from the considerable differences in average wind speed on the Peninsula, as is shown in Figure 2.12b. By using FLH which fluctuate around those obtained in this work, but supposing 10% cheaper turbines, Aghahosseini et al. [8] find almost the same range of LCOE for the country average values. More specifically, they report a range of 3.4-5.4 €c/kWh, whereas this study reports 3.2-5.9 €c/kWh. In both cases, Kuwait is at the lower boundary of this range, whereas the Arab Emirates have the highest cost on average. However, significant differences of country average values are observed for Saudi Arabia and Oman, where wind energy is 20% cheaper according to Aghahosseini et al. [8] due to higher FLH. As will be discussed in subsection 7.2.2, these FLH are however derived with a rather inaccurate approximation. Some analogies can also be found with the work of Fasihi and Breyer [208], although the only way to do is by referring to the colourmaps they created, as mentioned at the beginning of this subsection. By doing so, the FLH registered over the Arabian Peninsula seem to go up to 3500 h/a, which are then oversized to 3800 h/a by the authors. This is around 20 % less than the maximum value that can be observed by the naked eye for a similar colourmap obtained from this study. However, by using the same visual approach to find the cheapest LCOE value over the entire GCC area, the same value of around 2.5 €c/kWh is obtained from Fasihi and Breyer [208] as in this study. The reason is that the CAPEX used by these authors to model their wind turbines is 20% lower than the one adopted here according to Ryberg [135].
To satisfy the entire energy demand of the GCC countries, only 15% of the onshore wind potential would be sufficient, offering electricity for a price between 2.5 and 3.5 €c/kWh. Besides, 40% of wind energy is below the very competitive LCOE of 4.0 €c/kWh, while 70% is found below 5.0 €c/kWh, which translates into 10,000 TWh and 18,000 TWh for the two cases respectively. Typically, the registered wind potential is between 4 and 4.5 times lower than the solar potential at a country level, except in Saudi Arabia, where it is almost 5 times lower. This implies that only three states could be powered be wind turbines alone, namely the Arab Emirates, Oman and Saudi Arabia. However, the state with the lowest LCOE on average is Kuwait, although very cheap prices can also be found in some areas of Saudi Arabia and Oman. Moreover, each of these two countries could each theoretically satisfy the entire demand of the GCC area by itself.

The Peninsula does not benefit of significant offshore wind potential, as can be observed from the graph of Figure 7.1. More precisely, it totals 3300 TWh, with an average LCOE of around 15 €c/kWh, that is 2.5 and 5 times more than onshore wind and open-field PV respectively. However, a major contributor to this effect is the fact that the water depth constraint of the LEA excluded the Arabian Sea almost entirely, where the best wind conditions are found and which constitutes more than half of the GCC offshore area. In fact, close to Oman's coast, wind speeds reach values which are almost as high as in the North Sea [3]. This explains why a max value of 5400 h/a is registered for offshore wind turbines in this study, very close to the 6000 h/a obtained by Caglayan [6] for Europe when using the same turbine design. Accordingly, a minimum LCOE of 5.3 €c/kWh is obtained for the Peninsula, while Caglayan reports 4.9 €c/kWh. The same median value is however found, which can be explained by the fact that even though average FLH in Europe are higher, her analysis includes areas very far from the coast, which are connected with high coasts. Therefore, the methodology of Caglayan [6] seems to be correctly applied.
As already mentioned, due to the lack of literature on future LCOE costs for offshore wind on the region under exam, no further comparison is offered for this technology. Finally, it should be reminded that, by adopting a site-dependent turbine design, considerable cost reductions could be achieved [6]. Considering the average cost reduction in Europe found by Caglayan [6], less than 500 TWh would fall below the LCOE of 5.5 €c/kWh, which is the maximum nominal LCOE of installed VRES technologies in the simulations featuring all countries connected. The energy amount just indicated is around 20% of the electricity generated in the cooperation and export scenarios.

In general, this subsection has shown that important LCOE deviations between this and other studies are present due to different assumptions. However, these deviations can always be justified by comparing cost parameters or FLH, at least in the case of open-field PV and onshore wind. As for offshore wind, results are consistent with those of Caglayan [6] for Europe, whose methodology has been adopted for the current study. While cost parameters used here have been derived from other studies, FLH are a result of this work, which is why a plausibility check will be conducted in subsection 7.1.3. First, however, the same check is performed on the outcome of the LEA, which is one of the main results impacting the energy potential, together with FLH.

7.1.2 Plausibility check of the LEA

Clearly, the amount of eligible land calculated for the installations of VRES directly impacts their associated energy potential, which is subsequently found using time-dependent simulations. In this subsection, a comparison of the outcome of the LEA reported in chapter 5 with other studies is therefore conducted. In particular, the work of Chu and Hawkes [202] is kept as the main reference for this and the following subsection. In fact, their study is very recent and contains an analysis of the potential of all VRES technologies considered in this study. Besides, the methodology used by the authors is also very similar to that of Ryberg [135] and Caglayan [6] adopted here as indicated in chapter 3, with the advantage of offering results globally and not only for Europe. Moreover, Chu and Hawkes [202] also give an overview of other global studies on VRES potential, some of which offer additional material for comparison. In this and the following subsection, the analysis for each technology included in the study will be discussed separately, starting with open-field PV, to continue with onshore wind and finally offshore wind.

Although Chu and Hawkes [202] were able to include almost all type of onshore land constraints indicated by Ryberg [135], their study did not consider land instability. Although this particular constraint might not be highly influential on a global scale, it is of the utmost importance for the Arabian Peninsula, which is mostly covered by desert areas. As explained in section 3.2, excluding these areas entirely or not excluding them at all leads to a strong underestimation or overestimation of the VRES potential respectively. In fact, while Chu and Hawkes [202] and other global land eligibility analyses reported by them indicate desert areas as eligible, Almasoud and Gandayh [138] explicitly say that solar technologies cannot be installed over the "sand dunes and shifting sands" present on the Peninsula. Consequently, the same must apply for even heavier technologies such as onshore wind. Therefore, the DSMW database has been used here to exclude only the particular type of desert areas indicated by Almasoud and Gandayh [138].
The constraint just discussed has been found to be the main land exclusion criterion in section 5.1, being responsible for the classification of 25% of the onshore territory as ineligible. Consequently, the effect of this criterion would not allow to directly compare the outcome of the LEA conducted in this study with that of Chu and Hawkes [202] and other global analyses. Therefore, the effect of the moving sands constraint is filtered out from the results of this work presented in this chapter in order to allow for a meaningful comparison with literature.

Under the condition just explained, a good overlap is found between the amount of eligible land obtained here and in Chu and Hawkes's study [202] for open-field PV, as can be observed in Figure 7.2. An almost perfect

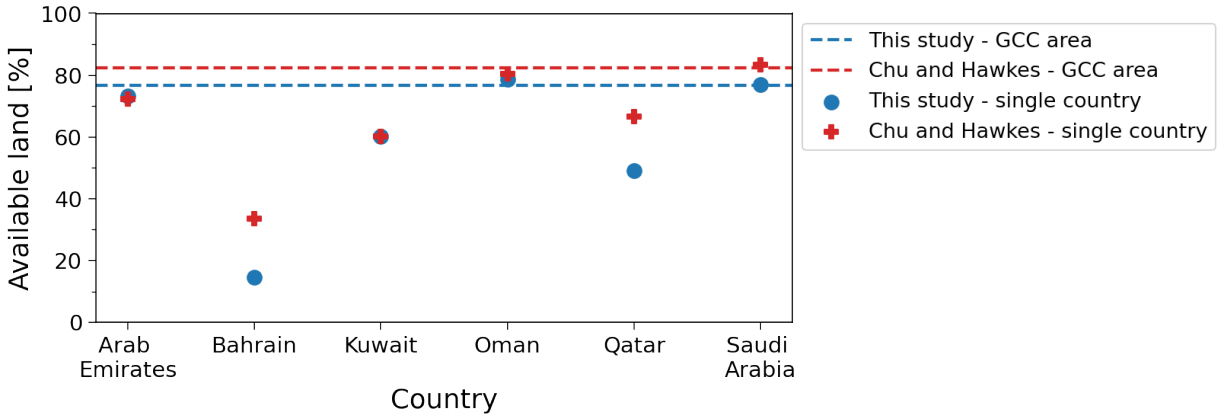

Figure 7.2: Comparison of the LEA for open-field PV panels with existing literature. The moving sand constraint is filtered out from the results of the current study for a more meaningful comparison

overlap is found for the four biggest countries in the region, while Bahrain and Qatar both feature around 20% less eligible land. It is difficult to state for certain which land eligibility criteria lead to this discrepancy, as only this study reports the breakdown of each constraint. The effect of the exclusion constraint and exclusion buffer of roads and coasts could be behind this pattern, since it has not been included by Chu and Hawkes [202], although this is only true for Bahrain as shown in Figure 5.3. For Qatar, it is most likely that the difference stems from the exclusion of rural settlements, considered only in this study, as well as the

exclusion buffer of agricultural areas, which is not applied by Chu and Hawkes [202]. The greater exclusion due to these constraints seems to outweigh the absence of a land suitability factor in the methdology of Ryberg [135], which is instead present in Chu and Hawkes [202] and other studies [203, 204]. The suitability factor allows to exclude only a fraction of geographical areas, while the tool GLAES developed by Ryberg [209] can only perform total exclusions, which is one of its main limitations. However, excluding the entire area also allows GLAES to perform a geographically explicit placement of VRES technologies, which is not possible otherwise. The use of a land suitability factor could also be behind the lower land exclusions of Chu and Hawkes [202] for Saudi Arabia, although this is most probably linked to the higher threshold for the elevation constraint used by them with respect to this study. In fact, the presence of mountains is significant on the western side of the Peninsula.

The trend just outlined for Bahrain and Qatar referring to open-field PV is even more visible when onshore wind is considered, as shown in Figure 7.3. This indicates that the discrepancy with the results of Chu and Hawkes [202] is even higher for these countries, while the other countries register deviations very close to those reported in section 5.1. Since sand dunes are excluded from the analyses and no mountains are present in Bahrain and Kuwait, the greater exclusion effects of the LEA with respect to Chu and Hawkes [202] can only be due to the higher buffer applied to rural settlements with respect to open-field PV, which are considered only in this study. This is true also for Kuwait, who also shows a slight negative deviation in terms of eligible land with respect to Chu and Hawkes [202]. Saudi Arabia, instead, features a better match with their work. This is line with the more similar assumptions for the elevation constraint with respect to the case of open-field PV. Besides, this may also indicate that the influence of the suitability factor is not very relevant for the present case compared to the choice of constraints and buffers. This is probably true because of the lack of areas covered by vegetation in the Peninsula, where the suitability factor is most relevant. It should also be noted that the closer match of Saudi Arabia also leads to a better match for the overall GCC area, since this country occupies most of the territory of the Arabian Peninsula.
Figure 7.3 also reports the outcome of the LEA conducted by Bosch et al. (2017) [204] and Eurek et al. [203]. In almost all cases, their results show higher values of eligible land, which is probably due to the fact that neither of these authors implemented an exclusion buffer around their selection of eligibility constraints. Also interesting is the fact that Bosch et al. (2017) [204] used the same constraints as Eurek et al. [203], but differences between their results can be appreciated. Although both their studies used the same landcover database, different versions might have been considered, which is also suggested by the different way in which the authors cite it, even though none of them reports the version explicitly. Alternatively, this outcome could also be due to the way in which the landcover database, featuring a native resolution of 300 m, was scaled to the resolution of 1 km used by Bosch et al. (2017) [204] and Eurek et al. [203]. Once again, a breakdown of the land exclusion effect of each constraint would prove beneficial, but it is not offered by the authors.

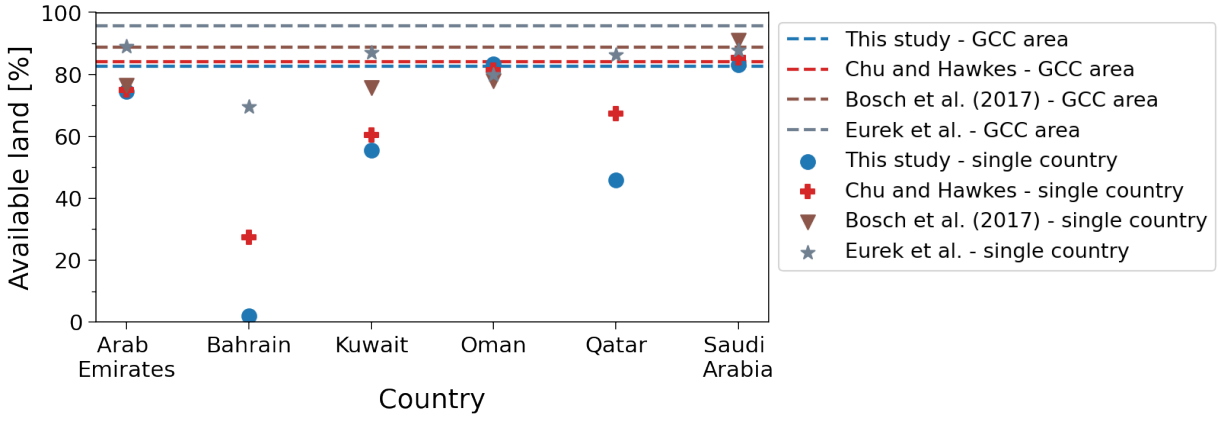

Figure 7.3: Comparison of the LEA for onshore wind turbines with existing literature. The moving sand constraint is filtered out from the results of the current study for a more meaningful comparison

The same paper published by Eurek et al. [203] also contains a study of offshore wind energy potential, whose LEA can therefore be compared to that of Chu and Hawkes [202] and of the present study. Although the

match with the study of Chu and Hawkes [202] is still good for the largest countries of Oman and Saudi Arabia, significant differences are found for the other states, as shown in Figure 7.4. This is due to the fact that their work does not include distance from coast as a constraint, which is instead the second most important constraint according to the findings of section 5.1. On the contrary, Eurek et al. [203] use a buffer of 9 km, which is behind the deviation observed with respect to the current work, where a buffer of 15 km is adopted following the example of Caglayan [6]. On top of this, the effect of the coast buffer in relation to small islands should also be pointed out, since it can lead to important exclusions, as observed in the southern portion of the Red Sea and of the Persian Gulf. In case the islands are not inhabited, the approach would in fact underestimate the space available for offshore turbines. In this work, all islands have been considered in the LEA, since this was the most conservative approach. This might also contribute to differences shown in Figure 7.4.
Interestingly enough, Chu and Hawkes [202] use a two times more conservative constraint on water depth than the one adopted in this study and in Eurek et al. [203], but their LEA still leads to lower sea exclusions in all countries except for Saudi Arabia. This highlights the importance of the coast distance constraint, which is therefore found to be more impactful than water depth in five countries out of six. Even in Saudi Arabia, the available sea area found by Chu and Hawkes [202] is still higher than that of the present study, falling below that of Eurek et al. [203].

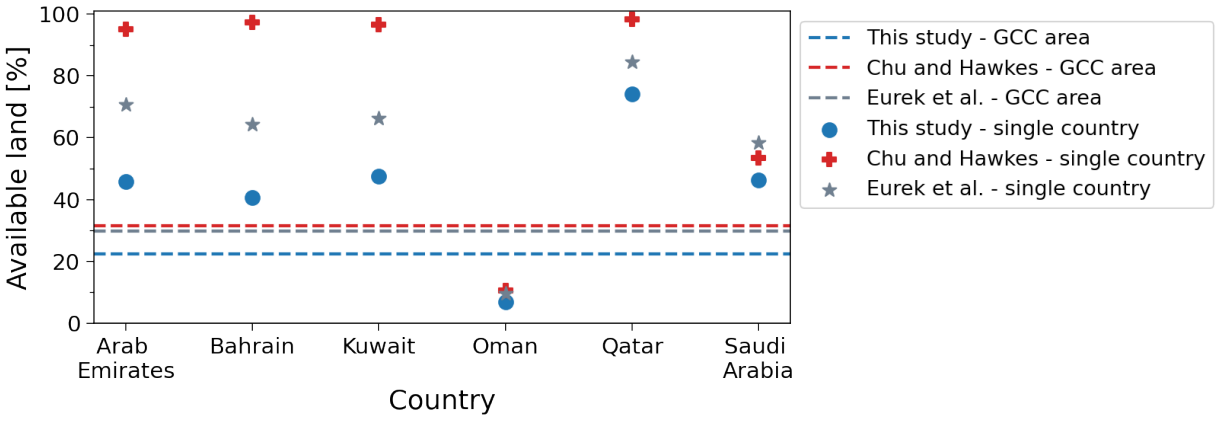

Figure 7.4: Comparison of the LEA for offshore wind with existing literature. The moving sand constraint is filtered out from the results of the current study for a more meaningful comparison

Overall, the LEA conducted in this work is found to be consistent with other studies. More conservative results are typically registered here, although significant deviations are only found for smaller countries. Most importantly, the differences can always be explained in the light of the methodology chosen in the current study and which is based on the models of Ryberg [135] for onshore technologies and Caglayan [6] for offshore technologies. As already explained, the biggest difference lies in the exclusion of moving sands from the eligible area, not considered by other global studies such as that of Chu and Hawkes [202], but absolutely necessary here as explained in Almasoud and Gandayh [138].
Finally, some aspects discussed earlier could not be stated with total certainty nor further expanded due to the fact that other studies do not sufficiently investigate the effect of the different land eligibility constraints. For example, no study reports the breakdown of the land exclusion according to the different constraints adopted, which is instead performed here. The lack of sufficient attention to this aspect was in fact already pointed out by Ryberg [119] as one of the main motivation for his work.

7.1.3 Plausibility check of the VRES simulations

The previous subsection has discussed the results of the first part of the methodology adopted to find VRES. In a similar way, this new subsection will deal with the outcome of the second part of the methodology, which consists in running simulations using the chosen VRES technologies to obtain their electricity feed-in time series. The same order used so far to discuss the three technologies, namely open-field PV, onshore wind and offshore wind, is also adopted here.

In order to check the reliability of the results now under exam, two main variables should be taken into account. First and foremost, the capacity of the installed VRES per unit of available land. Secondly, the FLH output by the simulations. Together with the LEA, in fact, these two variables combined return the value of the energy potential. While the simulations always depend on the workflow adopted to process weather data, the design of a technology can be independent of weather data. For example, in this work the same open-field PV panels and offshore wind turbines are installed everywhere, whereas onshore wind turbines are designed taking into account wind conditions in order to maximise power production. While global studies on VRES almost always assume the same design for fixed-tilt PV panels, some of them are able to implement a variable design on wind turbines. This should be kept in mind when comparing this work to existing literature. It should also be noted that among the studies mentioned in this chapter, only Pietzcker et al. [205] took into account improvement of VRES technologies in the future.

As in the case of the onshore LEA, Chu and Hawkes [202] show the best match with the current study also in terms of FLH. Even though the weighted average of their FLH is almost the same considering the GCC area as a whole, slight deviations can still be observed at a country level. It is difficult to know exactly where this difference comes from, but probably the fact that Chu and Hawkes [202] did not consider wind speed and pressure has an impact. Also important is the fact that they considered a 25% higher albedo coefficient, which increases the output of PV. On the other hand, they assumed a 15% greater temperature coefficient [1] in absolute terms, which impacts PV power in the opposite direction. As can be observed in Figure 7.5, the average efficiency of solar panels according to Pietzcker at al. [205] is way lower, since the FLH reported by them never surpass 1620 h/a. The workflow they adopted is totally different from that used here and in Chu and Hawkes [202], so that a comparison is difficult. However, the difference probably stems from the dataset they used. On the one hand, Pietzcker at al. [205] rely on an older dataset from the National Aeronautics and Space Administration (NASA) and reprocessed by the German Aerospace Center [210], which contains data at a lower temporal resolution, namely three hours vs one hour used here and in Chu and Hawkes [202], which makes their results less accurate. On the other hand, they consider a representative year based on a long-term average, which is better than considering a single year, as done in this study.

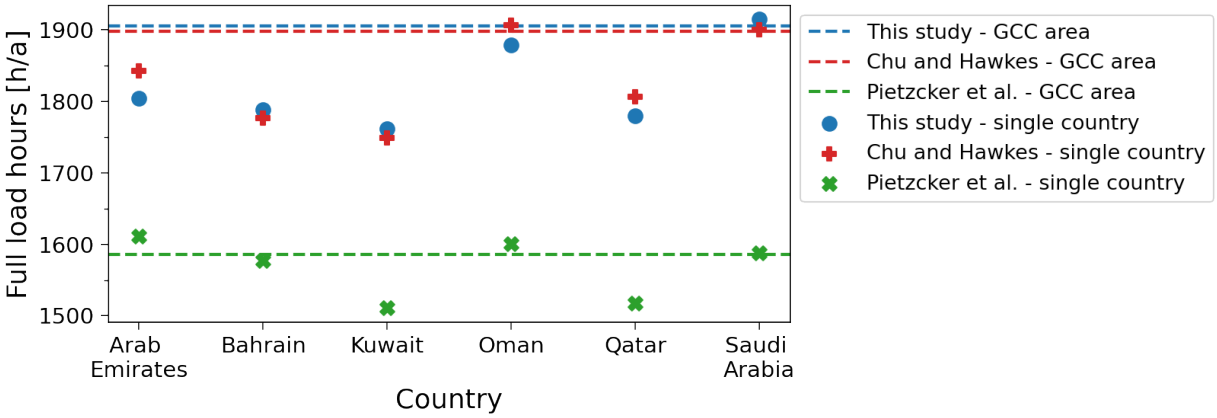

Figure 7.5: Comparison of the average FLH obtained for open-field PV panels with existing literature

Also difficult to explain are the differences with respect to Heuser [191]. Unfortunately, he only reports the value of FLH above which the top 25% of PV panels are found, and only for the countries of Oman and Saudi Arabia, which is also the reason why it cannot be included in Figure 7.5. In particular, 25% of the panels installed by Heuser [191] in Oman and Saudi Arabia feature a value of FLH higher than 2221 h/a and 2352 h/a respectively, while this study finds 1890 h/a and 1965 h/a. The difference is particularly unexpected, since Heuser [191] used the same workflow and PV panel specified in this study and suggested by Ryberg [135]. Although the FLH reported by Heuser [123] for the top 25% of PV panels are way higher than the average FLH reported by other studies considered here, his results may be more accurate than those obtained within this thesis. This is because The Modern-Era Retrospective Analysis for Research and Applications version 2

[1] This coefficient indicates the variation of power efficiency of the PV module as a linear function of the variation of the cell temperature. The coefficient is negative because an increase in temperature leads to a decrease in efficiency

(MERRA-2) weather dataset [211] chosen by Heuser [123] has been validated, whereas the one used in this study, namely the ERA5 [167], has not. If Heuser's results were indeed correct, the only possible explanation for the result of Heuser [191] would be that the choice of best panel identified by Ryberg [135] is responsible for the significantly better production over the year with respect to other studies. The nominal efficiency of the module, in fact, cannot impact the FLH as it also increases the rated power of the module itself.
In spite of the average FLH reported in Figure 7.5, the energy potential per unit of area is the highest for Pietzcker at al. [205] at 167 GWh/km^2, while Chu and Hawkes [202] show the lowest at 57 GWh/km^2. This study places itself between these two values at 97 GWh/km^2. These results are due to the different land coverage assumptions for PV. While Chu and Hawkes [202] use a value of 30 MW/km^2 considering current data reported by the NREL [148] and also mentioned by Ryberg [135], Ryberg [135] and therefore this study assume a value of 50 MW/km^2, which well reflects the 70% efficiency increase of PV panels by 2050. Pietzcker at al. [205] take a coverage value above 100 MW/km^2, which seems overly optimistic in the light of what reported by Chu and Hawkes [202], even considering future technology improvements.

Shifting the focus to the simulations run on onshore wind turbines, Figure 7.6 shows that the current work reports higher FLH with respect to all other studies considered. This is in line with the methodology outlined by Ryberg [135], who points out that future wind turbines such as that used as baseline here will typically have a lower specific power [2], which is linked to a higher efficiency and so higher FLH on average. However, this result is also due to the fact that the current study considers a site-dependent wind turbine design, which leads to better results than by using the same standard design everywhere. In particular, Chu and Hawkes [202] and Eurek et al. [204] used the standard International Electrotechnical Commission (IEC) class 2 wind turbine, even though this leads to very different FLH according to their studies. This is most likely due to the fact that Chu and Hawkes [202] used a more recent and accurate dataset, namely the MERRA-2 [211]. However, it should also be noted that Eurek et al. [203] did not use a minimum wind speed constraint, which could lead to lower average FLH. However, the biggest deviation from Chu and Hawkes [202] is observed in Kuwait and Qatar, where this constraint is not activated. Bosch et al. (2017) [204] also used the MERRA-2 dataset, but created a power curve based on the mix of multiple state-of-the-art turbines, which could then explain the negative deviation from Chu and Hawkes [202].

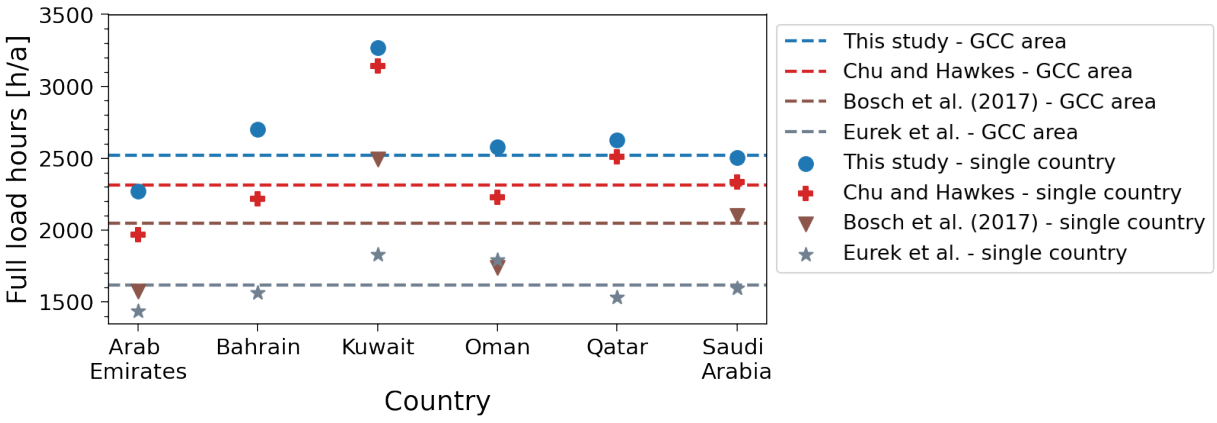

Figure 7.6: Comparison of the average FLH obtained for onshore wind turbines with existing literature

The effect of the design choices adopted here following Ryberg's [135] approach also impact the power density of the wind farms with respect to the eligible area identified. In fact, the power density reported in this study ranges from 7.5 MW/km^2 to 13 MW/km^2 depending on wind speed, whereas both Eurek et al. [203] and Chu and Hawkes [202] use a constant value of 5 MW/km^2, while Bosch et al. (2017) [204] take a power density of 6.5 MW/km^2. As both FLH and specific capacity per unit of eligible area have been found higher in this work due to future design assumptions, the potential per unit of eligible area is also way higher than the other studies indicated in Figure 7.6. On average, the energy potential is here found at 19 GWh/km^2,

[2]The specific power of a turbine is calculated dividing its rated power with the area swept by its rotor diameter. This should not be confused with the power density of wind turbines with respect to the land area they occupy, which is expressed in the same units and even sometimes called in the same way depending on the source

with a record-high value at the country level for Bahrain at 35 GWh/km^2. Differently, the other studies do not report any country with area-specific potential above 14 GWh/km^2, while the average values are found between 8 GWh/km^2 and 13 GWh/km^2.

Some considerations just made with respect to onshore wind turbines also apply to offshore ones. In fact, this study has followed the methodology adopted by Caglayan [6], who reportedly applied Ryberg's [135] approach to offshore wind turbines. However, as already mentioned in subsection 3.3.1, the future reference turbines considered for offshore installations has not been scaled according to wind site conditions due to the current limitations of the software used. According to Caglayan [173], using a single turbine design reduces the potential significantly; for example, the average capacity factor is reduced by 20% in Europe when design optimisation is not considered. Therefore, it could be expected that the deviation from other studies in terms of FLH is not as high as that observed for onshore wind turbines. However, Figure 7.7 indicates that the adopted methodology still returns considerably high values. Since the adopted methodology is the same, the difference can only be due to the fact that the baseline turbine adopted by Caglayan [6] implies greater technological improvements than that used as baseline for onshore installations. This, however, does not necessarily mean a higher cost efficiency, since the cost models adopted in the two cases are necessarily different. The other studies considered here showing the highest deviation in terms of FLH from the current work are those of Chu and Hawkes [202] and Eurek et al. [203], who adopted the same methodology described in the case of onshore wind, but using the IEC class 1 turbine model instead of the IEC class 2. Accordingly, Eurek et al. [203] report once again an average value of FLH around 30% lower than that of Chu and Hawkes [202], which in its turn has a deviation of -50% from the current study. The results of Bosch et al. (2018) [206] are those that come closer to those obtained within this work. In fact, differently from their study of onshore wind potential mentioned earlier [204], Bosch et al. (2018) [206] consider two different representative turbines depending on the site location, which improves the average FLH registered by their wind farms with respect to a single design. However, their results are still lower than those obtained within this work, as the representative turbines are still derived from contemporary technologies and not from a future one.
Compared to the case of onshore wind, the power density used in this study is not significantly higher the one used by Chu and Hawkes [202] and by Eurek et al. [203]: 6 MW/km^2 is the value in this study versus 5 MW/km^2 used by the other authors. Consequently, even if the FLH deviation is higher with respect to the onshore wind case, similar deviations for the area-specific energy potential are found. More precisely, this study finds an average potential of 17 GWh/km^2, while Chu and Hawkes [202] and Eurek et al. report 10 GWh/km^2 and 7 GWhh/km^2 respectively. As Bosch et al. (2018) [206] do not offer data for individual countries, the area-specific potential cannot be compared to their study.

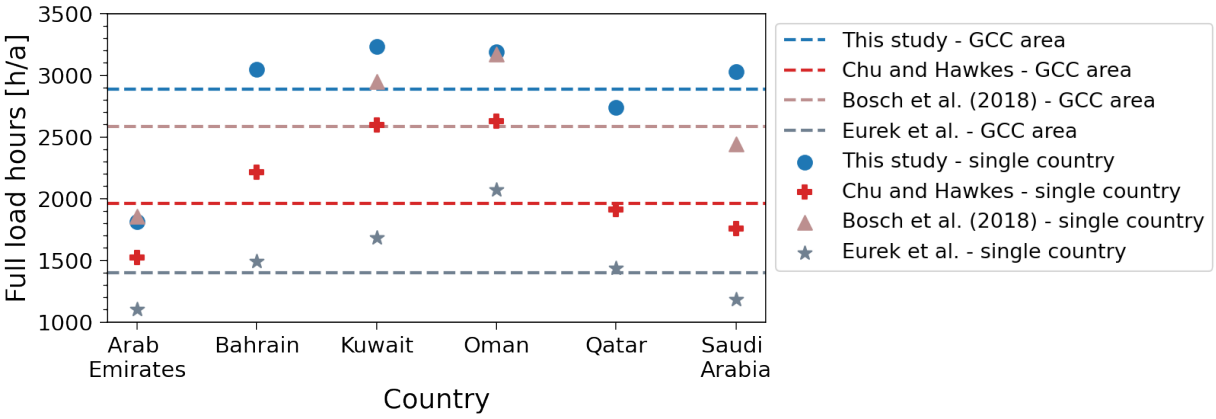

Figure 7.7: Comparison of the average FLH obtained for offshore wind turbines with existing literature

Overall, this subsection has shown that the models used in this study for VRES technologies lead to a higher area-specific energy potential than studies based on current technologies, which are the only sources offering both an extensive LEA and an energy potential analysis for the GCC area. In the case of open-field PV farms, this difference is mainly due to a higher area-specific power of PV panels, which is in turn caused by a

higher efficiency. In the case of onshore and offshore wind turbines this effect is also enhanced by an increase in FLH, although by different proportions between the two technologies.
The discussion has also revealed that studies which use the same database and even the same reference for the adopted methodology can end up reporting different FLH. In general, the FLH of wind technologies obtained by this work cannot be entirely verified, since no study considers future wind turbine designs to derive this value over the Arabian Peninsula.

7.2 ESM discussion

As done in the previous section, an overview of the main results obtained for the topic now considered, i.e. the ESM, is first reported. This is carried out in subsection 7.2.1, where the costs of the system are also related to those of fossil fuels. In order to discuss and partially validate the model created, the best approach is to compare those type of results which are also present in other studies. Therefore, the differences between the optimal VRES generation mix and LCOE obtained in this and other studies are discussed in subsection 7.2.2. Then, the LCOH found here is compared with that of Heuser et al. [191] in subsection 7.2.3. It should be noted that in order to perform these comparisons, specific functional scenarios had to be created featuring modeling assumptions more similar to those of the other studies chosen as reference. In particular, the isolation-electricity-demand scenario and the isolation-hydrogen-demand scenario are essential for subsection 7.2.2 and subsection 7.2.3 respectively.

7.2.1 Overview of the main features of the optimised ESM

Among the research goals of this study was the study of the behaviour of the optimised energy system model under different scenarios. These scenarios have been presented in section 4.1, while their related results have been reported in chapter 6. Given the considerable number of scenarios used in this study and the many different important aspects that have to be taken into account to fully understand the behaviour of the system, it is not possible to fully answer the research question regarding the behaviour of the system in a short and exclusively quantitative way, also due to the rather general and qualitative nature of the research question itself. However, a summary of the main features observed in the results is now offered to give the shortest possible answer to this research question. This subsection aims at discussing the different components of the system separately, although references to other components are very often necessary. Furthermore, differently from chapter 6, the insights derived from the functional scenarios of section 6.2 and from the comparison between the different system components are immediately incorporated in the discussion, so that a more direct understanding of the system can be achieved.

Focusing on the optimal VRES generation mix, this study has shown that wind energy has a major role in the system compared to solar energy. The reasons for this phenomenon are mainly two-fold. First, the profile of solar and wind energy with respect to that of power and hydrogen demand modeled in this study. In fact, the output of PV panels is lower in the summer, while power demand peaks in this season. Also, wind energy rarely drops to zero, whereas PV power is absent most hours of the day, while hydrogen demand is constant and power demand never falls to zero. The second reason is the profile of wind energy itself, which is very different over different regions of the Peninsula, allowing for the synchronisation of different wind farms in order to reduce the required overall capacity of VRES. This could also be the reason why the share of wind energy increases when the countries can exchange energy. Even if this could simply be due to the distribution of LCOE over the different regions of the system, the fact that multiple studies show this effect for very different regions of the world backs up the hypothesis just advanced. In particular, Aghahosseini et al. [8] observe this pattern for the MENA region, both Caglayan et al. [173] and Child et al. [5] report this trend for Europe, while the same effect can also be observed in Asia and North-America in the studies of Bogdanov and Breyer [212] and of Aghahosseini et al. [213] respectively. A plausibility check of the optimal generation mix found in this study will be discussed in detail in the next subsection, also offering comparison with some of the studies just mentioned.
Moreover, the current study has shown the importance of a sensitivity analysis on VRES installation costs, which is often not offered by other studies. For example, the functional scenarios of this study have shown that when the CAPEX of wind turbines is reduced by 30%, the ratio of wind to solar energy in the production mix changes significantly, namely from 2:1 to 1:1. Therefore, it is immediately clear that different cost assumptions have a huge impact on optimisation results, meaning that a comparison with other studies is

truly reliable only when similar economic parameters are implemented.

Comparing the location of the installation of VRES with that of energy demand has revealed that there is a connection between these components of the system: electricity production is mostly located where both electricity and hydrogen demand are concentrated. It should be noted that these two types of demand are very similar in each region given the methodology adopted to model them. However, comparing the cooperation and the electricity-demand scenario it is observed that VRES installations primarily drop in those regions which were exporting hydrogen after hydrogen demand is removed from the system, while VRES installations remain high where electricity demand is located. In particular, these high-exporting regions are SAU.5, Kuwait, OMN.6 and OMN.9. What has just been said can be explained with the fact that power losses are avoided if generation and electricity demand are located in the same region, while no hydrogen losses have been modeled for the hydrogen network. Consequently, only electricity demand is an important constraint for the location of VRES installations, together with LCOE. This is also confirmed by the fact that the maximum operation of electrolysers does not take place in the regions were hydrogen or electricity demand is primarily located, but rather where the best LCOE is found. These regions are the same as the exporting regions mentioned earlier in this paragraph. All of them feature the best LCOE in terms of both solar and wind energy, although in Kuwait this is true only for wind turbines. This suggests that wind energy is the main source for the production of hydrogen. Indeed, this is proven for both the cooperation and the export scenario by comparing the generation mix of VRES and the operation of electrolysers in different regions, particularly those where most hydrogen is produced. Besides, the share of wind energy in the electricity-demand and the hydrogen-demand scenarios is respectively lower and higher than in the cooperation scenario, confirming the trend just described.

While it is true that the location of hydrogen demand influences the location of VRES less than that of electricity, the location of both has an impact on the system. In fact, both powerlines and hydrogen pipelines are associated with costs. However, hydrogen pipelines are way less expensive than powerlines considering the same length and amount of transported power, as reported in subsection 4.2.2, which is another reason behind the lower dependence of VRES installations on hydrogen demand than on electricity demand. Another important consequence of the cost assumptions made in this study is that the capacity of the hydrogen transmission system is always greater than that of electricity, namely between 2 and 3 times in all three main scenarios, even though the cost of powerlines always surpasses that of hydrogen pipelines. In accord to what has just been described, the maximum value of net import and exports of hydrogen is always more than 3 times higher than that of electricity. In other words, the system is more flexible considering the hydrogen production and transport chain than the electricity one. In fact, isolating the countries impacts the hydrogen grid more: its capacity is reduced by three times, whereas the overall capacity of the powerlines is halved.

Thanks to the functional scenarios, a relationship has also been found between the share of the capacity of powerlines in the transmission system with respect to the share of PV in the generation mix. In fact, Figure 6.17 shows that as PV installations increase with respect to wind turbines, also powerlines do with respect to hydrogen pipelines. This trend is observed until the capacity of PV farms is around 2 times that of wind farms, so when the production of electricity from wind and solar energy is approximately the same. To explain this phenomenon, the role of storage has to be introduced. In fact, this study has shown that a growing share of solar energy in the generation mix increases the share of batteries in the storage system, whereas a growing share of wind energy increases the share of hydrogen vessels. The changing balance between the electricity and the hydrogen storage would then well explain the increased importance of the electricity or hydrogen transport system according to the different functional scenarios of Figure 6.17. Instead, the relationship between the type of energy source and the type of storage can only be explained with the different profile of the wind and solar feed-in time series with respect to the hydrogen and power demand. Taking the cooperation scenario as a reference, this phenomenon also leads to higher batteries installations in the eastern regions, where the share of PV is higher, and to higher installations of hydrogen vessels in the remaining regions, where wind has the greatest share of the mix.
Shifting the focus momentarily on all three main scenarios, the study also finds that the most efficient sizing of the storage technologies in terms of average operation rate is obtained in the cooperation scenario. In fact, the isolation scenario can rely less on the flexibility of the system due to the lack of country interconnections, whereas hydrogen demand is entirely concentrated in only three regions in the export scenario, which might result in a less cost-efficient use of technologies. However, in this case it should be mentioned that an

additional and constant electricity demand of around 170 TWh is also required by the system at the three ports due to liquefaction, which could also contribute to the oversizing of storage technologies. Moreover, the impact of removing country connections and so flexibility options is found to be higher on hydrogen technologies once again: batteries double in size in the isolation scenario with respect to the cooperation one, whereas hydrogen vessels quadruple. In fact, as observed for transmission technologies, storing compressed hydrogen is more than one order of magnitude cheaper than storing electricity in batteries considering the same amount of energy available under these two different forms, as shown in Table 4.4. It should be noted that the comparison just made between the relative increase of storage between the cooperation and isolation scenario does not account for the increase of vessels in Bahrain, which alone is ten times higher the total vessels installations of the cooperation scenario. This is because of the need of the country to exploit and therefore store the almost entire potential of its VRES.

A reduction in the average operation rate with respect to the cooperation scenario is also observed for the electrolysers in the export scenario and so in the isolation scenario, for the same reasons just mentioned. The higher use of wind energy to power these technologies and the consequent layout of installations over the Peninsula has already been discussed in this subsection referring to the profile of energy demand and production. The role of other conversion technologies is very limited, meaning that no more than 3% of electricity demand is satisfied in this way in any of the three main scenarios. Instead, batteries are preferred by optimisation, always providing more than 15% of overall electricity demand. In fact, apart from electrolysers, all conversion technologies available to the system are those able to reconvert hydrogen into electricity, which is a very inefficient process: even considering the most efficient reconversion system of this study, i.e. fuel cells, half of the electricity is lost after conversion and reconversion. However, it should be said that in the functional scenario where only wind energy is present, both batteries and reconversion technologies produce the same amount of electricity, namely 8% of the total demand. Furthermore, in the isolation scenario an important part of national electricity demand is satisfied through hydrogen reconversion in Kuwait (16%) as well as in Bahrain (21%), where reconversion even surpasses the use of batteries. However, as already mentioned, the associated values of electricity are very low compared to the total electricity demand in the GCC area. Therefore, from an economic point of view, the option of using hydrogen for long-term storage does not usually seem convenient, although it acquires importance when only wind energy is used or when countries cannot rely on a significant amount of VRES. However, this result is not valid in general for any energy system, as it depends on the profiles of electricity and hydrogen demand and on the distribution of solar and wind energy over the year.

As a final part of this subsection, we discuss the main findings regarding the costs of the system. The total annual costs in the cooperation scenario amount to 130 €bln. When the same amount of hydrogen is liquified at a constant rate in order to be transported at three main ports, costs rise by 18%, mainly due to installation of additional storage technologies and VRES. When the countries are isolated, these costs increase by 21%, with half of this surge due to storage and offshore wind installations in Bahrain. In order to evaluate the benefit of cooperation for each country, the LCOCEH parameter was created, which normalises total costs with the theoretical equivalent electricity demand of hydrogen and electricity demand combined. In this way, it is shown that only Saudi Arabia could slightly lose from this deal, with Oman saving 5% of total costs and all other countries more than 20%. The total annual costs expressed in terms of LCOCEH would amount to 5.5 €c/kWh. Due to the definition used to create the LCOCEH parameter, it is not very appropriate to compare the value found here with other studies. This is inevitably the case when systems are compared featuring a different share of electricity and hydrogen in the overall demand, since different technologies have to be installed in the two cases. More significant is the comparison of LCOE and LCOH, which have to be obtained with specific scenarios where only electricity and only hydrogen are considered. This is done in the upcoming subsection 7.2.2 and 7.2.3 for LCOE and LCOH respectively. The combination of the electricity-demand and the hydrogen-demand scenario have also shown that the coupling of these sectors allows for a 7% reduction of overall costs. However, this number depends on the amount of electricity and hydrogen supposed for the system, as well as the profile curves supposed. For example, Aghahosseini et al. [8] find an economic benefit of 20% by coupling the non-energetic industrial gas sector, which has a way lower demand with respect to electricity than in this study. Besides, the authors are considering power-to-gas technologies and can rely on more storage options than in this study.

When discussing costs, some considerations should also be made regarding the savings or additional expenses related to a fully renewable energy infrastructure. In section 7.1, the cheapest possible LCOE from fossil

fuels has been reported equal to 5.0 €c/kWh, which is way more than the LCOE from solar and most of the wind energy available in the Peninsula. However, these costs are exclusively related to generation of electricity, and do not take into account the need for storage, transmission and curtailment to balance the system. The full LCOE of the system is in fact found to be 6.6 €c/kWh in the electricity-demand scenario, although a value of 6.1 €c/kWh could be considered taking into account the effects of sector coupling. When comparing these costs to actual end-user electricity prices, it might look like the system modeled here is overly expensive. In fact, average end-user prices do not go higher than 2.5 €c/kWh [214,214]. This value, however, contradicts the lowest possible electricity generation price from fossil fuels reported earlier, something which is particularly remarkable since it also contains additional costs due to additional infrastructure and margin profits related to the role of utilities in the supply chain. The reason behind these prices is the heavy role of governmental subsidies in the oil and gas industry [214]. In fact, according to the World Bank [214], the actual costs incurred in by utilities acting in the GCC countries always exceed 8 €c/kWh. As for the cost of electricity generation itself in the region, the IEA [215] reports a price of 5 €c/kWh for gas and of 15 €c/kWh for oil, which are then brought down by as much as 40% and 70% respectively by governmental subsidies. Electricity production from fossil fuels is not subject to the same problems of variability related to VRES, so that only transmission costs would change this value. This study includes the inter-regional transmission costs of electricity while it ignores those related to the lower voltage / distribution level, so that the wholesale generation costs of natural gas can be indeed compared with the total system costs of electricity of this study. Therefore, it is found that the future fully renewable electricity system created in this work would still be more expensive than current gas-based systems in the Arabian Peninsula by 20%, as the LCOE of a gas-based system and of the renewable energy system of this study are of 5 €c/kWh and of 6.1 €c/kWh respectively.
Clearly, when the cost of hydrogen is compared to that of fossil fuels extracted in the GCC countries, the effect of subsidies is again altering the comparison. Therefore, looking at domestic prices is misleading, while export prices are very volatile [216]. A more meaningful comparison is accomplished by looking at breakeven costs. The ARC energy research insitute [217] reports that these are equal to 2 $/MMBtu for Qatar's LNG shipped towards northern Asia, so 0.5 €c/kWh. McKinsey [218], instead, reports a breakeven price slightly above 3 $/MMBtu for the same case, so around 0.8 €c/kWh. Adding shipping costs to the LCOH obtained with the hydrogen-demand scenario (3.2 €/kg) according to the model of Heuser et al. [191] and considering a 7% reduction due to sector coupling, the cost of liquid hydrogen found by this study becomes 3.5 €/kg, so 10.5 €c/kWh. This means that liquid hydrogen is between 13 and 21 times more expensive than LNG produced in Qatar. However, the gap is reduced if one considers the breakeven costs of other countries. In fact, LNG coming from outside the Middle East is in the range of 6-12 $/MMBtu, which corresponds to 1.5-3.0 €c/kWh [217]. This means that compared to these breakeven prices, liquid hydrogen is between 3.5 and 7 times more expensive than LNG. Besides, if liquefaction costs (including liquefiers and electricity needed to power them) are not considered in the LCOH of hydrogen, and if these costs are compared to the breakeven cost of crude oil for the GCC countries, the gap is reduced but hydrogen is still more expensive [219]. In fact, the LCOH drops to 2.5 €/kg, so 7.5 €c/kWh, while the breakeven costs of crude oil is between 51 $/barrel and 86 $/barrel [219], which corresponds to 2.5-4.1 €c/kWh, so between 2 and 3 times less.
The considerations made so far show that an energy system based on VRES and hydrogen in the GCC countries is less cost-competitive than current fossil-fuel-based systems in the same area. Gaseous hydrogen is 20% more expensive than gas when it comes to electricity generation, whereas it is 2-3 times more expensive than crude oil. Besides, liquid hydrogen is way more expensive than LNG, between 13 and 21 times more if compared to Qatari LNG, whereas it is 3.5-7 more expensive than LNG produced outside the Middle East. However, the considerations just made are not able to account for the significant changes in the economics of the energy sector that will necessarily follow from the climate policies being prepared by governments all over the world, most notably regarding a carbon tax and/or subsidies to renewables [220]. Delving deeper into this topic, however, is out of the scope of this thesis.

7.2.2 Plausibility check of optimal VRES generation and LCOE

Among the results of the optimisation mentioned in the previous subsection is the major role of onshore wind in the electricity production mix. Cross-checking this outcome with literature is particularly challenging, as no study exists to date creating an energy system model for the countries considered here and using the same type of technologies. However, the study of Aghahosseini et al. [8] can be used to discuss the results of the isolation-electricity-demand scenario, even though more technologies are considered in their study,

most notably single-axis tracking PV. The choice of excluding this technology from the current study has been made following to the results obtained by both Ryberg [135] and Caglayan et al. [173], according to whom single-axis tracking PV would not be competitive with fixed-tilt PV nowhere in Europe, including those areas showing high DNI values very close to the one observed in most regions of the Arabian Peninsula. Furthermore, interesting observations can be made referring to European studies, on which a greater amount of literature has been published. However, particular care should be used in this case, as very different geographical areas and thus systems are being compared.

The isolation-electricity-demand scenario has been designed exactly to offer a meaningful comparison with the results of Aghahosseini et al. [8]. In this scenario, each country acts independently to satisfy only the local electricity demand. Even though the two energy systems are similar, important differences exist in the methodology, which leads to very different results, as will be now discussed. This outcome can be observed in Figure 7.8.

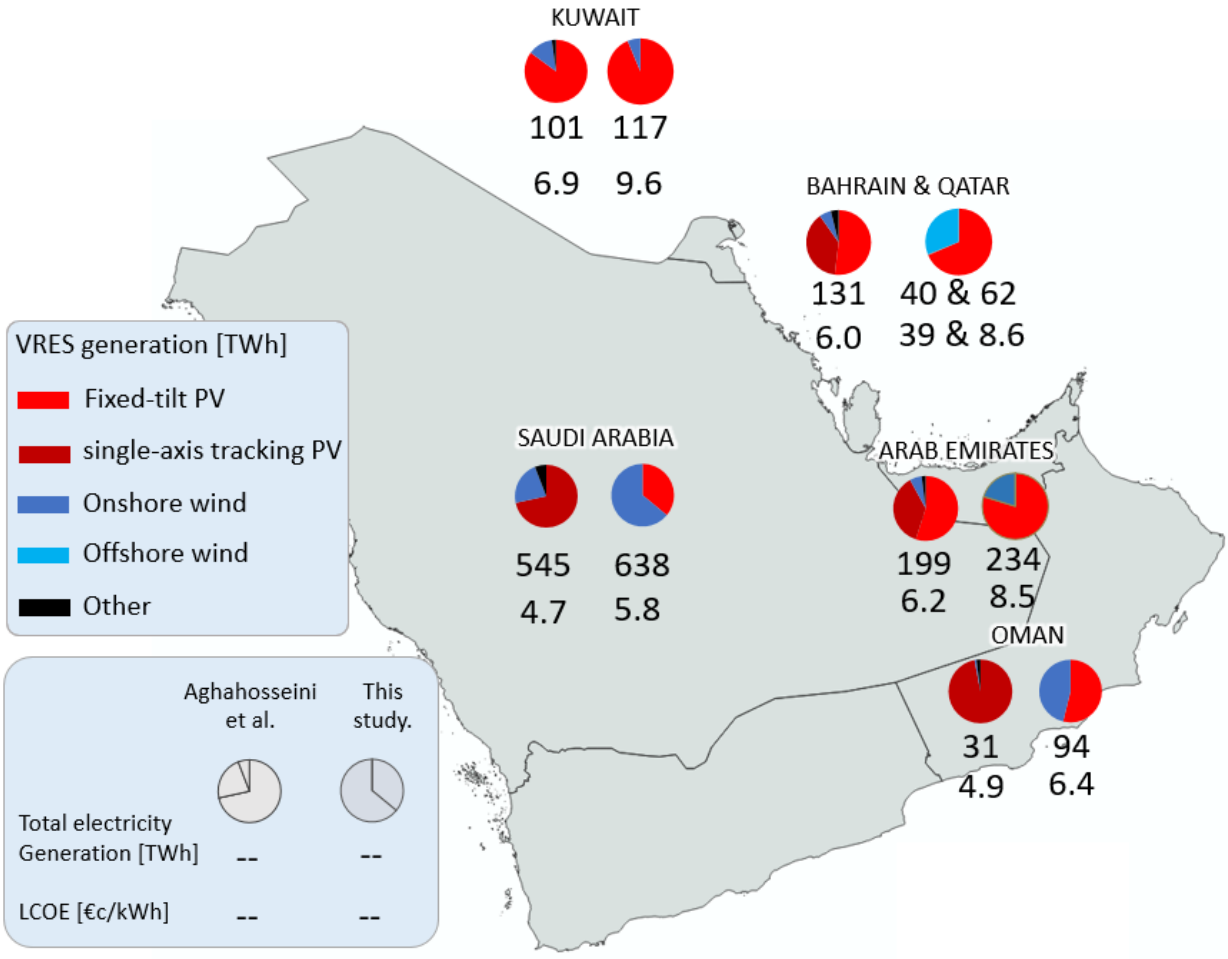

Figure 7.8: Comparison with literature of the optimal generation mix and LCOE in the isolation-electricity-demand scenario. For each country, the figures on the left are the result of Aghahosseini et al. [8], while the ones on the right come from this study. Aghahosseini et al. [8] group Bahrain and Qatar in a single node, whereas this study models them independently. The different values reported for generation are due to different values assumed for the power sector demand

First and foremost, a significantly higher share of solar energy is obtained by Aghahosseini et al. [8]. The explanation for this result depends on the countries being considered. Starting with the two largest countries of the GCC, it should be pointed out that while this analysis is able to classify VRES sources in different clusters based on LCOE price and location, Aghahosseini et al. [8] model their VRES sources as a single technology for each country, whose FLH are a weighted average of the best 50% potential installations.

Given the fact that wind energy shows way higher variations than solar energy over the Peninsula, as already reported in Figure 2.12 and confirmed by Figure 7.1, this assumption leads to overestimating the LCOE of wind turbines more than that of solar panels. Consequently, the optimal share of wind turbines found by Aghahosseini et al. [8] is underestimated. This effect is further enhanced by the fact that a single feed-in curve is available for each technology and country in their study, limiting the flexibility offered by installing independent clusters of wind turbines in different regions peaking at different moments. Solar technologies are less affected by this phenomenon, given their more regular energy production profile across different regions. The set-up of Aghahosseini et al. [8] is characterised also by a lower spatial resolution in terms of energy demand, since this is concentrated in a single node for each country. Therefore, the constraint of power losses minimisation that this work considers does not affect their system. However, this has important consequences, since this study has shown that production of electricity is considerably higher in those regions which show high electricity demand, while only hydrogen production is more flexible in terms of location. Hence, the choice of less efficient VRES by optimisation due to location constraints does not apply to Aghahosseini et al. [8], increasing the cost-competitiveness of their system. Besides, the fact that they model powerlines with losses around 4 times lower than this study based on a different (and commercial) source also contributes to the system achieving a better LCOE when all countries are connected: for the GCC, this study finds a LCOE of 6.6 €c/kWh, whereas Aghahosseini et al. [8] report 4.8 €c/kWh, although all countries of the MENA region are included in their system.
Another factor contributes to the higher costs obtained by this study, which is the greater need of curtailment. In fact, even though the specific storage costs are similar in the two cases, a way higher LCOE is registered in this study for VRES with respect to their potentially optimal value in case of no curtailment, namely the one reported in section 5.2 according to the VRES simulations. This phenomenon is observed in Aghahosseini et al. [8] only to a lower extent. A reason for this difference is offered by the option of using single-axis tracking PV by the authors: this technology is the only solar technology installed in Oman and Saudi Arabia. In fact, according to the feed-in time series reported by Aghahosseini et al. [8] and shown here in Figure 7.9, this technology would not only be more economically efficient than fixed-tilt PV, but could also reduce the need for storage and/or curtailment. This is because single-axis tracking PV reaches maximum production over the summer in the MENA region, exactly the opposite of fixed-tilt PV. This is the period when the power sector demand is also at his highest, as mentioned in subsection 4.2.5. Besides, additional advantages in this sense can also be observed on a daily basis. In fact, the capacity factor of single-axis tracking PV is above 0 for more hours those registered by fixed-tilt PV during the day, especially during the summer, which is also the period when power demand is higher. These features necessarily lead to a more efficient sizing of VRES technologies, which is behind the higher costs registered in the present work.

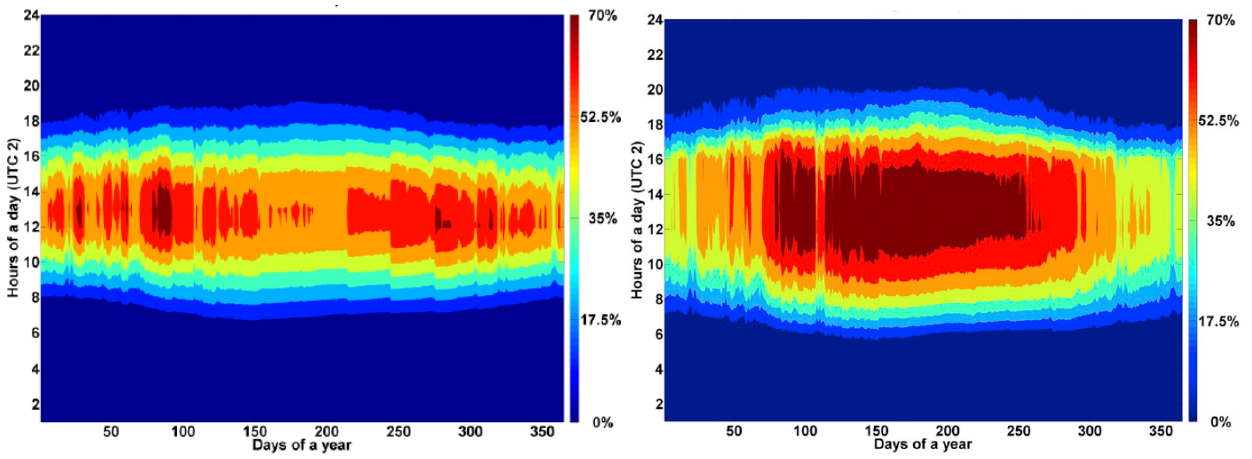

(a) fixed-tilt PV **(b)** single-axis tracking PV

Figure 7.9: Hourly operation-rate over the year for different PV systems as reported by Aghahosseini et al. [8] for the MENA region

In the case of the four smaller countries of the Gulf, the considerations about the lower spatial resolution of the system of Aghahosseini et al. [8] do not hold as strong, since the effect of averages over such small

territories is clearly reduced with respect to Oman and Saudi Arabia, as already shown in Figure 5.15 and 5.18. However, Aghahosseini et al. [8] arbitrarily assume coverage factors for both solar and wind technologies without running any LEA, which leads to significant underestimation of the potential of VRES, particularly of that of wind turbines. The deviation is due to Aghahosseini arbitrarily assuming way lower eligible area for VRES installations, while an higher and lower area-specific capacity values are also arbitrarily set for PV farms and onshore wind turbines respectively. As a consequence, it is not possible to know what the optimal generation mix would be without the upper constraints imposed on onshore wind by Aghahosseini et al. [8], which are in fact always activated in these countries. The LEA conducted in this study is also the reason why Bahrain is forced to rely on expensive offshore wind turbines, something which cannot be observed in Aghahosseini et al. [8] as they are assuming the same coverage factor there as everywhere else, while they are also coupling this country with Qatar, further increasing the VRES potential Bahrain can exploit.
In any case, the fact remains that even though the same VRES prices are more or less available to both Aghahosseini et al. [8] and this study, the present work always reports higher system costs in terms of LCOE, which mainly stem from more intense curtailment. While this could be explained with the role played by single-axis tracking PV in the Arab Emirates and Qatar, this cannot be the case for Kuwait, where only fixed-tilt PV is present as a solar technology. Since the power demand profile is modeled by Aghahosseini et al. [8] in the same way as this study, only two variables can lead to the differences observed in costs. One is the number of typical days used to aggregate the time series, although this is unlikely since the system modeled by Caglayan et al. [173] with the same software converges at this value, while featuring a greater number of technologies and nodes and thus complexity. What is more, they report a costs deviation of only 4% already at 15 typical days, meaning that 30 days can be considered a reliable value for aggregation. In spite of this, the time series aggregation algorithm might still impact results even if convergence is reached. In this case, the work of Aghahosseini et al. [8] would be more accurate, since they do not mention time series aggregation in their paper.
Another reason that could explain the higher curtailment operated by FINE with respect to the model of Aghahosseini et al. [8] could lie in the VRES time series themselves, which have been derived following different approaches. In particular, this study has the limitation of using only one weather year, whereas Aghahosseini et al. [8] considered the most representative year with respect to the last 38 ones. However, it should also be mentioned that the weather dataset considered here, i.e. ERA5, has a higher spatial resolution than the dataset used by Aghahosseini et al. [8] by more than two times. Moreover, Aghahosseini et al. [8] only dispose of GHI values at a three-hourly resolution, that is three times lower than in this study. Finally, Aghahosseini et al. [8] use the power curve of an existing Enercon turbine to derive the feed-in time series of their power plants, whereas the methodology adopted here and based on Ryberg [135] relies on a combination of different turbines, also implementing future technology improvements. All the differences just listed could well explain the different curtailment needs observed in this study and that of Aghahosseini et al. [8]. In any case, a validation of the weather dataset or the optimisation tool used here is out of the scope of this thesis.

As already suggested in the introduction of this subsection, considerably more extensive literature has been published on future fully renewable energy systems for Europe: Caglayan et al. [173], Child et al. [5] and Victoria et al. [7] all offer an overview of the optimal generation mix for 2050. Even though many differences can be found between the methodology and sources of these models and also in comparison with the present work, the model of Caglayan et al. [173] is probably the most important for comparison, since the same techno-economic assumptions were made regarding open-field PV and onshore wind technologies. Although they do not report the total operation of the selected technologies over the year, their system, which includes hydrogen demand, features 30% more capacity in terms of onshore wind farms than PV farms compared to 10% more obtained in the cooperation scenario of this study. This would be in line with the higher DNI values registered in Arabia with respect to the European countries.
However, the model of Child et al. [5] reports that the share of solar energy would be twice as high as that of onshore wind in an electricity-demand scenario, while this study finds the opposite. It should be noted, however, that the authors are adopting the same methodology of Aghahosseini et al. [8], which leads to overestimating the costs of wind energy due too coarse clustering of onshore wind turbines. Besides, the capital costs of PV panels they assume is 40% lower than that adopted here, whereas that of wind turbines is only 20% lower. Also interesting is the fact that when countries are isolated in a isolation-electricity-demand scenario, the share of solar and wind reported by Child et al. [5] becomes the same, while this study finds a 30% higher share of PV in the mix, meaning that this and their study show smaller differences than in the

electricity-demand scenario, while both are very sensitive to the presence of powerline connections.
A higher share of solar energy in the electricity production mix is also reported by Victoria et al. [7] for an electricity-only scenario, although the difference with wind is less than 10%, so less than 5% with respect to the total generation mix. It should be pointed out that this share is considerably lower than that reported by Child et al. [5], even though Victoria et al. [7] use half of the CAPEX considered by them for PV panels, while wind turbine costs are even 5% higher. However, Victoria et al. [7] include the required electricity demand to satisfy the heat sector, which is considerably higher during the winter, when the availability of wind potential is higher and that of solar potential lower in Europe [221].

As just mentioned, the modeling of energy demand is an important factor to consider when comparing energy systems in different areas. Even when a scenario including only power demand without any sector coupling is available for Europe and this study, the comparison is already rendered not very meaningful by the fact that the power sector demand has very different yearly profiles in the area considered here and Europe. In fact, while power demand is higher in summer in the GCC area by around two times, it is rather constant in Europe [5, 170] across the different seasons. Besides, the demand profile itself varies considerably once sector coupling is considered.
Furthermore, the Arabian Peninsula enjoys very different weather conditions from Europe, which leads to completely different distribution of wind and solar energy potential over the year [221]. In order to show this, Figure 7.10 is created showing the profile of the daily average capacity factor for fixed-tilt PV and onshore wind in the two regions. While in Europe fixed-tilt PV output peaks in the summer and wind production peaks in the winter, the time series is more irregular for the Arabian Peninsula. In particular, PV output decreases over the summer although only slightly, while wind turbine ouput is higher in spring and lower in autumn. Therefore, even if the same methodology and energy demand were adopted, very different results would be observed at the end of optimisation due to area-dependent weather conditions.
Finally, there is another feature of the European models that makes comparison with them less reliable, namely the fact that they can rely on other types of renewables sources for generation, namely biomass and hydropower. Although they never contribute to the total generation mix in the same proportion as wind and solar technologies, their input is always above 10%. Clearly, this can impact the optimal share of wind and solar in the generation mix, as particular synergies might be found between all these sources to minimise storage needs. Finally, the use of additional types of storage technologies in the European models mentioned so far might also lead to different results than those obtained in this study, where only Li-ion batteries and gaseous hydrogen vessels are possible options.

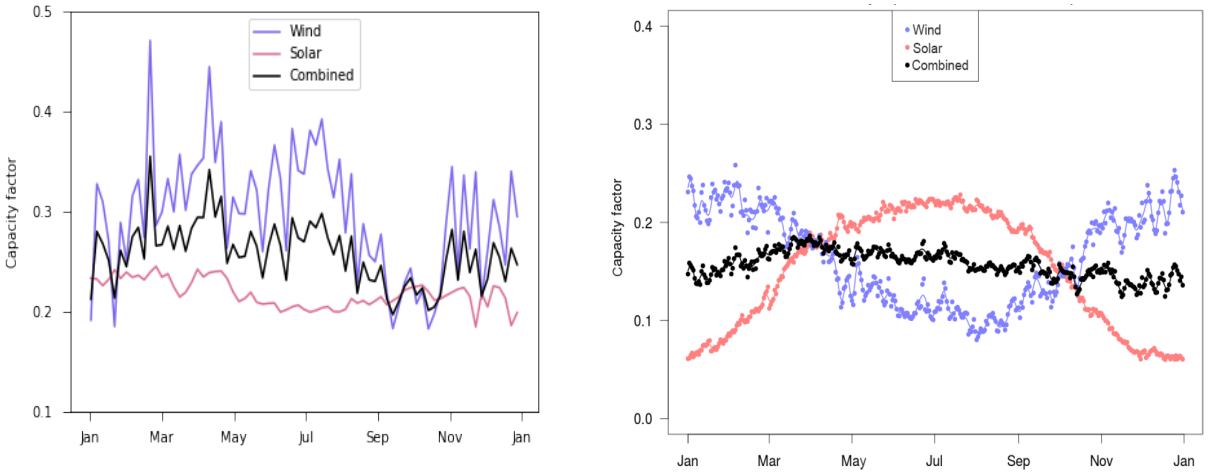

(a) Average over the GCC countries according to the VRES simulations of this study

(b) Average over Europe according to the VRES simulations of Kaspar et al. [221]

Figure 7.10: Comparison between the daily average capacity factor distribution over the year of onshore wind turbines and fixed-tilt PV panels over different geographical areas

7.2.3 Plausibility check of the LCOH

A meaningful comparison with other energy system models is already very difficult when only the price of electricity has to be compared, as many different assumptions can contribute to the results. Therefore, discussing the price of hydrogen, so the LCOH, is even more challenging as addional components are added to the system. However, the isolation-hydrogen-demand scenario allows to effectively compare the cost results obtained for Saudi Arabia and Oman with that of Heuser et al. [191]. In fact, even if important differences remain in the adopted methodology, the cost assumptions are the same in both cases. In any case, the fact should be stressed that the validity of the model created here mostly depends on the parts that have been discussed so far in this chapter.

As already described in section 4.1, the isolation-hydrogen-demand scenario considers the liquefaction and export of hydrogen at one port in each country and at a constant rate, while no electricity demand is required except for the one needed for liquefaction. In this way, all costs can be attributed to hydrogen and its LCOH can be derived. The total amount of hydrogen exported is the same as the national hydrogen demand, while no energy exchange is allowed between countries. Gaseous hydrogen storage is preferred over liquid hydrogen storage also in this scenario, as it is intrinsically more safe [178]. Most importantly, if one considers the fact that hydrogen demand would most likely be part of the local system in the case of a fully developed hydrogen economy, storing hydrogen in the gaseous form always allows for it to be transported back to the regions where demand is needed. This cannot happen if the hydrogen is liquefied at the port before being stored. However, the liquid storage strategy is the one adopted by Heuser et al. [191]. The fact of considering a variable liquefaction rate allows Heuser et al. [191] to optimise the installation of VRES, which then do not have to adapt to a constant demand profile. However, this also leads to oversizing electrolysers and liquefiers to account for an irregular production over the year. Besides, a significant liquefied hydrogen storage capacity has to be considered, which is equal to between 20 and 30 days according to Heuser et al. [191]. Therefore, even if specific investment costs for liquid hydrogen storage are lower by around ten times than those of gaseous hydrogen one [173, 191], Heuser et al. [191] still report higher total costs relative to the storage of hydrogen. Another different in methodology that should also be noted is that Heuser et al. [191] only take into account fixed-tilt PV, whereas this study also includes wind technologies.

In spite of the difference in the methodology adopted by Heuser et al. [123] and this study, a similar LCOH is found in both cases, as can be observed in Figure 7.11. More precisely, the current study finds a negative

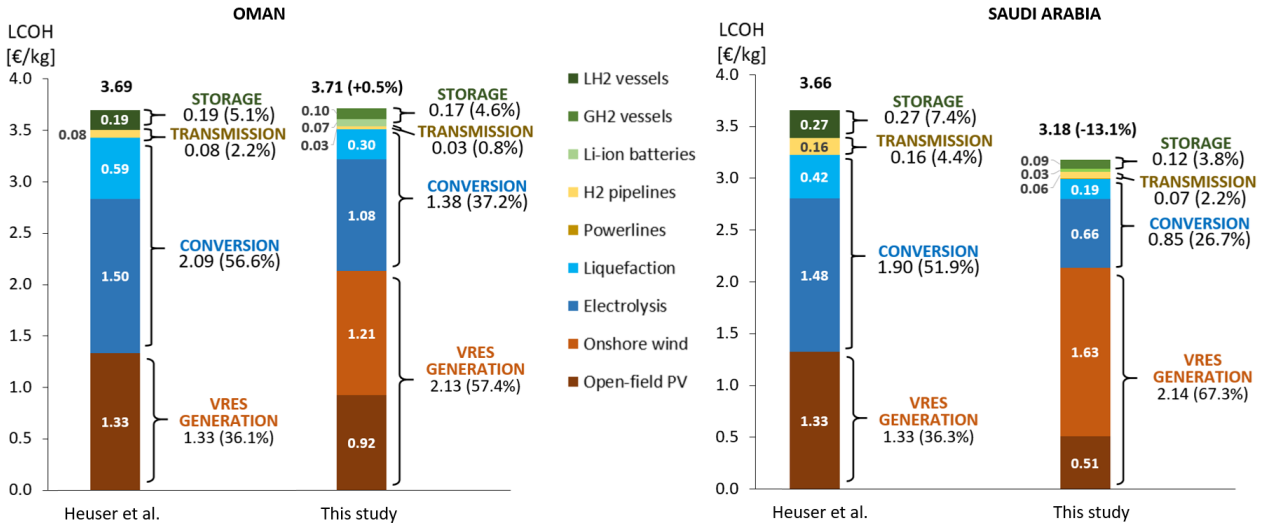

Figure 7.11: Comparison with literature of the specific costs in the isolation-LH2 scenario. Results are compared to Heuser et al. [191] for the countries of Oman (left) and Saudi Arabia (right)

deviation of 13% in the case of Saudi Arabia, while exactly the same costs are registered in Oman. However, the costs breakdown is significantly different. In fact, the optimisation process privileges the oversizing and consequent curtailment of VRES in order to reduce the installation costs of conversion technologies such as electrolysers and liquefiers. In fact, the share of conversion and VRES costs registered for Oman is

reversed with respect to Heuser et al. [191], while a role reversal in this sense can also be observed for Saudi Arabia. Here, the share of VRES costs registered by this study are even higher than the conversion ones of Heuser et al. [191], whereas the conversion costs obtained here are lower than the VRES costs of Heuser et al. [191].

It should also be noted that both this study and that of Heuser et al. [191] show no variation in specific costs of VRES between Oman and Saudi Arabia. This could have been expected in the case of Heuser et al. [191] since he is considering only the best PV farms in both countries, which indeed show the same LCOE. However, this result is less predictable when this study is considered, since an optimisation of the entire energy system is performed. In fact, even if total specific costs of VRES are unchanged, the share of solar and wind in the mix changes dramatically, also in accordance with the results of the electricity-demand-isolation scenario discussed in the previous subsection. In particular, the synergy of wind and solar technologies allows the system to find lower costs in Saudi Arabia with respect to Heuser et al. [191], while even with the use of both solar and wind energy no cost improvement can be obtained for Oman. This is because Heuser et al. [191] obtain higher FLH with their VRES simulations than those found in this study, meaning that they can rely on cheaper electricity.

8 | Conclusions and Recommendations

This last chapter will offer an answer to all research questions indicated in chapter 1. In order to do so, the main results relevant to each research goal are reported here together with the fundamental steps of the methodology adopted to achieve them.
Even though the various results found here are consistent with one another and can be reasonably compared with other studies, limitations apply to the energy system model created. These will be shortly repeated in this chapter. Moreover, ideas will be introduced suggesting how future research could build on the existing approach and analysis to improve it and/or further explain some of the results obtained from it.

Eligible land for VRES installations

In order to find out the potential of variable renewable energy sources (VRES), the first step was the derivation of the eligible land for open-field fixed-tilt PV farms, onshore wind farms and offshore wind farms following the methodology of Ryberg [135] and Caglayan et al. [6] for onshore and offshore technologies respectively. Existing land constraints and buffers were adapted to the context of the Arabian Peninsula, for example taking into account moving sands, political instabilities and the water-energy-food (WEF) nexus. The open-source tool GLAES [209] has been used to implement these constraints, applying a total land exclusion and a buffer distance to selected geographical elements featured in the chosen datasets. A resolution of 100 m was used.
Moving sands are by far the most impactful land constraint onshore (25%), while natural reserves and slope always feature in the four most dominant constraints. Offshore constraints like coasts and water depth result in the almost entirety of exclusions in the sea. Onshore results very well match the other global studies considered [202–204, 206], although only in the biggest countries and when moving sands are not included in the eligible land, as other authors did not investigate which portions of deserts should be excluded. For offshore areas, the different buffers and constraints adopted often results in important deviations from the other studies considered [202,203]. In general, other elements that can impact results are the the geographical datasets used, the resolution of the model, the scaling algorithm adapting the datasets to the chosen resolution and the land suitability factor. As this study was not focused on the validation of GLAES [209], sensitivity analyses were not performed, especially because of the good match with other studies considering the whole territory. However, these could provide interesting insights and might heavily impact the results obtained for the four smaller countries, where the LEA has an important role if no energy can be exchanged with the other countries.

VRES potential

As with the land eligibility analysis, the VRES technologies themselves were also modeled according to Ryberg [135] and Caglayan et al. [6]. Techno-economic improvements in the year 2050 are also considered as done by these authors. Since both Ryberg [135] and Caglayan et al. [6] show that single-axis tracking PV would not be economically efficient anywhere in Europe, where areas are found showing DNI comparable to that of most parts of the Arabian Peninsula, this technology was excluded from the system. However, other studies show that it might be part of an optimised energy system both in the case of Europe [5] and the MENA region [8], although they suppose cheaper costs for it than in this study.
To obtain the feed-in time series of VRES and consequently the electricity generation costs, the open-source tool RESKIT [164] was adopted. The ERA5 [167] weather data from the year 2015 is used having a temporal resolution of one hour and a spatial resolution of approximately 30 km. The GWA [3] and GSA [2] datasets are also used to improve the spatial resolution of the inputs.
Considering the overall GCC area, the results of the simulations show that both solar and onshore wind energy could cover the national hydrogen and electricity demand by more than one order of magnitude. However, at a country level, this is true only for solar energy. Compared with other energy sources, offshore wind has a lower potential approximately close to total energy demand, but it is particularly important for Bahrain, which cannot rely sufficiently on onshore technologies due to the LEA. When it comes to the area-specific potential, this study always reports higher values than those supposed by other authors [202–204,206], except for the values reported by Pietzcker [205]. Rather than the LEA, it is mainly the higher FLH found for VRES and particularly wind turbines which lead to this outcome. In turn, these are the result not only of the chosen weather datasets, but also of technological improvements assumed for VRES for the year 2050. This outcome,

however, does not always lead to lower costs, as will be explained next.

VRES-based electricity generation costs

Open-field PV would theoretically satisfy total energy needs for less than 2.5 €c/kWh, while onshore wind turbines could offer the same electricity for a price between 2.5 €c/kWh and 3.5 €c/kWh. These prices are very competitive when compared to the cheapest possible LCOE of gas turbines equal to 5.0 €c/kWh [118]. However, the true LCOE of VRES is considerably higher when the supply-demand balance is considered, as will be reported later in this chapter. Finally, offshore wind always scores above 5.5 €c/kWh. However, this value could actually be brought down by as much as 20% if a site-dependent turbine design was adopted [6]. In general, the electricity generation costs of open-field PV obtained here place themselves between the studies of Fasihi and Breyer [208] and Pietzcker et al. [205], thus being close to the work of Aghahosseini et al. [8]. As for onshore wind, prices are on average very close to that of Fasihi and Breyer [208] but lower than those registered by Aghahosseini et al. [8]. The registered deviations can always be explained looking at the assumptions made for CAPEX, OPEX, financial costs or FLH. In particular, the other studies mentioned here usually suppose lower CAPEX, especially in the case of PV technologies, but often obtain lower FLH, especially in the case of onshore wind technologies. As for the FLH registered for PV parks, only Pietzcker et al. [205] differ significantly from the results of this study due to the use of a different weather dataset [210]; in the case of wind turbines, the method created by Ryberg [135] and adopted here to implement future technological improvements is instead the main driver of higher FLH.

Creation and optimal operation of the ESM

An energy system model (ESM) was created using the tool FINE [185]. This includes technologies for the production, transmission, conversion and storage of green electricity and hydrogen. Future electricity and hydrogen demand were considered covering the power, transport, ammonia and steel sectors. For production, the feed-in time series of VRES output by simulations in RESKIT [164] are input, after applying averaging based on spatial and economic considerations. Finally, the optimal operation of the system is achieved by minimising total annual costs. To better study and understand the system, multiple scenarios are designed based on different assumptions.

The optimal generation mix reported by this study sees wind energy as the main source of electricity when all countries are able to exchange electricity, whereas it is slightly less used than solar energy when these are isolated. Also, hydrogen is mostly produced by wind energy when the system enjoys the maximum flexibility in terms of interconnection. These results depend on the assumed profiles of electricity and hydrogen demand used in the model, as well as the different hourly distribution of solar and wind energy derived from the VRES simulations. Studying the changes in the system when different demand profiles are assumed would shed more light on this topic. The comparison with the work of Aghahosseini et al. [8] has also shown the importance of the weather data selection and processing, since this is most likely behind the lower need of curtailment registered by their study for the GCC countries. In particular, the current study is significantly more accurate when it comes to averaging the feed-in time series of different technologies, but the adopted weather dataset, i.e. ERA5, has not been validated yet. The different generation profiles as well as the demand profiles are important factors also when comparing the optimal electricity mix of this study and those focused on other regions of the world, as shown for the case of Europe [5, 7, 173].

As just explained, LCOE and cost assumptions influence the results, but are not the only factors impacting optimisation. The presence of other technologies should also be considered, as well as the different regionalisation of the territory. Rerunning the optimisation process using both a higher and lower nodal resolution and/or VRES clusters in order to spot potential differences in the system costs or its optimal lay-out should be regarded as one of the best ways to further validate the results obtained with the optimisation tool. Specifying a different number of typical days for time series clustering for the optimisation could also contribute to prove the robustness of results. In any case, the sensitivity analysis conducted on the CAPEX of VRES shows that this parameter remains of the utmost importance for the outcome of optimisation, notably for the share of solar and wind energy in the electricity mix. Besides, the sensitivity analysis has also proven that a higher share of batteries in the storage system is needed when the optimal share of PV in the generation mix increases, whereas relatively more hydrogen vessels are installed if the optimal share of wind energy increases with respect to that of solar energy.

Due to the techno-economic parameters adopted in this work, the hydrogen transport and storage chain is more flexible than the electricity one, meaning that the location of VRES is more constrained by the distri-

bution of electricity demand over the territory. Besides, this also leads to more significant changes to the inter-regional flows of hydrogen than those of electricity when country connections are removed. It would be interesting to study the changes in the system once hydrogen storage in underground caverns is used, although not enough data is publicly available online to perform this analysis.
Finally, the system does not rely significantly on hydrogen reconversion technologies: in all main scenarios, less than 3% of electricity demand comes from reconversion, whereas 15% comes from battery storage. In fact, the conversion and reconversion process leads to an energy loss of at least 50% according to the present model parameters, making curtailment and battery storage a more cost-effective solution. However, the figures for the operation of batteries and reconversion are both equal to 8% of final electricity demand when only wind energy is made available to the system. Also, reconversion provides more than 15% of national electricity demand to both Kuwait and Bahrain when they cannot trade energy with other countries, meaning that scarcity of VRES can result in a higher dependence on hydrogen storage for electricity production.

Total costs and economic benefits of cooperation and sector coupling

To satisfy the overall energy demand assumed in this study, total annual costs would amount to 130 €bln when countries can exchange energy. Isolating the countries results in an increase of overall costs of 21%, which would then be avoided under a cooperation scheme. This would mainly benefit the smaller countries, particularly Bahrain, while it would leave energy costs almost unaltered for Saudi Arabia. In order to compare the costs found here with other studies, different scenarios were considered where only either electricity or liquid hydrogen demand was included. In this way, the LCOE and LCOH parameter could be derived and compared to other studies. An LCOE of 6.6 €c/kWh is therefore obtained, whereas an LCOH of 3.2 €/kg is found. Electricity costs are higher than those reported by Aghahosseini et al. [8], mainly due to a higher need for curtailment according to the optimisation tool used here. This is in turn partly due to the reportedly better performance of single-axis tracking PV with respect to fixed-tilt PV according to Aghahosseini et al. [8], excluded by this study following the results of Ryberg [135] and Caglayan et al. [173] in Europe, where regions with similar DNI to that observed in most regions of Saudi Arabia can be found. Due to the higher impact of curtailment, the costs of VRES alone are higher than the generation costs reported earlier. As for the LCOH, similar values are found by this study and that of Heuser et al. [123] in Oman and Saudi Arabia, although the adopted methodology differs for some aspects, notably the choice of the hydrogen storage medium, which is liquid hydrogen and not gaseous hydrogen in Heuser et al. [123].
Considering the combination of the scenarios with only one type of energy demand between electricity and liquid hydrogen, the economic benefits of sector coupling between these sectors were obtained. More precisely, a reduction of 7% in total system costs is obtained comparing the cost of the export scenario with the sum of the costs registered in the two scenarios similar to it but where only one type of demand is considered. Applying this reduction factor to the cost results obtained with the scenario featuring only electricity demand, it is found that the overall LCOE of the system is around 20% higher than that of modern natural gas turbines in the Middle East, namely 6.1 €c/kWh against 5 €c/kWh [174].
Applying the same cost reduction of 7% due to sector coupling to the LCOH found in the scenario including only liquid hydrogen demand, a comparison with the breakeven costs of LNG reveals that the cost gap between these two fuels is significantly high: liquid hydrogen costs are around 3.5 €/kg, between 13 and 21 times more than LNG, when production in Qatar and shipping to Asia is considered [217, 218]. Referring to LNG produced in other countries outside the Middle East, this difference reduces but never goes below 3.5 times [217]. Finally, gaseous green hydrogen is between around 2 and 3 times more expensive than crude oil produced in the GCC countries. [219].
Therefore, according to this study, a fully renewable energy system including the GCC countries in 2050 is found to be economically less competitive than the current fossil-fuel-based one. However, such a comparison cannot account for the important role of carbon pricing and of subsidies destined to clean technologies which are very likely to strongly impact the energy sector in the upcoming decades [220]. A detailed analysis of the consequences on the energy sector of climate change policies the might come into action in the future would allow for a more meaningful comparison between the VRES costs found in this study and those related to fossil fuels.

Bibliography

[1] European Commission, "A hydrogen strategy for a climate-neutral Europe," tech. rep., 2020.

[2] World Bank Group, "Global Solar Atlas", 2019. [online] Available at: <https://globalsolaratlas.info/map> [Accessed 17 November 2020].

[3] World Bank Group and Denmark Technical University (DTU), "Global Wind Atlas", 2019. [online] Available at: <https://globalwindatlas.info/> [Accessed 17 November 2020].

[4] International Renewable Energy Agency (IRENA), "Renewable Energy Market Analysis: GCC 2019", tech. rep., 2019.

[5] M. Child, C. Kemfert, D. Bogdanov, and C. Breyer, "Flexible electricity generation, grid exchange and storage for the transition to a 100% renewable energy system in Europe," *Renewable Energy*, vol. 139, pp. 80–101, 2019.

[6] D. G. Caglayan, D. S. Ryberg, H. Heinrichs, J. Linßen, D. Stolten, and M. Robinius, "The techno-economic potential of offshore wind energy with optimized future turbine designs in Europe," *Applied Energy*, vol. 255, no. September, p. 113794, 2019.

[7] M. Victoria, K. Zhu, T. Brown, G. B. Andresen, and M. Greiner, "Early decarbonisation of the European energy system pays off," *Nature Communications*, vol. 11, no. 1, pp. 1–9, 2020.

[8] A. Aghahosseini, D. Bogdanov, and C. Breyer, "Towards sustainable development in the MENA region: Analysing the feasibility of a 100% renewable electricity system in 2030," *Energy Strategy Reviews*, vol. 28, no. February, p. 100466, 2020.

[9] M. Beaudin, H. Zareipour, A. Schellenberglabe, and W. Rosehart, "Energy storage for mitigating the variability of renewable electricity sources: An updated review," *Energy for Sustainable Development*, vol. 14, no. 4, pp. 302–314, 2010.

[10] L. K. K. Maia and E. Zondervan, "Optimization of energy storage and system flexibility in the context of the energy transition: Germany's power grid as a case study," *BMC Energy*, vol. 1, no. 1, pp. 1–17, 2019.

[11] K. Schmietendorf, J. Peinke, and O. Kamps, "The impact of turbulent renewable energy production on power grid stability and quality," *European Physical Journal B*, vol. 90, no. 11, 2017.

[12] G. Strbac, "Demand side management: Benefits and challenges," *Energy Policy*, vol. 36, no. 12, pp. 4419–4426, 2008.

[13] A. Boretti and S. Castelletto, "Cost of wind energy generation should include energy storage allowance," *Scientific Reports*, vol. 10, no. 1, pp. 1–13, 2020.

[14] R. Irany, K. Aancha, G. Daniel, and G. Arwa, "Energy Storage Monitor," tech. rep., World Energy Council, 2019.

[15] International Renewable Energy Agency (IRENA), "Utility-Scale Batteries," tech. rep., 2019.

[16] A. Poullikkas, "Sustainable options for electric vehicle technologies," *Renewable and Sustainable Energy Reviews*, vol. 41, pp. 1277–1287, 2015.

[17] J. Wen, Y. Yu, and C. Chen, "A review on lithium-ion batteries safety issues: Existing problems and possible solutions," *Materials Express*, vol. 2, no. 3, pp. 197–212, 2012.

[18] D. B. Agusdinata, W. Liu, H. Eakin, and H. Romero, "Socio-environmental impacts of lithium mineral extraction: Towards a research agenda," *Environmental Research Letters*, vol. 13, no. 12, 2018.

[19] W. M. Seong, K. Y. Park, M. H. Lee, S. Moon, K. Oh, H. Park, S. Lee, and K. Kang, "Abnormal self-discharge in lithium-ion batteries," *Energy and Environmental Science*, vol. 11, no. 4, pp. 970–978, 2018.

[20] M. Uhrig, S. Koenig, M. R. Suriyah, and T. Leibfried, "Lithium-based vs. Vanadium Redox Flow Batteries - A Comparison for Home Storage Systems," *Energy Procedia*, vol. 99, pp. 35–43, 2016.

[21] Z. Li, M. S. Pan, L. Su, P. C. Tsai, A. F. Badel, J. M. Valle, S. L. Eiler, K. Xiang, F. R. Brushett, and Y. M. Chiang, "Air-Breathing Aqueous Sulfur Flow Battery for Ultralow-Cost Long-Duration Electrical Storage," *Joule*, vol. 1, no. 2, pp. 306–327, 2017.

[22] S. Hameer and J. L. van Niekerk, "A review of large-scale electrical energy storage," *International Journal of Energy Research*, vol. 39, no. 9, pp. 1179–1195, 2015.

[23] N. P. Brandon and Z. Kurban, "Clean energy and the hydrogen economy," *Philosophical Transactions of the Royal Society A: Mathematical, Physical and Engineering Sciences*, vol. 375, no. 2098, 2017.

[24] S. Cerniauskas, A. Jose Chavez Junco, T. Grube, M. Robinius, and D. Stolten, "Options of natural gas pipeline reassignment for hydrogen: Cost assessment for a Germany case study," *International Journal of Hydrogen Energy*, vol. 45, no. 21, pp. 12095–12107, 2020.

[25] A. Valera-Medina, H. Xiao, M. Owen-Jones, W. I. David, and P. J. Bowen, "Ammonia for power," *Progress in Energy and Combustion Science*, vol. 69, no. November, pp. 63–102, 2018.

[26] K. Keramidas, A. Diaz Vazquez, M. Weitzel, T. Vandyck, M. Tamba, S. Tchung-Ming, A. Soria Ramirez, J. Krause, R. Van Dingenen, Q. Chai, S. Fu, and X. Wen, "Global Energy and Climate Outlook 2019: Electrification for the low-carbon transition," tech. rep., Joint Research Center - European Commission, 2020.

[27] A. W. Mortensen, B. V. Mathiesen, A. B. Hansen, S. L. Pedersen, R. D. Grandal, and H. Wenzel, "The role of electrification and hydrogen in breaking the biomass bottleneck of the renewable energy system – A study on the Danish energy system," *Applied Energy*, vol. 275, p. 115331, 2020.

[28] United Nations Framework Convention on Climate Change (UNFCCC), "GHG Profiles - Annex I". [online] Available at: <https://di.unfccc.int/ghg_profile_annex1> [Accessed 12 November 2020].

[29] H. Ritchie, "Sector by sector: where do global greenhouse gas emissions come from?", Our World in Data and World Resource Institute, 2020. [online] Available at: <https://ourworldindata.org/ghg-emissions-by-sector> [Accessed 12 November 2020].

[30] International Energy Agency (IEA), "CO_2 emissions from fuel combustion", 2020. [online] Available at: <https://www.iea.org/subscribe-to-data-services/co2-emissions-statistics> [Accessed 14 November 2020].

[31] Istituto Superiore per la Protezione e la Ricerca Ambientale (ISPRA), "Fattori di emissione atmosferica di CO_2 e altri gas a effetto serra nel settore elettrico," tech. rep., 2017.

[32] International Energy Agency (IEA), "World Energy Outlook 2017," tech. rep., 2017.

[33] N. Sartori, "Tracking the decoupling of electricity demand and associated CO2 emissions", International Energy Agency (IEA), 2019. [online] Available at: <https://www.iea.org/commentaries/tracking-the-decoupling-of-electricity-demand-and-associated-co2-emissions> [Accessed 14 November 2020].

[34] International Energy Agency (IEA), "Data and statistics 2018", 2020. [online] Available at: <https://www.iea.org/data-and-statistics/data-tables?country=SAUDIARABIenergy=Balancesyear=2018> [Accessed 14 November 2020].

[35] P. Plötz, J. Axsen, S. A. Funke, and T. Gnann, "Designing car bans for sustainable transportation," *Nature Sustainability*, vol. 2, no. 7, pp. 534–536, 2019.

[36] International Energy Agency (IEA), "Global EV Outlook 2020," tech. rep., 2020.

[37] Mordor Intelligence, "Middle East & Africa Electric vehicle market - growth, trends, and forecast (2020 - 2025)," tech. rep., 2020.

[38] G. Morrison, J. Stevens, and F. Joseck, "Relative economic competitiveness of light-duty battery electric and fuel cell electric vehicles," *Transportation Research Part C: Emerging Technologies*, vol. 87, pp. 183–196, 2018.

[39] D. U. Eberle and D. R. von Helmolt, "Sustainable transportation based on electric vehicle concepts: a brief overview," *Energy Environ. Sci.*, vol. 3, pp. 689–699, 2010.

[40] G. J. Offer, D. Howey, M. Contestabile, R. Clague, and N. P. Brandon, "Comparative analysis of battery electric, hydrogen fuel cell and hybrid vehicles in a future sustainable road transport system," *Energy Policy*, vol. 38, no. 1, pp. 24–29, 2010.

[41] Energy Transitions Commission, "Electricity, hydrogen & hydrogen based fuels in a zero-carbon economy," tech. rep., 2019.

[42] International Energy Agency (IEA), "Transport sector CO2 emissions by mode in the Sustainable Development Scenario, 2000-2030", 2019. [online] Available at: <https://www.iea.org/data-and-statistics/charts/transport-sector-co2-emissions-by-mode-in-the-sustainable-development-scenario-2000-2030> [Accessed 12 November 2020].

[43] J. Kast, G. Morrison, J. J. Gangloff, R. Vijayagopal, and J. Marcinkoski, "Designing hydrogen fuel cell electric trucks in a diverse medium and heavy duty market," *Research in Transportation Economics*, vol. 70, no. November 2016, pp. 139–147, 2018.

[44] "Validation of robustness and fuel efficiency of a universal model-based energy management strategy for fuel cell hybrid trains: From analytical derivation via simulation to measurement on test bench," *Energy Conversion and Management*, vol. 229, p. 113734, 2021.

[45] United States Geological Survey (USGS), "Nitrogen Data Sheet - Mineral Commodity Summaries 2020", 2020. [online] Available at: <https://pubs.usgs.gov/periodicals/mcs2020/mcs2020-nitrogen.pdf> [Accessed 12 November 2020].

[46] X. Liu, A. Elgowainy, and M. Wang, "Life cycle energy use and greenhouse gas emissions of ammonia production from renewable resources and industrial by-products," *Green Chemistry*, vol. 22, no. 17, pp. 5751–5761, 2020.

[47] Gulf Petrochemicals and Chemicals Association (GPCA), "GCC fertilizer market outlook: challenges and opportunities for gcc fertilizer producers", tech. rep., 2020.

[48] P. H. Pfromm, "Towards sustainable agriculture: Fossil-free ammonia," *Journal of Renewable and Sustainable Energy*, vol. 9, no. 3, 2017.

[49] International Energy Agency (IEA), "Technology Roadmap - Hydrogen and Fuel Cells," tech. rep., 2015.

[50] C. Smith, A. K. Hill, and L. Torrente-Murciano, "Current and future role of Haber-Bosch ammonia in a carbon-free energy landscape," *Energy and Environmental Science*, vol. 13, no. 2, pp. 331–344, 2020.

[51] N. P. Cheremisinoff, P. Rosenfeld, and A. R. Davletshin, "Chapter Seven - P2 and Best Management Practices in Different Industries," in *Responsible Care* (N. P. Cheremisinoff, P. Rosenfeld, and A. R. Davletshin, eds.), Pergamon Texts in Inorganic Chemistry, pp. 435 – 476, Gulf Publishing Company, 2008.

[52] Worldsteel Association, "2020 World Steel in Figures," tech. rep., 2020.

[53] OECD, "Latest developments in steelmaking capacity 2020," tech. rep., 2020.

[54] M. Hvidt, "Economic diversification in GCC countries: Past record and future trends", Kuwait Programme on Development, Governance and Globalisation in the Gulf States,tech. rep., 2013.

[55] International Energy Agency (IEA), "Iron and Steel Technology Roadmap," tech. rep., 2020.

[56] Worldsteel Association, "Overview of the steelmaking process", 2020. [online] Available at: <https://www.worldsteel.org/publications/bookshop/product-details~Overview-of-the-steelmaking-process~PRODUCT~Poster2011~.html> [Accessed 12 November 2020].

[57] Worldsteel Association, "Steel's contribution to a low carbon future and climate resilient societies," tech. rep., 2020.

[58] L. D. Harvey, "Iron and steel recycling: Review, conceptual model, irreducible mining requirements, and energy implications," *Renewable and Sustainable Energy Reviews*, no. September 2019, p. 110553, 2020.

[59] B. B. Çiftçi, "The future of global scrap availability", Worldsteel Association, 2018. [online] Available at: <https://www.worldsteel.org/media-centre/blog/2018/future-of-global-scrap-availability.html> [Accessed 2 January 2020].

[60] International Energy Agency (IEA), "World Energy Outlook 2020," tech. rep., 2020.

[61] V. Vogl, M. Åhman, and L. J. Nilsson, "Assessment of hydrogen direct reduction for fossil-free steelmaking," *Journal of Cleaner Production*, vol. 203, pp. 736–745, 2018.

[62] Y. Gan and W. M. Griffin, "Analysis of life-cycle GHG emissions for iron ore mining and processing in China—Uncertainty and trends," *Resources Policy*, vol. 58, no. February, pp. 90–96, 2018.

[63] B. Osman Elasha, "Mapping of Climate Change Threats and Human Development Impacts in the Arab Region," tech. rep., United Nations Development Programme (UNDP), 2010.

[64] G. O. Odhiambo, "Water scarcity in the Arabian Peninsula and socio-economic implications," *Applied Water Science*, vol. 7, no. 5, pp. 2479–2492, 2017.

[65] K. A. Rambo, D. M. Warsinger, S. J. Shanbhogue, J. H. Lienhard, and A. F. Ghoniem, "Water-Energy Nexus in Saudi Arabia," *Energy Procedia*, vol. 105, pp. 3837–3843, 2017.

[66] U.S. Department of Energy , "Energy Demand on Water Resources - Report to congress on the interdependency of energy and water," tech. rep., 2006.

[67] M. E. Webber, "The water intensity of the transitional hydrogen economy," *Environmental Research Letters*, vol. 2, no. 3, 2007.

[68] C. B. Harto, M. Finster, J. Schroeder and C. Clark, "Saline water for power plant cooling - challenges and opportunities," tech. rep., Argonne National Laboratory, 2014.

[69] S. Dresp, F. Dionigi, M. Klingenhof, and P. Strasser, "Direct electrolytic splitting of seawater: Opportunities and challenges," *ACS Energy Letters*, vol. 4, no. 4, pp. 933–942, 2019.

[70] D. S. Ryberg, M. Robinius, and D. Stolten, "Evaluating land eligibility constraints of renewable energy sources in Europe," *Energies*, vol. 11, no. 5, pp. 1–19, 2018.

[71] M. Al-Saidi and S. Saliba, "Water, energy and food supply security in the Gulf Cooperation Council (GCC) countries-A risk perspective," *Water (Switzerland)*, vol. 11, no. 3, 2019.

[72] Nationsonline.org, "Map of the Arabian Peninsula, Middle East". [online] Available at: <http://nationsonline.org/oneworld/map/Arabia-Map.htm> [Accessed 13 November 2020].

[73] B. K. Nijim, R. B. Serjeant, *et al.* , "Arabia", Encyclopedia Britannica, 2019. [online] Available at: <https://www.britannica.com/place/Arabia-peninsula-Asia> [Accessed 13 November 2020].

[74] George S. Rentz, William L. Ochsenwald, W. L. Ochsenwald and G. S. Rentz, "Arabia", Encyclopedia Britannica, 2019. [online] Available at: <https://courses.lumenlearning.com/suny-worldgeography/chapter/8-5-arabs-islam-and-oil/> [Accessed 16 November 2020].

[75] Open Education Resources (OER) Services, "8.5 Arabs, Islam, and Oil", 2016. [online] Available at: <https://open.lib.umn.edu/worldgeography/chapter/8-5-arabs-islam-and-oil/> [Accessed 16 November 2020].

[76] European Space Agency (ESA), "Climate change Initiative: Land Cover", 2017. [online] Available at: <http://www.esa-landcover-cci.org/> [Accessed 16 December 2020].

[77] P. Patlakas, C. Stathopoulos, H. Flocas, C. Kalogeri, and G. Kallos, "Regional climatic features of the Arabian Peninsula," *Atmosphere*, vol. 10, no. 4, 2019.

[78] Encyclopedia Britannica, "Middle East", 2020. [online] Available at: <https://www.britannica.com/place/Middle-East> [Accessed 08 January 2021].

[79] D. Smith, *The State of the Middle East Atlas*. New Internationalist, 3 ed.

[80] US Central Intelligence Agency (CIA), "Middle East oil and gas", 2007. [online] Available at: <https://www.loc.gov/item/2007631392/> [Accessed 16 November 2020].

[81] British Petroleum (BP), "Statistical Review of World Energy 2020," tech. rep., 2020.

[82] D. Smith, *The political economy of the Middle East - Introduction to Economic Diversification in the GCC Region*, vol. 1. Palgrave Macmillan.

[83] J. . E. . Peterson, "The Emergence of Nation-States in the Arabian Peninsula," *GeoJournal*, vol. 13, no. 3, pp. 197–200, 1986.

[84] O. Schwab, *The Gulf Wars and the United States: Shaping the Twenty-first Century*. Greenwood, 1 ed., 2009.

[85] R. Burrowes, M. W. Wenner, *et al.* , "Arab Spring and civil war", Encyclopedia Britannica, 2020. [online] Available at: <https://www.britannica.com/place/Yemen/Arab-Spring-and-civil-war> [Accessed 13 November 2020].

[86] Statista, "Arab world: Gross domestic product (GDP) per capita in current prices in 2018 (in U.S. dollars), by country", 2019. [online] Available at: <https://www.statista.com/statistics/806152/gross-domestic-product-gdp-per-capita-in-the-arab-world/> [Accessed 14 November 2020].

[87] Statista, "Oil production in the Middle East in 2018, by country", 2019. [online] Available at: <https://www.statista.com/statistics/218302/oil-production-in-key-middle-eastern-countries/> [Accessed 14 November 2020].

[88] R. Parsapour. " Population in the Persian Gulf Region", Persian Gulf Studies Center, 2020. [online] Available at: <http://www.persiangulfstudies.com/en/index.asp?p=pagesid=240> [Accessed 13 November 2020].

[89] World Population Review, "Arabian Peninsula Countries 2020", 2020. [online] Available at: <https://worldpopulationreview.com/country-rankings/arabian-peninsula-countries> [Accessed 13 November 2020].

[90] K. C. Ulrichsen, "The GCC States and the Shifting Balance of Global Power," tech. rep., Center for International and Regional Studies (CIRS) - Georgetown University School of Foreign Service in Qatar, 2010.

[91] J. A. Sandwick, *The Gulf Cooperation Council: Moderation And Stability In An Interdependent World*. Routledge, 2019.

[92] T. Callen, R. Cherif, F. Hasanov, A. Hegazy, and P. Khandelwal, "Economic Diversification in the GCC : Past, Present, and Future," tech. rep., International Monetary Fund, 2014.

[93] F. H. Al-Marri, "The Impact of the Oil Crisis on Security and Foreign Policy in GCC Countries: Case Studies of Qatar, KSA and UAE," tech. rep., Arab Center for Research Policy Studies, 2017.

[94] K. C. Ulrichsen, *Qatar and the Gulf Crisis: A Study of Resilience*. Oxford University Press, 2020.

[95] Al Jazeera, "UN expert calls for immediate lifting of sanctions against Qatar", 2020. [online] Available at: <https://www.aljazeera.com/news/2020/11/12/un-expert-calls-for-immediate-lifting-of-sanctions-against-qatar> [Accessed 14 November 2020].

[96] F. Al-Muslimi, "A History of Missed Opportunities: Yemen and the GCC", Carnegie Middle East Center, 2016. [online] Available at: <https://carnegie-mec.org/diwan/62405> [Accessed 14 November 2020].

[97] M. Nichols, "Exclusive: U.N. investigators find Yemen's Houthis did not carry out Saudi oil attack", Reuters, 2020. [online] Available at: <https://www.reuters.com/article/us-saudi-aramco-attacks-un-exclusive-idUSKBN1Z72VX> [Accessed 14 November 2020].

[98] K. Selvik, "The War in Yemen: The view from Iran", NOREF, 2015. [online] Available at: <https://www.cmi.no/publications/5654-war-in-yemen-the-view-from-iran> [Accessed 14 November 2020].

[99] Flanders Marine Institute, "The intersect of the Exclusive Economic Zones and IHO sea areas", 2020. [online] Available at: < https://www.marineregions.org/.https://doi.org/10.14284/402> [Accessed 19 December 2020].

[100] C. E. Toffolo, *The Arab League*. Chelsea house publisher, 1 ed., 2008.

[101] United Nations Economic and Social Commission for Western Asia (UN-ESCWA), "Assessing Arab economic integration: towards the Arab Customs Union," tech. rep., 2015.

[102] US Energy Information Administration, "World Oil Transit Chokepoints," tech. rep., 2017.

[103] M. El-Said, "Qatari ships banned from entering suez canal ports: Mamish." Daily News Egypt, 2017. [online] Available at: <https://dailynewsegypt.com/2017/07/08/qatari-ships-banned-entering-suez-canal-ports-mamish/> [Accessed 17 November 2020].

[104] C. Emmerson and P. Stevens, "Maritime Choke Points and the global energy system: Charting a way forward," tech. rep., Chatam House - Energy, Environment and Resource Governance, 2012.

[105] M. Sullivan, *Hezbollah in Syria*. Institute for the Study of War, 2014.

[106] C. A. Ennis, "Situating the Gulf States in the Global Economic Redrawing: GCC-BICs Relations," in *Emerging Powers, Emerging Markets, Emerging Societies*, vol. 93, pp. 132–161, London: Palgrave Macmillan UK, 2016.

[107] W. Khadduri, "GCC petroleum investments growing in Asia", The Arab Weekly, 2017. [online] Available at: <https://thearabweekly.com/gcc-petroleum-investments-growing-asia> [Accessed 16 November 2020].

[108] World Bank, "GDP per capita 2017". [online] Available at: <https://ourworldindata.org/grapher/gdp-per-capita-worldbank?time=2013region=World> [Accessed 17 November 2020].

[109] K. Hyde and A. Ellis, "Feasibility of Hydrogen Bunkering," tech. rep., ITM Power & European Regional Development Fund, 2019.

[110] D. Saadi and G. Gentile, "Total, PTTEP win rights to explore, develop Omani gas deposits", SP Global Platts, 2020. [online] Available at: <https://www.spglobal.com/platts/en/market-insights/latest-news/natural-gas/021920-total-pttep-win-rights-to-explore-develop-omani-gas-depositsl> [Accessed 16 November 2020].

[111] S. Kamiya, M. Nishimura, and E. Harada, "Study on introduction of CO2 free energy to Japan with liquid hydrogen," *Physics Procedia*, vol. 67, pp. 11–19, 2015.

[112] Offshore Energy, "LNG Carrier Crossing Suez Canal with Qatari Cargo despite Row with Qatar", 2017. [online] Available at: <https://www.offshore-energy.biz/lng-carrier-crossing-suez-canal-with-qatari-lng-despite-row-with-qatar/> [Accessed 16 November 2020].

[113] L. Villar, M. Hamilton, "Three important oil trade chokepoints are located around the Arabian Peninsula", US Energy Information Administration, 2017. [online] Available at: <https://www.eia.gov/todayinenergy/detail.php?id=32352> [Accessed 16 November 2020].

[114] L. Coffey, "Bab el-Mandeb: The U.S. Ignores the Most Dangerous Strait in the World at Its Peril", The Heritage Foundation, 2018. [online] Available at: <https://www.heritage.org/middle-east/commentary/bab-el-mandeb-the-us-ignores-the-most-dangerous-strait-the-world-its-peril> [Accessed 16 November 2020].

[115] J. Bowlus, "How verbal threats to close oil transit chokepoints lead to military conflict," tech. rep., Global Political Trends Center (GPoT), 2012.

[116] Global Administrative Areas, "GADM database of Global Administrative Areas", 2018. [online] Available at: <https://gadm.org/> [Accessed 16 December 2020].

[117] D. Dudley, "The 10 strongest military forces in the middle east." Forbes, 2018. [online] Available at: <https://www.forbes.com/sites/dominicdudley/2018/02/26/ten-strongest-military-forces-middle-east/?sh=69c3ef7016a2> [Accessed 17 November 2020].

[118] International Renewable Energy Agency (IRENA), " Renewable Power Generation Costs in 2017", tech. rep., 2018.

[119] D. S. Ryberg, Z. Tulemat, D. Stolten, and M. Robinius, "Uniformly constrained land eligibility for onshore European wind power," *Renewable Energy*, vol. 146, pp. 921–931, 2020.

[120] J. P. Snyder, *Map Projections: A Working Manual. U.S. Geological Survey Professional Paper 1395*. United States Government Printing Office, 1987.

[121] J. P. Snyder, *Flattening the Earth. Two Thousand Years of Map Projections*. University of Chicago Press, 1993.

[122] P. M. V. J. P. Snyder, *Flattening the Earth. Two Thousand Years of Map Projections*. United States Government Printing Office, 1989.

[123] P. M. Heuser, "Worldwide hydrogen supply infrastructure based on renewable energy", Doctoral dissertation, Rheinisch-Westfälische Technische Hochschule (RWTH) Aachen and Institut für Energie- und Klimaforschung Elektrochemische Verfahrenstechnik (IEK-3), Germany, 2020.

[124] European Commission, "Global Human Settlements Layer", 2019. [online] Available at: <https://ghsl.jrc.ec.europa.eu/data.php> [Accessed 16 December 2020].

[125] OpenFlights.org, "Airport database", 2014. [online] Available at: <https://openflights.org/data.html> [Accessed 16 December 2020].

[126] Geofabrik-OpenStreetMap (OSM), "OpenStreetMap Data Extracts", 2018. [online] Available at: <https://download.geofabrik.de/> [Accessed 16 December 2020].

[127] World Bank Group, "Middle East North Africa - Electricity Transmission Network", 2017. [online] Available at: <https://energydata.info/dataset/mena-electricity-transmission-network-2017> [Accessed 16 December 2020].

[128] Telegeography, "Submarine Cable Map", 2020. [online] Available at: <https://www.submarinecablemap.com//> [Accessed 19 December 2020].

[129] ArcGIS, "Middle_East Oil&Gas Map by CIA", 2018. [online] Available at: <https://www.arcgis.com/home/webmap/viewer.html?layers=4a99caf63d6b4d3290ed27290e261a07> [Accessed 19 December 2020].

[130] B. Halpern, M. Frazier, J. Potapenko, K. Casey, Kellee Koenig, et al., "Cumulative human impacts: raw stressor data (2008 and 2013)", Knowledge Network for Biocomplexity (KNB), 2015. [online] Available at: <https://knb.ecoinformatics.org/view/doi:10.5063/F1S180FS> [Accessed 19 December 2020].

[131] Consultative Group on International Agricultural Research - Consortium for Spatial Information (CGIAR - CSI), "SRTM 90m Digital Elevation Database v4.1", 2008. [online] Available at: <https://www.arcgis.com/home/webmap/viewer.html?layers=4a99caf63d6b4d3290ed27290e261a07> [Accessed 16 December 2020].

[132] Food and Agriculture Organization - United Nations (FAO-UN), "Digital Soil Map of the World", 2007. [online] Available at: <https://www.arcgis.com/home/webmap/viewer.html?layers=4a99caf63d6b4d3290ed27290e261a07> [Accessed 16 December 2020].

[133] General bathymetric Chart of the Oceans (GEBCO), "GEBCO 2020 Gridded Bathymetry Data"2020. [online] Available at: <https://download.gebco.net/> [Accessed 19 December 2020].

[134] UN Environment Programme World Conservation Monitoring Centre (UNEP-WCMC), "World Database on Protected Areas", 2016. [online] Available at: <https://www.protectedplanet.net/en/thematic-areas/wdpa> [Accessed 16 December 2020].

[135] D. S. Ryberg, "Generation Lulls from the Future Potential of Wind and Solar Energy in Europe", Rheinisch-Westfälische Technische Hochschule (RWTH) Aachen and Institut für Energie- und Klimaforschung Elektrochemische Verfahrenstechnik (IEK-3), Germany, 2019.

[136] X. Li, D. L. Mauzerall, and M. H. Bergin, "Global reduction of solar power generation efficiency due to aerosols and panel soiling," *Nature Sustainability*, vol. 3, no. 9, pp. 720–727, 2020.

[137] H. Supe, R. Avtar, D. Singh, A. Gupta, A. P. Yunus, J. Dou, A. A. Ravankar, G. Mohan, S. K. Chapagain, V. Sharma, C. K. Singh, O. Tutubalina, and A. Kharrazi, "Google earth engine for the detection of soiling on photovoltaic solar panels in arid environments," *Remote Sensing*, vol. 12, no. 9, 2020.

[138] A. H. Almasoud and H. M. Gandayh, "Future of solar energy in Saudi Arabia," *Journal of King Saud University - Engineering Sciences*, vol. 27, no. 2, pp. 153–157, 2015.

[139] U. Kevin, W. David, "Desert Power: The Economics of Solar Thermal Electricity for Europe, North Africa, and the Middle East," tech. rep., Center for Global Development, 2008.

[140] O. Ugarteche, C. León, "The role of lithium in trade warfare", Observatorio Economico Latinoamericano (OBELA), 2019. [online] Available at: <http://www.obela.org/en-analisis/the-role-of-lithium-in-trade-warfare> [Accessed 19 December 2020].

[141] P. M. Heuser, D. S. Ryberg, T. Grube, M. Robinius, and D. Stolten, "Techno-economic analysis of a potential energy trading link between Patagonia and Japan based on CO2 free hydrogen," *International Journal of Hydrogen Energy*, vol. 44, no. 25, pp. 12733–12747, 2019.

[142] C. Noon, 'Just Deserts: Oman's New Wind Turbine Can Handle Sandstorms And Desert Sun", General Electric, 2018. [online] Available at: <https://www.ge.com/news/reports/just-deserts-wind-turbine-can-handle-sandstorms-desert-sun> [Accessed 26 December 2020].

[143] GDAL/OGR contributors, *GDAL/OGR Geospatial Data Abstraction software Library*. Open Source Geospatial Foundation, 2020. [online] Available at: <https://gdal.org> [Accessed 27 December 2020].

[144] E. Jones, T. Oliphant, P. Peterson, *et al.*, "SciPy: Open source scientific tools for Python," 2001. [online] Available at: <http://www.scipy.org> [Accessed 27 December 2020].

[145] R. T. Krämer , Techno-ökonomische Analyse des Nutzungspotentials von Windenergie in ausgewählten windreichen Regionen auf Basis globaler Wetter- und Geodaten, Master Thesis, Rheinisch-Westfälische Technische Hochschule (RWTH) Aachen and Institut für Energie- und Klimaforschung Elektrochemische Verfahrenstechnik (IEK-3), Germany, 2018.

[146] Statista, "Average solar energy project size globally in 2015, by region", 2016. [online] Available at: <https://www.statista.com/statistics/539644/average-solar-project-size-globally-by-region/> [Accessed 30 November 2020].

[147] P. Roddis, K. Roelich, K. Tran, S. Carver, M. Dallimer, and G. Ziv, "What shapes community acceptance of large-scale solar farms? A case study of the UK's first 'nationally significant' solar farm," *Solar Energy*, vol. 209, no. September, pp. 235–244, 2020.

[148] S. Ong, C. Campbell, P. Denholm, R. Margolis and G. Heath,"Land-Use Requirements for Solar Power Plants in the United States", National Renewable Energy Lab. (NREL), tech. rep., 2013.

[149] T. Jäger, R. McKenna, and W. Fichtner, "The feasible onshore wind energy potential in Baden-Württemberg: A bottom-up methodology considering socio-economic constraints," *Renewable Energy*, vol. 96, pp. 662–675, 2016.

[150] W. F. Holmgren, C. W. Hansen, and M. A. Mikofski. "pvlib python: a python package for modeling solar energy systems." Journal of Open Source Software, 3(29), 884, 2018.

[151] G. Richhariya, A. Kumar, and Samsher, *Solar cell technologies*. Elsevier Inc., 2020.

[152] M. Khalis, R. Masrour, G. Khrypunov, M. Kirichenko, D. Kudiy, and M. Zazoui, "Effects of Temperature and Concentration Mono and Polycrystalline Silicon Solar Cells: Extraction Parameters," *Journal of Physics: Conference Series*, vol. 758, no. 1, 2016.

[153] A. Ndiaye, C. M. F. Kébé, P. A. Ndiaye, A. Charki, A. Kobi, and V. Sambou, "Impact of dust on the photovoltaic (PV) modules characteristics after an exposition year in Sahelian environment: The case of Senegal," *International Journal of Physical Sciences*, vol. 8, no. 21, pp. 1166–1173, 2013.

[154] D. Olivares, P. Ferrada, C. D. Matos, A. Marzo, E. Cabrera, C. Portillo, and J. Llanos, "Characterization of soiling on PV modules in the Atacama Desert," *Energy Procedia*, vol. 124, pp. 547–553, 2017.

[155] J. N. Mayer, S. Philipps, N. S. Hussein, T. Schlegl, and C. Senkpiel, "Current and Future Cost of Photovoltaics Long-term Scenarios for Market Development.," tech. rep., Fraunhofer ISE, 2015.

[156] A. H. Shah, A. Hassan, M. S. Laghari, and A. Alraeesi, "The influence of cleaning frequency of photovoltaic modules on power losses in the desert climate," *Sustainability (Switzerland)*, vol. 12, no. 22, pp. 1–15, 2020.

[157] H. Apostoleris, S. Sgouridis, M. Stefancich, and M. Chiesa, "Evaluating the factors that led to low-priced solar electricity projects in the Middle East," *Nature Energy*, vol. 3, no. 12, pp. 1109–1114, 2018.

[158] A. Tim Umoette, "Development of Site Specific Optimal Tilt Angle Model for Fixed Tilted Plane PV Installation ın Akwa Ibom State, Nigeria," *Science Journal of Energy Engineering*, vol. 4, no. 6, p. 50, 2016.

[159] Vestas, "4 MW Platform - V136-3.45 MW® at a glance", 2020. [online] Available at: <https://www.vestas.com/en/products/4-mw-platform/v136-_3_45_mw#!> [Accessed 19 January 2021].

[160] L. Fingersh, M. Hand, and A. Laxson,"Wind Turbine Design Cost and Scaling Model", National Renewable Energy Lab. (NREL), tech. rep., 2006.

[161] B. Maples, M. Hand, and W. Musial,"Comparative assessment of direct drive high temperature superconducting generators in multi-megawatt class wind turbines", National Renewable Energy Lab. (NREL), tech. rep., 2010.

[162] Wind Europe, "Unleashing Europe's offshore wind potential", tech. rep., 2017.

[163] M. Maness , B. Maples , A. Smith ,'NREL offshore balance-of system model", National Renewable Energy Lab. (NREL), tech. rep., 2017.

[164] D. S. Ryberg, D. G. Caglayan, S. Schmitt, J. Linßen, D. Stolten, and M. Robinius, "The future of European onshore wind energy potential: Detailed distribution and simulation of advanced turbine designs," *Energy*, vol. 182, pp. 1222–1238, sep 2019.

[165] S. Hoyer and J. Hamman, "xarray: N-D labeled arrays and datasets in Python," *Journal of Open Research Software*, vol. 5, no. 1, 2017.

[166] Unidata, netCDF4 v. 1.5.3, UCAR/Unidata Program Center, 2019. [online] Available at: <https://doi.org/10.5065/D6H70CW6> [Accessed 16 January 2021].

[167] Copernicus Climate Change Service (C3S), "ERA5: Fifth generation of ECMWF atmospheric reanalyses of the global climate", Copernicus Climate Change Service Climate Data Store (CDS), 2019. [online] Available at: <https://cds.climate.copernicus.eu/cdsapp!/home> [Accessed 18 January 2021].

[168] European Environmental Agency (EEA), "Digital Elevation Model over Europe (EUDEM)", 2017. [online] Available at: <https://www.eea.europa.eu/data-and-maps/data/copernicus-land-monitoring-service-eu-dem> [Accessed 19 January 2021].

[169] W. De Soto, S. A. Klein, and W. A. Beckman, "Improvement and validation of a model for photovoltaic array performance," *Solar Energy*, vol. 80, no. 1, pp. 78–88, 2006.

[170] A. Toktarova, L. Gruber, M. Hlusiak, D. Bogdanov, and C. Breyer, "Long term load projection in high resolution for all countries globally," *International Journal of Electrical Power and Energy Systems*, vol. 111, no. April, pp. 160–181, 2019.

[171] International Energy Agency (IEA), "Data and statistics", 2021. [online] Available at: <https://www.iea.org/data-and-statistics/data-tables?country=WORLDenergy=Balancesyear=2018> [Accessed 21 February 2020].

[172] H. Liu, J. Ma, L. Tong, G. Ma, Z. Zheng, and M. Yao, "Investigation on the potential of high efficiency for internal combustion engines," *Energies*, vol. 11, no. 3, 2018.

[173] D. G. Caglayan, H. U. Heinrichs, M. Robinius, and D. Stolten, "Robust design of a future 100% renewable european energy supply system with hydrogen infrastructure," *International Journal of Hydrogen Energy*, Preprints, 2021.

[174] International Energy Agency (IEA), "World Energy Outlook 2016," tech. rep., 2016.

[175] N. Howarth, M. Galeotti, A. Lanza, and K. Dubey, "Economic development and energy consumption in the GCC: an international sectoral analysis," *Energy Transitions*, vol. 1, no. 2, pp. 1–19, 2017.

[176] World Bank, "GDP per capita", 2021. [online] Available at: <https://data.worldbank.org/indicator/NY.GDP.PCAP.PP.CD> [Accessed 14 November 2021].

[177] M. Rivarolo, G. Riveros-Godoy, L. Magistri, and A. F. Massardo, "Clean hydrogen and ammonia synthesis in paraguay from the Itaipu 14 GW hydroelectric plant," *ChemEngineering*, vol. 3, no. 4, pp. 1–11, 2019.

[178] M. Ni, "An overview of hydrogen storage technologies," *Energy Exploration and Exploitation*, vol. 24, no. 3, pp. 197–209, 2006.

[179] A. B. Awan, M. Zubair, R. P. Praveen, and A. R. Bhatti, "Design and comparative analysis of photovoltaic and parabolic trough based CSP plants," *Solar Energy*, vol. 183, no. March, pp. 551–565, 2019.

[180] A. Al-Mohaisen, L. Chaussé, and S. Sud, "Progress report on the GCC electricity grid system interconnection in the middle east," *2007 IEEE Power Engineering Society General Meeting, PES*, pp. 1–7, 2007.

[181] International Renewable Energy Agency (IRENA), "Renewable Energy Market Analysis: GCC 2016", tech. rep., 2016.

[182] S. Hasan, T. Al-aqeel, and N. Peerbocus, "Saudi Arabia ' s Unfolding Power Sector Reform : Features , Challenges and Opportunities for Market Integration Shahid Hasan , Turki Al-Aqeel and," no. May, 2020.

[183] T. M. Aljohani and A. M. Alzahrani, "The Operation of the GCCIA HVDC Project and Its Potential Impacts on the Electric Power Systems of the Region," *International Journal of Electronics and Electrical Engineering*, no. January 2014, pp. 207–213, 2014.

[184] WorldPop, "Population Countries - Unconstrained individual countries 2000-2020", 2021. [online] Available at: <https://www.worldpop.org/geodata/listing?id=74> [Accessed 21 February 2020].

[185] "Spatio-temporal optimization of a future energy system for power-to-hydrogen applications in germany," *Energy*, vol. 158, pp. 1130–1149, 2018.

[186] International Energy Agency - Energy Technology Systems Analysis Program (IEA-ETSAP), "Electricity Transmission and Distribution," tech. rep., 2014.

[187] J. Carlsson, "Energy Technology Reference Indicator (ETRI) Projections for 2010–2050," tech. rep., European Commission - Joint Research Center, 2014.

[188] D. N. S. Gonçalves, C. D. M. Gonçalves, T. F. D. Assis, and M. A. D. Silva, "Analysis of the difference between the euclidean distance and the actual road distance in Brazil," *Transportation Research Procedia*, vol. 3, no. July, pp. 876–885, 2014.

[189] O. E. Andreikiv, O. V. Hembara, O. T. Tsyrul'Nyk, and L. I. Nyrkova, "Evaluation of the residual lifetime of a section of a main gas pipeline after long-term operation," *Materials Science*, vol. 48, no. 2, pp. 231–238, 2012.

[190] S. Lechtenböhmer, C. Dienst, M. Fischedick, T. Hanke, R. Fernandez, D. Robinson, R. Kantamaneni, and B. Gillis, "Tapping the leakages: Methane losses, mitigation options and policy issues for russian long distance gas transmission pipelines," *International Journal of Greenhouse Gas Control*, vol. 1, no. 4, pp. 387–395, 2007.

[191] P. M. Heuser, "Worldwide hydrogen provision scheme based on renewable energy", Preprints, FZJ Jülich, Germany, 2020.

[192] P. Lá. Horváth, G. Schneider, H. Bernhardt, C. Weiler et al., "Update of SMRI´s Compilation of Worldwide Salt Deposits and Salt Cavern Fields", Solution Mining Research Institute (SMRI), tech. rep., 2018.

[193] Y. Almulla, Modelling electricity and water desalination demand in the Gulf Cooperation Council (GCC) countries, Master Thesis, Kungliga Tekniska högskolan (KTH), Industrial Engineering and Management, Sweden, 2014.

[194] Statista, "Electricity consumption in Saudi Arabia from 2012 to 2019", 2021. [online] Available at: <https://www.statista.com/statistics/975244/saudi-arabia-electricity-consumption/> [Accessed 14 November 2021].

[195] United Nations Economic and Social Commission for Western Asia (UN-ESCWA), "Survey of economic and social developments in the arab region 2014-2015," tech. rep.

[196] L. Kotzur, P. Markewitz, M. Robinius, and D. Stolten, "Time series aggregation for energy system design: Modeling seasonal storage," *Applied Energy*, vol. 213, pp. 123–135, 2018.

[197] M. Hoffmann, L. Kotzur, D. Stolten, and M. Robinius, "A review on time series aggregation methods for energy system models," *Energies*, vol. 13, no. 3, 2020.

[198] F. Jafarkazemi and S. A. Saadabadi, "Optimum tilt angle and orientation of solar surfaces in Abu Dhabi, UAE," *Renewable Energy*, vol. 56, pp. 44–49, 2013.

[199] Pacific Northwest National Laboratory, "Hydrogen Tools Portal". [online] Available at: <https://h2tools.org/hyarc/hydrogen-data/hydrogen-density-different-temperatures-and-pressures> [Accessed 24 March 2020].

[200] International Renewable Energy Agency (IRENA), "Renewable power generation costs," tech. rep., 2019.

[201] International Renewable Energy Agency (IRENA), "Energy transformation - Middle East and North Africa," tech. rep., 2019.

[202] C. T. Chu and A. D. Hawkes, "A geographic information system-based global variable renewable potential assessment using spatially resolved simulation," *Energy*, vol. 193, p. 116630, 2020.

[203] K. Eurek, P. Sullivan, M. Gleason, D. Hettinger, D. Heimiller, and A. Lopez, "An improved global wind resource estimate for integrated assessment models," *Energy Economics*, vol. 64, pp. 552–567, 2017.

[204] J. Bosch, I. Staffell, and A. D. Hawkes, "Temporally-explicit and spatially-resolved global onshore wind energy potentials," *Energy*, vol. 131, pp. 207–217, 2017.

[205] R. C. Pietzcker, D. Stetter, S. Manger, and G. Luderer, "Using the sun to decarbonize the power sector: The economic potential of photovoltaics and concentrating solar power," *Applied Energy*, vol. 135, pp. 704–720, 2014.

[206] J. Bosch, I. Staffell, and A. D. Hawkes, "Temporally explicit and spatially resolved global offshore wind energy potentials," *Energy*, vol. 163, pp. 766–781, 2018.

[207] P. Giani, F. Tagle, M. G. Genton, S. Castruccio, and P. Crippa, "Closing the gap between wind energy targets and implementation for emerging countries," *Applied Energy*, vol. 269, no. May, p. 115085, 2020.

[208] M. Fasihi and C. Breyer, "Baseload electricity and hydrogen supply based on hybrid PV-wind power plants," *Journal of Cleaner Production*, vol. 243, p. 118466, 2020.

[209] D. S. Ryberg, Z. Tulemat, M. Robinius, and D. Stolten, "Geospatial land availability for energy systems (glaes)," 2017. [online] Available at: <http://www.scipy.org> [Accessed 27 December 2020].

[210] D. Stetter, "Enhancement of the REMix energy system model: global renewable energy potentials optimized power plant siting and scenario validation.", Faculty of Energy-, Process- and Bio-Engineering, University of Stuttgart, Germany, 2012.

[211] R. Gelaro, W. McCarty, M. J. Suárez, R. Todling, A. Molod, L. Takacs, Randles, *et al.*, "The modern-era retrospective analysis for research and applications, version 2 (MERRA-2)," *Journal of Climate*, vol. 30, no. 14, pp. 5419–5454, 2017.

[212] D. Bogdanov and C. Breyer, "North-East Asian Super Grid for 100% renewable energy supply: Optimal mix of energy technologies for electricity, gas and heat supply options," *Energy Conversion and Management*, vol. 112, pp. 176–190, 2016.

[213] A. Aghahosseini, D. Bogdanov, and C. Breyer, "A techno-economic study of an entirely renewable energy-based power supply for North America for 2030 conditions," *Energies*, vol. 10, no. 8, 2017.

[214] D. Camos, R. Bacon, A. Estache and M. Hamid,"Shedding Light on Electricity Utilities in the Middle East and North Africa", World Bank Group, tech. rep., 2018.

[215] International Energy Agency (IEA), "World Energy Outlook 2014," tech. rep., 2014.

[216] P. Cochrane, "Supertanker state: How Qatar is gambling its future on global gas dominance", Middle East Eye, 2020. [online] Available at: <https://www.middleeasteye.net/news/qatar-gas-lng-market-oil-prices-dominance> [Accessed 21 March 2021].

[217] J. Forrest, "LNG breakeven cost comparisons: Costs for delivery to Northern Asia", ARC Energy Research Institute, 2019. [online] Available at: <https://www.arcenergyinstitute.com/snapchart-lng-breakeven-cost-comparisons/> [Accessed 21 March 2021].

[218] R. Chong, D. Dediu, R. Gupta, "Setting the bar for global LNG cost competitiveness", McKinsey Company, 2019. [online] Available at: <https://www.mckinsey.com/industries/oil-and-gas/our-insights/setting-the-bar-for-global-lng-cost-competitiveness> [Accessed 12 April 2021].

[219] D. Saadi, "Gulf breakeven oil prices to fall on non-oil revenue uptick, austerity measures: IIF", SP Global Platts, 2021. [online] Available at: <https://www.spglobal.com/platts/en/market-insights/latest-news/natural-gas/031821-gulf-breakeven-oil-prices-to-fall-on-non-oil-revenue-uptick-austerity-measures-iif> [Accessed 21 March 2021].

[220] International Monetary Fund (IMF) and Organisation for Economic Co-operation and Development (OECD), "Tax Policy and Climate Change IMF/OECD Report for the G20 Finance Ministers and Central Bank Governors"2021. [online] Available at: <https://www.oecd.org/tax/tax-policy/tax-policy-and-climate-change-imf-oecd-g20-report-april-2021.pdf> [Accessed 12 April 2021].

[221] F. Kaspar, M. Borsche, U. Pfeifroth, J. Trentmann, J. Drücke, and P. Becker, "A climatological assessment of balancing effects and shortfall risks of photovoltaics and wind energy in Germany and Europe," *Advances in Science and Research*, vol. 16, no. July, pp. 119–128, 2019.